



## 저작자표시-비영리-변경금지 2.0 대한민국

이용자는 아래의 조건을 따르는 경우에 한하여 자유롭게

- 이 저작물을 복제, 배포, 전송, 전시, 공연 및 방송할 수 있습니다.

다음과 같은 조건을 따라야 합니다:



저작자표시. 귀하는 원저작자를 표시하여야 합니다.



비영리. 귀하는 이 저작물을 영리 목적으로 이용할 수 없습니다.



변경금지. 귀하는 이 저작물을 개작, 변형 또는 가공할 수 없습니다.

- 귀하는, 이 저작물의 재이용이나 배포의 경우, 이 저작물에 적용된 이용허락조건을 명확하게 나타내어야 합니다.
- 저작권자로부터 별도의 허가를 받으면 이러한 조건들은 적용되지 않습니다.

저작권법에 따른 이용자의 권리는 위의 내용에 의하여 영향을 받지 않습니다.

이것은 [이용허락규약\(Legal Code\)](#)을 이해하기 쉽게 요약한 것입니다.

[Disclaimer](#)

이학박사 학위논문

**Polymerization of Multiynes to Give  
Conjugated Polyenes and Polyenynes:  
Cyclopolymerization and Cascade  
Metathesis/Metallotropy Polymerization**

멀티아인의 중합을 통한 공액 폴리엔과 폴리에나  
인의 합성: 고리화 중합 및 연속적인 복분해/금속  
옮김 반응을 이용한 중합

2020 년 8 월

서울대학교 대학원

화학부 유기화학 전공

강 철

**Abstract**  
**Polymerization of Multiynes to Give Conjugated**  
**Polyenes and Polyenyne:**  
**Cyclopolymerization and Cascade Metathesis/Metallotropy**  
**Polymerization**

Cheol Kang  
Department of Chemistry  
The Graduate School  
Seoul National University

The discovery of polyenes, such as polyacetylenes, led to intense interest in the use of organic compounds in optoelectronic materials. Notably, using  $\alpha,\omega$ -diyne derivatives as monomers involved cyclization reactions during polymerization, affording polyacetylene structures containing cycloalkene rings. Studies from the past decades provided efficient cyclopolymerization systems using Mo- and Ru-based catalysts, enhancing the monomer scope and the complexity of the resulting polymers. However, there had been constraints in using certain types of catalysts and monomers, limiting the utility of cyclopolymerization.

In addition to polyenes, conjugated polyenyne consisting of double bonds and triple bonds also received much attention due to their intriguing optical properties. However, their synthetic routes were limited to topochemical polymerization and step-growth polymerization, thus the controlled synthesis of conjugated polyenyne had remained elusive.

This dissertation describes the expansion of the scopes of catalysts and monomers for the cyclopolymerization of  $\alpha,\omega$ -dienes using Ru-based olefin metathesis catalysts. Furthermore, we broadened the utility of Ru catalysts for making conjugated polymers by developing cascade metathesis and metallotropy

polymerization, which is the only method thus far that yields conjugated polyenynes via chain-growth mechanism.

In Chapter 2, we demonstrate the successful cyclopolymerization using the first-generation Grubbs catalyst (G1), which had been known to be inactive toward cyclopolymerization. After the extensive additive screening, we found two additives, benzoic acid and sodium benzoates, are effective for enhancing the activity of G1, enabling the efficient cyclopolymerization of various 1,6-heptadiyne monomers. The roles of the additives were elucidated by control experiments combined with *in situ* NMR studies.

While most studies on cyclopolymerization used 1,6-heptadiynes as monomers, polymerization of 1,5-hexadiynes had been elusive due to the high ring strain of cyclobutenes in the resulting polymer structure. We describe, in Chapter 3, the cyclopolymerization of 1,5-hexadiynes, in which challenging cyclizations occur to give new polyacetylene structures containing four-membered rings. Sterically bulky groups in the catalysts and monomers facilitated the cyclization reactions, even allowing for the controlled polymerization as well as the preparation of block copolymers. Experimental and computational studies supported that these new polymers possess exceptionally delocalized  $\pi$ -systems.

We also became interested in making conjugated polyenynes by using Ru-alkylidenes. In Chapter 4, we demonstrate the design principle for various multiyne monomers to proceed polymerization via sequential and selective reactions of olefin metathesis and metallotropic 1,3-shift. This new polymerization, which we call cascade metathesis and metallotropy polymerization (i.e., M&M polymerization), afforded unique conjugated polyenyne motifs consisting of different numbers and sequences of double and triple bonds. Moreover, living polymerization gave access to the precise control over molecular weights of polymers as well as to the synthesis of block copolymers.

Lastly, the scope of M&M polymerization could be broadened by



switching the regioselectivity, as described in Chapter 5. Conventional Grubbs catalysts underwent M&M polymerization via  $\alpha$ -addition to give only five-membered rings in the backbone. In contrast, the use of a Ru catalyst containing a dithiolate ligand successfully switched the regioselectivity to  $\beta$ -addition, thereby providing new conjugated polyenynes having alternating six- and five-membered rings. Furthermore, it exhibited unique polymerization characteristics due to the formation of alkyne-chelated Ru complex, as confirmed by *in situ* NMR analysis.

**Keyword:** Cyclopolymerization, cascade M&M polymerization, conjugated polyenes, conjugated polyenynes, Ru-alkylidene, Grubbs catalyst, living polymerization

**Student number:** 2014-22387

# Table of Contents

<b>Abstract .....</b>	<b>i</b>
-----------------------	----------

<b>Table of Contents .....</b>	<b>iv</b>
--------------------------------	-----------

## **Chapter 1. Introduction**

1.1. Research background .....	1
1.2. Thesis research .....	5
1.3. References .....	7

## **Chapter 2. Cyclopolymerization of 1,6-Heptadiynes Using the First Generation Grubbs Catalyst**

2.1. Abstract .....	11
2.2. Introduction .....	12
2.3. Results and Discussion .....	15
2.3.1. Strategies to enhance cyclopolymerization using G1 .....	15
2.3.2. Optimization and monomer scope .....	21
2.3.3. Mechanistic studies to understand the roles of new additives .....	25
2.4. Conclusion .....	33
2.5. Supporting Figures .....	34
2.6. Experimental Section .....	46
2.7. References .....	55

## **Chapter 3. Controlled Cyclopolymerization of 1,5-Hexadiynes Involving Four-membered Ring-Forming Cyclization**

3.1. Abstract .....	59
3.2. Introduction .....	60
3.3. Results and Discussion .....	62

3.3.1. Polymer synthesis and kinetic analysis .....	62
3.3.2. Optoelectronic properties of polymers .....	68
3.4. Conclusion .....	70
3.5. Supporting Figures .....	71
3.6. Experimental Section .....	73
3.7. References.....	89

## **Chapter 4. Living Metathesis & Metallotropy Polymerization for the Synthesis of Conjugated Polyenynes from Multialkynes**

4.1. Abstract .....	92
4.2. Introduction.....	93
4.3. Results and Discussion .....	95
4.3.1. Polymerization of tetraynes .....	95
4.3.2. Polymerization of hexaynes / Block copolymerization.....	103
4.3.3. Polymerization of pentaynes .....	109
4.3.4. Optoelectronic properties of polymers .....	112
4.4. Conclusion .....	114
4.5. Supporting Figures.....	115
4.6. Experimental Section .....	127
4.7. References.....	167

## **Chapter 5. $\beta$ -Selective Cascade Metathesis and Metallotropy Polymerization**

5.1. Abstract .....	170
5.2. Introduction.....	171
5.3. Results and Discussion .....	173
5.3.1. Polymerization and characterization .....	173
5.3.2. <i>In situ</i> NMR and UV-Vis measurements .....	177

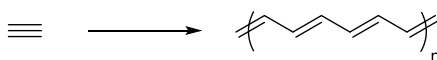
5.4. Conclusion .....	180
5.5. Supporting Figures .....	181
5.6. Experimental Section .....	191
5.7. References .....	214
 <b>Abstract (Korean)</b> .....	 216

# Chapter 1. Introduction

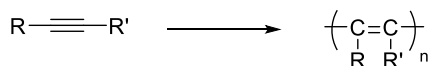
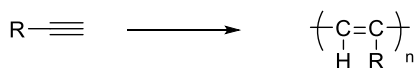
## 1.1. Research Background

Conjugated polymers, organic macromolecules having delocalized  $\pi$ -electron system in the backbone, received extensive attention due to their intriguing and useful optoelectronic properties.<sup>1</sup> Since the pioneering discovery of the metallic conductivity of the doped polyacetylene in the 1970s (Scheme 1.1.a),<sup>2</sup> people have developed various methods for the polymerization of acetylene derivatives. Despite its long effective conjugation length and high conductivity, simple polyacetylene could not be utilized for further applications because of its poor solubility and instability upon air exposure. These problems could be partially solved by using substituted alkynes as monomers to give mono- or disubstituted polyacetylenes, which exhibited improved solubility and oxidative stability (Scheme 1.1.b).<sup>3,4</sup> However, the steric repulsion between functional groups forced the polymer backbone out of coplanarity, resulting in short effective conjugation lengths.

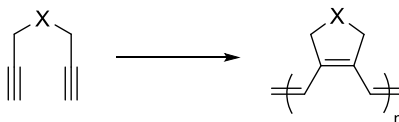
a) Polymerization of acetylene



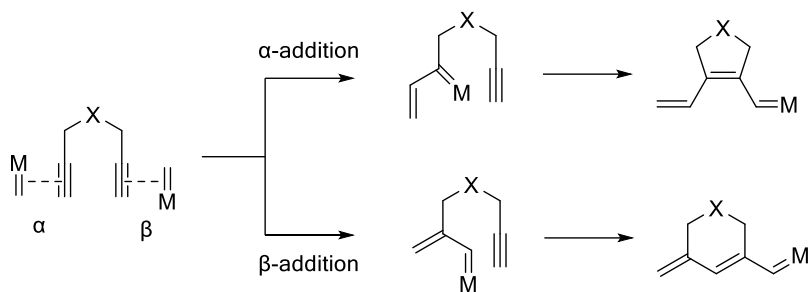
b) Polymerization of substituted alkynes



c) Cyclopolymerization of  $\alpha, \omega$ -diynes



**Scheme 1.1.** Syntheses of Functional Polyacetylenes

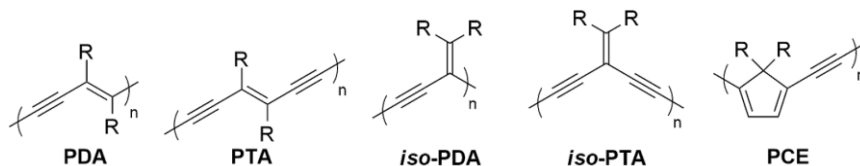


**Scheme 1.2.** Mechanism of Cyclopolymerization via  $\alpha$ - and  $\beta$ -Addition

In this regard, cyclopolymerization (CP) of  $\alpha,\omega$ -diynes became highly attractive as an efficient tool to prepare soluble and stable polyacetylenes with narrow band-gaps (Scheme 1.1.c).<sup>5-7</sup> In the early days, chemists used ill-defined catalysts such as Ziegler-Natta catalysts,<sup>8,9</sup>  $\text{MoCl}_5$ ,  $\text{Mo}(\text{CO})_6$ , and  $\text{WCl}_5$ <sup>10-13</sup> without understanding the detailed mechanism of CP. In 1992, the Schrock group reported the first living CP using a well-defined Mo-based catalyst and suggested the concept of  $\alpha$ - and  $\beta$ -addition to explain the mechanism and regioselectivity of the polymerization (Scheme 1.2).<sup>14,15</sup> Based on that study, Schrock and Buchmeiser groups independently solved the regioselectivity issue by modifying the ligands on the Mo-alkylidene catalysts, and prepared conjugated polyenes containing six-<sup>16,17</sup> or five-membered rings<sup>18,19</sup> via selective  $\beta$ - and  $\alpha$ -addition, respectively. Meanwhile, Ru-based Grubbs catalysts, which are air-stable and tolerant to various functional groups, had previously failed to promote CP and thus led to the misbelief that they were not sufficiently reactive for CP (Figure 1.1, **G1**, **G2**, and **HG2**). However, as a great breakthrough, the Buchmeiser group reported the first successful CP with Ru-based catalysts by modifying the second generation Hoveyda-Grubbs catalyst with electron-withdrawing groups such as trifluoroacetate or isocyanate (Figure 1.1, **Buch-I** and **Buch-II**).<sup>20-24</sup>



(Scheme 1.3).<sup>41,42</sup> Therefore, only certain monomers containing specific functional groups that induce proper alignment underwent successful polymerization in the solid state.<sup>43-45</sup> Moreover, the resulting polymers generally showed limited solubility, making solution fabrication challenging. To overcome these limitations, the synthesis of soluble polyenynes was realized by Glaser–Hay,<sup>46</sup> Sonogashira coupling<sup>47</sup> or alkyne metathesis reactions<sup>48</sup> via step-growth mechanism, while short oligoenynes could be prepared by multistep iterative syntheses.<sup>49-51</sup> Despite these efforts, only a handful of polyenylene motifs including polydiacetylene (PDA),<sup>49-52</sup> polytriacetylene (PTA),<sup>53-55</sup> their cross-conjugated isomers (*iso*-PDA<sup>56,57</sup> and *iso*-PTA<sup>58</sup>), and poly(cyclopentadienylene ethynylene) (PCE)<sup>47</sup> were reported (Figure 1.2). This narrow scope of available polymers and the difficulty of the methods by which they are prepared limit our understanding of how different sequences of C–C double bonds and triple bonds affect the properties of the  $\pi$ -conjugated polyenylene materials.



**Figure 1.2.** Previous examples of conjugated polyenynes.



## 1.2. Thesis Research

Despite extensive studies on the synthesis of conjugated polyenes and polyenynes, the preparation of new polymer structures with precise control is still desired. In this regard, we aimed to enhance the utility of Ru-based olefin metathesis catalysts for the synthesis of conjugated polymers, by enabling the use of a cheaper catalyst for the cyclopolymerization of 1,6-heptadiyne derivatives or by making new polyacetylenes containing four-membered rings. Furthermore, we report the first example of chain-growth polymerization to access conjugated polyenynes, which allowed for the elaborate design of the polymer structure and the precise control over the molecular weights via living polymerization.

Chapter 2 demonstrates the successful cyclopolymerization of 1,6-heptadiynes using the first-generation Grubbs catalyst. This phosphine-containing catalyst had been known to be inactive toward cyclopolymerization for several decades, but gratifyingly, we could activate the catalyst with the aid of simple additives; benzoic acid and sodium benzoate. Detailed mechanistic studies revealed the roles of additives, thus providing a comprehensive picture of cyclopolymerization using Grubbs catalysts.

Chapter 3 describes the cyclopolymerization of 1,5-hexadiyne derivatives, where challenging cyclizations to four-membered rings occur to afford new polyacetylenes containing cyclobutenes. Ru-based catalysts having a bulky N-heterocyclic ligand enabled the facile cyclization, allowing for the controlled polymerization as well as the preparation of block copolymers. Resulting polymers exhibited unexpectedly narrow band-gaps, as supported by experimental and computational studies.

In Chapter 4, we demonstrate the synthesis of conjugated polyenynes via cascade metathesis and metallotropy polymerization, i.e., M&M polymerization. Rational design of tetra-, penta-, and hexayne monomers enabled selective and

sequential reaction cascades of olefin metathesis and metallotropic 1,3-shift, affording unique conjugated polyenyne motifs with different sequences of double and triple bonds. Furthermore, living polymerization led to the synthesis of block copolymers consisting of fully conjugated polyenyne backbones.

Chapter 5 demonstrates the expansion of M&M polymerization by switching the regioselectivity from  $\alpha$ - to  $\beta$ -addition. The use of a Ru catalyst containing a dithiolate ligand enabled the M&M polymerization of tetrayne monomers via selective  $\beta$ -addition, thereby giving unique conjugated polyenyynes having alternating cyclohexene and cyclopentene rings in the backbone. *In situ* NMR studies revealed the formation of a stable alkyne-chelated Ru carbene during polymerization, providing detailed insights on the polymerization kinetics.

### 1.3. References

- (1) Guo, X.; Baumgarten, M.; Müllen, K. *Prog. Polym. Sci.* **2013**, *38*, 1832–1908.
- (2) Heeger, A. J. *Angew. Chem. Int. Ed.* **2001**, *40*, 2591–2611.
- (3) Liu, J.; Lam, J. W.; Tang, B. Z. *Chem. Rev.* **2009** *109*, 5799–5867.
- (4) Masuda, T. *J. Polym. Sci. Part A: Polym. Chem.* **2007**, *45*, 165–180.
- (5) Choi, S.-K.; Gal, Y.-S.; Jin, S.-H.; Kim, H.-K. *Chem. Rev.* **2000**, *100*, 1645–1681.
- (6) Buchmeiser, M. R. *Polym. Rev.* **2017**, *57*, 15–30.
- (7) Peterson, G. I.; Yang, S.; Choi, T. L. *Acc. Chem. Res.* **2019**, *52*, 994–1005.
- (8) Stille, J. K.; Frey, D. A. *J. Am. Chem. Soc.* **1961**, *83*, 1697–1701.
- (9) Gibson, H. W.; Bailey, F. C.; Epstein, A. J.; Rommelmann, H.; Kaplan, S.; Harbour, J.; Yang, X.-Q.; Tanner, D. B.; Pochan, J. M. *J. Am. Chem. Soc.* **1983**, *105*, 4417–4431.
- (10) Kim, Y.-H.; Gal, Y.-S.; Kim, U.-Y.; Choi, S.-K. *Macromolecules* **1988**, *21*, 1991–1995.
- (11) Ryoo, M.-S.; Lee, W.-C.; Choi, S.-K. *Macromolecules* **1990**, *23*, 3029–3031.
- (12) Kang, K.-L.; Kim, S.-H.; Cho, H.-N.; Choi, K.-Y.; Choi, S.-K. *Macromolecules* **1993**, *26*, 4539–4543.
- (13) Jeon, S. J.; Shim, S. C.; Cho, C. S.; Kim, T. J.; Gal, Y. S. *J. Polym. Sci., Part A: Polym. Chem.* **2000**, *38*, 2663–2670.
- (14) Fox, H. H.; Schrock, R. R. *Organometallics* **1992**, *11*, 2763–2765.
- (15) Fox, H. H.; Wolf, M. O.; O'Dell, R.; Lin, B. L.; Schrock, R. R.; Wrighton, M. S. *J. Am. Chem. Soc.* **1994**, *116*, 2827–2843.
- (16) Schattenmann, F. J.; Schrock, R. R.; Davis, W. M. *J. Am. Chem. Soc.* **1996**, *118*, 3295–3296.
- (17) Schattenmann, F. J.; Schrock, R. R. *Macromolecules* **1996**, *29*, 8990–8991.
- (18) Anders, U.; Nuyken, O.; Buchmeiser, M. R. *Angew. Chem., Int. Ed.* **2002**, *41*, 4044–4047.

- (19) Anders, U.; Nuyken, O.; Buchmeiser, M. R.; Wurst, K. *Macromolecules* **2002**, *35*, 9029–9038.
- (20) Krause, J. O.; Zarka, M. T.; Anders, U.; Weberskirch, R.; Nuyken, O.; Buchmeiser, M. R. *Angew. Chem., Int. Ed.* **2003**, *42*, 5965–5969.
- (21) Krause, J. O.; Nuyken, O.; Buchmeiser, M. R. *Chem. - Eur. J.* **2004**, *10*, 2029–2035.
- (22) Kumar, P. S.; Wurst, K.; Buchmeiser, M. R. *J. Am. Chem. Soc.* **2009**, *131*, 387–395.
- (23) Buchmeiser, M. R.; Schmidt, C.; Wang, D. *Macromol. Chem. Phys.* **2011**, *212*, 1999–2008.
- (24) Sudheendran, M.; Horecha, M.; Kiriy, A.; Gevorgyan, S. A.; Krebs, F. C.; Buchmeiser, M. R. *Polym. Chem.* **2013**, *4*, 1590–1599.
- (25) Kang, E.-H.; Lee, I. S.; Choi, T.-L. *J. Am. Chem. Soc.* **2011**, *133*, 11904–11907.
- (26) Kang, E.-H.; Yu, S. Y.; Lee, I. S.; Park, S. E.; Choi, T.-L. *J. Am. Chem. Soc.* **2014**, *136*, 10508–10514.
- (27) Kang, E.-H.; Lee, I.-H.; Choi, T.-L. *ACS Macro Lett.* **2012**, *1*, 1098–1102.
- (28) Mayershofer, M. G.; Nuyken, O.; Buchmeiser, M. R. *Macromolecules* **2006**, *39*, 3484–3493.
- (29) Vygodskii, Y. S.; Shaplov, A. S.; Lozinskaya, E. I.; Vlasov, P. S.; Malyshkina, I. A.; Gavrilova, N. D.; Kumar, P. S.; Buchmeiser, M. R. *Macromolecules* **2008**, *41*, 1919–1928.
- (30) Song, W.; Han, H.; Liao, X.; Sun, R.; Wu, J.; Xie, M. *Macromolecules* **2014**, *47*, 6181–6188.
- (31) Naumann, S.; Unold, J.; Frey, W.; Buchmeiser, M. R. *Macromolecules* **2011**, *44*, 8380–8387.
- (32) Lee, I. S.; Kang, E.-H.; Park, H.; Choi, T.-L. *Chem. Sci.* **2012**, *3*, 761–765.
- (33) Park, H.; Lee, H.-K.; Choi, T.-L. *Polym. Chem.* **2013**, *4*, 4676–4681.

- (34) Park, H.; Lee, H.-K.; Kang, E.-H.; Choi, T.-L. *J. Polym. Sci., Part A: Polym. Chem.* **2015**, *53*, 274–279.
- (35) Song, J. -A.; Park, S.; Kim, T. -S.; Choi, T. -L. *ACS Macro Lett.* **2014**, *3*, 795–798.
- (36) Song, J. A.; Choi, T. L. *Macromolecules* **2017**, *50*, 2724–2735.
- (37) Jung, K.; Ahmed, T. S.; Lee, J.; Sung, J. C.; Keum, H.; Grubbs, R. H.; Choi, T. L. *Chem. Sci.* **2019**, *10*, 8955–8963.
- (38) Yoon, B.; Lee, S.; Kim, J. M. *Chem. Soc. Rev.* **2009**, *38*, 1958–1968.
- (39) Sun, X.; Chen, T.; Huang, S.; Li, L.; Peng, H. *Chem. Soc. Rev.* **2010**, *39*, 4244–4257.
- (40) Lee, S.; Kim, J. Y.; Chen, X.; Yoon, J. *Chem. Commun.* **2016**, *52*, 9178–9196.
- (41) Eichele, H.; Schwoerer, M.; Huber, R.; Bloor, D. *Chem. Phys. Lett.* **1976**, *42*, 342–346.
- (42) Stevens, G. C.; Bloor, D. *Chem. Phys. Lett.* **1976**, *40*, 37–40.
- (43) Lu, Y.; Yang, Y.; Sellinger, A.; Lu, M.; Huang, J.; Fan, H.; Haddad, R.; Lopez, G.; Burns, A. R.; Sasaki, D. Y.; Shelnutt, J.; Brinker, C. J. *Nature* **2001**, *410*, 913–917.
- (44) Mosley, D. W.; Sellmyer, M. A.; Daida, E. J.; Jacobson, J. M. *J. Am. Chem. Soc.* **2003**, *125*, 10532–10533.
- (45) Lauher, J. W.; Fowler, F. W.; Goroff, N. S. *Acc. Chem. Res.* **2008**, *41*, 1215–1229.
- (46) Hu, K.; Qin, Y. *J. Polym. Sci., Part A: Polym. Chem.* **2016**, *54*, 1391–1395.
- (47) Rahman, M. M.; Zhao, X.; Harrell, J.; Chen, L.; Pietrangelo, A. *ACS Macro Letters* **2017**, *6*, 632–636.
- (48) Hu, K.; Yang, H.; Zhang, W.; Qin, Y. *Chem. Sci.* **2013**, *4*, 3649–3653.
- (49) Kohler, B. E.; Schilke, D. E. *J. Chem. Phys.* **1987**, *86*, 5214–5215.
- (50) Takayama, Y.; Delas, C.; Muraoka, K.; Uemura, M.; Sato, F. *J. Am. Chem. Soc.* **2003**, *125*, 14163–14167.

- (51) Pilzak, G. S.; van Lagen, B.; Hendrikx, C. C.; Sudhölter, E. J.; Zuilhof, H. *Chem.–Eur. J.* **2008**, *14*, 7939–7950.
- (52) Fujiwara, Y. I.; Kadota, K.; Nagarkar, S. S.; Tobori, N.; Kitagawa, S.; Horike, S. *J. Am. Chem. Soc.* **2017**, *139*, 13876–13881.
- (53) Martin, R. E.; Mäder, T.; Diederich, F. *Angew. Chem., Int. Ed.* **1999**, *38*, 817–821.
- (54) Schreiber, M.; Anthony, J.; Diederich, F.; Spahr, M. E.; Nesper, R.; Hubrich, M.; Bommeli, F.; Degiorgi, L.; Wachter, P.; Kaatz, P.; Bosshard, C.; Günter, P.; Colussi, M.; Suter, U. W.; Boudon, C.; Gisselbrecht, J.-P.; Gross, M. *Adv. Mater.* **1994**, *6*, 786–790.
- (55) Anthony, J.; Boudon, C.; Diederich, F.; Gisselbrecht, J.-P.; Gramlich, M.; Gross, M.; Hobi, M.; Seiler, P. *Angew. Chem., Int. Ed. Engl.* **1994**, *33*, 763–766.
- (56) Zhao, Y.; Tykwinski, R. R. *J. Am. Chem. Soc.* **1999**, *121*, 458–459.
- (57) Zhao, Y.; Campbell, K.; Tykwinski, R. R. *J. Org. Chem.* **2002**, *67*, 336–344.
- (58) Boldi, A. M.; Anthony, J.; Gramlich, V.; Knobler, C. B.; Boudon, C.; Gisselbrecht, J.-P.; Gross, M.; Diederich, F. *Helv. Chim. Acta* **1995**, *78*, 779–796.

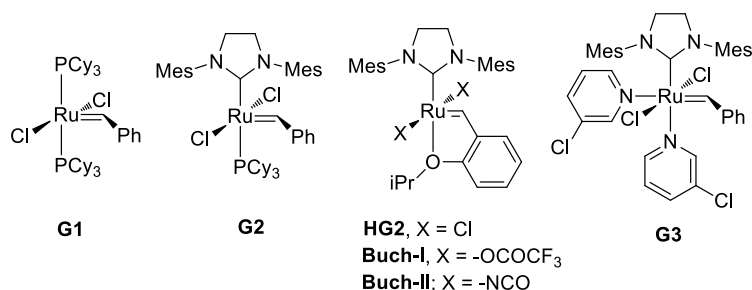
## Chapter 2. Cyclopolymerization of 1,6-Heptadiynes Using the First Generation Grubbs Catalyst

### 2.1. Abstract

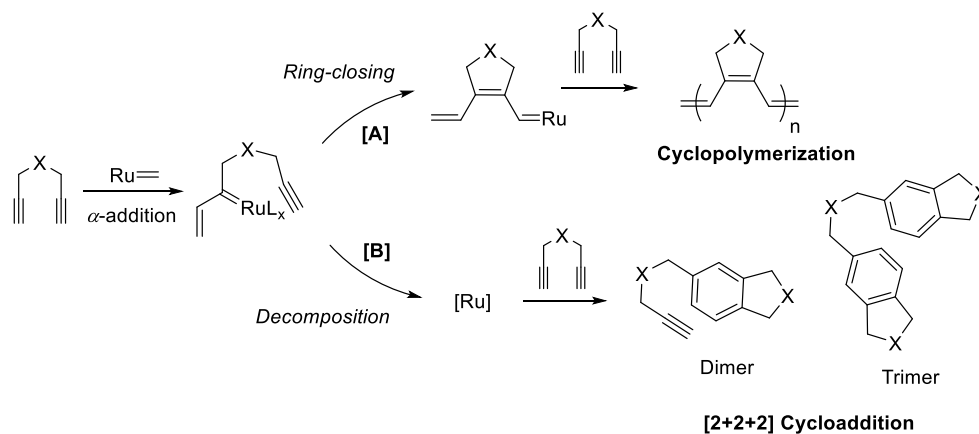
Cyclopolymerization (CP) of 1,6-heptadiynes using olefin metathesis catalysts is a useful method for producing soluble and stable polyacetylenes. Even though it had been well-known that highly reactive Grubbs catalysts containing an *N*-heterocyclic carbene ligand can promote CP, there was no report of successful CP using the much cheaper but less active first-generation Grubbs catalyst (G1). Based on the previous mechanistic studies on CP, we came up with three strategies to enhance the activity of G1. By categorizing numerous additives into three distinct classes and conducting extensive reaction screening, we discovered two additives: benzoic acid and sodium benzoate, both of which successfully produced various *trans*-selective conjugated polyenes with molecular weights of up to 23 kDa. We also conducted mechanistic studies by *in situ*  $^1\text{H}$  and  $^{31}\text{P}$  NMR spectroscopy to reveal that these two additives, despite having very similar chemical structures, enhance the CP efficiency via very different mechanisms; benzoic acid accelerated phosphine dissociation by protonation, while sodium benzoate mediated the exchange of an anionic ligand to afford a more active Ru complex. Also, these additives suppressed the carbene decomposition and retarded the [2+2+2] cycloaddition side reaction to enhance the selectivity of CP.

## 2.2. Introduction

Ru-based Grubbs catalysts (Figure 2.1, **G1**, **G2**, and **HG2**), which are air-stable and tolerant to various functional groups, had previously failed to promote CP (Scheme 2.1-[A]). However, the Buchmeiser group reported the first successful CP with Ru-based catalysts by modifying the second generation Hoveyda-Grubbs catalyst with electron-withdrawing groups such as trifluoroacetate or isocyanate (Figure 2.1, **Buch-I** and **Buch-II**).<sup>1-5</sup>



**Figure 2.1.** Chemical structures of conventional Ru catalysts.



**Scheme 2.1.** Competition between Cyclopolymerization and [2+2+2] Cycloaddition of 1,6-Heptadiynes Using Grubbs Catalysts

Since the Buchmeiser group's pioneering work using these new Ru-alkylidene catalysts, several reports suggested that certain aromatic side products such as the dimer and trimer of 1,6-heptadiyne derivatives were generated instead of the desired conjugated polymers (Scheme 2.1-[B]).<sup>3,5</sup> In those reports, they



suggested that a series of backbiting olefin metathesis reaction is competing with CP to generate these side products. This mechanism seemed plausible as it was also proposed by other organic chemists (e.g., the Blechert and Witulski groups) who had reported the same cyclization reaction of either triynes, or a combination of diynes and terminal alkynes by using Grubbs catalysts.<sup>6,7</sup> In contrast, the Pérez-Castells group suggested that the cyclization reaction (leading to the aromatic side products) proceeded by a completely different [2+2+2] cycloaddition mechanism, catalyzed by unknown Ru complexes generated after the decomposition of Grubbs catalysts.<sup>8-10</sup> Recent mechanistic studies revealed that it was indeed the decomposed Ru complex that generated those aromatic side products via a [2+2+2] cycloaddition mechanism.<sup>11</sup> In other words, the key to a successful CP using Grubbs catalysts was not to enhance the reactivity of the catalysts, but mainly about the stabilization of the propagating carbenes in order to suppress their decomposition and the competing [2+2+2] cycloaddition reaction. In this regard, living cyclopolymerization became possible using a fast-initiating third-generation Grubbs catalyst in tetrahydrofuran solvent or with the addition of pyridine ligands.

Despite extensive studies on CP using Grubbs catalysts, only highly active and expensive Grubbs catalysts containing *N*-heterocyclic carbene (NHC) ligands were known to promote CP. Nevertheless, a less active but much cheaper first-generation Grubbs catalyst containing two tricyclohexylphosphine ligands (Figure 2.1, **G1**) has been widely used in the past two decades in many organic and polymerization reactions such as cross-metathesis (CM), ring-closing metathesis (RCM), acyclic diene metathesis (ADMET) polymerization, and ring-opening metathesis polymerization (ROMP).<sup>12,13</sup> Particularly, **G1** showed decent activities for both intra- and intermolecular enyne metathesis reactions which are essential steps for CP.<sup>14,15</sup> Based on our previous reports on the importance of catalyst stability during CP,<sup>11</sup> as well as other studies that highlighted the enhancement of **G1**'s activity by controlling the equilibrium between the 16-electron precatalyst and the 14-electron active catalyst,<sup>16-24</sup> we believed that CP using **G1** would be

possible as well.

In this chapter, we demonstrate successful CP of 1,6-heptadiyne derivatives by using **G1** with simple additives. Various types of additives were screened to identify the optimal reaction condition, thereby maximizing the polymerization efficiency to afford conjugated polyenes with  $M_n$  values of up to 23 kDa. Additionally, extensive kinetic studies were carried out, especially by monitoring the propagating carbenes using  $^1\text{H}$  and  $^{31}\text{P}$  NMR spectroscopy to reveal how the additives affected CP and its competing side reaction, [2+2+2] cycloaddition.

## 2.3 Results & Discussion

### 2.3.1. Strategies to enhance cyclopolymerization using **G1**

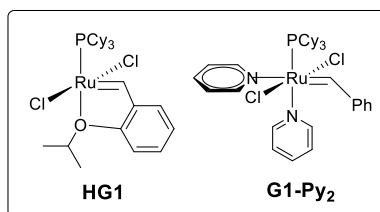
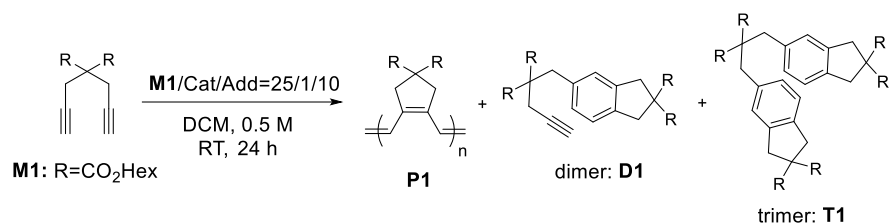
First, as a control experiment, we tested the reactivity of **G1** with **M1** monomer ( $M/I = 25$ ) in dichloromethane (DCM) and found that the competing [2+2+2] cycloaddition reaction predominates over the desired CP reaction (52% + 38% vs 8%) (Table 2.1, entry 1), analogous to previous CP results using **G2** and **HG2** catalysts in DCM.<sup>11</sup> Our first strategy to enhance CP focused on increasing the concentration of the active 14-electron complex, by using catalysts without free phosphine<sup>25,26</sup> or by adding various phosphine trapping agents to facilitate the dissociation of phosphine.<sup>16-24</sup> Without having a free phosphine that would reversibly coordinate to Ru complex, **HG1** produced a slightly higher amount of **P1** (18%); however, 44% of the dimer (**D1**) and 17% of the trimer (**T1**) were formed (entry 2). With **G1-Py**<sub>2</sub> catalyst containing labile pyridine ligands, the yield of **P1** increased only slightly to 23% even though the formation of the side products, **D1** and **T1**, were highly suppressed (entry 3). This was a big disappointment because the analogous **G3** (containing the NHC ligand) is the best catalyst for living CP, thus implying that the stabilization mechanism of **G1** might differ from those NHC ligand-containing catalysts. Next, Lewis acid additives were used since these are known to increase the reactivity of **G1** toward RCM.<sup>22,23</sup> With AlCl<sub>3</sub>, large amounts of **D1** and **T1** were formed over **P1** (38% + 7% vs 16%, entry 4). Another Lewis acid CuCl seemed to deactivate both pathways (entry 5). In response, various Brønsted acids were screened, and a strong acid such as trifluoroacetic acid ( $pK_a = 0.5$ ) completely shut down the CP pathway (entry 6). To our delight, other carboxylic acids with  $pK_a$  of ca. 4–5 significantly improved the efficiency of CP and significantly suppressed dimer formations (entries 7–10). Among them, benzoic acid was the best additive, affording 86% conversion to **P1** with minimal formation of side products (entry 8). Therefore, using an acid additive with a proper  $pK_a$  value was important as the catalyst might become

unstable with stronger acids, while weaker acids might not trap the phosphine effectively to activate the catalyst sufficiently. Meanwhile, the  $pK_a$  of the additive was not the only determining factor because 2,4-dinitrophenol, which has a similar  $pK_a$  to benzoic acid, completely suppressed CP but promoted [2+2+2] cycloaddition exclusively (entry 11). In short, achieving a proper balance between the dissociation of phosphine by protonation and weak coordination of benzoic acid to Ru center greatly enhanced CP, while removing the free phosphines was unhelpful because ensuring the stability of the catalyst by reversible coordination of the phosphine was crucial as well.

As the second strategy, we added various weakly coordinating ligands to stabilize the propagating carbene, thereby suppressing the catalyst decomposition. Firstly, we tested THF solvent since it worked well for **HG2** and **G3**,<sup>11,27-29</sup> but disappointingly, aromatic products were formed almost exclusively with **G1** (entry 12). Moreover, various pyridine ligands, which also functioned as good additives for **HG2** and **G3**,<sup>11,28</sup> produced only 16–26% of **P1** with almost no or small amounts of **D1** (entries 13–15). These results showed that the simple stabilization of **G1** via weak coordination could not enhance CP sufficiently.

Inspired by the results of using carboxylic acids as additives, we screened various carboxylate salts and observed that sodium acetate and sodium benzoate were excellent additives, while sodium trifluoroacetate showed only a moderate effect (entries 16–18). Other acetate salts containing different counter cations such as  $Li^+$ ,  $K^+$ , and  $NH_4^+$  were less efficient compared to sodium acetate (entries 19–21). Among the carboxylate salts tested, sodium benzoate gave the best result, showing full consumption of the monomer with a production of 91% of **P1** (entry 17). Additionally, **HG1** was re-tested with the two best-performing additives – benzoic acid and sodium benzoate – but both could not sufficiently enhance the CP efficiency, suggesting that the presence of labile phosphine ligand in **G1** was essential for the successful CP.

**Table 2.1.** Screening Various Additives to Enhance CP Efficiency and Selectivity



entry	cat	additive (pK <sub>a</sub> )	conv (%) <sup>a</sup>	P1 (%) <sup>a</sup>	D1 (T1) (%) <sup>a</sup>
1	<b>G1</b>	None	> 99	8	52 (38)
2	<b>HG1</b>	None	82	18	44 (17)
3	<b>G1-Py<sub>2</sub></b>	None	34	23	6 (3)
4	<b>G1</b>	AlCl <sub>3</sub> (5 eq)	62	16	38 (7)
5	<b>G1</b>	CuCl	42	2	26 (8)
6	<b>G1</b>	Trifluoroacetic acid (0.5)	98	0	41 (8)
7	<b>G1</b>	4-Nitrobenzoic acid (3.85)	67	39	28
8	<b>G1</b>	PhCOOH (4.20)	88	86	2
9	<b>G1</b>	Hexanoic acid (4.88)	56	46	7
10	<b>G1</b>	Pivalic acid (5.03)	54	40	6
11	<b>G1</b>	2,4-Dinitrophenol (4.11)	> 99	0	59 (36)
12	<b>G1</b>	THF (solvent)	94	3	59 (29)
13	<b>G1</b>	Pyridine	25	23	0
14	<b>G1</b>	3-Chloropyridine	31	26	3
15	<b>G1</b>	3,5-Dichloropyridine	36	16	16

**Table 2.1.** continued

entry	cat	additive (pK <sub>a</sub> )	conv (%) <sup>a</sup>	P1 (%) <sup>a</sup>	D1 (T1) (%) <sup>a</sup>
16	<b>G1</b>	CH <sub>3</sub> COONa	99	93	0
17	<b>G1</b>	PhCOONa	> 99	97	0
18	<b>G1</b>	CF <sub>3</sub> COONa	67	48	13
19	<b>G1</b>	CH <sub>3</sub> COOLi	92	19	48 (19)
20	<b>G1</b>	CH <sub>3</sub> COOK	92	84	0
21	<b>G1</b>	CH <sub>3</sub> COONH <sub>4</sub>	35	23	0
22	<b>HG1</b>	PhCOOH	44	8	15
23	<b>HG1</b>	PhCOONa	77	42	18
24	<b>G1</b>	CH <sub>3</sub> COOAg (1 eq)	98	29	37 (31)
25	<b>G1</b>	CH <sub>3</sub> COOAg (2 eq)	81	30	26 (5)
26	<b>G1</b>	PhCOOAg (1 eq)	81	11	55 (12)
27	<b>G1</b>	PhCOOAg (2 eq)	36	18	12 (2)
28	<b>G1</b>	CF <sub>3</sub> COOAg (2 eq)	99	62	27 (5)
29	<b>G1</b>	CF <sub>3</sub> COOAg (5 eq)	97	84	6
30 <sup>b</sup>	<b>G2</b>	None	80	17	49 (11)
31 <sup>b</sup>	<b>G2</b>	PhCOOH	68	66	1
32 <sup>b</sup>	<b>G2</b>	PhCOONa	58	41	16
33 <sup>c</sup>	<b>HG2</b>	None	94	8	54 (22)
34 <sup>c</sup>	<b>HG2</b>	PhCOOH	84	68	8
35 <sup>c</sup>	<b>HG2</b>	PhCOONa	84	11	51 (12)

<sup>a</sup>Calculated from <sup>1</sup>H NMR spectroscopy (Figure S2.14). <sup>b</sup>20 h reaction. <sup>c</sup>1 h reaction.

The last strategy to enhance CP involved exchanging the anionic X-type ligand (chlorides in **G1**) as inspired by the reports from the Buchmeiser group who demonstrated the successful CP using **Buch-I** via this strategy.<sup>1-4</sup> They treated various silver salts to **HG2** and isolated the corresponding modified Ru catalysts, which contained NHC and electron-withdrawing ligands such as trifluoroacetate or isocyanate. Likewise, we compared the efficiencies of CP by adding various silver carboxylates to **G1** in order to produce the corresponding carboxylated Ru complexes *in situ*.<sup>30-38</sup> The addition of 1 or 2 equiv of silver acetate to **G1** (entries 24 and 25) gave only 30% of **P1**, which was only scarcely better than just using **G1**. It was also disappointing to find that 1 or 2 equiv of silver benzoate led to even poorer results (11-18% **P1**, entries 26 and 27). However, using 2 equiv of silver trifluoroacetate significantly increased the formation of **P1** up to 62%, with 32% of side products (entry 28). Furthermore, using a higher loading of the additive (5 equiv) increased the **P1** formation to 84% (entry 29). Overall, new Ru complexes containing carboxylate ligands showed slightly higher activities towards CP than **G1** alone, but these results were still worse than that afforded by benzoic acid or sodium benzoate, presumably because of the lower stability of the modified complexes.<sup>34</sup> In order to get a better insight, we monitored the changes in carbene signals by <sup>1</sup>H NMR after adding silver benzoate to **G1** and observed multiple complicated carbene signals, implying the formation of various complex carbenes (Figure S2.1). However, adding silver trifluoroacetate to **G1** produced only a couple of new carbene signals, hence suggesting that these more well-defined Ru complexes substituted by electron-withdrawing trifluoroacetate ligands were much more efficient for CP (Figure S2.2).

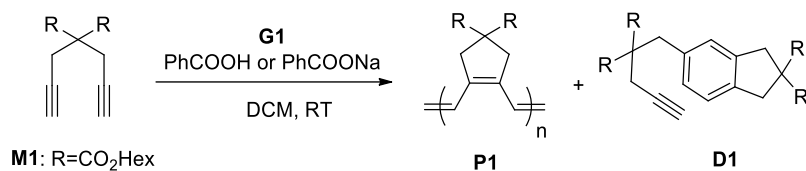
Since we discovered that the benzoic acid and sodium benzoate additives greatly improved CP of **G1**, we became curious how these new additives would affect CP involving the NHC-containing Grubbs catalysts such as **G2** and **HG2**. Analogous to the previous report,<sup>11</sup> CP of **M1** by **G2** and **HG2**, without any additive, mainly produced **D1** and **T1** (entries 30 and 33). Interestingly, both

benzoic acid and sodium benzoate somewhat enhanced the CP efficiency of **G2**, respectively producing 66% and 41% of **P1** (entries 31 and 32). The addition of benzoic acid to another NHC-containing **HG2** moderately increased the conversion toward **P1** to 68% (entry 34), but replacing it with sodium benzoate resulted in an unsuccessful CP (entry 35). In short, the optimal additives for **G1** were not the best additives for **G2** and **HG2**, whereas the best condition for **G2** and **HG2** did not improve the CP of **G1**. These results implied that an appropriate choice of additive, based on the specific type of catalysts, is essential for a successful CP because the activation mechanisms of phosphine-containing **G1** and NHC-containing **G2** and **HG2** might be different.



### 2.3.2. Optimization and monomer scope

With benzoic acid and sodium benzoate as the best additives, the reaction conditions were further optimized (Table 2.2). As the concentration of the monomer increased from 0.5 to 2.0 M, the polymerization efficiency increased to give 98% of **P1** with  $M_n$  of 15 kDa using the benzoic acid additive ( $M/I = 25$ , entries 1–3). Furthermore, using a higher amount of sodium benzoate (from 5 to 8 equivalents) and a higher concentration (1.0 M) improved the CP efficiency up to 96% in just 3 hours to give **P1** with  $M_n$  of 12 kDa exclusively (entries 5 and 6). With a higher  $M/I$  ratio of 50, both additives showed similar results of 82%–83% conversion to **P1** as well as high  $M_n$  of up to 23 kDa (entries 4 and 7). Nevertheless, the dispersities ( $D$ ) in all cases were broad mainly due to slow initiation and the catalyst decomposition. The possibility of chain transfer reaction via intermolecular olefin metathesis was ruled out since the reaction of narrow dispersity polymer with **G1** did not change the dispersity at all (Figure S2.3). We also confirmed that only a five-membered ring repeat unit was formed via exclusive  $\alpha$ -addition of **G1**, similar to the cases of **G2**, **HG2**, and **G3** (Figure S2.4). In addition, the polymers synthesized by **G1** contained *trans* olefin almost exclusively in all cases ( $> 97\%$ , Figure S2.5), while **G3** produced a 5.4:1 mixture of *E*:*Z* olefins.<sup>39</sup>

**Table 2.2.** Optimization of CP with Benzoic Acid and Sodium Benzoate Additives

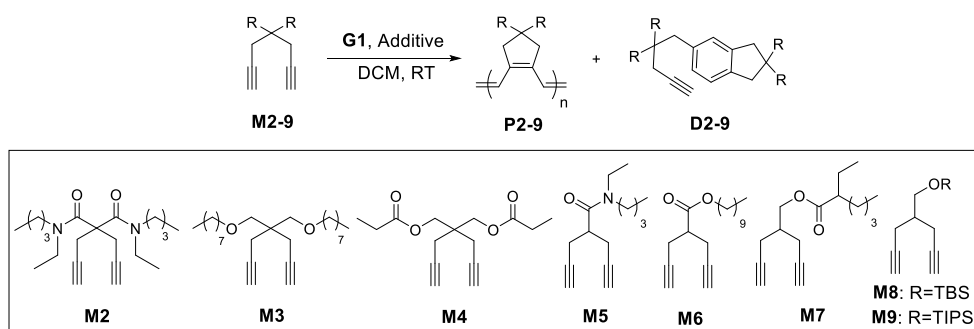
entry	additive	M/I/Add	conc (M)	time (h)	conv (%) <sup>a</sup>	P1 (%) <sup>a</sup>	D1 (%) <sup>a</sup>	yield (%)	<i>M<sub>n</sub></i> (kDa) <sup>b</sup>	<i>Đ</i> <sup>b</sup>
1	PhCOOH	25/1/10	0.5	23	88	86	2	82	12.5	1.70
2	PhCOOH	25/1/10	1.0	20	90	90	0	87	14.7	1.64
3	PhCOOH	25/1/10	2.0	24	98	98	0	93	14.6	1.60
4	PhCOOH	50/1/15	2.0	48	85	83	2	72	20.2	1.68
5	PhCOONa	25/1/5	0.5	24	92	83	9	62	11.7	1.69
6	PhCOONa	25/1/8	1.0	3	99	96	0	90	12.3	1.67
7	PhCOONa	50/1/8	1.0	24	87	82	0	74	23.3	1.53

<sup>a</sup>Calculated from <sup>1</sup>H NMR. <sup>b</sup>Determined by THF size-exclusion chromatography (SEC) calibrated using polystyrene (PS) standards.

In order to broaden the monomer scope, various 4-bis-substituted 1,6-heptadiyne monomers (**M2–4**) and 4-mono-substituted monomers (**M5–9**) were polymerized with the addition of benzoic acid and sodium benzoate, respectively (Table 2.3). Surprisingly, a bis-amide group-containing monomer **M2**, which gave no polymer with the intrinsically more reactive **G3** catalyst (Figure S2.6), was successfully polymerized by **G1** (entry 1). The reaction afforded 65% and 87% conversion to **P2** (with *M<sub>n</sub>* of 10 kDa) using the benzoic acid and sodium benzoate additives, respectively. Another bis-substituted octyl ether-containing monomer **M3** produced 75% of **P3** (*M<sub>n</sub>* of 12 kDa) with benzoic acid, while sodium benzoate resulted in a lower conversion to **P3** (49%, *M<sub>n</sub>* of 7 kDa) (entry 2). Furthermore, a bis-substituted ester monomer **M4**, coupled with benzoic acid, gave 88% and 76% of polymer conversion in M/I = 25 and 50, while sodium benzoate gave 95% and

44% conversions, respectively (entries 3 and 4). For mono-substituted monomers, we initially tested an amide-substituted monomer **M5** and obtained a moderate reaction efficiency of 46% using benzoic acid, while the use of sodium benzoate gave 68% of **P5** with  $M_n$  of 7 kDa (entry 5). An analogous ester-containing monomer **M6** was polymerized at conversions of 80% (benzoic acid) and 71% (sodium benzoate) to give **P6** with  $M_n$  of up to 11 kDa (entry 6). The CP of another ester-containing monomer **M7** using benzoic acid showed excellent conversion to **P7** with  $M_n$  of up to 15.7 kDa (89% and 81% for M/I = 25 and 50, respectively), while sodium benzoate showed slightly decreased reaction efficiency of 87% and 57% for M/I = 25 and 50, respectively (entries 7 and 8). Furthermore, **M8** containing a *tert*-butyldimethylsilyl (TBS) ether group with benzoic acid produced 84% and 55% of **P8** for M/I = 25 and 50, respectively. Using sodium benzoate for this reaction resulted in 93% (M/I = 25) and 82% (M/I = 50) conversions to **P8**, as well as a high  $M_n$  of 12 kDa (entries 9 and 10). Lastly, the triisopropylsilyl (TIPS) ether-containing monomer **M9** gave 75% and 58% conversions to **P9** ( $M_n$  of 8 kDa) using benzoic acid and sodium benzoate, respectively (entry 11). Based on the results obtained from the monomer screening, the CP of **G1** with the two additives showed comparable or complementary results, but dimer formation was more effectively suppressed using sodium benzoate. These results implied that these two additives might work differently during CP.

**Table 2.3.** Cyclopolymerization of Various Monomers by G1



			PhCOOH Additive <sup>a</sup>					PhCOONa Additive <sup>b</sup>				
entry	M	M/I	conv (%) <sup>c</sup>	polymer, dimer (%) <sup>c</sup>	yield (%)	$M_n$ (kDa) <sup>d</sup>	$\bar{D}^d$	conv (%) <sup>c</sup>	polymer, dimer (%) <sup>c</sup>	yield (%)	$M_n$ (kDa) <sup>d</sup>	$\bar{D}^d$
1	<b>M2</b>	25	73	65, 1	62	10.2	1.46	91	87, 0	87	9.8	1.58
2	<b>M3</b>	25	84	75, 6	70	11.7	1.67	61	49, 4	45	7.4	1.57
3	<b>M4</b>	25	98	88, 10	64	9.5	1.45	97	95, 0	91	9.0	1.71
4	<b>M4</b>	50	90	76, 14	64	9.9	1.62	58	44, 6	38	8.9	1.60
5	<b>M5</b>	25	74	46, 11	46	6.4	1.39	89	68, 0	64	7.2	1.32
6	<b>M6</b>	25	88	80, 5	76	11.1	1.70	93	71, 0	71	7.0	2.13
7	<b>M7</b>	25	97	89, 8	78	12.0	1.53	> 99	87, 0	82	11.5	1.77
8	<b>M7</b>	50	88	81, 7	73	15.7	1.71	63	57, <1	32	12.0	1.83
9	<b>M8</b>	25	95	84, 6	77	9.7	1.76	99	93, 0	78	8.7	1.55
10	<b>M8</b>	50	65	55, 6	43	10.7	1.88	93	82, 3	53	11.8	1.71
11	<b>M9</b>	25	98	75, 4	59	7.7	1.56	87	58, 6	58	8.2	1.59

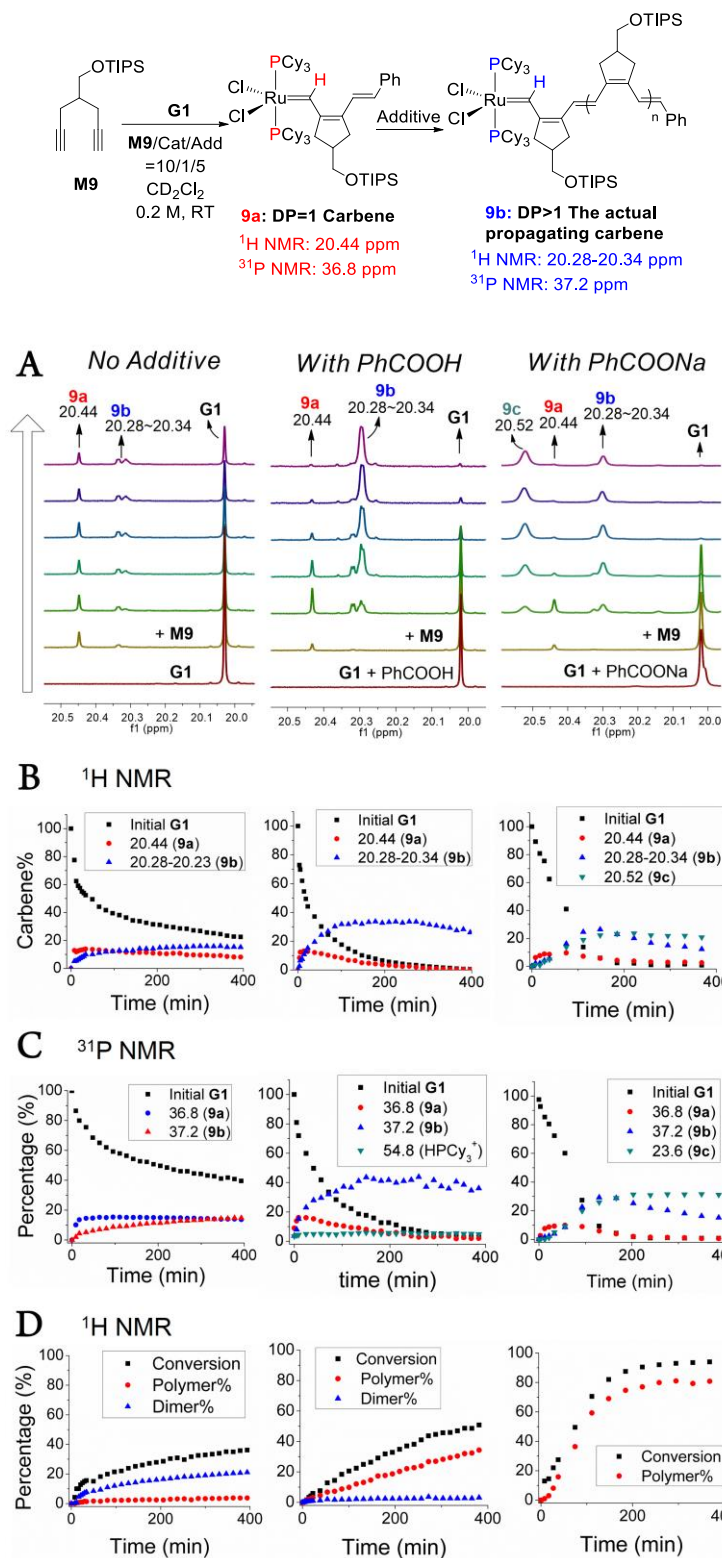
<sup>a</sup>Reaction performed in 2.0 M with the addition of 10 and 15 equivalents of PhCOOH for M/I = 25 (24 h) and 50 (48 h), respectively. <sup>b</sup>Reaction performed in 1.0 M for 3 h (M/I = 25) or 24 h (M/I = 50) with the addition of 8 equivalents of PhCOONa. <sup>c</sup>Calculated from <sup>1</sup>H NMR. <sup>d</sup>Determined by THF SEC calibrated using PS standards.

### 2.3.3. Mechanistic studies to understand the roles new of additives

In order to investigate how the additives enhanced CP, a series of *in situ* NMR experiments was carried out to monitor the reaction kinetics of CP and changes in the propagating carbenes (Figure 2.2). Initially, the carbene signal of the original **G1** appeared at 20.02 ppm, and adding **M9** alone generated a new sharp singlet peak at 20.44 ppm (Figure 2.2, **A-left**), whose intensity increased up to 14% during the early stage and decreased very slowly throughout the reaction. Subsequently, other new broad signals appeared at 20.28–20.34 ppm and gradually increased to 20%. (Figure 2.2, **A** and **B-left**). We assigned the singlet peak at 20.44 ppm to the Ru carbene with a degree of polymerization (DP) of 1 generated by the first monomer addition to the catalyst (Figure 2.2, **9a**). The broad peak at 20.28–20.34 ppm was assigned to the actual propagating carbene with DP > 1 (Figure 2.2, **9b**), formed by further monomer additions.<sup>40</sup> To support this argument, we conducted a control experiment using a just 1:1 mixture of **G1** and **M9** (M/I = 1) and observed that the 20.44 ppm singlet formed exclusively (Figure S2.7). Additionally, we also observed a similar phenomenon from the reaction using **G3** with pyridine additives, whereby two different signals corresponding to the DP = 1 carbene and the DP > 1 propagating carbene were detected separately (Figure S2.8). Similar to the <sup>1</sup>H NMR result, the two new neighboring peaks at 36.8 and 37.2 ppm of the <sup>31</sup>P NMR spectrum were observed (Figure S2.9), which were assigned to the DP = 1 carbene (**9a**) and the DP > 1 propagating carbene (**9b**), respectively, since their changes in population were consistent with those of <sup>1</sup>H NMR (Figure 2.2, **B** and **C-left**). Based on these results, we realized that the amount of the actual propagating carbene (**9b**) without any additive was very low (below 20%), and more importantly, the transition from **9a** to **9b** was very slow and inefficient. This observation agreed with the previous studies, which reported that initiation of ruthenium vinylidene was much slower than that of ruthenium benzylidene during ROMP.<sup>41</sup> This implied that further propagation was retarded because of the low efficiency of phosphine dissociation from the conjugated carbene **9a**, thus leading

to an inefficient polymerization and eventual carbene decomposition to produce the dimer as a major side product by [2+2+2] cycloaddition (Figure 2.2, **D**-left).

In order to understand how the additives facilitated the polymerization, we carried out the same investigation using the benzoic acid additive. Compared to the previous case, the initial consumption of **G1** with the additive was twice as fast (0.61 vs. 1.2 mM/min), leading to a complete initiation in 6 hours. The DP = 1 carbene at 20.44 ppm (**9a**) increased and decreased quickly at the early stage, and the DP > 1 propagating carbene (**9b**) formed rapidly (up to 34%, Figure 2.2, **A** and **B**-middle). It indicates that benzoic acid accelerated both the initiation of **G1** and the transition from **9a** to **9b**, presumably by protonating the phosphines to facilitate the formation of active 14-electron species. Furthermore, benzoic acid seemed to act as a weakly coordinating ligand to stabilize the propagating carbene, thereby suppressing its decomposition. As a result, the initial polymerization was six times faster than that without using any additive (0.043 vs 0.25 mM/min, Figure 2.2, **D**-middle). Moreover,  $^{31}\text{P}$  NMR analysis showed the formation of 3–5% of  $\text{HPCy}_3^+$  at 54.8 ppm (Figure S2.10), confirming that benzoic acid indeed protonated the phosphines. Still, a majority of the free tricyclohexylphosphine reversibly coordinated to Ru, achieving appropriate equilibrium between the active (14-electron Ru) and the dormant species (16-electron Ru) of the catalyst. This could be the reason why the polymerization was not efficient using **HG1** and **G1-Py**<sub>2</sub>, whose propagating carbenes could not be stabilized due to the lack of free phosphines. Additionally, we observed that the amount of the DP > 1 propagating carbene increased by 11% (from 31% to 42% using **M1**, Figure S2.12) as the concentration increased from 0.2 to 0.6 M, suggesting that a high concentration (2.0 M) enhanced the CP efficiency (Table 2.2, entries 1–3).



**Figure 2.2.** (A) <sup>1</sup>H NMR spectra monitoring the initial and propagating carbenes

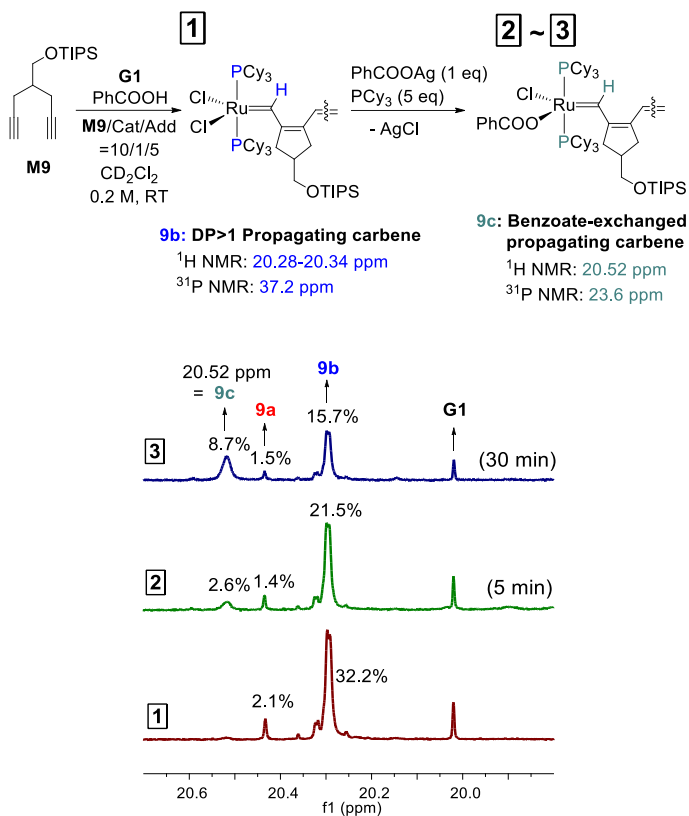
with  $M/I = 10$ . (B) Plots of changes for various carbene signals obtained from  $^1\text{H}$  NMR vs time. (C) Plots of changes for various  $^{31}\text{P}$  NMR signals vs time. (D) Plots of total conversion, conversions of polymerization, and dimerization vs time.

Lastly, further investigations with sodium benzoate revealed that the initial consumption of **G1** was ironically 0.36 times slower than that even without any additive (0.61 vs 0.22 mM/min). This might result from the competitive coordination of the benzoate anion against the monomer. However, the conversion of **9a** to **9b** was rather fast, and more interestingly, a completely new propagating carbene appeared at 20.52 ppm (**9c**). The intensity of **9b** and **9c** grew up to 24% each, giving a combined value of close to 50% (Figure 2.2, **A** and **B-right**). The changes in the population of **9a** (36.8 ppm), **9b** (37.2 ppm), and the new peak at 23.6 ppm (**9c**) from  $^{31}\text{P}$  NMR analysis matched with those from  $^1\text{H}$  NMR analysis (Figure 2.2, **B** and **C-right**, Figure S2.11). Interestingly, there was a significant upfield shift for this new **9c** peak compared to the carbenes of **9a–b** (23.6 ppm vs 36.8 and 37.2 ppm), and this implied for some changes in the ligand sphere of the Ru complex.

Even though the initiation rate was the slowest with the sodium benzoate additive, the propagation was the fastest as the initial polymerization rate was 23 times faster than using only **G1**, or 4 times faster than utilizing the benzoic acid additive (0.043 vs 0.25 vs 0.98 mM/min, Figure 2.2-**D**). We suspected that this high reactivity was due to the formation of the more active carbene species **9c**. Thus, we carried out several control experiments to identify the origin of this new peak. Initially, we added sodium benzoate to **G1**, but this did not produce any new carbene species, which meant that the benzyldiene **G1** on its own did not react with sodium benzoate at all (Figure S2.13). However, after the *in situ* preparation of the  $\text{DP} > 1$  propagating carbene (**9b**) (the major species resulting from a mixture of **M9**, **G1**, and benzoic acid additive), we added just one equivalent of silver benzoate and five equivalents of tricyclohexylphosphine to promote X-type ligand exchanges

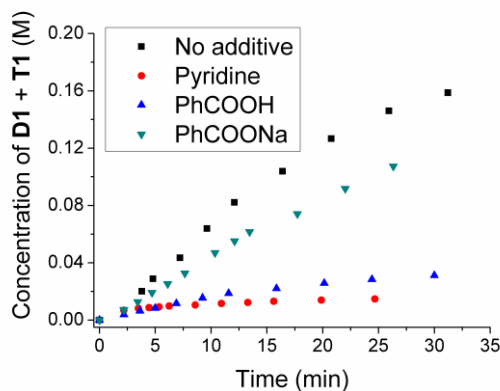
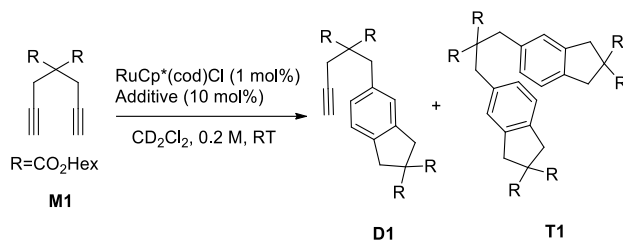


and observed the same new peak appearing at 20.52 ppm (Figure 2.3). Therefore, we identified the new peak as a Ru carbene species containing one chloride ligand and one benzoate ligand each (**9c**). Based on these investigations, we concluded that sodium benzoate enhanced the reactivity of **G1** by partially exchanging one chloride ligand with a benzoate ligand (**9c**), while other benzoate anions stabilized the propagating species (**9b** and **9c**) by weak coordination to suppress carbene decomposition, similar to the role of benzoic acid. Ironically, silver benzoate – a much stronger exchanging reagent compared to sodium benzoate – gave complex mixtures of unstable carbenes, and thus, was a poor additive (Table 2.1, entries 26 and 27, Figure S2.1). However, it is clear that Buchmeiser’s original strategy for activating Hoveyda-Grubbs catalysts by exchanging the chloride ligand with electron-withdrawing acetates<sup>14</sup> certainly worked for the CP of **G1** as well.



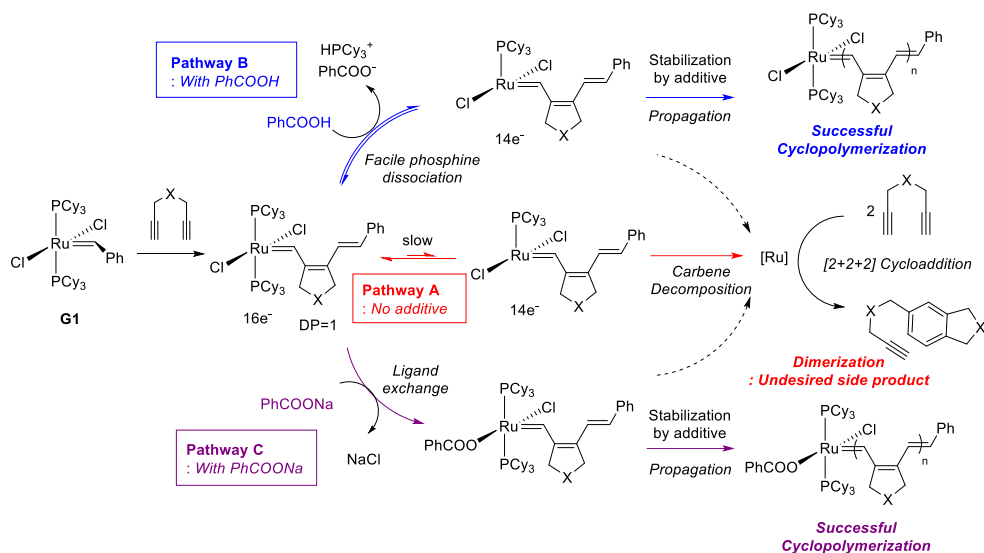
**Figure 2.3.** An exchange reaction of chloride ligand with silver benzoate on the propagating carbene.

Lastly, we investigated how various additives affected the undesired side reaction by testing the same [2+2+2] cycloaddition reaction using another catalyst, RuCp\*(cod)Cl, to produce aromatic dimers (**D1**) and trimers (**T1**) independently (Figure 2.4).<sup>42,43</sup> Without using any additive, 1 mol% of the catalyst rapidly generated **D1** and **T1**, at an initial reaction rate of 6.0 mM/min. Interestingly, adding pyridine to the reaction almost stopped the conversion, presumably because its coordination to RuCp\*(cod)Cl poisoned the catalyst. This agreed with our previous observation that pyridine also suppressed the [2+2+2] cycloaddition during CP catalyzed by **HG2**.<sup>11</sup> Furthermore, benzoic acid also significantly retarded the [2+2+2] cycloaddition catalyzed by RuCp\*(cod)Cl (1.7 mM/min), presumably via a similar mechanism. Adding sodium benzoate also slowed down the reaction by 28%, with an initial rate of 4.3 mM/min. From these results, one could suggest that these additives not only activated and stabilized the propagating carbenes of **G1**, but also suppressed or retarded the [2+2+2] cycloaddition side reaction by poisoning or coordinating to the decomposed **G1**.



**Figure 2.4.** Kinetic profiles of [2+2+2] cycloaddition by RuCp\*(cod)Cl with various additives.

By combining all the data, we could finally reveal a comprehensive picture of how the reactions between **G1** and 1,6-heptadiyne monomers proceeded with and without additive, as summarized in Scheme 2.2. **G1** without additive could form DP = 1 conjugated carbene, but it was difficult for this vinylidene carbene species to undergo further propagation due to slow or inefficient phosphine dissociation. Without any external stabilizing ligands, it inevitably decomposed, and this decomposed Ru complexes predominantly catalyzed the [2+2+2] cycloaddition reaction to produce aromatic products (Scheme 2.2, **Pathway A**). On the other hand, the addition of benzoic acid helped both phosphine dissociation and the initiation of **G1** by protonating the phosphine. More importantly, it also accelerated the formation of the actual propagating carbene from the DP = 1 carbene species, whose phosphine dissociation was very sluggish. Also, benzoic acid suppressed the side reactions by stabilizing the propagating carbene species by weak coordination, as well as by poisoning the decomposed catalyst to hamper the dimerization (**Pathway B**). Interestingly, another excellent additive – sodium benzoate – successfully promoted CP via a different mechanism from that of benzoic acid despite their similar structures. The benzoate anion partially substituted one chloride ligand on **G1**, and this *in situ* formation of the new catalyst afforded a more active catalytic species to facilitate CP. Furthermore, sodium benzoate also seemed to stabilize the propagating species similarly to benzoic acid, thus enhancing the polymerization (**Pathway C**).



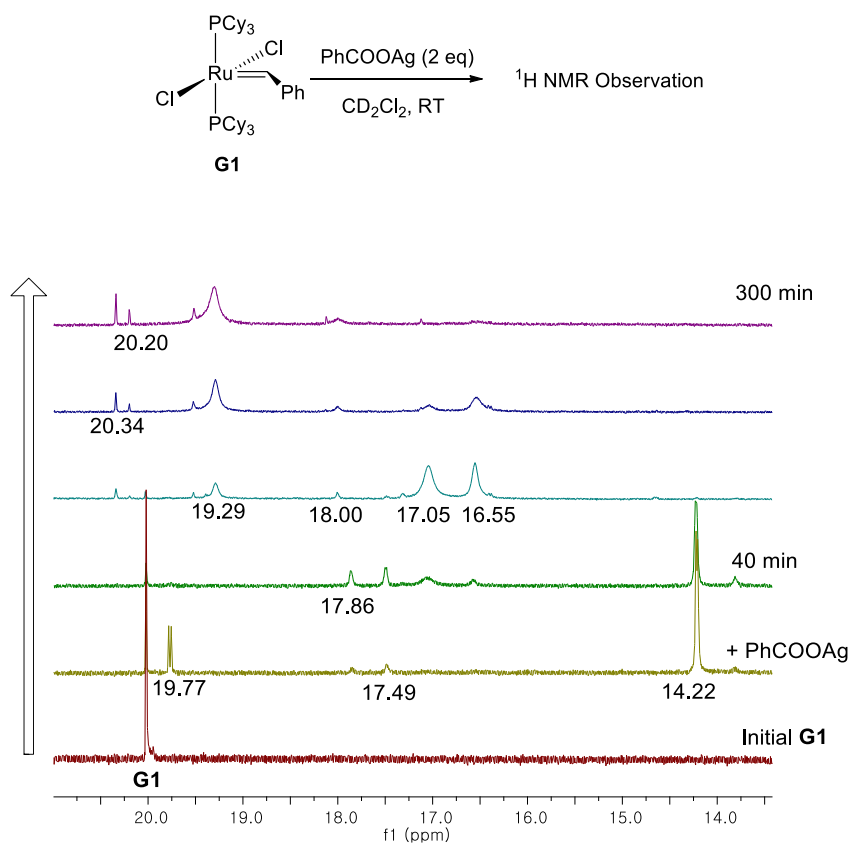
**Scheme 2.2.** Proposed Scheme Showing How the Additives Affect CP Catalyzed by **G1**

## 2.4. Conclusion

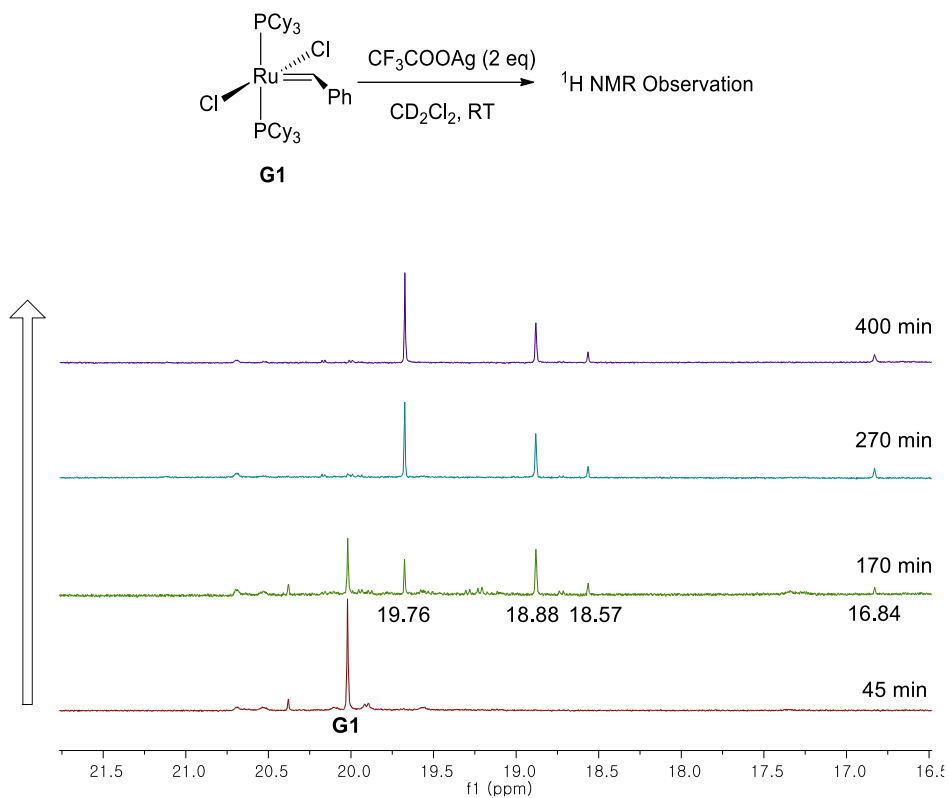
In conclusion, we demonstrated successful cyclopolymerization of 1,6-heptadiyne derivatives by using simple additives to activate **G1**. To achieve successful CP, we attempted three strategies: 1) using phosphine-free catalysts or phosphine trapping agents to activate the catalyst, 2) stabilizing the propagating carbene by adding coordinating ligands, and 3) promoting anionic ligand exchange of **G1**. Through an extensive screening of three different classes of additives, both benzoic acid and sodium benzoate proved to be the best additives to facilitate the polymerization, being compatible with a broad monomer scope and capable of producing various conjugated polyenes with  $M_n$  of up to 23 kDa. Furthermore, detailed mechanistic investigations by kinetic studies and monitoring the changes in the carbene complexes by  $^1\text{H}$  and  $^{31}\text{P}$  NMR analyses revealed how these two additives enhanced the CP efficiency via two different mechanisms. Benzoic acid increased both the initiation and propagation rates by partially trapping phosphine and stabilizing the catalyst via weak coordination, respectively. In contrast, sodium benzoate produced more active propagating carbene species by partially exchanging a chloride ligand with a benzoate ligand, which significantly accelerated CP. Finally, we conducted independent control experiments of [2+2+2] cycloaddition (catalyzed by  $\text{RuCp}^*(\text{cod})\text{Cl}$  with and without additives) and concluded that these additives retarded the side reaction. This also explained why these additives provided a high CP selectivity over the side reaction. In short, these results not only enabled the use of **G1** for efficient CP but also have provided detailed insights to improve our understanding of cyclopolymerization using Grubbs catalysts.

## 2.5. Supporting Figures

### Carbene observation for the mixtures of **G1** and silver salts

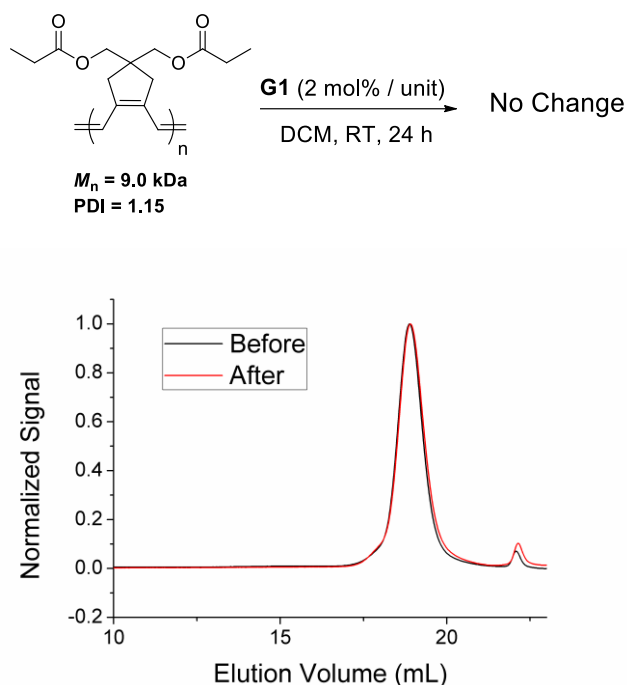


**Figure S2.1.**  $^1\text{H}$  NMR spectra monitoring the carbene change of **G1** with silver benzoate additive.



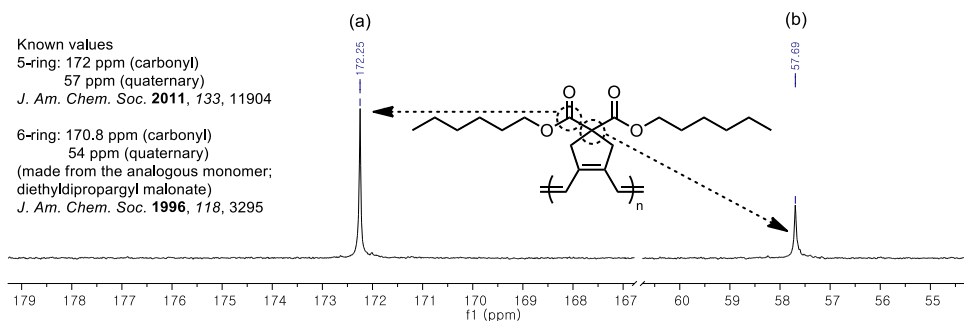
**Figure S2.2.**  $^1\text{H}$  NMR spectra monitoring the carbene change of **G1** with silver trifluoroacetate additive.

## Investigation for the possibility of chain transfer reaction using G1



**Figure S2.3.** Addition of **G1** to a solution of preformed polymer having a low dispersity (synthesized by **G3**).

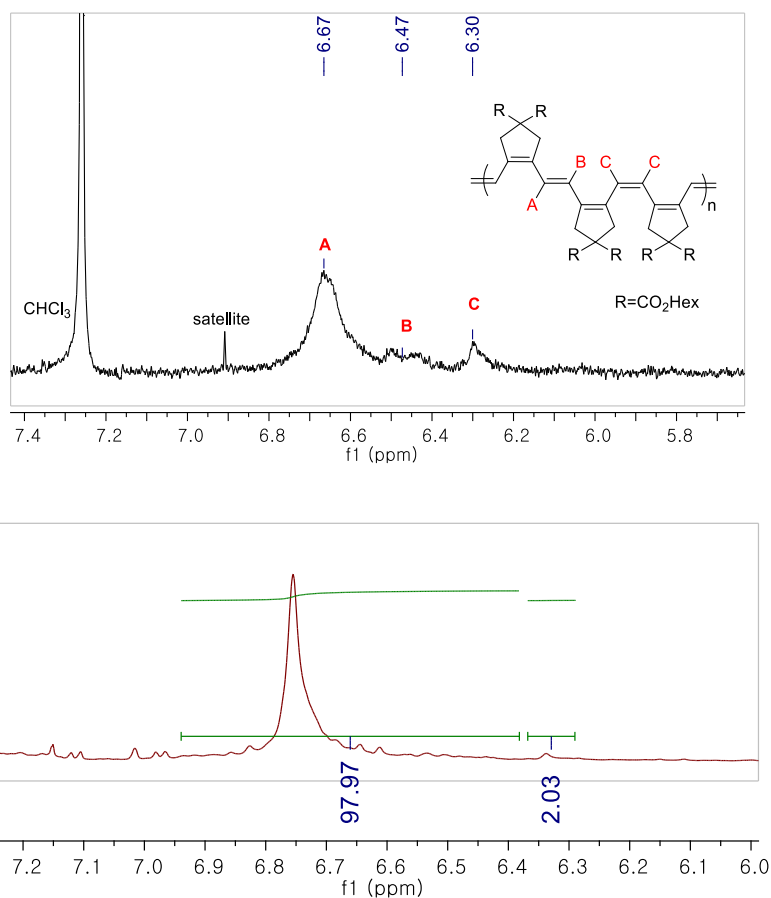
## Ring structure of the polymer synthesized by G1: $^{13}\text{C}$ NMR spectroscopy (in $\text{CDCl}_3$ )



**Figure S2.4.**  $^{13}\text{C}$ -NMR peaks for (a) carbonyl carbon and (b) quaternary carbon of malonate.

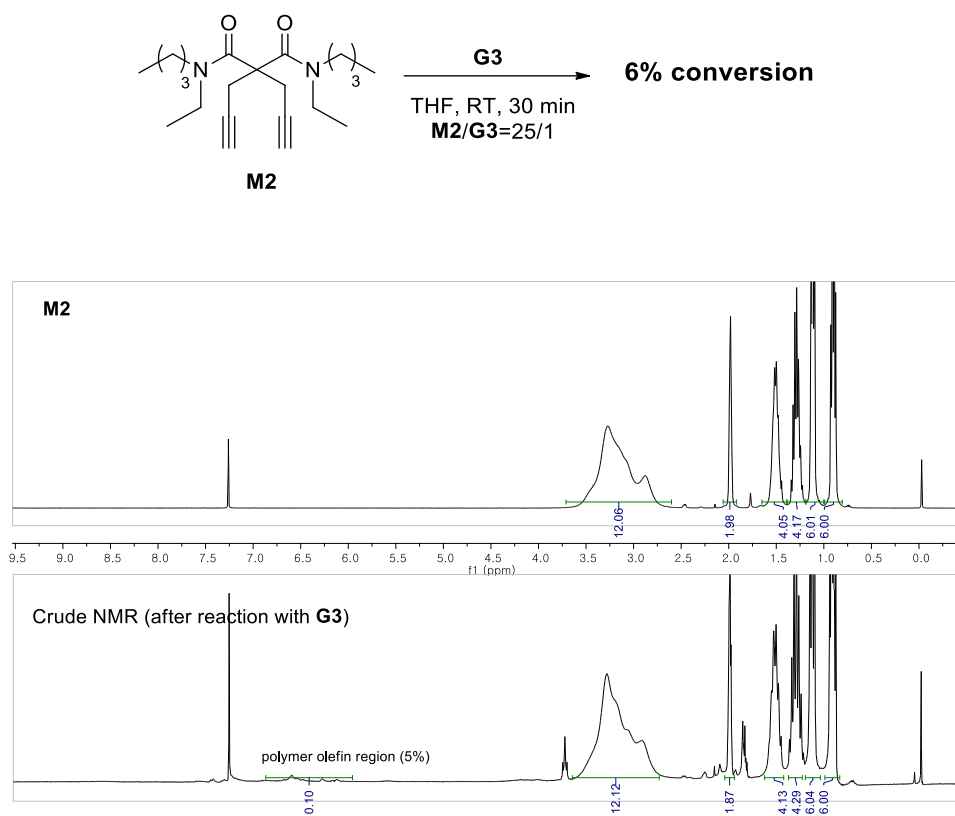


## NMR analysis showing the conformation of olefins in the polymer backbone



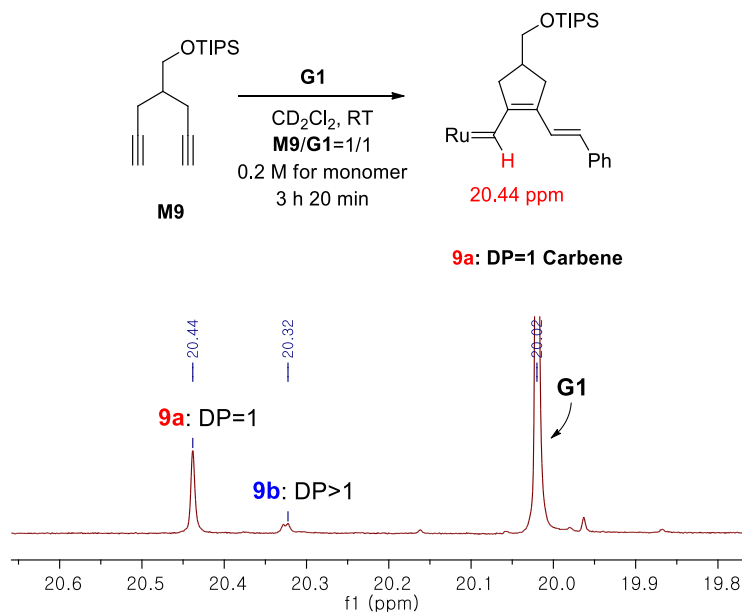
**Figure S2.5.**  $^1\text{H}$  NMR spectra of **P1** synthesized by **G3** (up) and **G1** (down), respectively. The former one shows a mixture of *trans*- and *cis*-olefins (in  $\text{CDCl}_3$ ) while the latter one contains 98% of *trans*-olefin.

### Control experiment showing the inactivity of G3 toward CP of M2

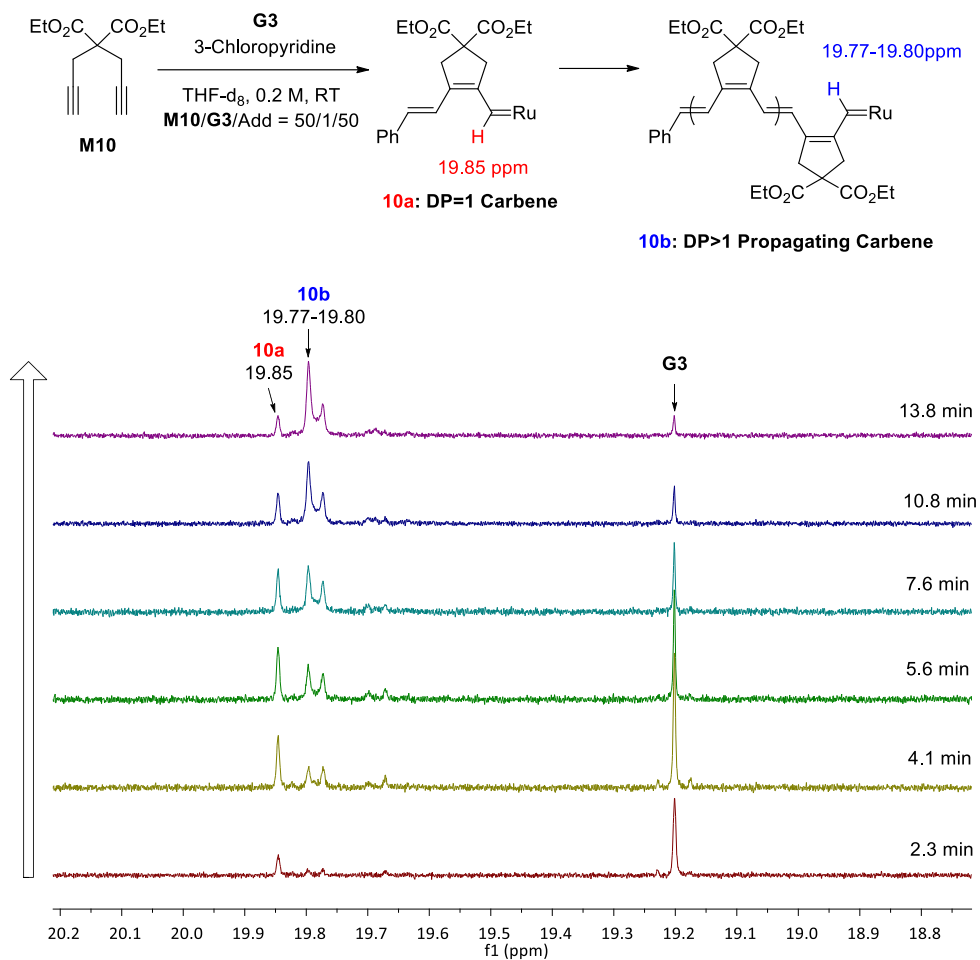


**Figure S2.6.** A crude NMR spectrum ( $^1\text{H}$  NMR, in  $\text{CDCl}_3$ ) after the reaction between **G3** and **M2** in THF.

**Investigation for the new carbenes generated by reaction between monomers and Grubbs catalysts**

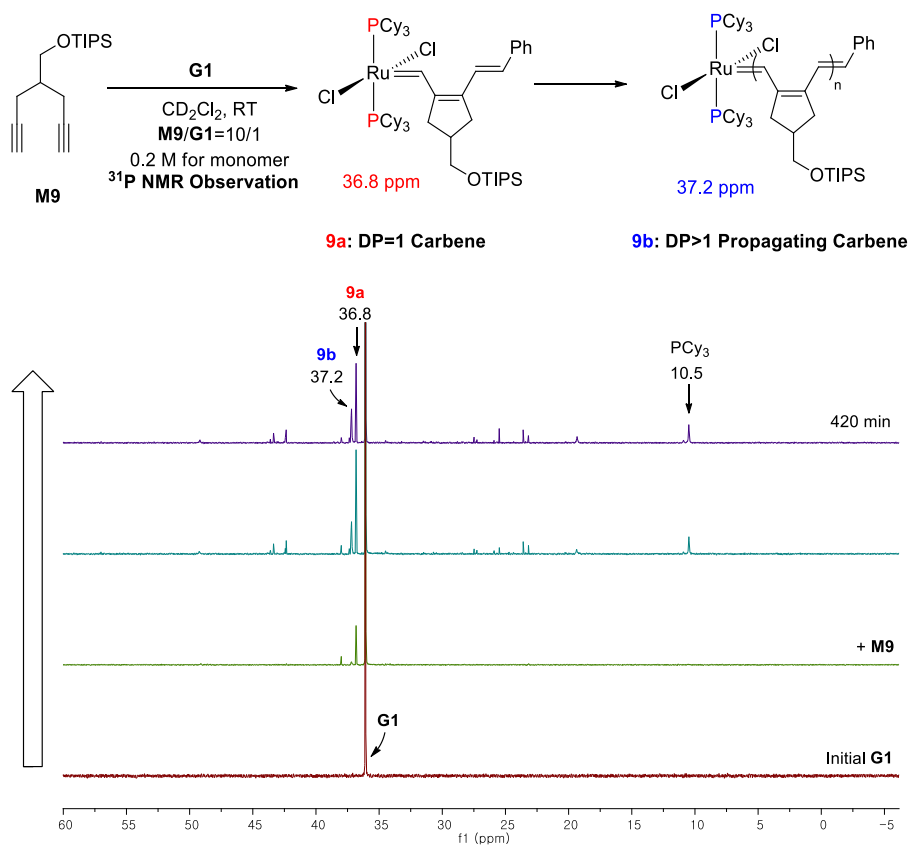


**Figure S2.7.** A  $^1\text{H}$  NMR spectrum from a 1:1 mixture of **G1** and **M9**

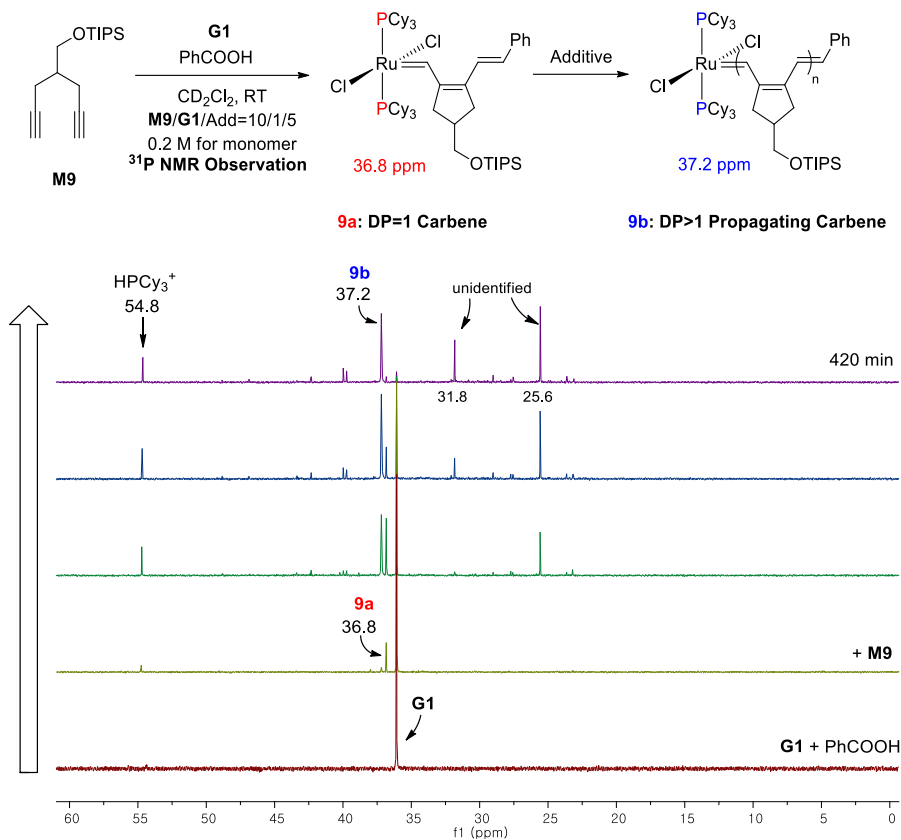


**Figure S2.8.**  $^1\text{H}$  NMR spectra monitoring the generation of new carbenes from **G3**. The carbene peaks having different DPs were separately observed in the early stage of the reaction because the propagation was significantly retarded by the addition of excess pyridine.

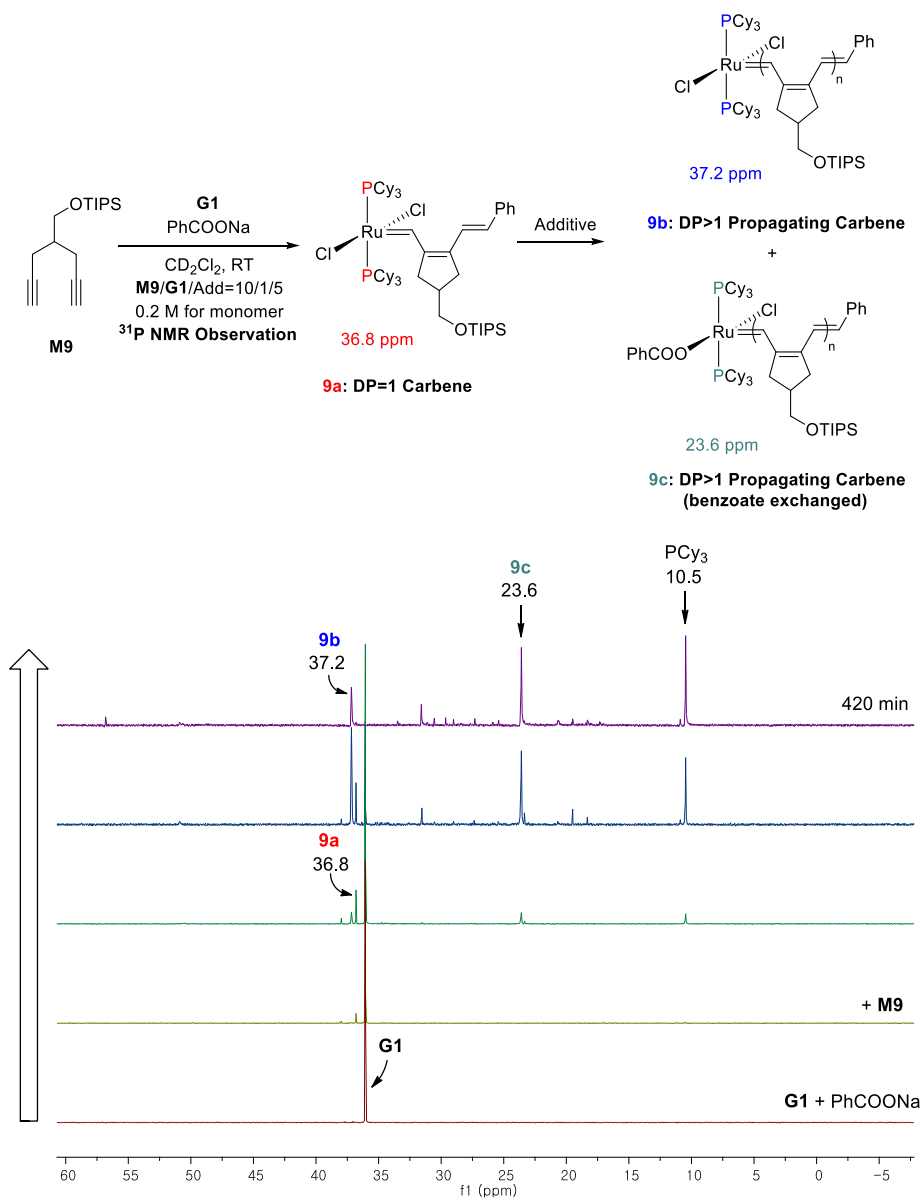
### <sup>31</sup>P NMR spectra monitoring the reaction between G1 and monomer



**Figure S2.9.** <sup>31</sup>P NMR spectra monitoring the reaction between **M9** and **G1** without additive.

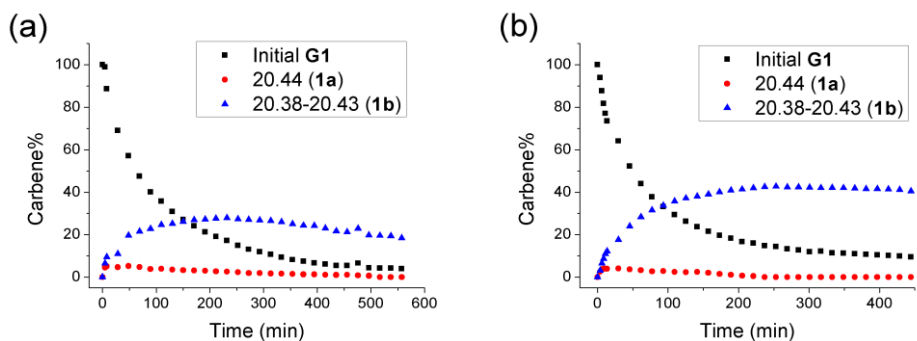
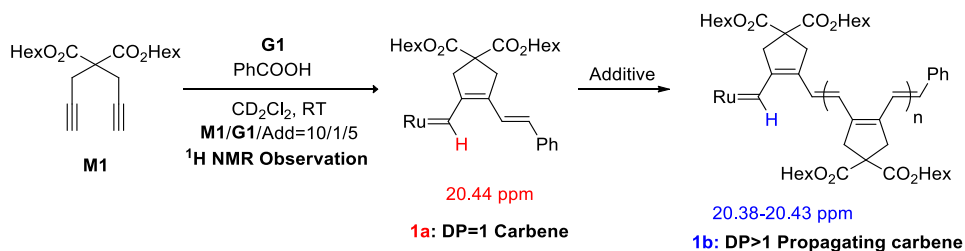


**Figure S2.10.** <sup>31</sup>P NMR spectra monitoring the reaction between **M9** and **G1** with benzoic acid.



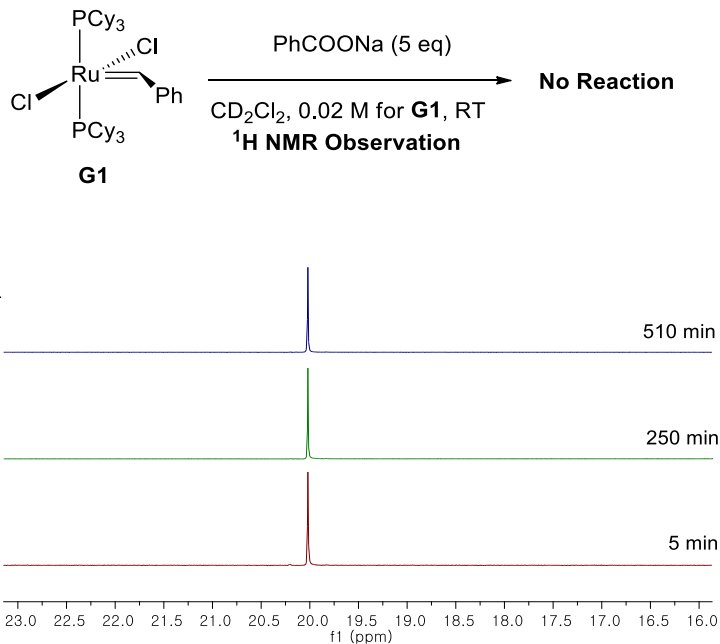
**Figure S2.11.**  $^{31}\text{P}$  NMR spectra monitoring the reaction between **M9** and **G1** with sodium benzoate.

## Effect of concentration to the amount of DP>1 propagating carbene



**Figure S2.12.** Plots of changes for various carbene signals vs time in (a) 0.2 M and (b) 0.6 M.

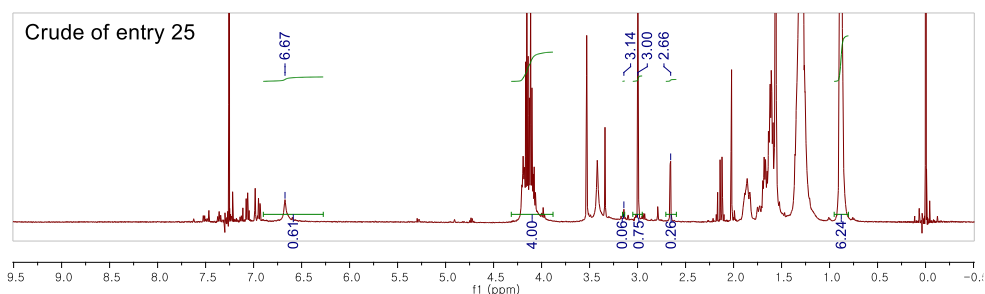
## Reaction between **G1** and sodium benzoate



**Figure S2.13.** <sup>1</sup>H NMR spectra monitoring the carbene change of **G1** with sodium benzoate additive.



## Calculation of conversion, **P1**, **D1**, and **T1**



**Figure S2.14.** An example of calculating conversion and the formations of **P1**, **D1**, and **T1** (Table 2.1, entry 25)

(All the conversion, **P1**, **D1**, and **T1** were calculated from the corresponding integration values in <sup>1</sup>H NMR; conversion from 3.00 ppm (remaining **M1**), **P1** from 6.67 ppm, **D1** from 2.66 ppm, and **T1** from 3.14 ppm. For example, the percentage of **P1** was calculated as [(integration of the olefin conjugated proton at 6.67 ppm)/2]. In general, the sp<sup>2</sup> olefin proton of the conjugated backbone showed varied integration in <sup>1</sup>H NMR spectra of purified polymers (1.7 – 2). Due to this reason, some of the cases in Table 2.1, Table 2.3, and Figure 2.2 showed discrepancies between conversion and **P1** + **D1** + **T1**.)

## 2.6. Experimental Section

### Characterization

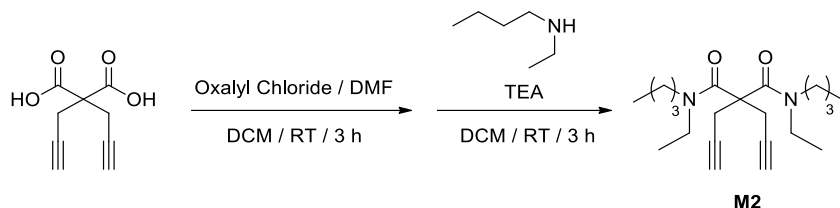
$^1\text{H}$  NMR,  $^{13}\text{C}$  NMR and  $^{31}\text{P}$  NMR were recorded by Varian/Oxford As-500 (500 MHz for  $^1\text{H}$  and 125 MHz for  $^{13}\text{C}$ ), Agilent 400-MR (400 MHz for  $^1\text{H}$ , 100 MHz for  $^{13}\text{C}$ , and 162 MHz for  $^{31}\text{P}$ ) and Bruker DRX-300 (300 MHz for  $^1\text{H}$ , 75 MHz for  $^{13}\text{C}$ ) spectrometers. Size exclusion chromatography (SEC) analyses were carried out with Waters system (1515 pump, 2414 refractive index detector) and Shodex GPC LF-804 column eluted with THF (GPC grade, Honeywell Burdick & Jackson®) and filtered with a 0.2  $\mu\text{m}$  PTFE filter (Whatman®). Flow rate was 1.0 mL/min and temperature of column was maintained at 35 °C.

### Materials

All reagents which are commercially available from Sigma-Aldrich®, Tokyo Chemical Industry Co. Ltd., Acros Organics, Alfa Aesar®, without additional notes, were used without further purification. **M1**,<sup>27</sup> **M3**,<sup>5</sup> **M4**,<sup>27</sup> **M6**,<sup>11</sup> **M7**,<sup>28</sup> **M8**,<sup>44</sup> **M9**<sup>11</sup> and **G1-py**<sub>2</sub><sup>26</sup> were prepared by literature methods. Dichloromethane (DCM) and tetrahydrofuran (THF) for the polymerization were purified by Glass Contour Organic Solvent Purification System, and degassed further by Ar bubbling for 10 minutes before performing reactions. DCM-*d*<sub>2</sub> (99.90% D, 0.75mL) was purchased from Euriso-top® and used without further purification.

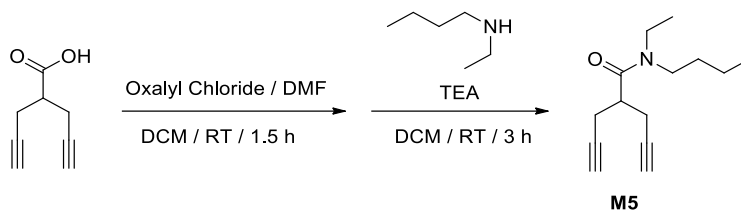
## Experimental procedures for the preparation of monomers

### Synthesis of M2



Dipropargylmalonic acid<sup>45</sup> (271.1 mg, 1.505 mmol) was added to a 25-mL round-bottom flask containing a magnetic stirring bar, and the flask was purged with argon. DCM (10 mL) was added and the mixture was cooled down to 0 °C. A solution of oxalyl chloride (2.0 M in DCM, 2.26 mL, 4.52 mmol) was added, and 10 drops of DMF was added under the control of atmospheric pressure. Generated CO<sub>2</sub> gas was trapped by a balloon. The reaction mixture was stirred for 3 h at room temperature, and concentrated to give yellow colored solid. After this flask was filled with argon, it was re-dissolved in DCM (12 mL) and the solution was cooled to 0 °C. Then, *N*-ethylbutylamine (0.62 mL, 4.52 mmol) and triethylamine (0.63 mL, 4.52 mmol) were added dropwise. After stirring 3 hours at room temperature, the reaction was quenched by saturated NaHCO<sub>3</sub> aqueous solution. The organic layer was washed with water and extracted by ethyl acetate, dried with MgSO<sub>4</sub>, and concentrated. The product was purified by flash column chromatography on silica gel (ethyl acetate:hexane = 1:5) to afford **M2** as white solid (455.0 mg, 1.31 mmol, 87%). <sup>1</sup>H NMR (400 MHz, CDCl<sub>3</sub>) δ 3.27 (br, 12H), 2.02 – 1.94 (m, 2H), 1.62 – 1.41 (m, 4H), 1.38 – 1.19 (m, 4H), 1.16 – 1.07 (m, 6H), 0.95 – 0.85 (m, 6H). <sup>13</sup>C NMR (100 MHz, CDCl<sub>3</sub>) δ 168.74, 79.69, 72.01, 55.93, 47.36, 46.74, 42.10, 30.85, 29.59, 24.88, 20.73, 20.40, 14.12, 13.95, 12.91. HRMS (ESI): *m/z* for C<sub>21</sub>H<sub>34</sub>N<sub>2</sub>NaO<sub>2</sub> [M+Na]<sup>+</sup>, calcd. 369.2512, found: 369.2514

## Synthesis of M5



4-Carboxy-1,6-heptadiyne<sup>45</sup> (238.2 mg, 1.75 mmol) was added to a 25-mL round-bottom flask containing a magnetic stirring bar, and the flask was purged with argon. DCM (5 mL) was added and the mixture was cooled down to 0 °C. A solution of oxalyl chloride (2.0 M in DCM, 1.31 mL, 2.63 mmol) was added, and 8 drops of DMF was added under the control of atmospheric pressure. Generated CO<sub>2</sub> gas was trapped by a balloon. The reaction mixture was stirred for 1.5 h at room temperature, and concentrated to give yellow colored liquid. After this flask was filled with argon, it was re-dissolved in DCM (5 mL) and the solution was cooled to 0 °C. Then, *N*-ethylbutylamine (0.36 mL, 2.63 mmol) and triethylamine (0.21 mL, 2.63 mmol) were added dropwise. After stirring 3 hours at room temperature, the reaction was quenched by saturated NaHCO<sub>3</sub> aqueous solution. The organic layer was washed with water and extracted by ethyl acetate, dried with MgSO<sub>4</sub>, and concentrated. The product was purified by flash column chromatography on silica gel (ethyl acetate:hexane = 1:5) to afford **M5** as colorless liquid (293.8 mg, 1.34 mmol, 77%). <sup>1</sup>H NMR (500 MHz, CDCl<sub>3</sub>) δ 3.47 – 3.38 (m, 2H), 3.34 (dd, *J* = 15.2, 7.0 Hz, 2H), 3.09 – 3.00 (m, 1H), 2.55 – 2.42 (m, 4H), 1.98 (t, *J* = 2.6 Hz, 2H), 1.65 – 1.47 (m, 2H), 1.40 – 1.27 (m, 2H), 1.17 (dt, *J* = 56.0, 7.1 Hz, 3H), 0.93 (dt, *J* = 22.6, 7.4 Hz, 3H). <sup>13</sup>C NMR (125 MHz, CDCl<sub>3</sub>) δ 172.41, 81.81, 70.37, 47.96, 46.18, 43.00, 41.75, 40.19, 39.98, 32.24, 30.31, 22.23, 20.53, 15.24, 14.18, 13.24. HRMS (ESI): *m/z* for C<sub>14</sub>H<sub>21</sub>NNaO [M+Na]<sup>+</sup>, calcd. 242.1515, found: 242.1516

## General procedure for cyclopolymerization

Catalyst, additive and a magnetic bar were added to a 4-mL vial with a cap containing PTFE-silicon septum. Dry solvent was added after the vial was purged with argon three times, and the solution of monomer (0.1 mmol) prepared from inert atmosphere was rapidly injected at room temperature. The reaction was quenched by excess ethyl vinyl ether (0.2 mL) after desired reaction time, and dried under vacuum. The ratio of products was calculated from the crude  $^1\text{H}$  NMR spectrum, then, the mixture was precipitated in methanol (10 mL). The polymer was filtered, and the dimer was purified from the filtrate by flash column chromatography on silica gel.

## Procedure of general *in situ* NMR experiments

**Method A:** Monitoring a reaction between catalyst and additive (without monomer).

A 4-mL vial was filled with catalyst, purged by argon, and hexamethyl disilane was added as an internal standard. An NMR tube containing additive was purged with argon and dissolved by deuterated solvent. The 4-mL vial containing the catalyst was dissolved by deuterated solvent and a partial amount of the catalyst solution was diluted to measure NMR for checking the ratio between initial carbene and the internal standard. The rest of the catalyst solution was added to the NMR tube containing additive solution and NMR measurement was recorded over time.

**Method B:** Monitoring a reaction between monomer and catalyst with and without additive.

A 4-mL vial was filled with catalyst, purged with argon, and hexamethyl disilane

was added as an internal standard. Monomer was added to another 4-mL vial, purged by argon, and dissolved by deuterated solvent. An NMR tube containing additive was purged with argon and dissolved by deuterated solvent. The catalyst in the 4-mL vial was dissolved by deuterated solvent, and a partial amount of the solution was diluted to measure NMR for checking the ratio between initial carbene and the internal standard. The rest of the catalyst solution was added to the NMR tube containing additive solution, followed by NMR measurement. After that, the monomer solution was injected to the NMR tube and NMR measurement was recorded over time.

### **$^1\text{H}$ and $^{13}\text{C}$ NMR characterization of polymers and dimers**

The spectroscopic data of **P1**,<sup>27</sup> **P3**,<sup>5</sup> **P4**,<sup>27</sup> **P6**,<sup>11</sup> **P7**,<sup>28</sup> and **P9**<sup>11</sup> were reported in the literature.

**P2**  $^1\text{H}$  NMR (500 MHz,  $\text{CDCl}_3$ )  $\delta$  6.90 – 6.07 (br, 2H), 4.67 – 2.23 (br, 12H), 1.67 – 1.45 (br, 4H), 1.38 – 1.23 (br, 4H), 1.20 – 1.02 (br, 6H), 0.99 – 0.85 (br, 6H).  $^{13}\text{C}$  NMR (75 MHz,  $\text{CDCl}_3$ )  $\delta$  172.09, 136.56, 123.21, 57.19, 47.38, 46.14, 43.49, 41.99, 30.70, 29.53, 20.74, 14.10, 13.43.

**P5**  $^1\text{H}$  NMR (400 MHz,  $\text{CDCl}_3$ )  $\delta$  7.01 – 5.94 (br, 2H), 3.40 (br, 5H), 3.14 – 2.38 (br, 4H), 1.57 (br, 2H), 1.34 (br, 2H), 1.01 (br, 6H).  $^{13}\text{C}$  NMR (100 MHz,  $\text{CDCl}_3$ )  $\delta$  174.80, 138.59, 123.39, 53.75, 48.01, 46.11, 41.50, 38.50, 32.23, 30.46, 29.98, 20.66, 15.21, 14.21, 13.50.

**P8**  $^1\text{H}$  NMR (500 MHz,  $\text{CDCl}_3$ )  $\delta$  6.72 (br, 2H), 3.56 (br, 2H), 2.67 (br, 4H), 0.93 (br, 9H), 0.08 (br, 6H).  $^{13}\text{C}$  NMR (125 MHz,  $\text{CDCl}_3$ )  $\delta$  139.33, 123.35, 67.46, 38.26, 36.75, 26.38, 18.82, -4.82.

The spectroscopic data of **D1**,<sup>11</sup> **D3**,<sup>5</sup> **D6**,<sup>11</sup> and **T1**<sup>11</sup> were reported in the literature.

**D2** <sup>1</sup>H NMR (400 MHz, CDCl<sub>3</sub>) δ 6.99 (d, *J* = 7.6 Hz, 1H), 6.91 (s, 1H), 6.86 (d, *J* = 7.6 Hz, 1H), 5.05 – 2.22 (m, 24H), 2.13 – 2.04 (m, 1H), 1.72 – 1.38 (m, 8H), 1.38 – 1.22 (m, 8H), 1.22 – 1.00 (m, 12H), 0.99 – 0.78 (m, 12H). <sup>13</sup>C NMR (100 MHz, CDCl<sub>3</sub>) δ 172.03, 169.83, 140.38, 139.16, 134.80, 134.40, 129.22, 126.25, 123.70, 80.81, 72.13, 60.29, 56.86, 47.89, 46.96, 45.98, 42.52, 41.61, 39.07, 30.71, 29.85, 29.49, 24.08, 20.69, 14.25, 12.73. HRMS (ESI): *m/z* for C<sub>42</sub>H<sub>68</sub>N<sub>4</sub>NaO<sub>4</sub> [M+Na]<sup>+</sup>, calcd. 715.5133, found: 715.5132.

**D4** <sup>1</sup>H NMR (500 MHz, CDCl<sub>3</sub>) δ 7.07 (d, *J* = 7.6 Hz, 1H), 6.99 (s, 1H), 6.97 (d, *J* = 7.7 Hz, 1H), 4.09 (s, 4H), 3.98 (dd, *J* = 32.3, 11.1 Hz, 4H), 2.85 (d, *J* = 4.2 Hz, 4H), 2.75 (s, 2H), 2.35 (dq, *J* = 15.2, 7.6 Hz, 8H), 2.18 (d, *J* = 2.6 Hz, 2H), 2.12 (t, *J* = 2.6 Hz, 1H), 1.16 (t, *J* = 7.6 Hz, 6H), 1.13 (t, *J* = 7.6 Hz, 6H). <sup>13</sup>C NMR (125 MHz, CDCl<sub>3</sub>) δ 174.64, 174.25, 141.61, 139.91, 134.57, 129.27, 127.06, 125.08, 80.12, 72.29, 67.06, 65.23, 47.06, 41.46, 39.21, 38.89, 37.26, 27.91, 22.23, 9.47. HRMS (ESI): *m/z* for C<sub>30</sub>H<sub>40</sub>NaO<sub>8</sub> [M+Na]<sup>+</sup>, calcd. 551.2615, found: 551.2613.

**D5** <sup>1</sup>H NMR (300 MHz, CDCl<sub>3</sub>) δ 7.09 (t, *J* = 7.4 Hz, 1H), 7.05 – 6.91 (m, 2H), 3.61 – 3.21 (m, 8H), 3.21 – 2.74 (m, 8H), 2.65 – 2.30 (m, 2H), 1.99 (t, *J* = 2.5 Hz, 1H), 1.72 – 1.46 (m, 4H), 1.41 – 1.29 (m, 4H), 1.27 – 0.81 (m, 12H). <sup>13</sup>C NMR (75 MHz, CDCl<sub>3</sub>) δ 174.21, 173.31, 142.57, 140.57, 137.75, 127.62, 125.18, 124.35, 82.82, 69.93, 47.77, 45.76, 43.69, 42.47, 41.23, 39.27, 37.42, 32.18, 30.37, 20.62, 15.17, 14.26, 13.36. HRMS (ESI): *m/z* for C<sub>28</sub>H<sub>42</sub>N<sub>2</sub>NaO<sub>2</sub> [M+Na]<sup>+</sup>, calcd. 461.3138, found: 461.3140.

**D7** <sup>1</sup>H NMR (500 MHz, CDCl<sub>3</sub>) δ 7.11 (d, *J* = 7.6 Hz, 1H), 7.02 (s, 1H), 6.96 (d, *J* = 7.6 Hz, 1H), 4.18 – 4.01 (m, 4H), 3.04 (dd, *J* = 15.7, 8.0 Hz, 2H), 2.88 – 2.77 (m, 1H), 2.75 – 2.63 (m, 4H), 2.34 – 2.19 (m, 4H), 2.18 – 2.11 (m, 1H), 2.02 (t, *J* = 2.4 Hz, 1H), 1.68 – 1.59 (m, 4H), 1.56 – 1.41 (m, 4H), 1.35 – 1.22 (m, 8H), 0.94 – 0.86 (m, 12H). <sup>13</sup>C NMR (125 MHz, CDCl<sub>3</sub>) δ 176.82, 176.63, 143.11, 140.78, 137.67,

127.66, 125.64, 124.85, 81.85, 70.69, 67.59, 65.47, 47.78, 39.23, 38.86, 36.61, 36.29, 36.00, 32.15, 30.01, 25.85, 22.97, 20.23, 14.31, 12.25. HRMS (ESI):  $m/z$  for  $C_{32}H_{48}NaO_4$   $[M+Na]^+$ , calcd. 519.3445, found: 519.3444.

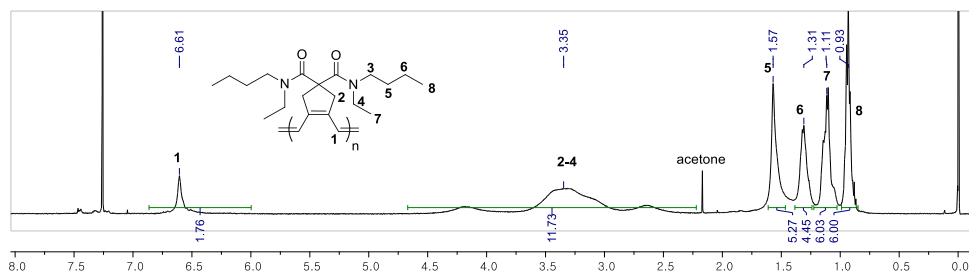
**D8**  $^1H$  NMR (300 MHz,  $CDCl_3$ )  $\delta$  7.09 (d,  $J = 7.6$  Hz, 1H), 7.02 (s, 1H), 6.95 (d,  $J = 7.6$  Hz, 1H), 3.72 – 3.45 (m, 4H), 2.97 (dd,  $J = 16.8, 8.9$  Hz, 2H), 2.81 – 2.52 (m, 5H), 2.31 – 2.11 (m, 2H), 1.98 (t,  $J = 2.6$  Hz, 1H), 1.96 – 1.85 (m, 1H), 0.90 (d,  $J = 3.9$  Hz, 18H), 0.05 (s, 12H).  $^{13}C$  NMR (75 MHz,  $CDCl_3$ )  $\delta$  143.58, 141.05, 138.43, 127.44, 125.78, 124.64, 83.31, 69.83, 66.94, 64.12, 42.56, 35.96, 30.06, 26.30, 18.71, -4.93. HRMS (ESI):  $m/z$  for  $C_{28}H_{48}NaO_2Si_2$   $[M+Na]^+$ , calcd. 495.3083, found: 495.3083.

**D9**  $^1H$  NMR (500 MHz,  $CDCl_3$ )  $\delta$  7.09 (d,  $J = 7.6$  Hz, 1H), 7.04 (s, 1H), 6.95 (d,  $J = 7.6$  Hz, 1H), 3.73 – 3.63 (m, 4H), 3.01 – 2.91 (m, 2H), 2.78 – 2.66 (m, 4H), 2.63 (dd,  $J = 13.5, 7.7$  Hz, 1H), 2.31 – 2.19 (m, 2H), 1.97 (t,  $J = 2.6$  Hz, 1H), 2.00 – 1.91 (m, 1H), 1.13 – 1.01 (m, 42H).  $^{13}C$  NMR (125 MHz,  $CDCl_3$ )  $\delta$  143.67, 141.13, 138.44, 127.43, 125.84, 124.64, 83.49, 69.79, 67.16, 64.68, 43.03, 42.55, 36.52, 36.00, 35.70, 19.98, 18.41, 12.44. HRMS (ESI):  $m/z$  for  $C_{34}H_{60}NaO_2Si_2$   $[M+Na]^+$ , calcd. 579.4024, found: 579.4022.

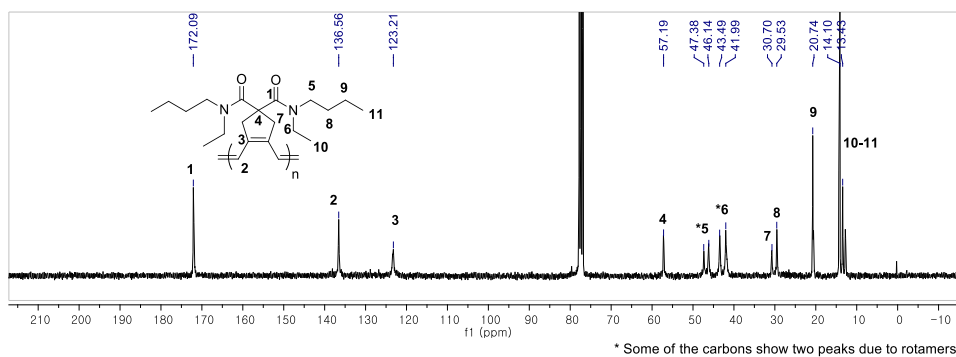


# $^1\text{H}$ and $^{13}\text{C}$ NMR Spectra of polymers

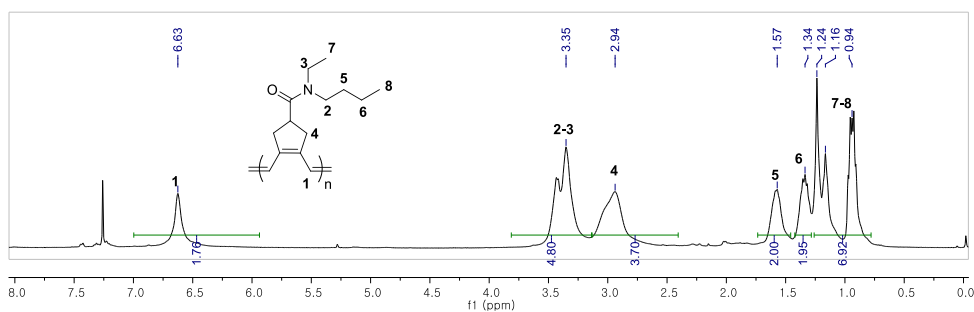
## P2 ( $^1\text{H}$ NMR, $\text{CDCl}_3$ )



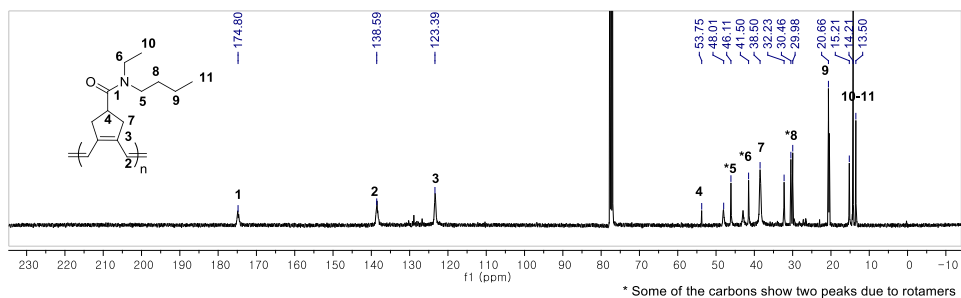
## P2 ( $^{13}\text{C}$ NMR, $\text{CDCl}_3$ )



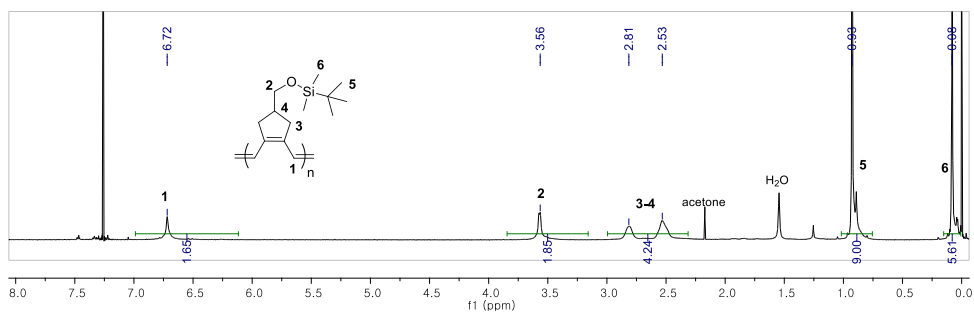
## P5 ( $^1\text{H}$ NMR, $\text{CDCl}_3$ )



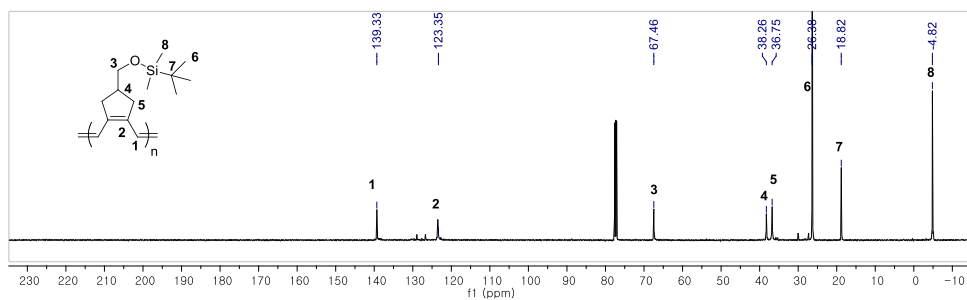
**P5** ( $^{13}\text{C}$  NMR,  $\text{CDCl}_3$ )



**P8** ( $^1\text{H}$  NMR,  $\text{CDCl}_3$ )



**P8** ( $^{13}\text{C}$  NMR,  $\text{CDCl}_3$ )



## 2.7. References

† This chapter was previously reported: Kang, C.; Kang, E. H.; Choi, T. L. *Macromolecules*, **2017**, *50*, 3153-3163.

- (1) Krause, J. O.; Zarka, M. T.; Anders, U.; Weberskirch, R.; Nuyken, O.; Buchmeiser, M. R. *Angew. Chem., Int. Ed.* **2003**, *42*, 5965–5969.
- (2) Krause, J. O.; Nuyken, O.; Buchmeiser, M. R. *Chem. - Eur. J.* **2004**, *10*, 2029–2035.
- (3) Kumar, P. S.; Wurst, K.; Buchmeiser, M. R. *J. Am. Chem. Soc.* **2009**, *131*, 387–395.
- (4) Buchmeiser, M. R.; Schmidt, C.; Wang, D. *Macromol. Chem. Phys.* **2011**, *212*, 1999–2008.
- (5) Sudheendran, M.; Horecha, M.; Kiriy, A.; Gevorgyan, S. A.; Krebs, F. C.; Buchmeiser, M. R. *Polym. Chem.* **2013**, *4*, 1590–1599.
- (6) Peters, J.-U.; Blechert, S. *Chem. Commun.* **1997**, 1983–1984.
- (7) Witulski, B.; Stengel, T.; Fernández-Hernández, J. M. *Chem. Commun.* **2000**, 1965–1966.
- (8) Medina, S.; Domínguez, G.; Pérez-Castells, J. *J. Org. Lett.* **2012**, *14*, 4982–4985.
- (9) Alvarez, S.; Medina, S.; Domínguez, G.; Pérez-Castells, J. *J. Org. Chem.* **2013**, *78*, 9995–10001.
- (10) Alvarez, S.; Medina, S.; Domínguez, G.; Pérez-Castells, J. *J. Org. Chem.* **2015**, *80*, 2436–2442.
- (11) Kang, E. H.; Kang, C.; Yang, S.; Oks, E.; Choi, T. L. *Macromolecules* **2016**, *49*, 6240–6250.
- (12) Grubbs, R. H. *Handbook of Metathesis*, 2nd ed., Vols. 2, 3; Wiley-VCH: Weinheim, 2015.
- (13) Grela, K. *Olefin Metathesis: Theory and Practice*. Wiley-VCH: Weinheim, 2014.
- (14) Poulsen, C. S.; Madsen, R. *Synthesis* **2003**, *1*, 1-18.

- (15) Diver, S. T.; Giessert, A. J. *Chem. Rev.* **2004**, *104*, 1317.
- (16) Dias, E. L.; Nguyen, S. T.; Grubbs, R. H. *J. Am. Chem. Soc.* **1997**, *119*, 3887-3897.
- (17) Sanford, M. S.; Henling, L. M.; Grubbs, R. H. *Organometallics*, **1998**, *17*, 5384-5389.
- (18) Lynn, D. M.; Mohr, B.; Grubbs, R. H. *J. Am. Chem. Soc.* **1998**, *120*, 1627-1628.
- (19) Lynn, D. M.; Mohr, B.; Grubbs, R. H.; Henling, L. M.; Day, M. W. *J. Am. Chem. Soc.* **2000**, *122*, 6601-6609.
- (20) Gallivan, J. P.; Jordan, J. P.; Grubbs, R. H. *Tetrahedron Lett.* **2005**, *46*, 2577-2580.
- (21) Forman, G. S.; McConnell, A. E.; Tooze, R. P.; Janse van Rensburg, W.; Meyer, W. H.; Kirk, M. M.; Dwyer, C. L.; Serfontein, D. W. *Organometallics* **2005**, *24*, 4528-4542.
- (22) Ledoux, N.; Allaert, B.; Schaubroeck, D.; Monsaert, S.; Drozdak, R.; Van Der Voort, P.; Verpoort, F. *J. Organomet. Chem.* **2006**, *691*, 5482-5486.
- (23) Meyer, W. H.; McConnell, A. E.; Forman, G. S.; Dwyer, C. L.; Kirk, M. M.; Ngidi, E. L.; Blignaut, A.; Saku, D.; Slawin, A. M. *Inorganica chimica acta* **2006**, *359*, 2910-2917.
- (24) Simocko, C.; Wagener, K. B. *Organometallics* **2013**, *32*, 2513-2516.
- (25) Kingsbury, J. S.; Harrity, J. P. A.; Bonitatebus, P. J.; Hoveyda, A. H. *J. Am. Chem. Soc.* **1999**, *121*, 791.
- (26) Trnka, T. M.; Dias, E. L.; Day, M. W.; Grubbs, R. H. *Arkivoc* **2002**, *13*, 28-41.
- (27) Kang, E.-H.; Lee, I. S.; Choi, T.-L. *J. Am. Chem. Soc.* **2011**, *133*, 11904-11907.
- (28) Kang, E.-H.; Yu, S. Y.; Lee, I. S.; Park, S. E.; Choi, T.-L. *J. Am. Chem. Soc.* **2014**, *136*, 10508-10514.
- (29) Kang, E.-H.; Lee, I.-H.; Choi, T.-L. *ACS Macro Lett.* **2012**, *1*, 1098-1102.
- (30) Wu, Z.; Nguyen, S. T.; Grubbs, R. H.; Ziller, J. W. *J. Am. Chem. Soc.* **1995**,

117, 5503-5511.

- (31) Chang, S.; Jones, L.; Wang, C.; Henling, L. M.; Grubbs, R. H. *SOrganometallics* **1998**, *17*, 3460-3465.
- (32) Buchowicz, W.; Mol, J. C.; Lutz, M.; Spek, A. L. *J. Organomet. Chem.* **1999**, *588*, 205-210.
- (33) Sanford, M. S.; Henling, L. M.; Day, M. W.; Grubbs, R. H. *Angew. Chem., Int. Ed.* **2000**, *39*, 3451-3453.
- (34) Buchowicz, W.; Ingold, F.; Mol, J. C.; Lutz, M.; Spek, A. L. *Chem. Eur. J.* **2001**, *7*, 2842-2847.
- (35) Nieczypor, P.; Buchowicz, W.; Meester, W. J.; Rutjes, F. P.; Mol, J. C. *Tetrahedron Lett.* **2001**, *42*, 7103-7105.
- (36) Conrad, J. C.; Amoroso, D.; Czechura, P.; Yap, G. P.; Fogg, D. E. *Organometallics* **2003**, *22*, 3634-3636.
- (37) Vehlow, K.; Maechling, S.; Köhler, K.; Blechert, S. *J. Organomet. Chem.* **2006**, *691*, 5267-5277.
- (38) Buchowicz, W.; Makal, A.; Woźniak, K. *J. Organomet. Chem.* **2009**, *694*, 3179-3183.
- (39) Kang, E.-H.; Choi, T.-L. *ACS Macro Lett.* **2013**, *2*, 780-784.
- (40) It seems that even DP=2 and DP > 2 carbene peaks are observed separately since this broad peak contains two distinct peaks. As shown in Figure 2A-middle, the peak at 20.32 ppm disappears and 20.29 ppm increases as polymerization proceeds implying that those two peaks would be DP=2 and DP>2 carbenes respectively.
- (41) Schwab, P.; France, M. B.; Ziller, J. W.; Grubbs, R. H. *Angew. Chem., Int. Ed. Engl.* **1995**, *34*, 2039-2041.
- (42) Kirchner, K.; Calhorda, M. J.; Schmid, R.; Veiros, L. F. *J. Am. Chem. Soc.* **2003**, *125*, 11721-11729.
- (43) Yamamoto, Y.; Arakawa, T.; Ogawa, R.; Itoh, K. *J. Am. Chem. Soc.* **2003**, *125*, 12143-12160.

- (44) Wang, X.; Chakrapani, H.; Madine, J. W.; Keyerleber, M. A.; Widenhoefer, R. *A.J. Org. Chem.* **2002**, 67, 2778-2788.
- (45) Atkinson, R. S.; Grimshire, M. J. *J. Chem. Soc. Perkin Trans. 1* **1986**, 1215-1224.

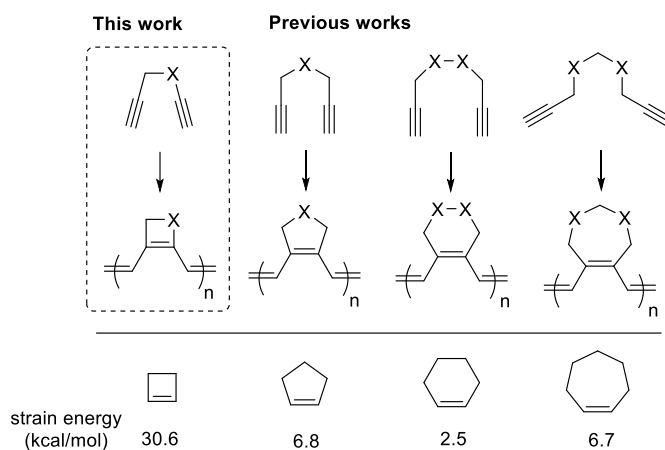
## Chapter 3. Controlled Cyclopolymerization of 1,5-Hexadiynes Involving Four-membered Ring-Forming Cyclization

### 3.1. Abstract

For decades, cyclopolymerization of  $\alpha,\omega$ -diynes has proven to be an effective method to synthesize various substituted polyacetylenes containing five- to seven-membered rings in the backbone. However, cyclopolymerization forming four-membered carbocycles was considered impossible due to their exceptionally high ring strain. In this chapter, we demonstrate the successful cyclopolymerization of rationally designed 1,5-hexadiyne derivatives to give polyacetylenes containing cyclobutene rings in each repeat unit. By using Ru catalysts containing bulky diisopropylphenyl groups, challenging four-membered ring-forming cyclization proceeded efficiently from various monomers, enabling the synthesis of high molecular weight polymers in a controlled manner and block copolymers as well. These new polymers unexpectedly showed narrow band-gaps, which was supported by computational studies showing that their small bond length alternation in the conjugated backbone resulted in highly delocalized  $\pi$ -electrons along the polymer chain.

### 3.2. Introduction

Cyclopolymerization (CP) of  $\alpha,\omega$ -diyne derivatives is a powerful tool for preparing various substituted polyacetylenes.<sup>1-3</sup> While extensive studies were mainly conducted using 1,6-heptadiyne monomers, which gave five- or six-membered rings in the conjugated backbone via  $\alpha$ -<sup>4-7</sup> or  $\beta$ -addition,<sup>8-11</sup> respectively, recent studies expanded the scope of CP where 1,7-octadiyne<sup>12-18</sup> and 1,8-nonadiyne derivatives<sup>19</sup> successfully produced polyacetylenes containing six- and seven-membered rings, respectively (Scheme 3.1). However, cyclization to form four-membered ring is far more challenging due to high strain energy of cyclobutenes (30.6 kcal/mol),<sup>20</sup> making them rather excellent monomers for ring-opening metathesis polymerization (ROMP)<sup>21-23</sup> or tandem ring-opening/cross-metathesis reactions.<sup>24-28</sup>



**Scheme 3.1.** Cyclopolymerization of  $\alpha,\omega$ -Diynes and the Strain Energies of Cycloalkenes

Then, we were intrigued by the reports on CP of 1,2-diethynyldisilane derivatives, which produced random copolymers containing both four- and five-membered rings due to the lack of regioselectivity of W and Mo catalysts.<sup>29-31</sup> Furthermore, Campagne *et al.* prepared challenging cyclobutenes by 1,5-enyne ring-closing metathesis reaction using the Hoveyda-Grubbs catalyst in high



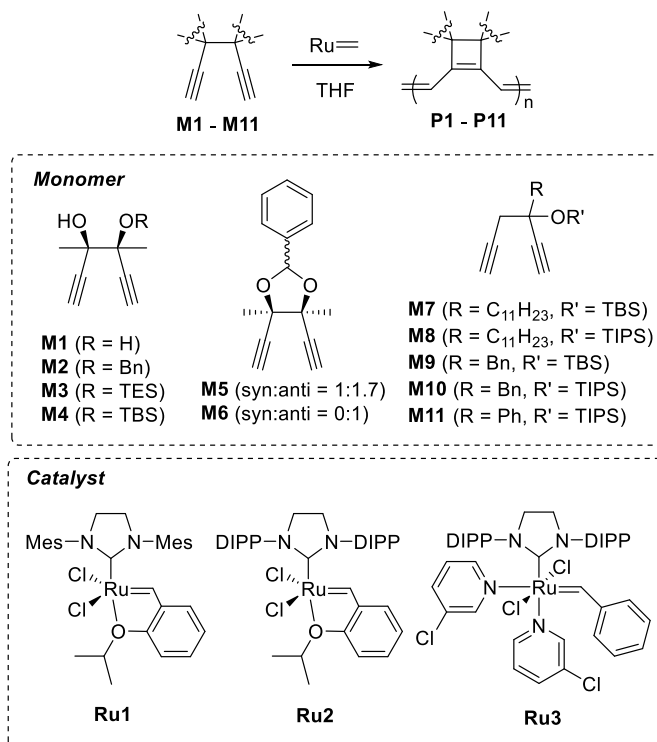
dilution to prevent cross-metathesis, although the max turnover number was less than five even under microwave condition.<sup>32</sup> Inspired by these works, we envisioned that CP of properly designed 1,5-hexadiyne derivatives would be possible to give more planar poly(cyclobutenylene vinylene)s, where the conjugated cyclobutenes with large substituents would be stable against ROMP. In this chapter, we demonstrate the successful CP of various 1,5-hexadiyne monomers to give polyacetylenes containing cyclobutenes with perfect selectivity, and their intriguing optoelectronic properties were discussed based on experimental and computational studies.

### 3.3. Results and Discussion

#### 3.3.1. Polymer synthesis and kinetic analysis

First, we tried polymerization of simple 1,5-hexadiyne using 2<sup>nd</sup> generation Hoveyda-Grubbs catalyst (**Ru1**) in tetrahydrofuran (THF), but disappointingly, it showed almost no reactivity for CP (Table S3.1). To accelerate the cyclization, we prepared tetra-substituted *meso*-3,4-dimethylhexa-1,5-diyne-3,4-diol (**M1**) to maximize Thorpe-Ingold effect, and obtained some CP product of insoluble purple solid (Table 3.1, entry 1). Encouraged by the initial success, we attached benzyl group to both alcohols to enhance solubility. Interestingly, polymerization of **M2**, a mono-benzyl substituted derivative of **M1** (R/S and S/R mixture), yielded soluble reddish-purple polymer despite the low conversion (35% at 50 °C, M/I=30, entry 2), while its other diastereomeric isomers (R/R and S/S mixture) and bis-benzyl substituted monomer showed no reactivity (Table S3.1). Instead of using **Ru1** containing conventional mesityl (Mes) substituted *N*-heterocyclic carbene (NHC), switching to **Ru2** containing 2,6-diisopropylphenyl (DIPP) group<sup>33</sup> enhanced the polymerization efficiency to 54% conversion (entry 3). Finally, with bulkier substituents such as triethylsilyl (TES, **M3**) and *tert*-butyldimethylsilyl (TBS, **M4**) groups, excellent conversions (> 99%) were obtained to give **P3** and **P4** with high  $M_n$ s of ca. 20 kDa (entries 4 and 5). To restrict the bond rotation, we introduced benzylidene acetal substituent having *syn:anti* = 1:1.7 mixture (**M5**), but even at a higher temperature of 70 °C, polymerization was rather sluggish with 47% conversion (entry 6). However, **M6** with *anti*-stereoisomer showed much higher reactivity to give >99% conversion and  $M_n$  of 16.1 kDa, presumably because of the facile cyclization when the phenyl group is in sterically less hindered *anti*-position to alkynes (entries 7).

**Table 3.1. Cyclopolymerization of Various 1,5-Hexadiyne Derivatives**



entry	M	cat	M/I	temp (°C)	conc (M)	time (h)	conv (%) <sup>a</sup>	yield (%) <sup>b</sup>	<i>M<sub>n</sub></i> (kDa) <sup>c</sup>	<i>Đ</i> <sup>c</sup>
1	<b>M1</b>	<b>Ru1</b>	20	rt	0.5	14	-	58	-	-
2	<b>M2</b>	<b>Ru1</b>	30	50	0.5	3	35	-	-	-
3	<b>M2</b>	<b>Ru2</b>	30	50	0.5	3	54	-	-	-
4	<b>M3</b>	<b>Ru2</b>	30	50	1.0	3	>99	76	21.6	1.80
5	<b>M4</b>	<b>Ru2</b>	30	50	1.0	3	>99	56	19.5	1.56
6	<b>M5</b>	<b>Ru2</b>	30	70	1.0	4	47	35	4.1	1.67
7	<b>M6</b>	<b>Ru2</b>	30	70	1.0	4	> 99	94	16.1	1.88
8	<b>M7</b>	<b>Ru2</b>	30	50	0.5	4	70	69	8.7	1.68
9	<b>M8</b>	<b>Ru2</b>	30	50	0.5	4	>99	86	19.7	1.61
10	<b>M9</b>	<b>Ru2</b>	30	50	0.5	4	> 99	98	15.1	1.91
11	<b>M10</b>	<b>Ru2</b>	30	50	0.5	3.5	>99	99	16.2	2.07

**Table 3.1. continued**

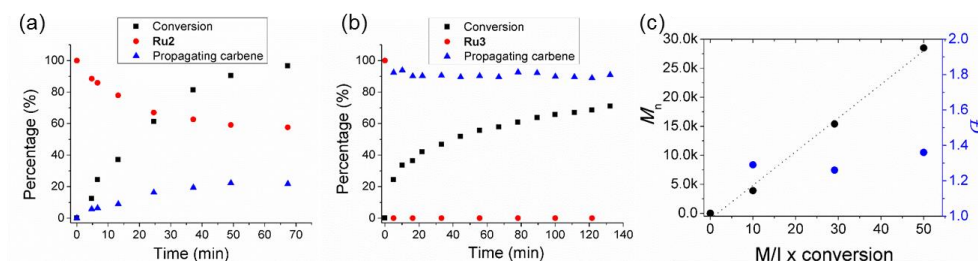
entry	M	cat	M/I	temp (°C)	conc (M)	time (h)	conv (%) <sup>a</sup>	yield (%) <sup>b</sup>	<i>M<sub>n</sub></i> (kDa) <sup>c</sup>	<i>Đ</i> <sup>c</sup>
12	<b>M11</b>	<b>Ru2</b>	30	70	0.5	6	> 99	83	6.4	2.41
13	<b>M8</b>	<b>Ru3</b>	10	50	0.5	1	> 99	58	3.9	1.29
14 <sup>d</sup>	<b>M8</b>	<b>Ru3</b>	30	50	0.5	6	97	83	15.4	1.26
15 <sup>d</sup>	<b>M8</b>	<b>Ru3</b>	50	50	0.5	15	>99	90	28.5	1.36
16 <sup>d</sup>	<b>M8</b>	<b>Ru3</b>	70	50	0.5	20	88	81	39.3	1.87
17	<b>M10</b>	<b>Ru3</b>	30	50	0.5	6	> 99	84	13.6	1.55
18	<b>M10</b>	<b>Ru3</b>	50	50	0.35	15	> 99	90	21.2	1.63

<sup>a</sup>Calculated from crude <sup>1</sup>H NMR. <sup>b</sup>Isolated yield. <sup>c</sup>Determined by tetrahydrofuran (THF) size-exclusion chromatography (SEC) calibrated using polystyrene standards. <sup>d</sup>1,3-Dioxane was used as solvent.

Despite the initial success, monomer design for tetra-substituted **M1-M6** was rather restricted because the polymerization efficiency seemed to be sensitive to certain stereochemistry. Therefore, to broaden the monomer scope, we designed 3,3-disubstituted 1,5-hexadiyne monomers (**M7-M11**), where catalyst would approach easily to less hindered alkyne at 5-position. Polymerization of undecyl- and TBS-substituted monomer (**M7**) at 50°C gave blue-colored polymer with 8.7 kDa from 70% conversion (M/I = 30, entry 8), and substitution with sterically bulkier triisopropylsilyl (TIPS) group (**M8**) improved the polymerization efficiency to give > 99% conversion and a high *M<sub>n</sub>* of 20 kDa (entry 9). Benzyl-substituted monomers with TBS (**M9**) and TIPS (**M10**) groups also showed high reactivity to give > 99% conversion and *M<sub>n</sub>*s of 15 – 16 kDa (entry 10 and 11). However, **M11** containing even larger phenyl- and TIPS substituents required a higher temperature of 70 °C for > 99% conversion (*M<sub>n</sub>* = 6.4 kDa), presumably due to too high steric congestion (entry 12). It seems that bulkier groups in the catalyst (Mes < DIPP)

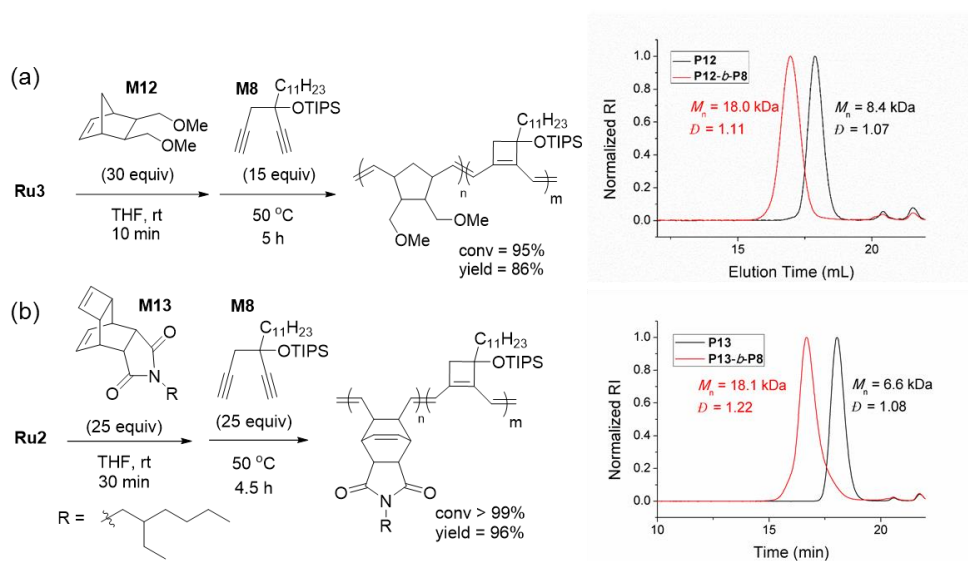
and monomers improved the polymerization by suppressing catalyst decomposition<sup>6</sup> as well as by enhancing Thorpe-Ingold effect for facile cyclization.<sup>35</sup>

Even though these monomers showed good reactivity with **Ru2**, all the resulting polymers showed uncontrolled molecular weights with broad dispersities (1.56 – 2.41) due to the slow initiation. When the reaction of **M8** with **Ru2** (M/I = 10) was monitored by *in situ* NMR experiment in THF-*d*<sub>8</sub> (0.25 M, 50 °C), it showed slow initiation leaving more than 50 % of the initial catalyst at the end of the reaction, thereby giving a low  $k_i/k_p$  value of 0.027 (Figure 3.1.a). In contrast, similar to widely used fast-initiating 3<sup>rd</sup> generation Grubbs catalyst,<sup>36</sup> **Ru3** having 3-chloropyridine and DIPP-NHC ligands showed rapid initiation upon monomer addition, generating a large amount of propagating carbene (Figure 3.1.b). Notably, the propagation rate was approximately 8 times lower than that using **Ru2**, presumably because the pyridine coordination to the propagating carbene (from **Ru3**, 18.74 ppm) significantly retarded CP compared to the propagating carbene with weaker coordination of putatively assigned olefin chelation<sup>37</sup> (from **Ru2**, 18.19 ppm) (Figure S3.1). As a result, **Ru3** gave a high  $k_i/k_p$  value of > 4.4, which enabled controlled polymerization of **M8** to give  $M_n$  from 4 to 29 kDa according to the M/I ratio from M/I = 10 to 50 with relatively narrow dispersities (<1.4) (entries 13-15, Figure 3.1.c). The maximum  $M_n$  up to 40 kDa was achieved with M/I=70, from a turnover number of 62, despite the broad dispersity (entry 16). Polymerization of **M10** with **Ru3** also showed a proportional increase of  $M_n$  values up to M/I=50 (entries 17 and 18). All the polymer structures were characterized by <sup>1</sup>H & <sup>13</sup>C NMR, which supported all-*trans* olefin stereochemistry in the polymer backbones.



**Figure 3.1.** Plots of conversions and carbene changes monitored by *in situ*  $^1\text{H}$  NMR analysis during the polymerization of **M8** ( $M/I = 10$ ) in  $\text{THF-}d_8$  (0.25 M, 50  $^\circ\text{C}$ ) using (a) **Ru2** and (b) **Ru3**, respectively. (c) Plots of  $M_n$  vs.  $M/I$  and corresponding  $D$  values for **P8** synthesized by **Ru3**.

Furthermore, block copolymers with polyacetylenes having four-membered rings were successfully synthesized by combining with living ROMP. First, a norbornene derivative (**M12**, 30 equiv) was polymerized by **Ru3** at room temperature, and the addition of **M8** (15 equiv) to the same reaction pot at 50  $^\circ\text{C}$  resulted in a successful block copolymerization as shown by a clear shift of SEC traces with an increase in  $M_n$  from 8.4 to 18.0 kDa and a narrow dispersity of 1.11 (Figure 3.2.a). Additionally, from the fact that olefin chelation allowed the living polymerization of endo-tricyclo-[4.2.2.0<sup>2,5</sup>]deca-3,9-diene derivatives even with the relatively slow-initiating Hoveyda-Grubbs catalyst,<sup>38</sup> polymerization of **M13** (25 equiv) was carried out by **Ru2** to give the first block with  $M_n$  of 6.6 kDa. Then the addition of **M8** (25 equiv) at 50  $^\circ\text{C}$  produced another block copolymer having  $M_n$  of 18.1 kDa with a narrow dispersity of 1.22 (Figure 3.2.b).



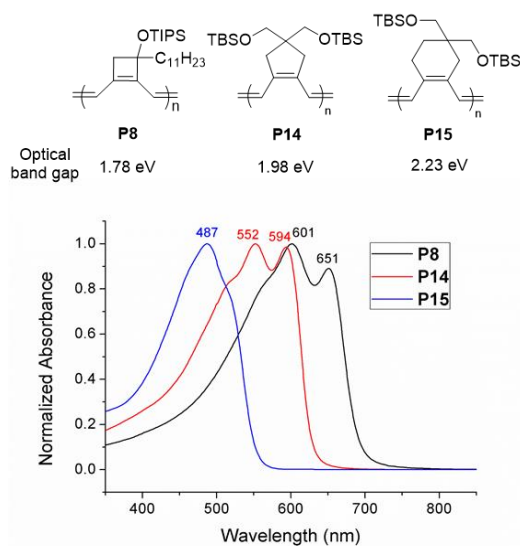
**Figure 3.2.** Syntheses of block copolymers by combining CP of **M8** with ROMP of (a) **M12** and (b) **M13**, respectively.

### 3.3.2. Optoelectronic properties of polymers

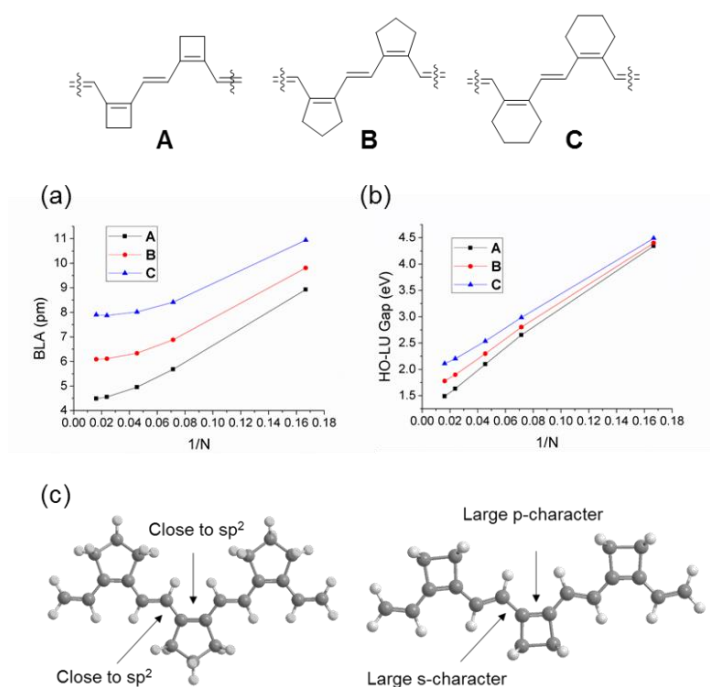
Interestingly, polymers from 3,3-disubstituted monomers (**P7**, **P8**, **P10**, and **P11**) exhibited dark blue color both in solid and solution state, implying for the absorption of long-wavelength visible light. Indeed, UV-Vis analysis indicated that **P8** showed significantly higher  $\lambda_{\text{max}}$  at 601 and 651 nm than those from analogous polyacetylenes containing five- (**P14**, 552 and 594 nm)<sup>8</sup> and six-membered rings (**P15**, 487 nm)<sup>13</sup> prepared by CP of 1,6-heptadiynes and 1,7-octadiynes, respectively (Figure 3.3). In order to understand the origin of this longest absorption values for highly soluble substituted polyacetylenes,<sup>3,39</sup> we conducted density functional theory (DFT) calculations on model oligoacetylenes containing four- (**A**), five- (**B**), and six-membered rings (**C**) (DP = 1-15, N=number of carbon atoms in the polyacetylene backbone) (Figure 3.4).<sup>40-42</sup> Bond length alternation (BLA),<sup>48</sup> the difference between the length of central single and double bonds, was much smaller for **A** (4.5 pm with DP = 15) compared to those from **B** (6.1 pm) and **C** (7.9 pm) (Figure 3.4.a). Also, consistent with the experimental observation, the band-gap decreased with the smaller ring (**A** = 1.49, **B** = 1.78, **C** = 2.11 eV for DP = 15, Figure 3.4.b). This unexpectedly smaller BLA and narrower band-gap of **A** might be due to the small bond angle of the cyclobutene which gives more p-orbital character to the endocyclic double bonds thereby making them longer than the analogous cyclopentene model compound (**B**), while making the exocyclic single bonds shorter by rendering more s-orbital character to them (Figure 3.4.c). As a result, the difference between the lengths of single and double bonds decreased, making the  $\pi$ -electrons more delocalized.<sup>43</sup> Compared to **P8**, polymers **P3**, **P4**, and **P6** from tetra-substituted monomers showed blue-shifted absorption spectra ( $\lambda_{\text{max}}$  = 550 – 600 nm) presumably because the steric repulsion between the substituents distorted the backbone planarity (Figure S3.2). We also measured the highest occupied molecular orbital (HOMO) energies of **P3-P11** by cyclic voltammetry (-5.12 – -5.34 eV), which were similar to or slightly deeper than that of



polyacetylene containing five-membered rings (-5.14 eV) (Table S3.2).



**Figure 3.3.** UV-Vis spectra of various polyacetylenes containing four-, five-, and six-membered rings.



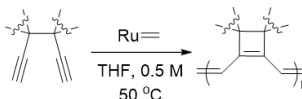
**Figure 3.4.** Comparison of (a) bond length alternation (BLA) and (b) HOMO-LUMO gaps of polyacetylenes having different ring sizes calculated by DFT using B3LYP method with 6-31G(d) basis set.

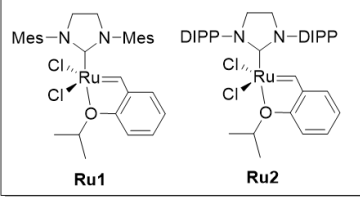
### 3.4. Conclusion

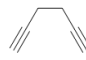

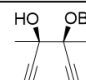

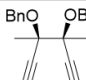
In conclusion, we have demonstrated the successful cyclopolymerization of 1,5-hexadiyne derivatives, which continuously forms highly strained cyclobutenes. From various monomers, high molecular weight polymers up to 40 kDa could be synthesized, and even controlled polymerization as well as the preparation of block copolymers was possible by using Ru catalysts containing a bulky NHC ligand. These new polyacetylenes containing four-membered rings showed surprisingly long-wavelength absorption, which is among the longest reported for soluble polyacetylenes. Computations using density functional theory has shed light on the origin of narrow band-gaps of conjugated polymer containing cyclobutenes, whose  $\pi$ -electrons are highly delocalized as supported by short bond length alternation. This study not only broadened the utility of the Grubbs catalyst for the synthesis of conjugated polymers but also provided more profound insights on the structure-property relationship of conjugated polymers having different ring sizes in the backbone.

### 3.5. Supporting Figures

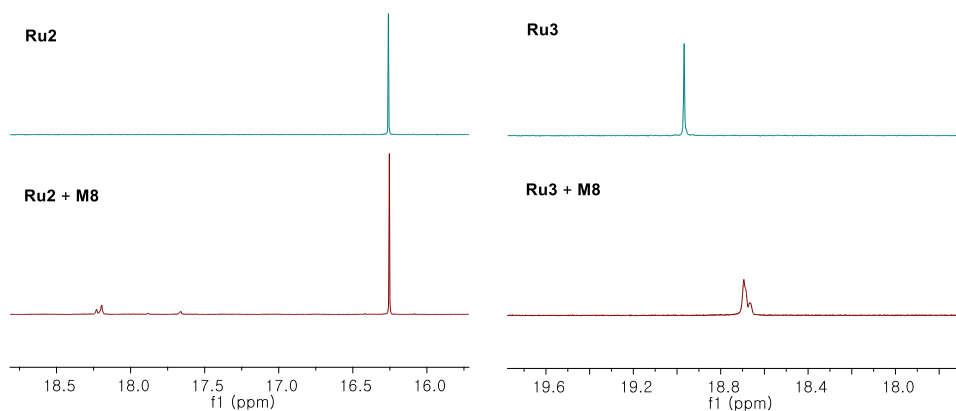
**Table 3.1.** Polymerization of a simple 1,5-hexadiyne and tetra-substituted 1,5-hexadiyne derivatives





monomer	cat	M/I	conc	time	conv <sup>a</sup>	yield <sup>b</sup>
	<b>Ru1</b>	20	0.5 M	3	10%	-
	<b>Ru2</b>	30	0.5 M	3	54%	-
	<b>Ru2</b>	30	1 M	3	54%	-
	<b>Ru2</b>	30	0.5 M	3	0%	0%
	<b>Ru1</b>	20	0.5 M	24	0%	0%

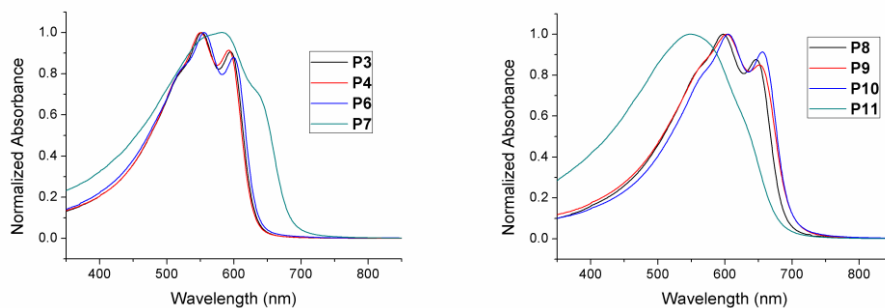
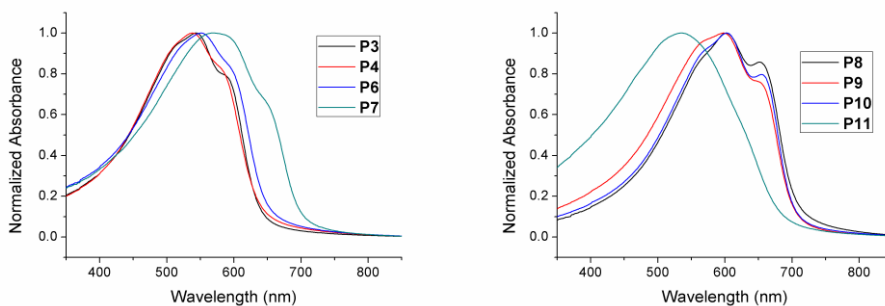
<sup>a</sup>Calculated from crude <sup>1</sup>H NMR. <sup>b</sup>Isolated yield.



**Figure S3.1.** Carbene regions in <sup>1</sup>H NMR spectra from the reaction of **M8** with **Ru2** (left) and **Ru3** (right), respectively (M/I = 10, THF-*d*<sub>8</sub>, 0.25 M, 50 °C)

**Table S3.2.** Optical and Electrical Properties of Polymers

	Solution		Film		$E_{\text{HOMO}}$ (eV)
	$\lambda_{\text{abs}}$ (nm)	$E_{\text{g}}^{\text{opt}}$ (eV)	$\lambda_{\text{abs}}$ (nm)	$E_{\text{g}}^{\text{opt}}$ (eV)	
<b>P3</b>	552, 595	1.96	544	1.94	-5.12
<b>P4</b>	550, 592	1.97	538	1.92	-5.17
<b>P6</b>	556, 600	1.95	551	1.90	-5.23
<b>P7</b>	582	1.81	569	1.77	-5.26
<b>P8</b>	597, 646	1.80	602, 652	1.74	-5.34
<b>P9</b>	603, 652	1.77	598	1.75	-5.15
<b>P10</b>	605, 656	1.77	603, 655	1.75	-5.20
<b>P11</b>	549	1.82	535	1.80	-5.21

**Figure S3.2.** UV-Vis spectra of **P3** – **P11** in THF solution (ca. 0.01 g/L).**Figure S3.3.** UV-Vis spectra of **P3** – **P11** in film state.

### 3.6. Experimental Section

#### Characterization

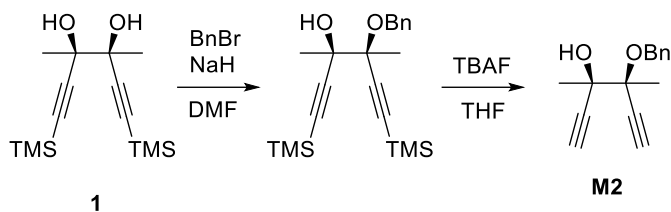
$^1\text{H}$  NMR and  $^{13}\text{C}$  NMR were recorded by Varian/Oxford As-500 (500 MHz for  $^1\text{H}$ , 125 MHz for  $^{13}\text{C}$ ) and Bruker AVANCE 600 (600 MHz for  $^1\text{H}$  and 150 MHz for  $^{13}\text{C}$ ). Size exclusion chromatography (SEC) analyses were carried out with Waters system (1515 pump and 2707 autosampler) and Shodex GPC LF-804 column eluted with THF (GPC grade, Honeywell Burdick & Jackson<sup>®</sup>) and filtered through a 0.2  $\mu\text{m}$  PTFE filter (Whatman<sup>®</sup>). The flow rate was 1.0 mL/min and temperature of the column was maintained at 35 °C. Wyatt OptiLab T-rEx refractive index detector was used for molecular weight measurement. High-resolution mass spectroscopy (HRMS) analyses were performed by ultra high resolution ESI Q-TOF mass spectrometer (Bruker, Germany) in the Sogang Organic Chemistry Research Center. UV/Vis spectra were obtained by UV-vis Spectrometer V-650 (Jasco Inc.). Cyclic voltammetry (CV) measurements were carried out by CHI 660 Electrochemical Analyzer (CH Instruments, Inc., Texas, USA).

#### Materials

All reagents which are commercially available from Sigma-Aldrich<sup>®</sup>, Tokyo Chemical Industry Co. Ltd., Acros Organics, Alfa Aesar<sup>®</sup>, Umicore (**Ru2**) without additional notes, were used without further purification. Tetrahydrofuran (THF) for the polymerization were purified by distillation and degassed further by Ar bubbling for 10 minutes before performing reactions. THF- $d_8$  (99.50% D, 0.75mL) was purchased from Deutero GmbH and used without further purification.

## Experimental procedures for the preparation of monomers

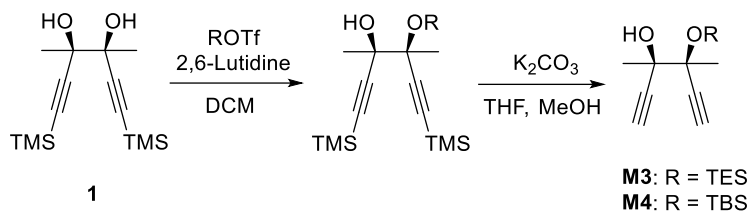
Compounds **1**,<sup>44</sup> **2**,<sup>45</sup> **3**,<sup>46</sup> and **4**,<sup>47</sup> were prepared by literature methods.



### Synthesis of **M2**

Compound **1** (139 mg, 1.01 mmol) was dissolved in  $\text{DMF}$  (3 ml), and  $\text{NaH}$  (60% dispersion in mineral oil, 44 mg, 1.1 mmol) was slowly added to the solution at  $0\text{ }^{\circ}\text{C}$ . Then, benzyl bromide (0.13 ml, 1.1 mmol) was added and the reaction mixture was stirred at room temperature for 2.5 h. After quenching with a saturated  $\text{NH}_4\text{Cl}$  aqueous solution, the organic layer was washed with brine and extracted by ethyl acetate, dried with  $\text{MgSO}_4$ , and concentrated. Purification with flash column chromatography afforded a mixture of the desired product and its TMS-deprotected derivatives. This mixture was dissolved in  $\text{THF}$  (3 ml), then tetrabutylammonium fluoride solution (1.0 M in  $\text{THF}$ , 0.77 ml, 0.77 mmol) was added. After stirring for 40 min, the reaction mixture was quenched with  $\text{NH}_4\text{Cl}$  aqueous solution. The organic layer was washed with water and extracted by ethyl acetate, dried with  $\text{MgSO}_4$ , and concentrated. The product was purified by flash column chromatography on silica gel to afford **M2** as white powder (46 mg, 0.20 mmol, 20%).

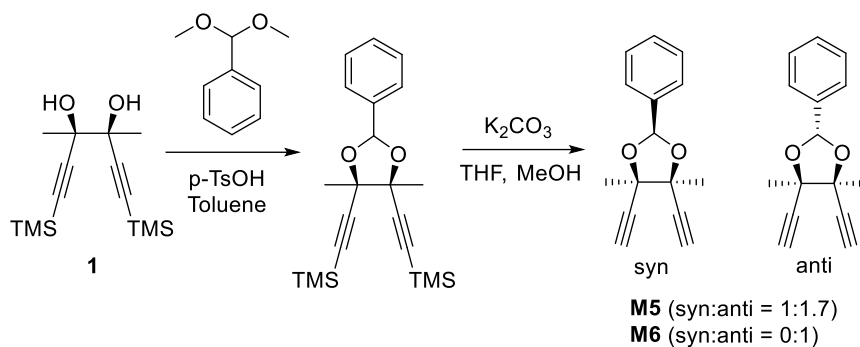
## Synthesis of M3 and M4



Compound **1** (720 mg, 2.5 mmol) was dissolved in DCM. Then, 2,6-lutidine (90  $\mu$ l, 0.77 mmol) and triethylsilyl trifluoromethanesulfonate (0.16 ml, 0.77 mmol) was added sequentially at 0 °C. After stirring 1 h, the reaction was quenched by saturated  $\text{NH}_4\text{Cl}$  aqueous solution. The organic layer was washed with brine and extracted by ethyl acetate, dried with  $\text{MgSO}_4$ , and concentrated. This product was mixed with  $\text{K}_2\text{CO}_3$  (67 mg), and dissolved in THF (0.6 ml) and methanol (0.6 ml). After 4 h, the reaction was quenched by saturated  $\text{NH}_4\text{Cl}$  aqueous solution. The organic layer was washed with brine and extracted by ethyl acetate, dried with  $\text{MgSO}_4$ , and concentrated. The product was purified by flash column chromatography on silica gel to afford **M3** as colorless liquid (88 mg, 0.35 mmol, 45%).  $^1\text{H}$  NMR (500 MHz,  $\text{CDCl}_3$ )  $\delta$  2.74 (br, 1H), 2.54 (s, 1H), 2.41 (s, 1H), 1.54 (d,  $J$  = 1.6 Hz, 6H), 0.98 (t,  $J$  = 7.9 Hz, 9H), 0.81 – 0.67 (m, 6H).  $^{13}\text{C}$  NMR (125 MHz,  $\text{CDCl}_3$ )  $\delta$  86.12, 85.40, 74.60, 74.58, 74.23, 72.13, 25.34, 24.05, 7.11, 6.04. HRMS (ESI):  $m/z$  for  $\text{C}_{14}\text{H}_{24}\text{NaO}_2\text{Si}$   $[\text{M}+\text{Na}]^+$ , calcd: 275.1438, found: 275.1440.

Following the same procedure, compound **1** (2.07 g, 7.34 mmol) was reacted with *tert*-butyldimethylsilyl trifluoromethanesulfonate (0.51 ml, 2.20 mmol) to afford **M4** as colorless liquid (333 mg, 1.32 mmol, 60%).  $^1\text{H}$  NMR (500 MHz,  $\text{CDCl}_3$ )  $\delta$  2.71 (br, 1H), 2.55 (s, 1H), 2.41 (s, 1H), 1.55 (s, 3H), 1.54 (s, 3H), 0.90 (s, 9H), 0.24 (s, 3H), 0.23 (s, 3H).  $^{13}\text{C}$  NMR (125 MHz,  $\text{CDCl}_3$ )  $\delta$  86.02, 85.18, 74.90, 74.70, 74.22, 72.15, 25.82, 25.23, 24.07, 18.28, -2.97, -3.27. HRMS (ESI):  $m/z$  for  $\text{C}_{14}\text{H}_{24}\text{NaO}_2\text{Si}$   $[\text{M}+\text{Na}]^+$ , calcd: 275.1438, found 275.1439.

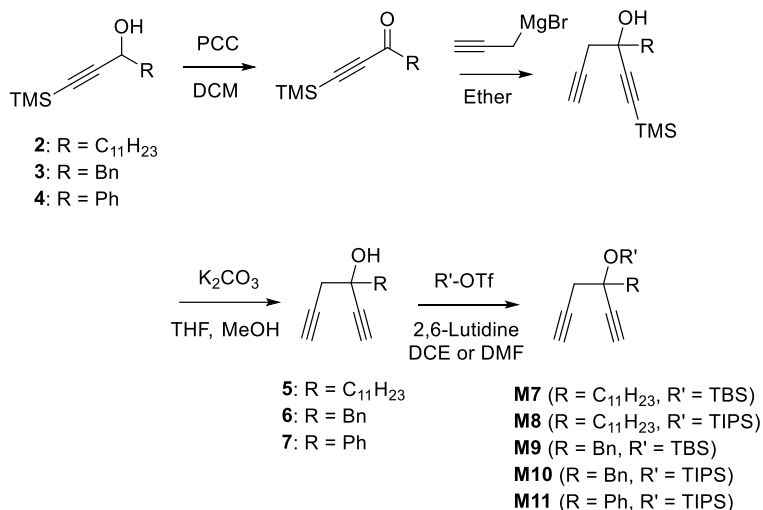
## Synthesis of **M5** and **M6**



To a dried round-bottom flask containing a stirring bar, compound **1** (412 mg, 1.46 mmol) and p-toluenesulfonic acid (56 mg, 0.29 mmol) was added and purged with Ar gas. The mixture was dissolved in toluene (1.5 ml), then benzaldehyde dimethyl acetal (0.26 ml, 1.75 mmol) was added. After stirring for 6 h at 70 °C, the organic layer was washed with brine and extracted by ethyl acetate, dried with MgSO<sub>4</sub>, and concentrated. This crude was dissolved in THF (2 ml) and methanol (2 ml), then K<sub>2</sub>CO<sub>3</sub> (508 mg, 3.63 mmol) was added. After vigorous stirring for 3 h, the reaction was quenched by saturated NH<sub>4</sub>Cl aqueous solution. The organic layer was washed with brine and extracted by ethyl acetate, dried with MgSO<sub>4</sub>, and concentrated. The product was purified by flash column chromatography on silica gel to afford **M5** (syn:anti = 1:1.7) as colorless liquid (264 mg, 1.17 mmol, 80%). Further purification by recrystallization afforded **M6** (syn:anti = 0:1) as white solid (90 mg). <sup>1</sup>H NMR (500 MHz, CDCl<sub>3</sub>) δ 7.54 – 7.45 (m, 2H), 7.42 – 7.35 (m, 3H), 6.27 (s, 1H), 2.70 (s, 2H), 1.62 (s, 6H). <sup>13</sup>C NMR (125 MHz, CDCl<sub>3</sub>) δ 129.58, 128.52, 126.76, 102.29, 82.64, 80.32, 75.51, 23.87. HRMS (ESI): m/z for C<sub>15</sub>H<sub>14</sub>NaO<sub>2</sub> [M+Na]<sup>+</sup>, calcd: 249.0886, found: 249.0887.



## General procedure for the synthesis of compounds 5-7



Compound **2** (5.25 g, 18.6 mmol) was dissolved in DCM (62 ml), and pyridinium chlorochromate (6.01 g, 27.9 mmol) was added. After stirring for 5 h, the crude mixture was filtered with celite. Purification with flash column chromatography afforded a mixture of the desired oxidized product and its TMS-deprotected derivative. A portion of this product (2.21 g) was dissolved in degassed diethyl ether (30 ml), then propargyl magnesium bromide solution (30 ml)\* was added at -30 °C. After checking the complete consumption of the starting materials by thin layer chromatography, the reaction was quenched by saturated NH<sub>4</sub>Cl aqueous solution. The organic layer was washed with brine and extracted by ethyl acetate, dried with MgSO<sub>4</sub>, and concentrated. This crude mixture was dissolved in THF (10 ml) and methanol (10 ml), then K<sub>2</sub>CO<sub>3</sub> (5.9 g, 43 mmol) was added. After vigorous stirring for 2 h, the reaction was quenched by saturated NH<sub>4</sub>Cl aqueous solution. The organic layer was washed with water and extracted by ethyl acetate, dried with MgSO<sub>4</sub>, and concentrated. The product was purified by flash column chromatography on silica gel to afford **5** as colorless liquid (1.74 g, 7.0 mmol). <sup>1</sup>H NMR (500 MHz, CDCl<sub>3</sub>) δ 2.62 (ddd, *J* = 40.5, 16.6, 2.6 Hz, 2H), 2.50 (s, 1H), 2.38 (br, 1H), 2.16 (t, *J* = 2.6 Hz, 1H), 1.80 – 1.70 (m, 2H), 1.55 – 1.49 (m, 2H),

1.38 – 1.23 (m, 16H), 0.88 (t,  $J = 6.9$  Hz, 3H).  $^{13}\text{C}$  NMR (125 MHz,  $\text{CDCl}_3$ )  $\delta$  85.52, 79.40, 72.82, 72.06, 69.70, 40.97, 33.33, 32.07, 29.79, 29.77, 29.75, 29.71, 29.65, 29.50, 24.41, 22.84, 14.28. HRMS (ESI):  $m/z$  for  $\text{C}_{17}\text{H}_{28}\text{NaO}$   $[\text{M}+\text{Na}]^+$ , calcd: 271.2032, found: 271.2031.

\* Preparation of propargyl magnesium bromide (Grignard reagent)

To a two-neck round-bottom flask with a reflux condenser, magnesium turnings (2.2 g, 90 mmol) and mercury (II) chloride (610 mg, 2.3 mmol) was added. After drying it with a torch, diethyl ether (30 ml) was added. Propargyl bromide solution (80% in toluene, 5.0 ml, 45 mmol) was slowly added, then the reaction mixture is warmed over a water bath for 1 h. After seeing that bubbling stopped, the reagent was directly used for the Grignard reaction.

Following the same procedure, compound **3** was used to afford **6** as colorless liquid.

$^1\text{H}$  NMR (500 MHz,  $\text{CDCl}_3$ )  $\delta$  7.39 – 7.27 (m, 5H), 3.11 (q,  $J = 13.4$  Hz, 2H), 2.64 (d,  $J = 2.6$  Hz, 2H), 2.54 (s, 1H), 2.42 (s, 1H), 2.22 (t,  $J = 2.6$  Hz, 1H).  $^{13}\text{C}$  NMR (125 MHz,  $\text{CDCl}_3$ )  $\delta$  135.41, 130.89, 128.36, 127.37, 85.12, 79.41, 74.18, 72.33, 69.72, 46.58, 32.63. HRMS (ESI):  $m/z$  for  $\text{C}_{13}\text{H}_{12}\text{NaO}$   $[\text{M}+\text{Na}]^+$ , calcd: 207.0780, found: 207.0783.

Following the same procedure, compound **4** was used to afford **7** as colorless liquid.

$^1\text{H}$  NMR (500 MHz,  $\text{CDCl}_3$ )  $\delta$  7.70 – 7.65 (m, 2H), 7.42 – 7.36 (m, 2H), 7.36 – 7.31 (m, 1H), 2.97 (s, 1H), 2.86 (d,  $J = 2.6$  Hz, 2H), 2.74 (s, 1H), 2.15 (t,  $J = 2.6$  Hz, 1H).  $^{13}\text{C}$  NMR (125 MHz,  $\text{CDCl}_3$ )  $\delta$  142.25, 128.44, 125.43, 85.16, 79.23, 74.47, 72.11, 71.42, 36.70. HRMS (ESI):  $m/z$  for  $\text{C}_{12}\text{H}_{10}\text{NaO}$   $[\text{M}+\text{Na}]^+$ , calcd: 193.0624, found: 193.0627.

## General procedure for the synthesis of **M7** – **M11**

Compound **5** (150 mg, 0.61 mmol) was dissolved in DCE (3 ml). Then, 2,6-lutidine (0.35 ml, 3.0 mmol) and tert-butyldimethylsilyl trifluoromethanesulfonate (0.42 ml, 1.8 mmol) was added. After stirring for 5 h at 50 °C, the reaction was quenched by saturated NaHCO<sub>3</sub> aqueous solution. The organic layer was washed with water and extracted by dichloromethane, dried with MgSO<sub>4</sub>, and concentrated. The product was purified by flash column chromatography on silica gel to afford **M7** as colorless liquid (188 mg, 0.518 mmol, 85%). <sup>1</sup>H NMR (500 MHz, CDCl<sub>3</sub>) δ 2.56 (dd, *J* = 2.5, 1.5 Hz, 2H), 2.50 (s, 1H), 2.04 (t, *J* = 2.6 Hz, 1H), 1.81 – 1.71 (m, 2H), 1.51 – 1.39 (m, 2H), 1.37 – 1.19 (m, 17H), 0.91 – 0.85 (m, 12H), 0.19 (d, *J* = 8.9 Hz, 6H). <sup>13</sup>C NMR (125 MHz, CDCl<sub>3</sub>) δ 86.41, 80.37, 73.70, 70.99, 70.77, 42.14, 33.80, 32.08, 29.80, 29.76, 29.73, 29.69, 29.51, 25.84, 24.14, 22.85, 18.33, 14.28, -2.84, -2.95. HRMS (ESI): *m/z* for C<sub>23</sub>H<sub>42</sub>NaOSi [M+Na]<sup>+</sup>, calcd: 385.2897, found: 385.2899.

From the reaction of compound **5** (550 mg, 2.2 mmol) with triisopropylsilyl trifluoromethanesulfonate (1.8 ml, 6.6 mmol) in DCE (50 °C, 17 h), **M8** was obtained as colorless liquid (818 mg, 2.02 mmol, 91%). <sup>1</sup>H NMR (500 MHz, CDCl<sub>3</sub>) δ 2.64 (d, *J* = 2.7 Hz, 2H), 2.47 (s, 1H), 2.03 (t, *J* = 2.7 Hz, 1H), 1.93 – 1.81 (m, 2H), 1.49 – 1.42 (m, 2H), 1.40 – 1.21 (m, 18H), 1.21 – 1.14 (m, 3H), 1.08 (dd, *J* = 7.3, 2.4 Hz, 18H), 0.88 (t, *J* = 7.0 Hz, 3H). <sup>13</sup>C NMR (125 MHz, CDCl<sub>3</sub>) δ 86.85, 80.31, 73.22, 70.89, 70.79, 42.01, 33.11, 32.08, 29.80, 29.79, 29.71, 29.67, 29.51, 24.09, 22.85, 18.51, 14.28, 13.18. HRMS (ESI): *m/z* for C<sub>26</sub>H<sub>48</sub>NaOSi [M+Na]<sup>+</sup>, calcd: 427.3367, found: 427.3369.

From the reaction of compound **6** (109 mg, 0.59 mmol) with tert-butyldimethylsilyl trifluoromethanesulfonate (0.54 ml, 2.4 mmol) in DMF (80 °C, 4 h), **M9** was obtained as colorless liquid (138 mg, 0.46 mmol, 78%). <sup>1</sup>H NMR (500 MHz, CDCl<sub>3</sub>) δ 7.38 (d, *J* = 6.9 Hz, 2H), 7.33 – 7.24 (m, 3H), 3.10 (qd, *J* = 13.2, 2.3 Hz,

2H), 2.58 (d,  $J = 2.9$  Hz, 1H), 2.56 (s, 2H), 2.16 (q,  $J = 2.6$  Hz, 1H), 0.88 (d,  $J = 2.8$  Hz, 9H), 0.17 (d,  $J = 2.6$  Hz, 3H), -0.06 (d,  $J = 2.6$  Hz, 3H).  $^{13}\text{C}$  NMR (125 MHz,  $\text{CDCl}_3$ )  $\delta$  136.34, 131.35, 127.75, 126.83, 85.75, 80.38, 75.45, 71.53, 71.28, 47.76, 33.68, 25.96, 18.37, -2.80, -3.35. HRMS (ESI):  $m/z$  for  $\text{C}_{19}\text{H}_{26}\text{NaOSi}$   $[\text{M}+\text{Na}]^+$ , calcd: 321.1645, found: 321.1648.

From the reaction of compound **6** (150 mg, 0.83 mmol) with triisopropylsilyl trifluoromethanesulfonate (0.90 ml, 3.3 mmol) in DMF (80 °C, 40 h), **M10** was obtained as colorless liquid (143 mg, 0.42 mmol, 51%).  $^1\text{H}$  NMR (500 MHz,  $\text{CDCl}_3$ )  $\delta$  7.41 (d,  $J = 6.8$  Hz, 2H), 7.32 – 7.22 (m, 3H), 3.20 (dd,  $J = 40.7, 13.2$  Hz, 2H), 2.57 – 2.52 (m, 3H), 2.17 (t,  $J = 2.6$  Hz, 1H), 1.25 – 1.16 (m, 3H), 1.07 (dd,  $J = 7.4, 4.4$  Hz, 18H).  $^{13}\text{C}$  NMR (125 MHz,  $\text{CDCl}_3$ )  $\delta$  136.28, 131.21, 127.90, 126.89, 80.52, 74.95, 71.77, 71.26, 47.39, 32.75, 18.53, 18.49, 13.20. HRMS (ESI):  $m/z$  for  $\text{C}_{22}\text{H}_{32}\text{NaOSi}$   $[\text{M}+\text{Na}]^+$ , calcd: 363.2115, found: 363.2117.

From the reaction of compound **7** (180 mg, 1.1 mmol) with triisopropylsilyl trifluoromethanesulfonate (0.85 ml, 3.2 mmol) in DMF (40 °C, 2 d), **M11** was obtained as colorless liquid (233 mg, 0.71 mmol, 65%).  $^1\text{H}$  NMR (500 MHz,  $\text{CDCl}_3$ )  $\delta$  7.76 – 7.70 (m, 2H), 7.39 – 7.28 (m, 3H), 2.91 (ddd,  $J = 51.2, 16.3, 2.6$  Hz, 2H), 2.79 (s, 1H), 1.95 (t,  $J = 2.6$  Hz, 1H), 1.29 – 1.19 (m, 3H), 1.05 (dd,  $J = 26.0, 7.5$  Hz, 18H).  $^{13}\text{C}$  NMR (125 MHz,  $\text{CDCl}_3$ )  $\delta$  143.57, 127.97, 127.81, 126.11, 85.44, 79.91, 76.17, 73.07, 71.21, 39.07, 18.54, 18.49, 13.24. HRMS (ESI):  $m/z$  for  $\text{C}_{21}\text{H}_{30}\text{NaOSi}$   $[\text{M}+\text{Na}]^+$ , calcd: 349.1958, found: 349.1956.

### General procedure for cyclopolymerization

A 4-mL sized screw-cap vial with septum was flame dried and charged with monomer (ca. 20 ~ 30 mg). The vial was purged with Ar three times, and degassed anhydrous solvent was added. A mixture of initiator and additive in another 4-mL

vial was dissolved in solvent under Ar atmosphere. The initiator solution was rapidly injected to the monomer solution at experimental temperature under vigorous stirring. The reaction was quenched by excess ethyl vinyl ether after desired reaction time, and resulting polymer was partially precipitated in methanol, remaining small amount of crude mixture (c.a. 2 mg). Obtained solid was filtered and dried *in vacuo*. Monomer conversion was calculated from the  $^1\text{H}$  NMR spectrum of the remained crude mixture.

### $^1\text{H}$ and $^{13}\text{C}$ NMR characterization of polymers

**P3:**  $^1\text{H}$  NMR (500 MHz,  $\text{CD}_2\text{Cl}_2$ )  $\delta$  6.83 – 6.27 (m, 2H), 3.12 – 2.89 (m, 1H), 1.58 (s, 3H), 1.43 (s, 3H), 1.06 – 0.93 (m, 9H), 0.79 – 0.64 (m, 6H).

$^{13}\text{C}$  NMR (150 MHz,  $\text{CDCl}_3$ )  $\delta$  148.45, 145.75, 123.57, 122.94, 82.71, 79.18, 20.91, 19.91, 7.20, 6.72.

**P4:**  $^1\text{H}$  NMR (500 MHz,  $\text{CD}_2\text{Cl}_2$ )  $\delta$  6.79 – 6.29 (m, 2H), 3.06 – 2.79 (m, 1H), 1.58 (br, 3H), 1.42 (s, 3H), 0.91 (s, 9H), 0.38 – 0.12 (m, 6H).

$^{13}\text{C}$  NMR (150 MHz,  $\text{CDCl}_3$ )  $\delta$  148.16, 145.76, 123.34, 123.02, 82.78, 79.60, 26.06, 20.88, 19.96, 18.48, -2.25.

**P6:**  $^1\text{H}$  NMR (500 MHz,  $\text{CD}_2\text{Cl}_2$ )  $\delta$  7.47 (br, 2H), 7.36 (d,  $J$  = 12.1 Hz, 3H), 6.64 (s, 2H), 5.64 (s, 1H), 1.54 (s, 6H).

$^{13}\text{C}$  NMR (125 MHz,  $\text{CD}_2\text{Cl}_2$ )  $\delta$  142.52, 136.99, 129.80, 128.58, 127.80, 124.03, 100.77, 87.82, 16.92.

**P8:**  $^1\text{H}$  NMR (500 MHz,  $\text{CD}_2\text{Cl}_2$ )  $\delta$  6.80 (d,  $J$  = 12.7 Hz, 1H), 6.24 (d,  $J$  = 12.7 Hz, 1H), 2.76 (s, 1H), 2.60 (s, 1H), 1.95 (s,  $J$  = 84.6 Hz, 1H), 1.75 (s, 1H), 1.65 – 1.12 (m, 18H), 1.05 (s, 18H), 0.88 (t,  $J$  = 6.1 Hz, 3H).

$^{13}\text{C}$  NMR (125 MHz,  $\text{CD}_2\text{Cl}_2$ )  $\delta$  147.26, 140.04, 123.97, 121.88, 78.74, 42.44, 41.10, 40.68, 32.39, 30.51, 30.10, 29.81, 25.54, 23.15, 18.64, 14.35, 13.61.

**P9:**  $^1\text{H}$  NMR (500 MHz,  $\text{CD}_2\text{Cl}_2$ )  $\delta$  7.48 – 6.89 (m, 5H), 6.54 – 6.11 (m, 1H), 6.11 – 5.84 (m, 1H), 3.44 – 2.94 (m, 2H), 2.94 – 2.27 (m, 2H), 1.12 – 0.56 (m, 9H), 0.28 – -0.33 (m, 6H).

$^{13}\text{C}$  NMR (150 MHz,  $\text{CD}_2\text{Cl}_2$ )  $\delta$  146.53, 140.20, 138.96, 131.30, 127.95, 126.64, 124.43, 122.14, 79.30, 47.32, 41.83, 26.34, 18.69, -2.59, -3.44.

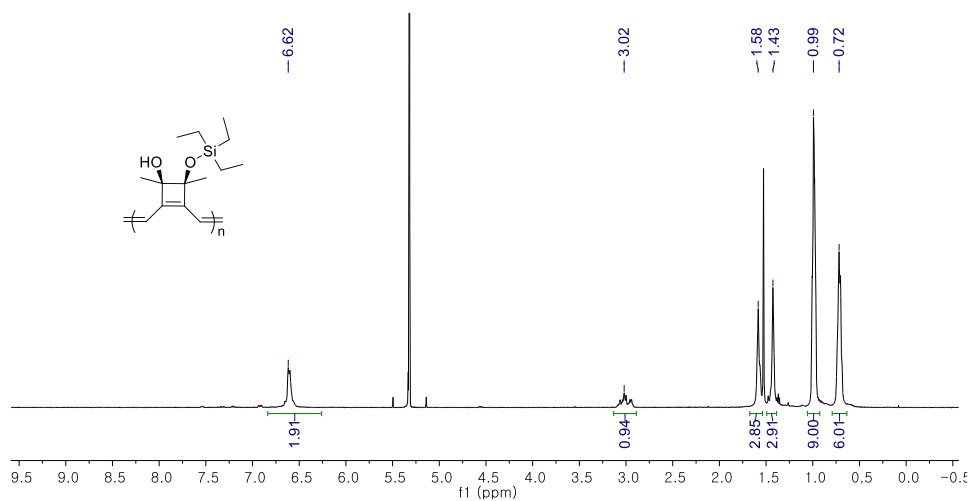
**P11:**  $^1\text{H}$  NMR (500 MHz,  $\text{CD}_2\text{Cl}_2$ )  $\delta$  7.68 – 6.78 (m, 5H), 6.53 (br, 1H), 6.13 (br, 1H), 3.53 – 2.22 (m, 2H), 1.25 – 0.65 (m, 21H).

### General procedure for *in situ* NMR experiments

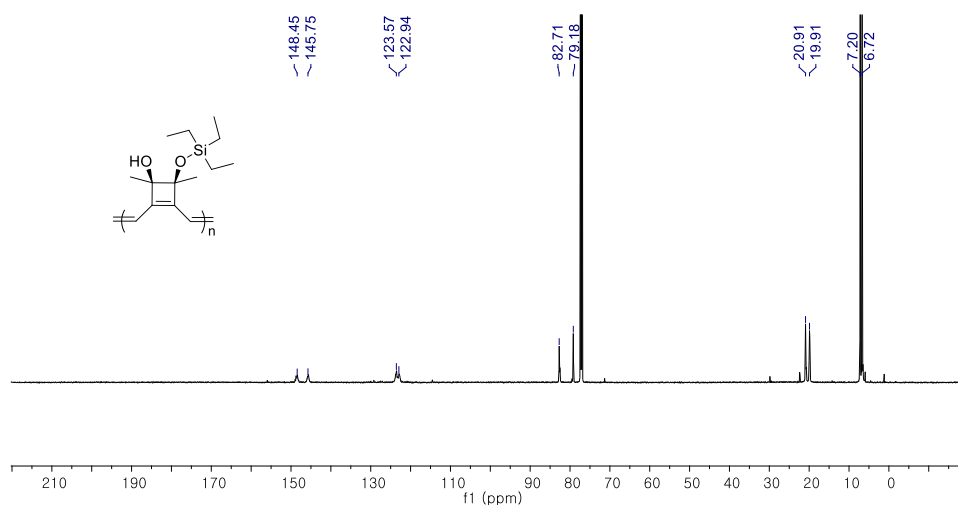
An NMR tube was filled with monomer (0.125 mmol, 10 eq), purged with argon, and  $\text{DCM-}d_2$  (300  $\mu\text{L}$ ) was added. A 4-mL vial containing initiator (0.0156 mmol, 1.25 eq) was argon-purged, and hexamethyldisilane was added as an internal standard. The total amount of initiator was 5/4 of the amount used for the reaction; after dissolving those using  $\text{THF-}d_8$  (250  $\mu\text{L}$ ), 1/5 (50  $\mu\text{L}$ ) of it was diluted in another NMR tube and used for checking the ratio between initial carbene and the internal standard. Then, the remaining 200  $\mu\text{L}$  of initiator solution was added to monomer solution and  $^1\text{H}$  NMR measurement was recorded over time.

## <sup>1</sup>H and <sup>13</sup>C NMR spectra of polymers

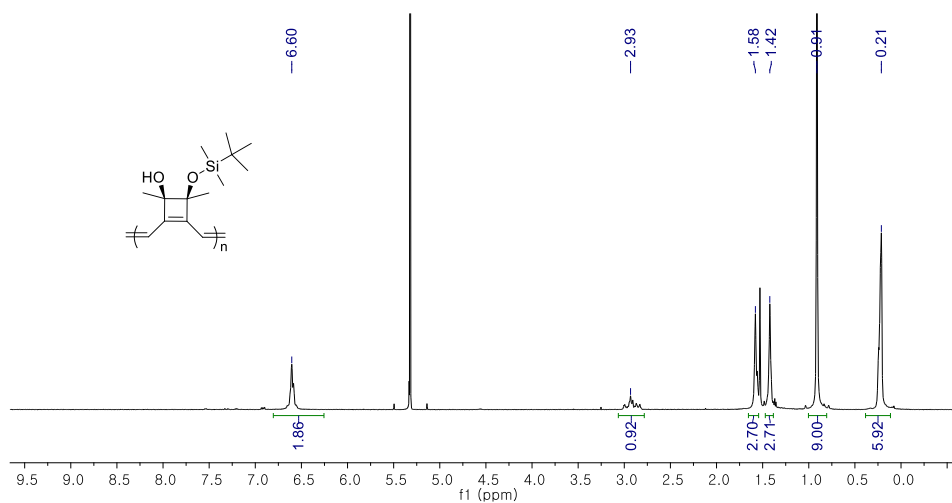
**P3** ( $^1\text{H}$  NMR,  $\text{CD}_2\text{Cl}_2$ )



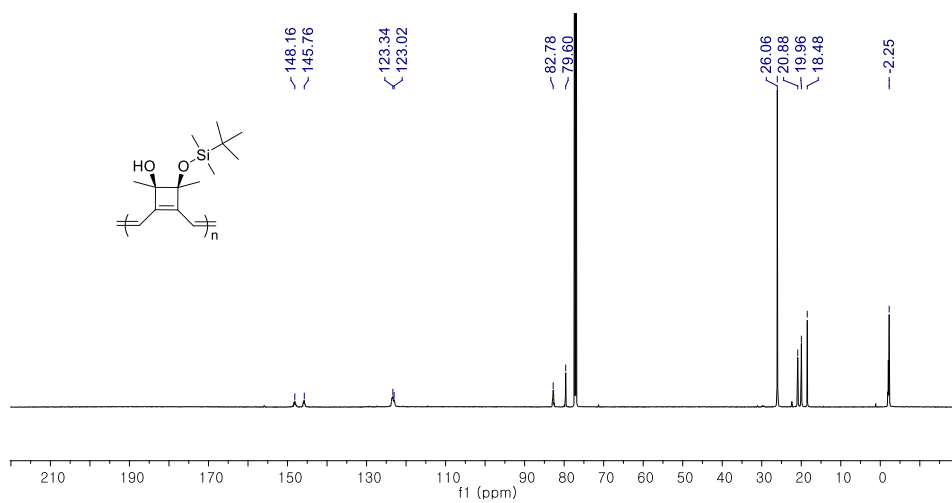
**P3** ( $^{13}\text{C}$  NMR,  $\text{CDCl}_3$ )



**P4** ( $^1\text{H}$  NMR,  $\text{CD}_2\text{Cl}_2$ )

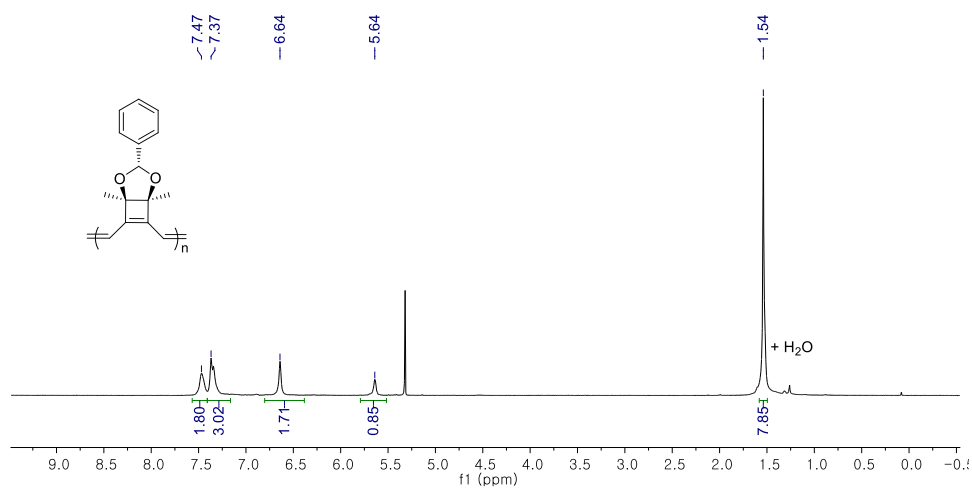


**P4** ( $^{13}\text{C}$  NMR,  $\text{CDCl}_3$ )

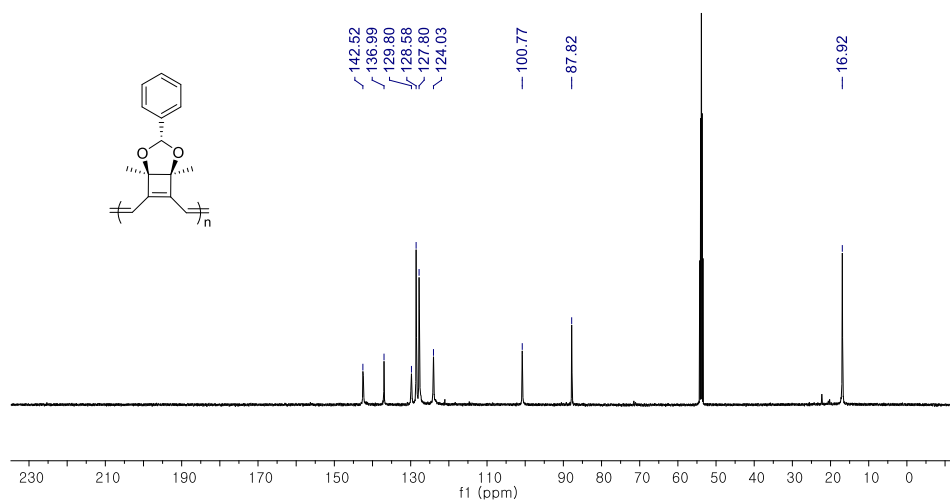




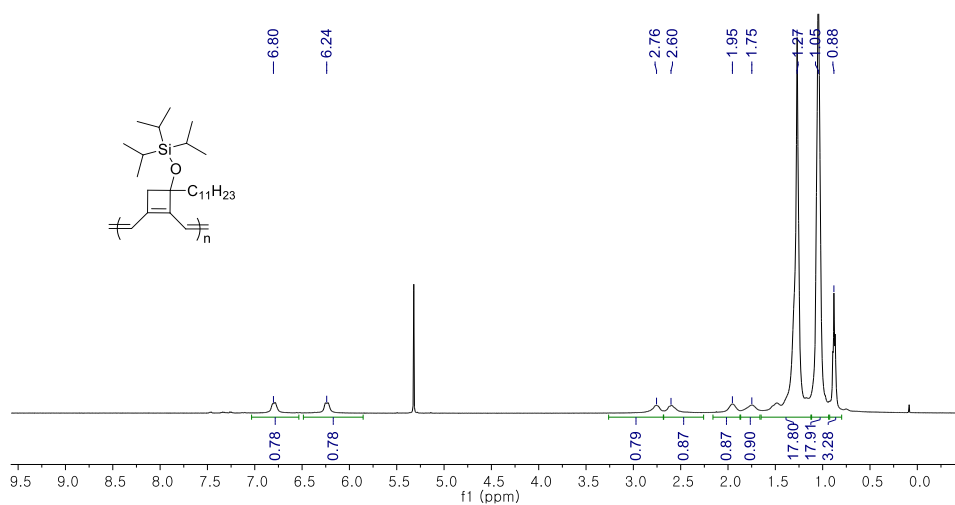
**P6** ( $^1\text{H}$  NMR,  $\text{CD}_2\text{Cl}_2$ )



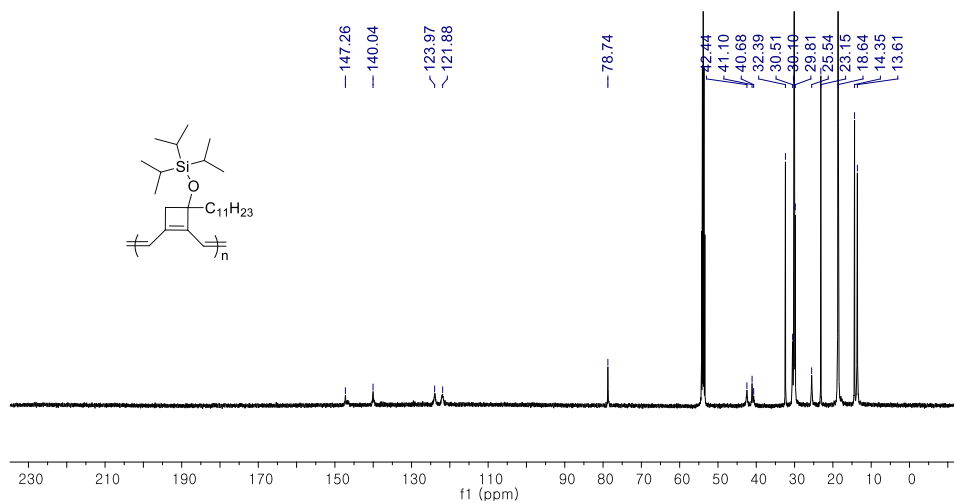
**P6** ( $^{13}\text{C}$  NMR,  $\text{CD}_2\text{Cl}_2$ )



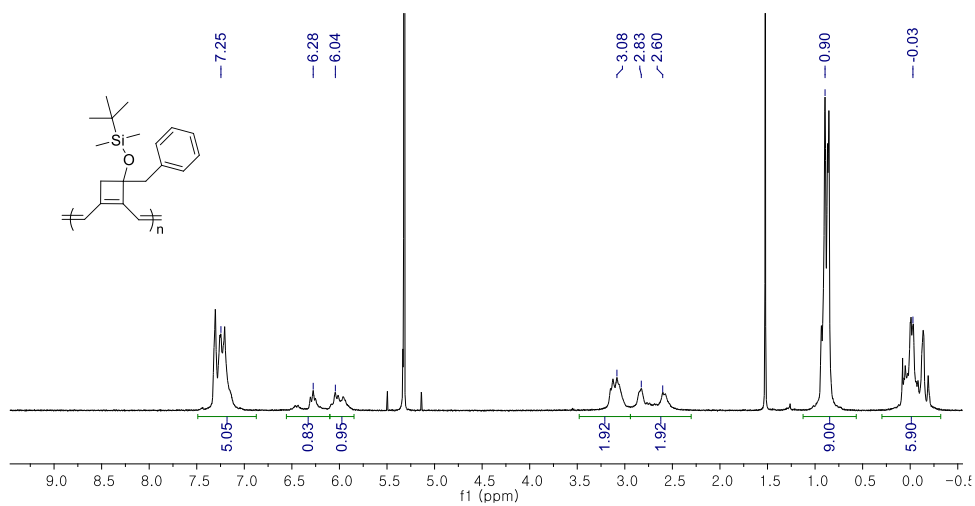
**P8** ( $^1\text{H}$  NMR,  $\text{CD}_2\text{Cl}_2$ )



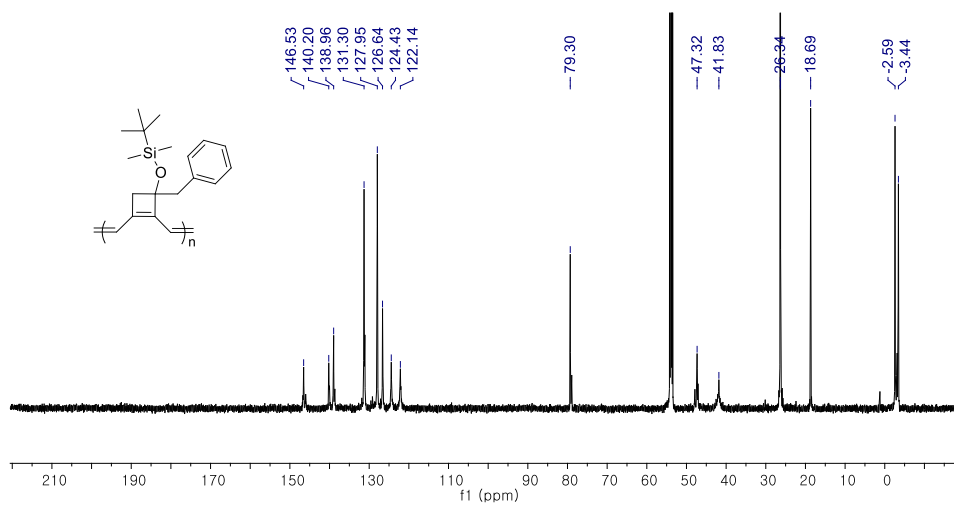
**P8** ( $^{13}\text{C}$  NMR,  $\text{CD}_2\text{Cl}_2$ )



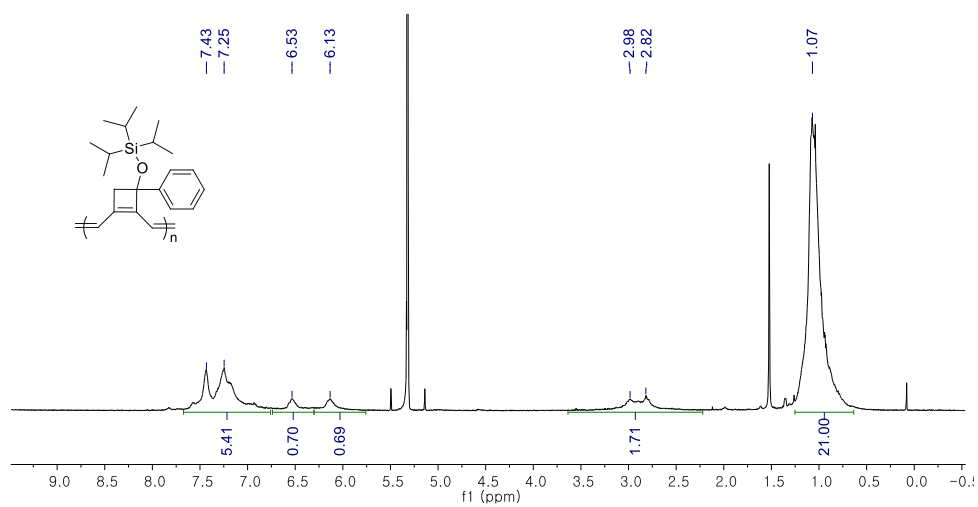
**P9** ( $^1\text{H}$  NMR,  $\text{CD}_2\text{Cl}_2$ )



**P9** ( $^{13}\text{C}$  NMR,  $\text{CD}_2\text{Cl}_2$ )



**P11** ( $^1\text{H}$  NMR,  $\text{CD}_2\text{Cl}_2$ )



### 3.7. References

- (1) Peterson, G. I.; Yang, S.; Choi, T. L. *Acc. Chem. Res.* **2019**, *52*, 994–1005.
- (2) Buchmeiser, M. R. *Polymer Reviews*, **2017**, *57*, 15-30.
- (3) Choi, S.-K.; Gal, Y.-S.; Jin, S.-H.; Kim, H.-K. *Chem. Rev.* **2000**, *100*, 1645–1681.
- (4) Krause, J. O.; Zarka, M. T.; Anders, U.; Weberskirch, R.; Nuyken, O.; Buchmeiser, M. R. *Angew. Chem., Int. Ed.* **2003**, *42*, 5965–5969.
- (5) Kang, E.-H.; Lee, I. S.; Choi, T.-L. *J. Am. Chem. Soc.* **2011**, *133*, 11904–11907.
- (6) Kang, E.-H.; Yu, S. Y.; Lee, I. S.; Park, S. E.; Choi, T.-L. *J. Am. Chem. Soc.* **2014**, *136*, 10508–10514.
- (7) Kang, E. H.; Kang, C.; Yang, S.; Oks, E.; Choi, T. L. *Macromolecules* **2016**, *49*, 6240–6250.
- (8) Jung, K.; Kang, E. H.; Sohn, J. H.; Choi, T. L. *J. Am. Chem. Soc.* **2016**, *138*, 11227–11233.
- (9) Jung, K.; Hong, M.; Kwon, S.; Kim, K.; Hong, S. H.; Choi, T.-L.; Baik, M. H. *J. Am. Chem. Soc.* **2018**, *140*, 834–841.
- (10) Jung, K.; Kim, K.; Sung, J. C.; Ahmed, T. S.; Hong, S. H.; Grubbs, R. H.; Choi, T. L. *Macromolecules* **2018**, *51*, 4564–4571.
- (11) Jung, K.; Ahmed, T. S.; Lee, J.; Sung, J. C.; Keum, H.; Grubbs, R. H.; Choi, T. L. *Chem. Sci.* **2019**, *10*, 8955–8963.
- (12) Naumann, S.; Unold, J.; Frey, W.; Buchmeiser, M. R. *Macromolecules* **2011**, *44*, 8380–8387.
- (13) Lee, I. S.; Kang, E.-H.; Park, H.; Choi, T.-L. *Chem. Sci.* **2012**, *3*, 761–765.
- (14) Unold, J.; Wang, D.; Frey, W.; Buchmeiser, M. R. *Polym. Chem.* **2013**, *4*, 4219–4233.
- (15) Park, H.; Lee, H.-K.; Choi, T.-L. *Polym. Chem.* **2013**, *4*, 4676–4681.

- (16) Park, H.; Lee, H.-K.; Kang, E.-H.; Choi, T.-L. *J. Polym. Sci., Part A: Polym. Chem.* **2015**, *53*, 274–279.
- (17) Herz, K.; Unold, J.; Hännle, J.; Schowner, R.; Sen, S.; Frey, W.; Buchmeiser, M. R. *Macromolecules* **2015**, *48*, 4768–4778.
- (18) Song, J.-A.; Park, S.; Kim, T.-S.; Choi, T.-L. *ACS Macro Lett.* **2014**, *3*, 795–798.
- (19) Song, J. -A.; Choi, T. L. *Macromolecules* **2017**, *50*, 2724–2735.
- (20) Bach, R. D.; Dmitrenko, O. *J. Am. Chem. Soc.* **2004**, *126*, 4444-4452.
- (21) Lee, K. S.; Choi, T.-L. *Org. Lett.* **2011**, *13*, 3908–3911.
- (22) Maughon, B. R.; Grubbs, R. H. *Macromolecules* **1997**, *30*, 3459–3469.
- (23) Parker, K. A.; Sampson, N. S. *Acc. Chem. Res.* **2016**, *49*, 408–417.
- (24) Randall, M. L.; Tallarico, J. A.; Snapper, M. L. *J. Am. Chem. Soc.* **1995**, *117*, 9610-9611.
- (25) Zuercher, W. J.; Hashimoto, M.; Grubbs, R. H. *J. Am. Chem. Soc.* **1996**, *118*, 6634-6640.
- (26) Nicolaou, K. C.; Vega, J. A.; Vassilikogiannakis, G. *Angew. Chem., Int. Ed.* **2001**, *40*, 4441-4445.
- (27) Mori, M.; Wakamatsu, H.; Tonogaki, K.; Fujita, R.; Kitamura, T.; Sato, Y. *J. Org. Chem.* **2005**, *70*, 1066-1069.
- (28) Weatherhead, G. S.; Ford, J. G.; Alexanian, E. J.; Schrock, R. R.; Hoveyda, A. H. *J. Am. Chem. Soc.* **2000**, *122*, 1828-1829.
- (29) Kusumoto, T.; Hiyama, T. *Chem. Lett.* **1988**, *7*, 1149-1152.
- (30) Maciejewski, J. L.; Bazan, G. C.; Rodriguez, G. *Organometallics* **1995**, *14*, 3357-3363.
- (31) Anders, U.; Krause, J. O.; Wang, D.; Nuyken, O.; Buchmeiser, M. R. *Designed Monomers and Polymers*, **2004**, *7*, 151– 163.
- (32) Debleds, O.; Campagne, J. M. *J. Am. Chem. Soc.* **2008**, *130*, 1562-1563.
- (33) Fürstner, A.; Ackermann, L.; Gabor, B.; Goddard, R.; Lehmann, C.W.; Mynott,

- R.; Stelzer, F.; Thiel, O.R. *Chem.–A Eur. J.* **2001**, *7*, 3236-3253.
- (34) Kim, K. O.; Kim, J.; Choi, T. L. *Macromolecules*, **2014**, *47*, 4525-4529.
- (35) Park, H.; Lee, H.-K.; Choi, T.-L. *Polym. Chem.* **2013**, *4*, 4676-4681.
- (36) Love, J. A.; Morgan, J. P.; Trnka, T. M.; Grubbs, R. H. *Angew. Chem., Int. Ed.* **2002**, *41*, 4035-4037.
- (37) Song, J. A.; Park, B.; Kim, S.; Kang, C.; Lee, D.; Baik, M. H.; Grubbs, R. H.; Choi, T. L. *J. Am. Chem. Soc.* **2019**, *141*, 10039–10047.
- (38) Kim, K. O.; Shin, S. Y.; Kim, J. Y.; Choi, T.-L. *Macromolecules* **2014**, *47*, 1351-1359.
- (39) Scriban, C.; Amagai, B. S.; Stemmler, E. A.; Christensen, R. L.; Schrock, R. R. *J. Am. Chem. Soc.*, **2009**, *131*, 13441-13452.
- (40) Peach, M. J.; Tellgren, E. I.; Salek, P.; Helgaker, T.; Tozer, D. J. *J. Phys. Chem. A*, **2007**, *111*, 11930-11935.
- (41) Gutzler, R.; Perepichka, D. F. *J. Am. Chem. Soc.* **2013**, *135*, 16585-16594.
- (42) Sancho-García, J. C.; Pérez-Jiménez, A. J. *Phys. Chem. Chem. Phys.* **2007**, *9*, 5874-5879.
- (43) Kertesz, M.; Choi, C. H.; Yang, S. *Chem. Rev.*, **2005**, *105*, 3448-3481.
- (44) Alabugin, I. V.; Timokhin, V. I.; Abrams, J. N.; Manoharan, M.; Abrams, R.; Ghiviriga, I. *J. Am. Chem. Soc.* **2008**, *130*, 10984-10995.
- (45) Shiina, I.; Umezaki, Y.; Kuroda, N.; Iizumi, T.; Nagai, S.; Katoh, T. *J. Org. Chem.* **2012**, *77*, 4885-4901.
- (46) López, F.; Castedo, L.; Mascareñas, J. L. *J. Am. Chem. Soc.* **2002**, *124*, 4218-4219.
- (47) Yan, W.; Wang, Q.; Chen, Y.; Petersen, J. L.; Shi, X. *Org. Lett.* **2010**, *12*, 3308-3311.

## **Chapter 4. Living Metathesis & Metallotropy Polymerization for the Synthesis of Conjugated Polyenynes from Multialkynes**

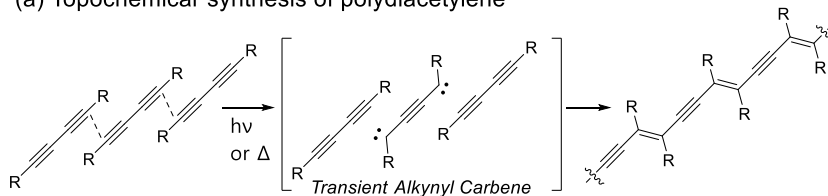
### **4.1. Abstract**

To date, olefin metathesis polymerizations using Grubbs catalysts have been widely used to produce well-defined polyalkenomers. In this chapter, we demonstrate cascade polymerization where olefin metathesis and metallotropic 1,3-shift reactions occur to form unique conjugated polymers consisting of sequence-specific polyenynes. By rationally designing a series of tetra-, penta-, and hexayne monomers, we achieved highly selective cascade transformations via ring-closing/metallotropic 1,3-shift/ring-closing reactions to produce polyenynes with high molecular weights. Furthermore, living polymerization was realized to give controlled molecular weights and narrow dispersities ( $\bar{D}$ ). Detailed kinetic investigations of the polymerization mechanism conducted using *in situ* NMR analysis confirmed that the metallotropic 1,3-shift was a fast process and the stability of the propagating carbene improved upon addition of a pyridine ligand. Thus, block copolymers were successfully synthesized, making this cascade polymerization approach a useful tool for preparing a new class of conjugated polymers.

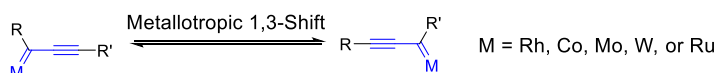


## 4.2. Introduction

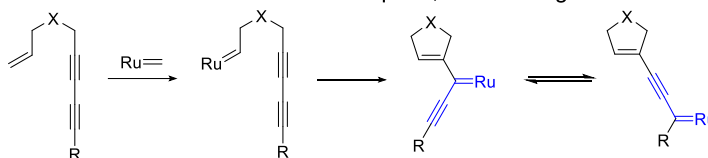
### (a) Topochemical synthesis of polydiacetylene



### (b) Metallotropic 1,3-shift of alkynyl carbenes involving transition metals



### (c) Tandem olefin metathesis/metallotropic 1,3-shift using Grubbs catalyst



**Scheme 4.1.** Previous Reactions Involving Alkynyl Carbenes

Conjugated polyenynes, such as polydiacetylenes, received much attention for their intriguing optoelectronic properties.<sup>1-3</sup> Most synthetic routes to conjugated polyenynes relied on topochemical polymerization, where transient alkynyl carbenes generated upon light irradiation or heating promotes polymerization when the diacetylene monomers are strictly aligned in proximity (Scheme 4.1.a).<sup>4,5</sup>

In contrast to the transient alkynyl carbenes generated by light or heat during topochemical polymerization, transition metal complexes can form stable yet reactive alkynyl carbenes.<sup>6</sup> In particular, various alkynyl carbenes of Rh,<sup>7</sup> Co,<sup>8,9</sup> Mo,<sup>8</sup> W,<sup>8</sup> and Ru<sup>11-16</sup> undergo a unique rearrangement with an adjacent carbon–carbon triple bond, known as a metallotropic 1,3-shift (Scheme 4.1.b). More interestingly, the Lee group reported a ring-closing metathesis reaction followed by a metallotropic 1,3-shift from Ru-alkylidenes<sup>11-16</sup> to prepare various complex

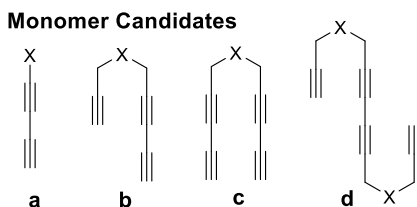
oligoenynes and natural products<sup>17,18</sup> (Scheme 4.1.c). We envisioned that this reaction could be a genuine way to incorporate internal triple bonds in the polymer backbone for the synthesis of conjugated polyenynes.

In Chapter 3, we describe the synthesis of a new class of conjugated polyenynes by combining olefin metathesis and metallotropic 1,3-shift reactions using Grubbs catalyst, which we call cascade metathesis and metallotropy (M&M) polymerization. In contrast to previously reported olefin metathesis polymerizations such as ring-opening metathesis polymerization (ROMP), acyclic diene metathesis (ADMET) polymerization,<sup>19,20</sup> cyclopolymerization (CP)<sup>21,22</sup>, and tandem olefin metathesis polymerizations,<sup>23-26</sup> M&M polymerization exploits two fundamentally different transformations, olefin metathesis and a nonmetathesis reaction (metallotropic 1,3-shift). As a result, unique conjugated polyenynes containing specific sequences of double bonds and triple bonds were prepared in a highly selective manner. Furthermore, we even achieved living cascade polymerization, making this a rare example of forming new triple bonds in a conjugated backbone by chain-growth polymerization.<sup>27,28</sup>

## 4.3 Results & Discussion

### 4.3.1. Polymerization of tetraynes

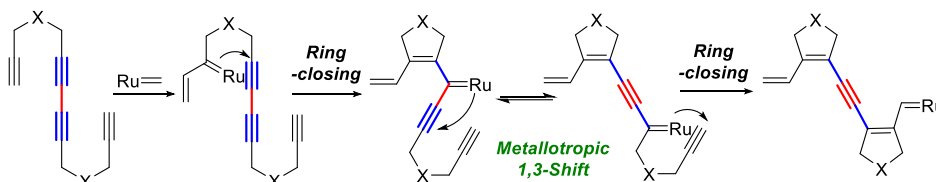
To realize successful tandem/cascade reactions, high efficiency of the whole process, as well as excellent selectivity of each reaction, is crucial. If each reaction deviates from the intended perfect relay owing to nonselective transformations or side reactions, the formation of ill-defined polymers is inevitable, especially in cascade polymerization. Therefore, understanding how to control the whole cascade sequence and designing appropriate monomers is the key to success.



**Figure 4.1.** Design of monomers for cascade M&M polymerization.

For this cascade M&M polymerization, we designed a series of monomers (**a–d**) that could potentially undergo both olefin metathesis and metallotropic 1,3-shift reactions to give conjugated polyenynes (Figure 4.1). The simplest diyne structure **a** was expected to form a polydiacetylene, but the desired M&M polymerization failed (Table S4.1). Moreover, another monomer containing a terminal diyne, **b**, also showed low polymerization efficiencies (Table S4.2). We suspected that the resulting propagating species from **a**, consisting of a 1,1-disubstituted Ru carbene, became less active for the desired cascade polymerization, analogous to terminal alkyne polymerization,<sup>29,30</sup> or new alkynyl carbenes (propagating species for **a** or **b**) were not reactive enough for further propagation.<sup>13,17</sup> Unfortunately, structure **c** containing two terminal diynes

decomposed rapidly. Finally, we designed monomer **d**, tetradeca-1,6,8,13-tetrayne, as the symmetric and stable internal diyne moiety should produce a uniform polyenyne backbone (Scheme 4.2).



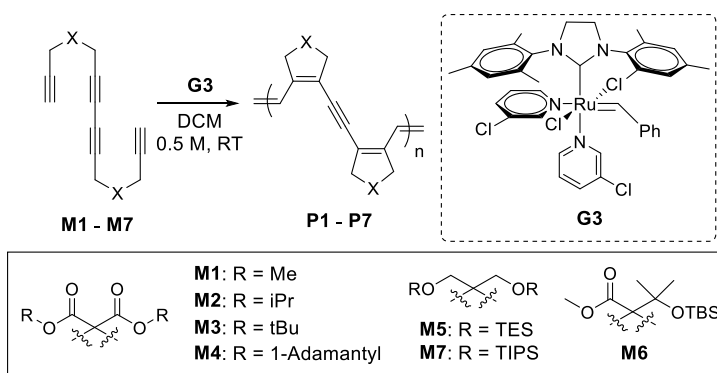
**Scheme 4.2.** Mechanism of Cascade M&M Polymerization of Tetradeca-1,6,8,13-tetrayne Derivatives

Based on this design principle, we prepared various monomers, **M1–M7**, by 3–5 simple synthetic steps, and tested M&M polymerization using a fast-initiating third generation Grubbs catalyst (**G3**), which was the optimal catalyst for successful CP (Table 4.1).<sup>21,22</sup> First, monomer **M1** containing a dimethyl malonate moiety was polymerized in dichloromethane (DCM) with a monomer to initiator ratio (M/I) of 25, and the reaction solution rapidly turned red. Complete conversion was achieved within 1 h at room temperature, giving a high yield (95%) of **P1**. This polymer was highly soluble in common organic solvents, such as chloroform, DCM, and tetrahydrofuran (THF), and its molecular weight ( $M_n = 14.8$  kDa) and dispersity ( $\mathcal{D} = 1.64$ ) were measured by SEC in THF (entry 1). At M/I = 50, **P1** with a higher  $M_n$  (26.6 kDa) was obtained in 84% conversion (entry 2). With **M2**, which contained larger isopropyl side chains, the polymerization efficiency increased slightly to 91% conversion at M/I = 50 ( $M_n = 33.9$  kDa, entry 3). Monomer **M3**, with an even bulkier di-*tert*-butyl malonate moiety, showed better polymerization efficiency, giving 98% conversion at M/I = 50 ( $M_n = 34.9$  kDa,

entry 4). The molecular weight of this polymer further increased to 42.7 kDa at M/I = 75 (80% conversion, entry 5).

Encouraged by the positive influence of the steric effect, we maximized the size by introducing an adamantyl group (**M4**), but the conversion decreased to 76% at M/I = 50 (entry 6), suggesting that steric factors only improved the polymerization efficiency to a certain degree. Another monomer containing triethylsilyl (TES) ether groups (**M5**) was polymerized successfully, resulting in >99% and 95% conversion at M/I = 25 ( $M_n$  = 15.8 kDa, entry 7) and M/I = 50 ( $M_n$  = 22.0 kDa, entry 8), respectively. Furthermore, monomer **M6**, containing methyl ester and *gem*-dimethyl *tert*-butyldimethylsilyl (TBS) ether groups, also showed good polymerization, giving >99% and 84% conversion at M/I = 25 ( $M_n$  = 20.0 kDa, entry 9) and M/I = 50 ( $M_n$  = 27.0 kDa, entry 10), respectively.

**Table 4.1. Cascade M&M Polymerization of Various Monomers**



entry	monomer	M/I	time (h)	conv (%) <sup>a</sup>	yield (%)	<i>M<sub>n</sub></i> (kDa) <sup>b</sup>	<i>D<sup>b</sup></i>
1	<b>M1</b>	25	1	> 99	95	14.8	1.64
2	<b>M1</b>	50	2	84	79	26.6	2.33
3	<b>M2</b>	50	1	91	82	33.9	1.69
4	<b>M3</b>	50	2	98	94	34.9	1.62
5	<b>M3</b>	75	4	80	74	42.7	1.77
6	<b>M4</b>	50	3	76	74	28.0	1.99
7	<b>M5</b>	25	1	> 99	96	15.8	1.45
8	<b>M5</b>	50	2	95	88	22.0	1.90
9	<b>M6</b>	25	2	> 99	86	20.0	1.45
10	<b>M6</b>	50	4	84	84	27.0	1.75
11 <sup>c</sup>	<b>M3</b>	50	4	89	81	31.3	1.45
12 <sup>d</sup>	<b>M3</b>	50	2	83	76	33.7	1.84
13 <sup>e</sup>	<b>M3</b>	50	3	97	93	36.4	1.39
14 <sup>e</sup>	<b>M3</b>	10	0.33	99	95	8.4	1.11
15 <sup>e</sup>	<b>M3</b>	25	0.83	98	98	22.2	1.15
16 <sup>e</sup>	<b>M3</b>	40	2.5	97	91	30.6	1.29
17 <sup>e</sup>	<b>M1</b>	25	0.42	97	93	12.8	1.30
18 <sup>e</sup>	<b>M2</b>	25	0.67	> 99	98	16.8	1.15
19 <sup>e</sup>	<b>M2</b>	50	1.5	91	91	35.8	1.32

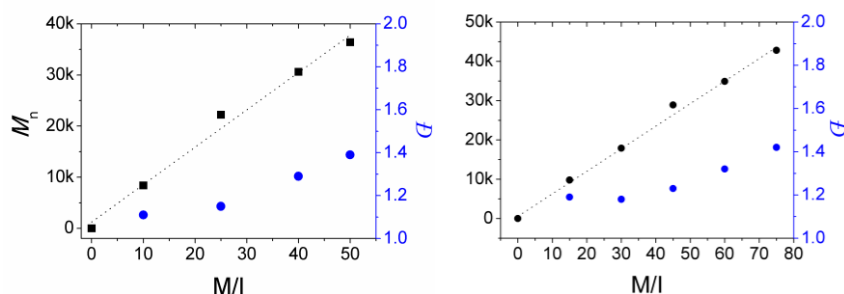
**Table 4.1. Continued**

entry	monomer	M/I	time (h)	conv (%) <sup>a</sup>	yield (%)	<i>M<sub>n</sub></i> (kDa) <sup>b</sup>	<i>Đ</i> <sup>b</sup>
20 <sup>e</sup>	<b>M5</b>	25	0.83	> 99	97	18.1	1.14
21 <sup>e</sup>	<b>M5</b>	50	3	> 99	98	31.2	1.38
22 <sup>e</sup>	<b>M6</b>	25	0.83	90	84	18.0	1.33
23 <sup>f</sup>	<b>M7</b>	15	1	98	94	9.8	1.19
24 <sup>f</sup>	<b>M7</b>	30	1.7	> 99	97	17.9	1.18
25 <sup>f</sup>	<b>M7</b>	45	2.5	96	95	28.9	1.23
26 <sup>f</sup>	<b>M7</b>	60	4	97	97	34.9	1.32
27 <sup>f</sup>	<b>M7</b>	75	5	91	83	42.8	1.42

<sup>a</sup>Calculated from <sup>1</sup>H NMR. <sup>b</sup>Determined by THF size-exclusion chromatography (SEC) calibrated using polystyrene standards <sup>c</sup>Reaction conducted at 0 °C. <sup>d</sup>THF was used as solvent. <sup>e</sup>20 mol% of 3,5-dichloropyridine was added. <sup>f</sup>13 mol% of 3,5-dichloropyridine was added and chloroform was used as solvent (0.15 M) for better solubility. *M<sub>n</sub>* and *Đ* were determined by chloroform SEC calibrated using polystyrene standards.

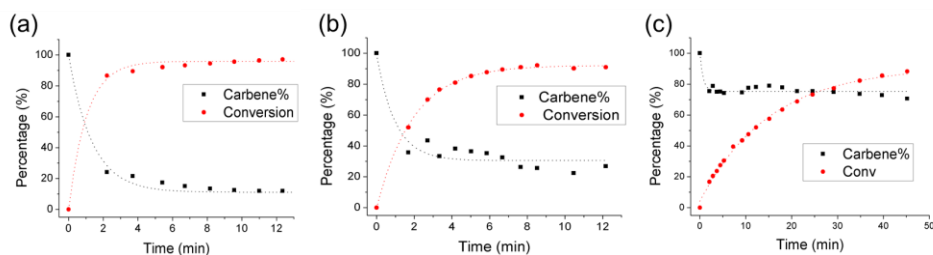
However, all the resulting polymers (in Table 4.1, entries 1–10) generally showed broad SEC traces and *Đ* values due to the chain transfer reaction and the catalyst decomposition. Based on the mechanistic similarity between cascade M&M polymerization and CP, we also tried several strategies that have been effective for improving the control of CP to suppress carbene decomposition during polymerization.<sup>32</sup> First, polymerization at a lower temperature (0 °C) was tested with the best monomer, **M3**, but despite a narrower *Đ* (1.45), the conversion was lower (89% at M/I = 50, entry 11). Second, THF, the optimal solvent for CP, was used as a weakly coordinating solvent, but the result was even less satisfactory (83% conversion at M/I = 50, *Đ* = 1.84, entry 12). Gratifyingly, with a weakly

coordinating ligand, 3,5-dichloropyridine, as an additive, **P3** with a high conversion of 97% ( $M/I = 50$ ) and the lowest  $\bar{D}$  of 1.39 was obtained (entry 13) because the additive effectively hindered the catalyst decomposition and also chain transfer reaction (Figure S4.1). Under the optimized condition, the  $M_n$  of **P3** increased linearly for  $M/I$  of 10–50 with excellent conversions and yields. Further, narrow  $\bar{D}$  values were obtained at  $M/I = 10$  (1.11), 15 (1.15), and 40 (1.29) (Table 4.1, entries 14–16, Figure 4.3, Figure S4.2). Gratifyingly, under the same condition, other monomers (**M1**, **M2**, **M5**, and **M6**) also underwent such controlled polymerization to give excellent yields (up to 98%) and narrow  $\bar{D}$  ( $<1.4$ ) (entries 17–22). Finally, another monomer (**M7**) having even bulkier substituents, triisopropylsilyl (TIPS) ether groups, showed the best living polymerization in chloroform to give a linear increase in  $M_n$  with increasing  $M/I$  from 15 (9.8 kDa) to 75 (42.8 kDa, 137 cyclopentene units in one chain) with excellent conversions and yields as well as narrow  $\bar{D}$  values with  $M/I = 15$  (1.19), 30 (1.18), 45 (1.23), and 60 (1.32) (Table 4.1, entries 23–27, Figure 4.3, Figure S4.2).



**Figure 4.3.** Plots of  $M_n$  vs  $M/I$  and corresponding  $\bar{D}$  values for **M3** (left) and **M7** (right).





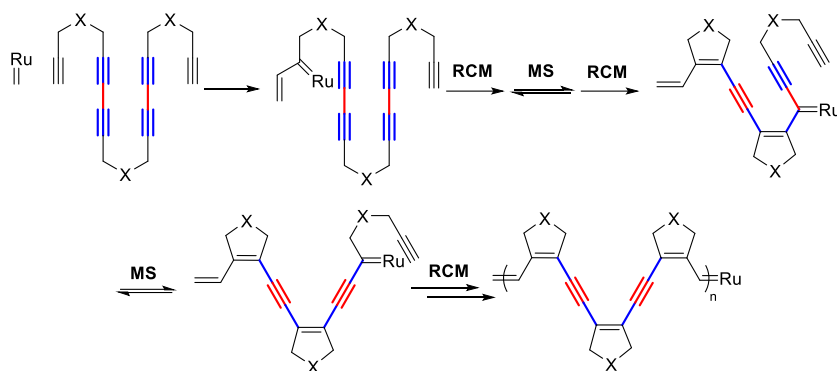
**Figure 4.4.** Conversions and carbene changes monitored by *in situ* NMR analysis during M&M polymerization ( $M/I = 20$ ) in  $CD_2Cl_2$  using (a) **M1**, (b) **M3**, and (c) **M3** with 3,5-dichloropyridine (10 equiv to **G3**).

To investigate M&M polymerization in detail, we conducted a kinetic analysis of **M1** ( $M/I = 20$ ) by *in situ* NMR in  $CD_2Cl_2$  at room temperature, and found that the conversion reached almost 90% in 2 min (Figure 4.4.a). This rate was comparable to that of CP using 1,6-heptadiyne monomers,<sup>31</sup> implying that the metallotropic 1,3-shift was a fast transformation. However, the lifetime of the propagating carbene from **M1** was short, with only 22% of the carbene remaining after 2 min. We also conducted this kinetic experiment using one of the best monomer, **M3**, thinking that its high activity arises from the Thorpe–Ingold effect of the bulky *tert*-butyl group, which should accelerate cyclization.<sup>33</sup> However, the polymerization of **M3** was slower than that of **M1**, taking 8 min to reach 90% conversion (Figure 4.4.b, Figure S4.3). Instead, decomposition of the propagating carbene from **M3** was also slower, with 40% of the carbene remaining after 2 min, suggesting that the bulky side chain suppressed carbene decomposition, thereby increasing polymerization efficiency. Moreover, adding 10 equiv of 3,5-dichloropyridine further suppressed carbene decomposition, resulting in 70% of the carbene remaining at 90% conversion, even though the propagation rate also

decreased owing to competitive coordination between the additive and **M3** (Figure 4.4.c). Analogous to the conclusions from previous mechanistic studies on CP,<sup>31,32</sup> the weakly coordinating ligand improved the stability of the propagating carbene during M&M polymerization. The polymerization followed first-order kinetics with respect to the monomer concentration indicating that all the intramolecular reaction steps, especially the metallotropic 1,3-shift, are faster than the intermolecular propagation reaction.

Furthermore, the structures of the polymers were fully characterized by <sup>1</sup>H and <sup>13</sup>C NMR, MALDI (Figure S4.4), IR analyses (Figure S4.5), and also by comparing NMR spectra with an analogous model compound (Scheme S4.1), confirming that the cascade M&M polymerization proceeded via a ring-closing/metallotropic 1,3-shift/ring-closing sequence, as designed. The  $\alpha$ -addition and 5-membered ring cyclization steps occurred exclusively, as confirmed by <sup>13</sup>C NMR (Figure S4.6). The metallotropic 1,3-shift must have been selective and efficient, otherwise neither the second cyclization nor the selective polymerization would occur. Additionally, two olefin peaks were observed at 6.6 and 6.3 ppm by <sup>1</sup>H NMR (7.8:1 ratio), corresponding to *trans*- and *cis*-olefins (in the polymer backbone), respectively. This minor amount of *cis*-olefin readily isomerized to *trans*-olefin when the polymer solution in chloroform was irradiated with a blue LED, analogous to the case of CP (Figure S4.7).<sup>34</sup>

### 4.3.2. Polymerization of hexaynes / Block copolymerization



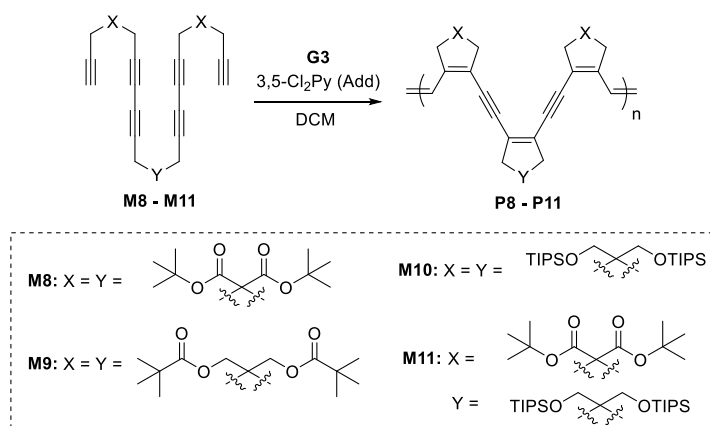
**Scheme 4.3.** Mechanism of Cascade M&M Polymerization of Henicosa-1,6,8,13,15,20-hexayne Derivatives Undergoing Three Ring-Closing Metathesis (RCM) and Two Metallotropic 1,3-Shift (MS)

To broaden the scope of cascade M&M polymerization, we attempted increasing the number of the cascade sequences. In this regard, another class of complex monomers was designed to contain a total of six alkynes including two internal diynes. They were envisioned to undergo three RCM and two MS reactions sequentially to generate conjugated polymers with four double bonds, two triple bonds, and three cyclopentene moieties in each repeat unit (Scheme 4.3). Accordingly, four new monomers containing various bulky substituents were prepared, and their M&M polymerizations were tested using **G3** catalyst with 3,5-Cl<sub>2</sub>Py additive (Table 4.2, **M8** – **M11**). First, a monomer **M8** having di-*tert*-butylmalonate moiety was polymerized in DCM, reaching only 68% conversion with M/I = 25 (entry 1). Slightly higher temperature (35 °C) enhanced polymerization of **M8**, giving 96% and 88% conversions with better control for M/I = 10 ( $M_n$  = 9.6 kDa,  $\bar{D}$  = 1.20) and M/I = 25 ( $M_n$  = 19.9 kDa,  $\bar{D}$  = 1.35) respectively (entries 2 and 3). Another hexayne monomer **M9** containing pivaloyl

groups was also polymerized successfully giving > 99% and 90% conversions with  $M/I = 10$  ( $M_n = 9.9$  kDa,  $\bar{D} = 1.23$ ) and  $M/I = 25$  ( $M_n = 24.1$  kDa,  $\bar{D} = 1.38$ ) at room temperature (entries 4 and 5). Similar to the case for the analogous tetrayne monomer, **M7**, a hexayne monomer **M10** having bulky TIPS ether group showed the best result in chloroform with excellent conversions, yields, and control to give linear increase in  $M_n$  up to 30 kDa from  $M/I = 10$  to 35 (up to 105 cyclopentene units in one chain corresponding to 105 RCM and 70 MS reactions) with narrow  $\bar{D}$  values below 1.3 (entries 6 – 9, Figure 4.5).

Furthermore, the good living character of **M10** was indicated by *in situ* NMR analysis, which showed a high ratio of the propagating carbene (ca. 70%) during polymerization. Also, clear first-order kinetic relationship with the monomer concentration suggested that even with the long series of cascade reactions involving five independent steps, the intermolecular propagation reaction remains rate-limiting (Figure S4.8). Finally, from a monomer **M11** containing two different substituents, di-*tert*-butylmalonate (X) and TIPS ether groups (Y), **P11** having substituents with the specific YXX sequence in a repeat unit was successfully obtained with excellent conversion and high  $M_n$  of 30.8 kDa (entry 10).  $^1\text{H}$  and  $^{13}\text{C}$  NMR analyses confirmed that only one well-defined microstructure was produced, suggesting that the cascade sequence of RCM–MS–RCM–MS–RCM proceeded selectively and exclusively.

**Table 4.2. Cascade M&M Polymerization of Various Hexayne Monomers**

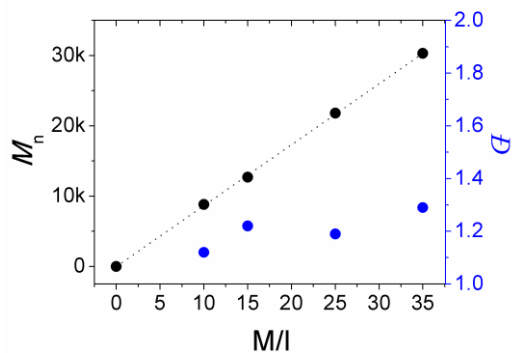


entry	monomer	M/I/Add	conc (M)	temp (°C)	time (h)	conv (%) <sup>a</sup>	yield (%) <sup>b</sup>	<i>M<sub>n</sub></i> (kDa) <sup>c</sup>	<i>Đ</i> <sup>c</sup>
1	<b>M8</b>	25/1/5	0.1	RT	1	68	66	16.7	1.48
2	<b>M8</b>	10/1/2	0.3	35	0.33	96	95	9.6	1.20
3	<b>M8</b>	25/1/5	0.3	35	0.67	88	82	19.9	1.35
4	<b>M9</b>	10/1/4	0.1	RT	1	> 99	91	9.9	1.23
5	<b>M9</b>	25/1/10	0.1	RT	2	90	90	24.1	1.38
6 <sup>d</sup>	<b>M10</b>	10/1/2	0.1	RT	1.5	92	88	8.8	1.12
7 <sup>d</sup>	<b>M10</b>	15/1/3	0.1	RT	2	96	91	12.7	1.22
8 <sup>d</sup>	<b>M10</b>	25/1/5	0.1	RT	4	94	86	21.8	1.19
9 <sup>d</sup>	<b>M10</b>	35/1/7	0.1	RT	6	> 99	87	30.3	1.29
10	<b>M11</b>	25/1/5	0.15	RT	1	> 99	92	30.8	1.59

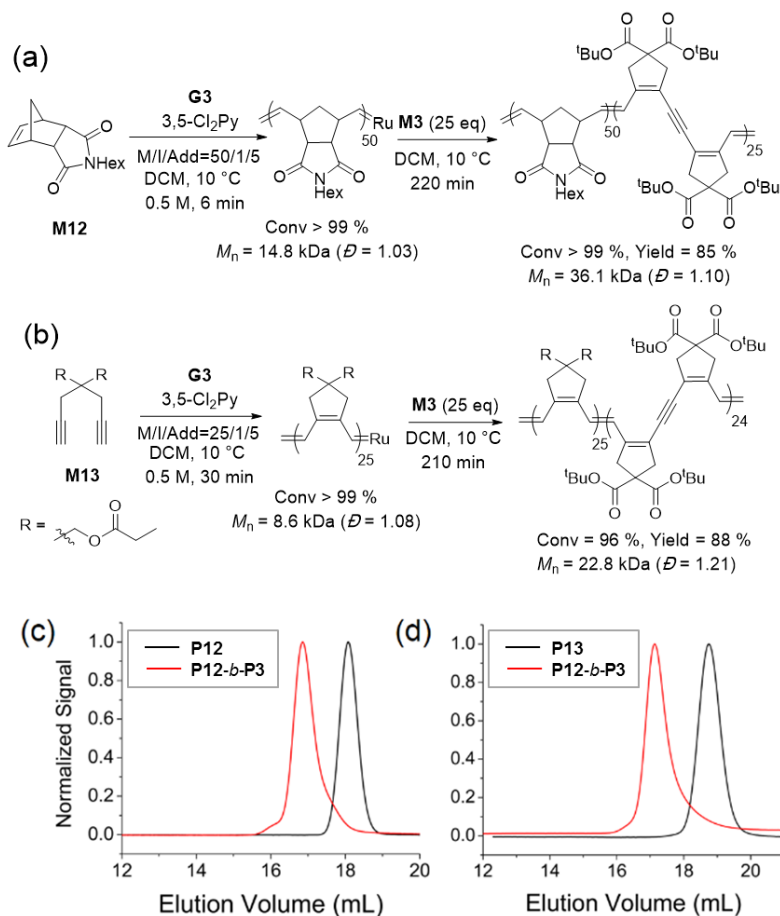
<sup>a</sup>Calculated from crude <sup>1</sup>H NMR. <sup>b</sup>Isolated yield. <sup>c</sup>Determined by chloroform

size-exclusion chromatography (SEC) calibrated using polystyrene standards.

<sup>d</sup>Chloroform was used as solvent.



**Figure 4.5.** A Plot of  $M_n$  vs  $M/I$  and corresponding  $D$  values for **P10**.

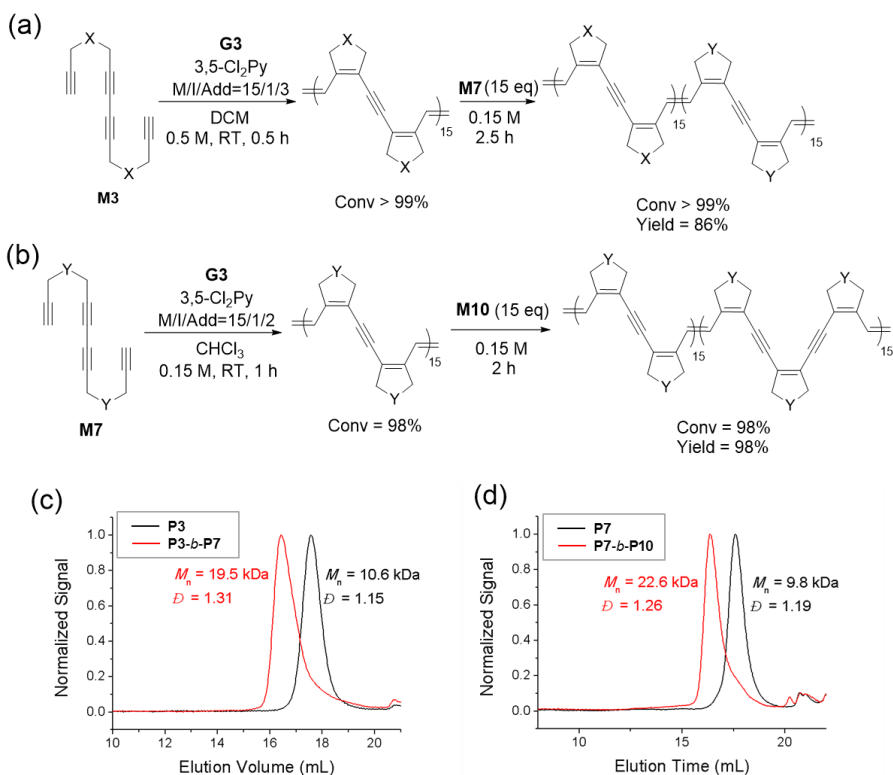


**Figure 4.6.** Syntheses of block copolymers by combining M&M polymerization with (a) ROMP of norbornene monomer **M12** and (b) CP of 1,6-heptadiyne monomer **M13**, and (c) and (d) corresponding SEC traces.

To synthesize block copolymers, we combined this new controlled cascade M&M polymerization with other living polymerization methods. First, ROMP of norbornene derivative **M12** was conducted using **G3** and 3,5-dichloropyridine (M/I/Add = 50/1/10) to prepare the first block, and then **M3** (25 equiv) was added to the same reaction pot to successfully produce block copolymer with an increase of  $M_n$  from 14.8 to 36.1 kDa and a narrow  $D$  of 1.10 (Figure 4.6.a). Furthermore, a new fully conjugated block copolymer was synthesized by first carrying out CP of 1,6-heptadiyne monomer **M13** (M/I/Add = 25/1/5), followed by M&M polymerization of **M3** (25 equiv) to increase  $M_n$  from 8.6 to 22.8 kDa with a narrow  $D$  of 1.21 (Figure 4.6.b). All block copolymerizations were conducted at 10 °C to optimize control, and both cases showed clear and complete shifts in the SEC traces (Figure 4.6. c,d).

In addition, using tetrayne and hexayne monomers that showed good controlled M&M polymerizations, we synthesized block copolymers having fully conjugated enyne chains in both blocks. First, **M3** was polymerized under the optimized condition to prepare the first block (M/I = 15,  $M_n$  = 10.6 kDa,  $D$  = 1.15), followed by addition of 15 equiv of **M7**. This resulted in the clear shift of SEC trace corresponding to **P3-b-P7** ( $M_n$  = 19.5 kDa,  $D$  = 1.31), confirming the successful block copolymerization from two tetraynes (Figure 4.7. a,c). Furthermore, another block copolymer was constructed by polymerizing a tetrayne **M7** as the first block (M/I = 15,  $M_n$  = 9.8 kDa,  $D$  = 1.19) followed by the

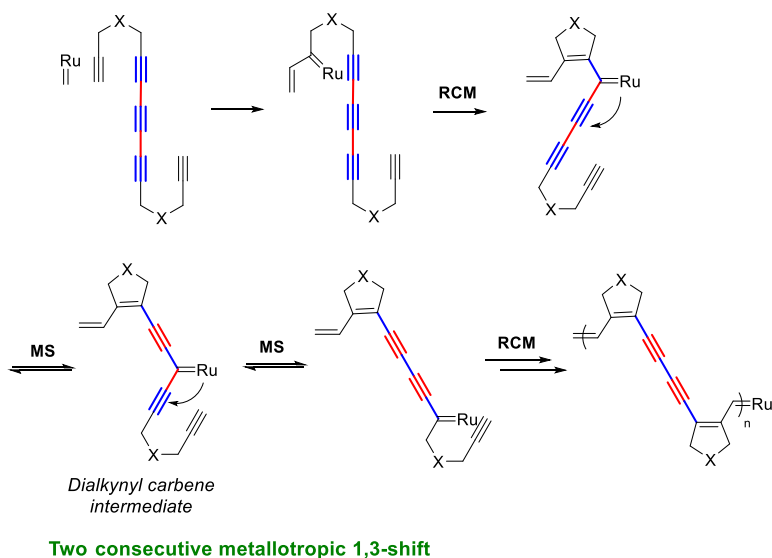
polymerization of a hexayne monomer **M10** (15 equiv) to cause complete shift of SEC trace, thereby making **P7-b-P10** with  $M_n$  of 22.6 kDa and  $\bar{D}$  of 1.26 (Figure 4.7. b,d). This is the first example of block copolymer syntheses consisting of fully conjugated polyenynes only, highlighting the uniqueness and versatility of this chain-growth M&M polymerization.



**Figure 4.7.** Syntheses of block copolymers via sequential M&M polymerization of (a) **M3** and **M7**, and (b) **M7** and **M10**, and (c), (d) their corresponding SEC traces.



### 4.3.3. Polymerization of pentaynes

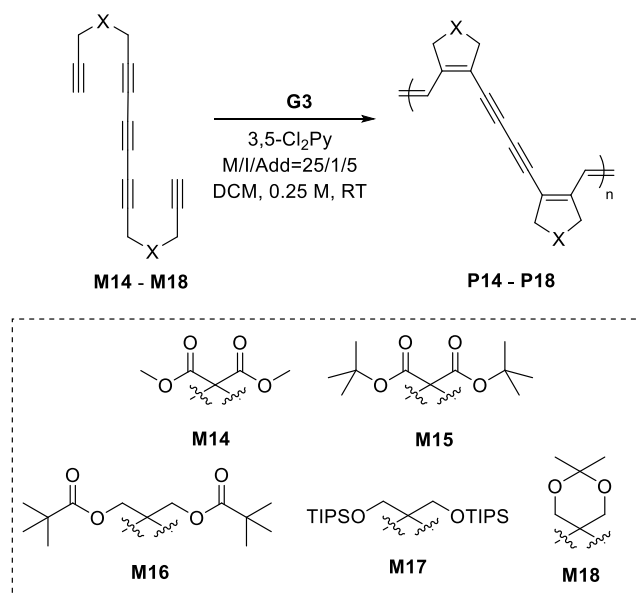


**Scheme 4.4.** Mechanism of Cascade M&M Polymerization of Hexadeca-1,6,8,10,15-pentayne Moiety Undergoing Two RCM and Two MS Sequences

The third class of new monomers was designed by introducing an internally conjugated 1,3,5-triynes functionality so that two consecutive metallotropic 1,3-shift may occur and form conjugated diyne structures.<sup>10,14</sup> We expected that hexadeca-1,6,8,10,15-pentayne derivatives would undergo the cascade M&M polymerization via the RCM–MS–MS–RCM sequence, as illustrated in Scheme 4.4, to give an unprecedented polyendiyne structure containing three conjugated alkenes (*Z-E-Z*) and one conjugated diyne in each repeat unit. Using the similar optimized polymerization condition, **M14** containing dimethylmalonate moiety was polymerized to 59% conversion by using **G3** (*M/I* = 25) and 3,5-Cl<sub>2</sub>Py in DCM (Table 4.3, entry 1, *M<sub>n</sub>* = 10.5 kDa, *D* = 2.32). We switched to monomers having bulkier ester groups such as di-*tert*-butylmalonate (**M15**) and pivaloyl group (**M16**) hoping that the conversion would improve. But under the same conditions, the

conversions were still 59% and 43% to give **P15** and **P16** with  $M_n$  of 17.4 kDa and 11.9 kDa respectively (entries 2 and 3). Furthermore, other monomers containing an ether such as TIPS (**M17**) and acetal (**M18**) were polymerized to give similar conversions (43% and 53%) with  $M_n$  of 14.4 kDa and 12.0 kDa respectively (entries 4 and 5). Unlike the previous M&M polymerizations, sterically bulky substituents did not enhance the polymerization efficiency of pentayne monomers, likely because the distance between Ru-carbene in dialkynyl carbene intermediate and the side chain (Scheme 4.4) is too far to stabilize the propagating carbene effectively (Figure S4.9). Despite relatively low turnover numbers and loss of control,  $M_n$ s of **P14** – **P18** were fairly high from 11 kDa to 17 kDa performing up to the average of 60 selective and specific transformations without any side reactions or defects which was confirmed by various characterizations such as  $^1\text{H}$  and  $^{13}\text{C}$  NMR, MALDI (**Figure S4.10**), and IR (**Figure S4.11**) analyses. In short, from various tetrayne, pentayne, and hexayne monomers, 16 different conjugated polyenynes having unique sequences of double and triple bonds were successfully synthesized with perfect cascade sequences.

**Table 4.3. Cascade M&M Polymerization of Various Pentayne Monomers**



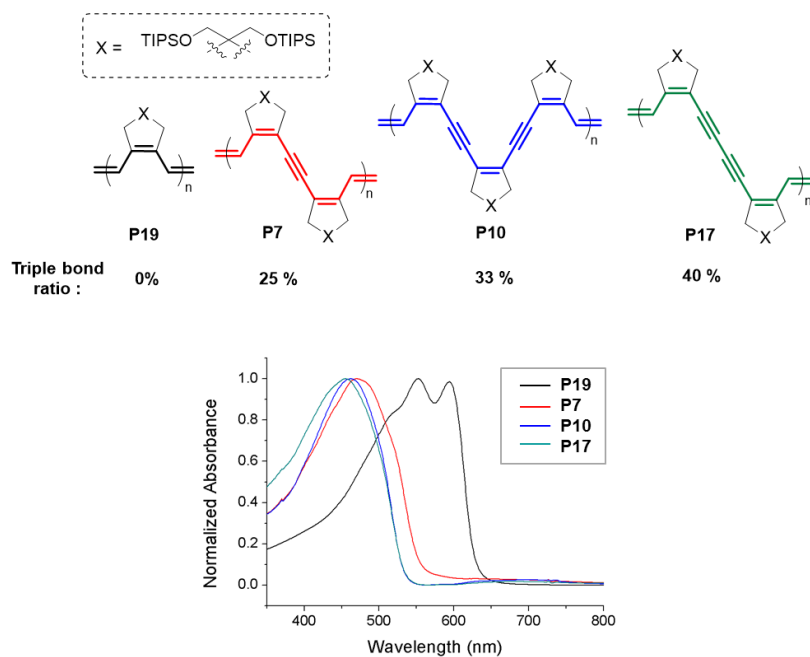
entry	monomer	time (h)	conv (%) <sup>a</sup>	yield (%) <sup>b</sup>	<i>M<sub>n</sub></i> (kDa) <sup>c</sup>	<i>D</i> <sup>c</sup>
1	<b>M14</b>	1	59	50	10.5	2.32
2	<b>M15</b>	1	59	53	17.4	1.57
3	<b>M16</b>	1	43	43	11.9	1.39
4	<b>M17</b>	2	43	43	14.4	1.61
5	<b>M18</b>	1	53	49	12.0	2.05

<sup>a</sup>Calculated from crude <sup>1</sup>H NMR. <sup>b</sup>Isolated yield. <sup>c</sup>Determined by chloroform

SEC calibrated using polystyrene standards.

#### 4.3.4. Optoelectronic properties of polymers

After preparing a library of diverse conjugated polyenynes, we measured their optical and electronic properties (**Table S4.3**). As shown in Figure 4.8, compared to the analogous conjugated polyene (**P19**) prepared by cyclopolymerization<sup>21,22</sup> which showed absorption maxima ( $\lambda_{\max}$ ) at 552 and 594 nm, polyenynes presented here having different portions of triple bond (**P7**: 25 %, **P10**: 33 %, **P17**: 40 %) showed much more blue-shifted UV-Vis spectra without any 0 – 0 vibronic peak. In particular, **P7** consisting of less triple bond (25 %) exhibited a higher  $\lambda_{\max}$  value (470 nm) compared to those of **P10** (33 %,  $\lambda_{\max} = 462$  nm), **P17** (40 %,  $\lambda_{\max} = 457$  nm), and conventional soluble polydiacetylenes (50%,  $\lambda_{\text{abs}} = 450 - 460$  nm)<sup>35</sup>. This implies that higher ratio of triple bond in the backbone tends to lower the conjugation length due to higher rotational freedom of single bonds adjacent to triple bonds.<sup>36,37</sup> Accordingly, the optical band gaps of **P7**, **P10**, and **P17** (2.2 – 2.3 eV) were significantly higher than that of **P19** (2.0 eV).<sup>38</sup> In addition, most polymers showed similar UV-Vis spectra in both solution and film, but interestingly, TIPS ether containing polymers **P7** and **P10** exhibited strong 0 – 0 vibronic peaks in the film state (Figure S4.12 and S4.13) presumably because the sterically bulky side chains would extend the backbone more rigidly. Furthermore, all the polymers **P1** – **P18** showed weak emission at  $\lambda_{\max} = 522 - 553$  nm (Figure S4.14,  $\phi_{\text{PL}} < 0.3$  %), analogous to soluble yellow polydiacetylenes.<sup>39</sup>



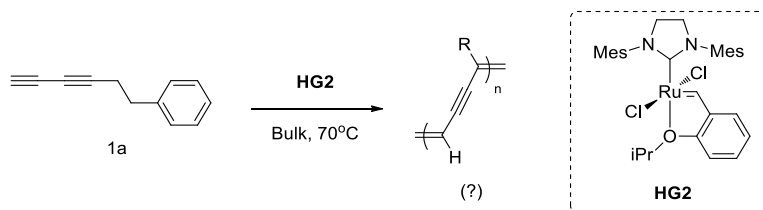
**Figure 4.8.** Various conjugated polyene and polyenynes synthesized by **G3** and their UV-Vis spectra in chloroform solution.

## 4.4. Conclusion

In conclusion, with the rational design of multialkyne monomers, we demonstrated a new cascade olefin metathesis/metallotropic 1,3-shift (M&M) polymerization, which expands the utility of user-friendly Grubbs catalysts in polymer synthesis. Thus far, this is the only example that uses metallotropic 1,3-shift of alkynyl transition metal carbenes in polymerization, allowing efficient generation of unique conjugated polyenylene backbones via a chain-growth mechanism with a specific ring-closing/metallotropic 1,3-shift/ring-closing sequence. The living polymerization efficiency of the tetradeca-1,6,8,13-tetrayne monomer could be enhanced by increasing the steric bulk of the side chains to give controlled  $M_n$  up to  $DP = 75$  and narrow  $D$ . More exotic substrates such as heneicosa-1,6,8,13,15,20-hexayne monomers underwent successful cascade living polymerization via five independent sequences of the intramolecular transformations to give new conjugated polyenyne consisting of four double bonds and two triple bonds in the repeat unit. Mechanistic studies using *in situ* NMR analyses revealed that tetrayne and hexayne monomers followed first-order kinetics, indicating that metallotropic 1,3-shift is a fast transformation. From tetrayne and hexayne monomers, block copolymers having fully conjugated polyenylene motifs in both blocks were successfully synthesized, highlighting the utility of M&M polymerization. Furthermore, other unique conjugated polyenyne containing conjugated diynes were prepared from hexadeca-1,6,8,10,15-pentayne monomers, undergoing two consecutive migratory shifts in a row. In brief, genuine designs of multi-yne monomers allowed easy and efficient syntheses of conjugated polyenyne with unique backbone motifs.

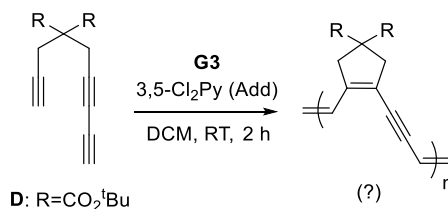
## 4.5. Supporting Figures

**Table S4.1.** Polymerization results of monomer **1a** (Structure ‘a’ in Figure 4.1)



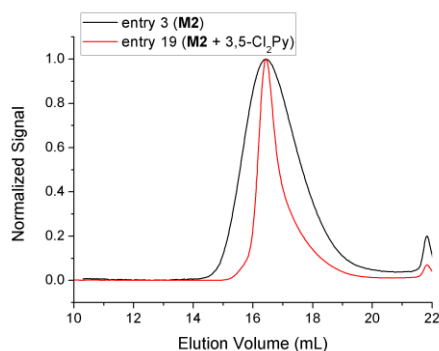
entry	M/I	time (h)	$M_n$ (kDa)	$\bar{D}$	yield (%)
1	50	17 h	4.3	1.32	14
2	100	24 h	3.3	1.34	13

**Table S4.2.** Polymerization results of monomer **D** (Structure ‘b’ in Figure 4.1)

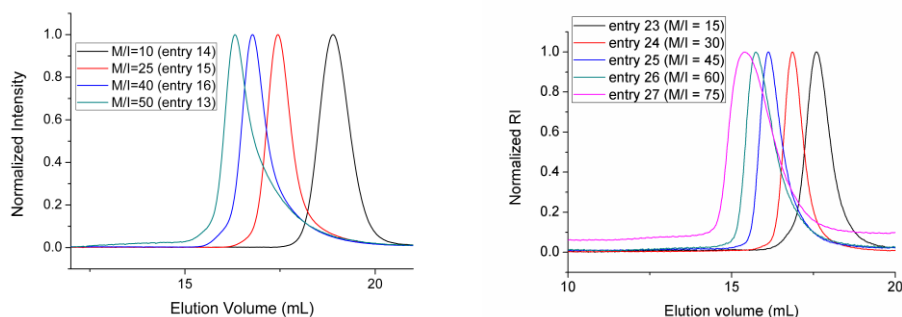


entry	M/I/Add	conc (M)	conv (%)
1	25/1	0.25 M	45%
2	25/1/5	0.25 M	34%

**Note:** **HG2** catalyst, which was the optimal catalyst for terminal alkyne polymerization,<sup>46,47</sup> was used for **1a**. Both monomers **1a** and **D** seemed to produce oligomeric products upon the noted polymerization conditions. However, the conversions and yields were low, and the NMR spectra of resulting products were not matched with the desired polymer structures.



**Figure S4.1.** SEC traces of **P2** (Table 4.1) synthesized by **G3** without (entry 3) and with 3,5-dichloropyridine additive (entry 19).



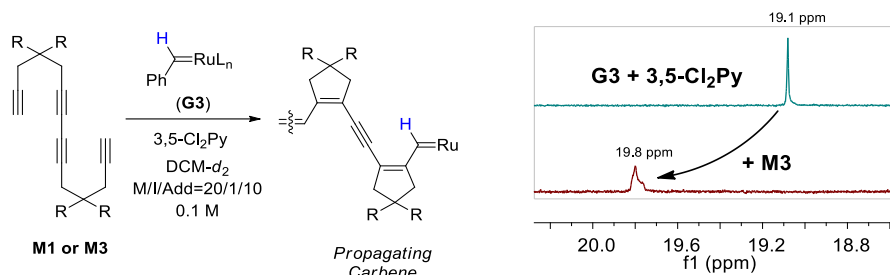
**Figure S4.2.** SEC traces of **P3** (Table 4.1, entries 13-16) and **P7** (entries 23-27).

### ***In situ* NMR experiment: procedure and data**

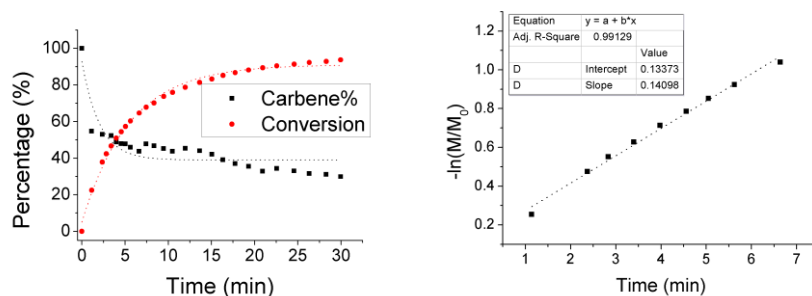
An NMR tube was filled with monomer (0.05 mmol, 20 eq), purged with argon, and DCM-*d*<sub>2</sub> (300 μL) was added. A 5-mL vial containing initiator (0.0025 mmol, 1 eq) (and 10 eq of additive) was argon-purged, and hexamethyl disilane was added as an internal standard. The total amount of initiator and additive was 5/4 of original value; after dissolving those using DCM-*d*<sub>2</sub> (250 μL), 1/5 (50 μL) of it was diluted in another NMR tube and used for checking the ratio between initial carbene and internal standard. Then, 200 μL of initiator solution was added to monomer solution and <sup>1</sup>H NMR measurement was recorded over time. The *k<sub>p</sub>* values were obtained based on the following equation;  $-d[M]/dt = k_p[M][Cat]$ . The



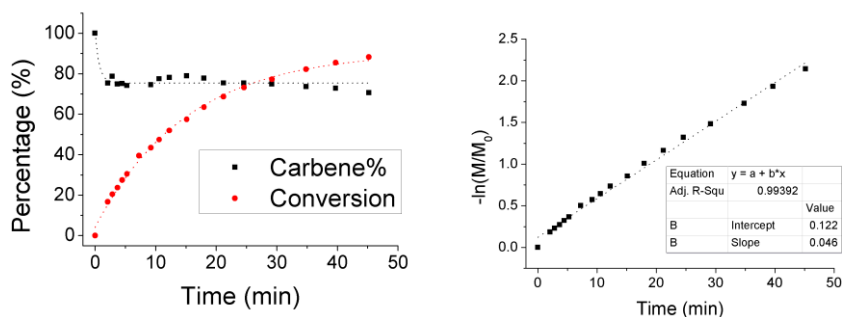
$k_{\text{obs}}$  values could be obtained only with the addition of 3,5-dichloropyridine because, otherwise, the propagation rates were too fast and carbene decomposed so quickly that linear  $-\ln [M]/[M]_0$  vs. time graphs were not obtained. The propagation rate of **M1** was 3 times higher than that of **M3** even with the shorter lifetime of propagating carbene.



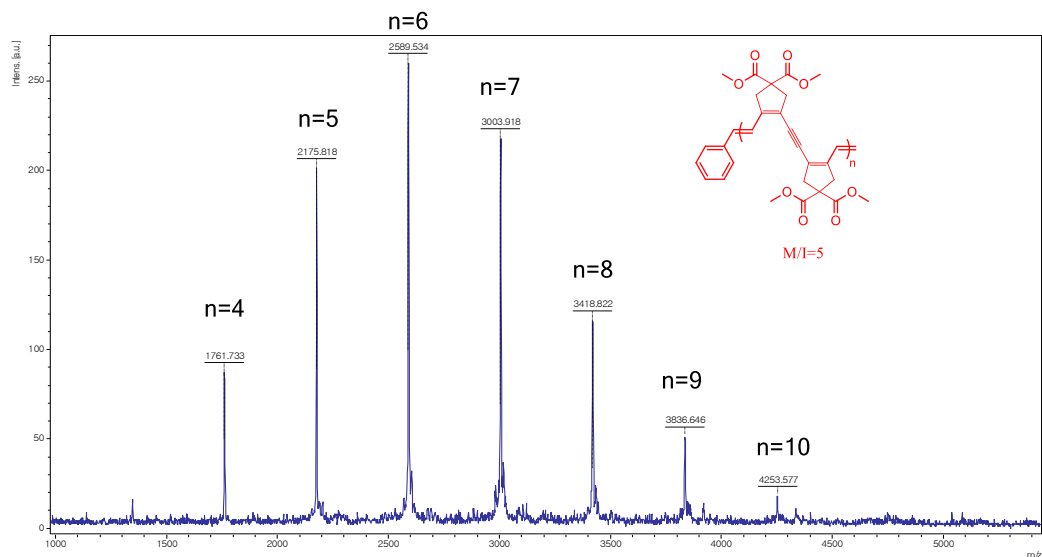
(a) **M1** ( $k_{\text{obs}} = 0.14 \text{ min}^{-1}$ )



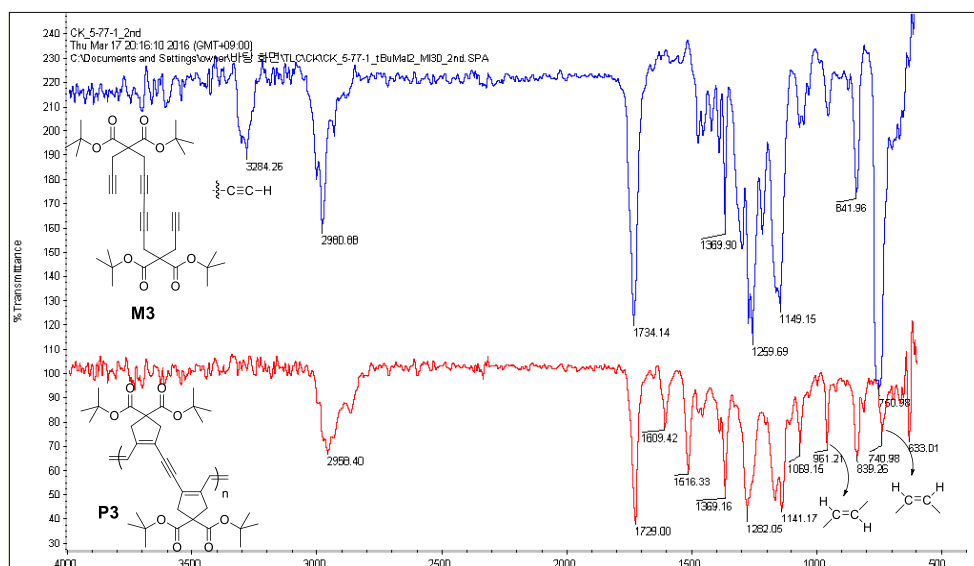
(b) **M3** ( $k_{\text{obs}} = 0.046 \text{ min}^{-1}$ )



**Figure S4.3.** Conversions, carbene changes and linear plots of  $-\ln [M]/[M]_0$  vs. time for the polymerizations of (a) **M1** and (b) **M3** with  $\text{M/I/Add} = 20/1/10$ .

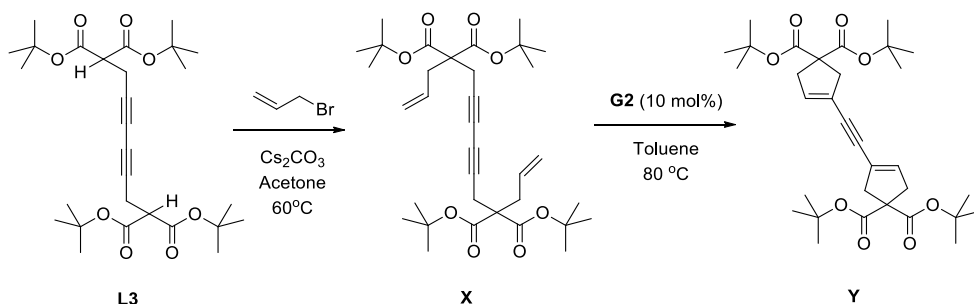


**Figure S4.4.** MALDI spectrum of the oligomers of **M1** synthesized by **G3** at  $M/I = 5$ .



**Figure S4.5.** IR spectra of **M3** and **P3** indicating the disappearance of terminal alkyne (C-H stretching) and the generation of backbone olefins (*trans* and *cis*).

## Synthesis of Model Compound

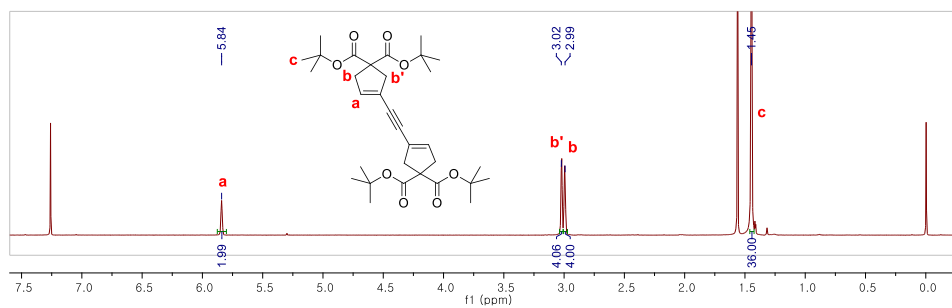


**Scheme S4.1.** Synthesis of tetradeca-1,13-dien-6,8-diyne moiety and its cascade ring-closing metathesis and 1,3-metallotropic shift reactions.

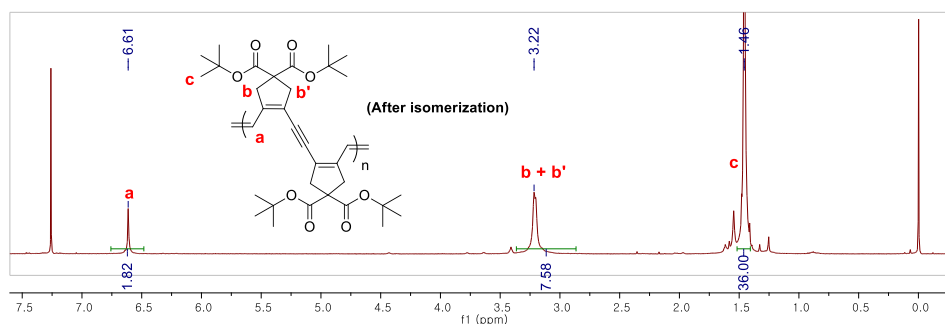
To a solution mixture of **L3** (21 mg, 0.041 mmol) and  $\text{Cs}_2\text{CO}_3$  (54 mg, 0.165 mmol) in acetone (0.4 ml), allyl bromide (14  $\mu\text{l}$ , 0.165 mmol) was added. The reaction mixture was heated to 60  $^\circ\text{C}$  and stirred for 6 h. Then, the reaction mixture was filtered and purified by flash column chromatography on silica gel (ethyl acetate : hexane = 1 : 20) to afford **X** as colorless liquid (22 mg, 0.038 mmol, 93%).  $^1\text{H}$  NMR (500 MHz,  $\text{CDCl}_3$ )  $\delta$  5.60 (ddt,  $J$  = 17.5, 10.1, 7.5 Hz, 2H), 5.16 (dd,  $J$  = 17.0, 2.0 Hz, 2H), 5.11 (dd,  $J$  = 10.1, 2.0 Hz, 2H), 2.74 (s, 4H), 2.67 (d,  $J$  = 7.5 Hz, 4H), 1.44 (s, 36H).  $^{13}\text{C}$  NMR (125 MHz,  $\text{CDCl}_3$ )  $\delta$  169.02, 132.38, 120.01, 82.21, 73.09, 68.01, 57.79, 36.92, 28.18, 23.65. HRMS (ESI):  $m/z$  for  $\text{C}_{34}\text{H}_{50}\text{NaO}_8$   $[\text{M}+\text{Na}]^+$ , calcd. 609.3398, found: 609.3400.

Compound **X** (8.0 mg, 0.014 mmol) was dissolved in toluene (0.1 ml), and 2<sup>nd</sup> generation Grubbs catalyst (**G2**) solution (1.2 mg in 40  $\mu\text{l}$  toluene) was added. The reaction mixture was heated to 80  $^\circ\text{C}$  and stirred for 9 h. Then, the product was purified by flash column chromatography on silica gel (ethyl acetate : hexane = 1 : 20) to afford **Y** as white solid (4.9 mg, 8.8  $\mu\text{mol}$ , 63%).  $^1\text{H}$  NMR (500 MHz,  $\text{CDCl}_3$ )  $\delta$  5.84 (s, 2H), 3.02 (d,  $J$  = 1.6 Hz, 4H), 2.99 (d,  $J$  = 1.8 Hz, 4H), 1.45 (s, 36H). HRMS (ESI):  $m/z$  for  $\text{C}_{32}\text{H}_{46}\text{NaO}_8$   $[\text{M}+\text{Na}]^+$ , calcd. 581.3085, found: 581.3088.

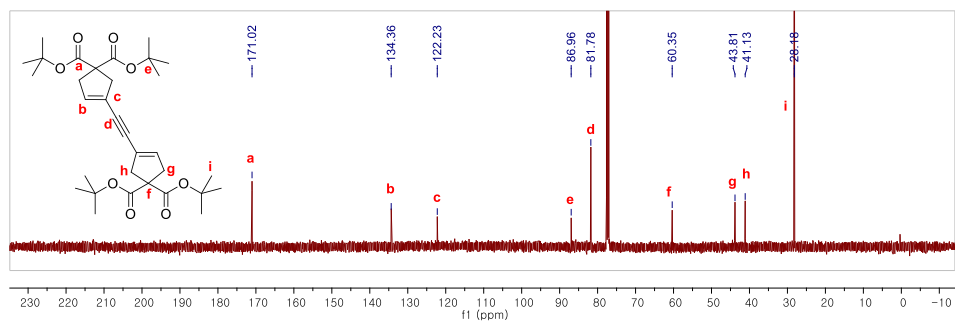
### $^1\text{H}$ NMR of **Y**



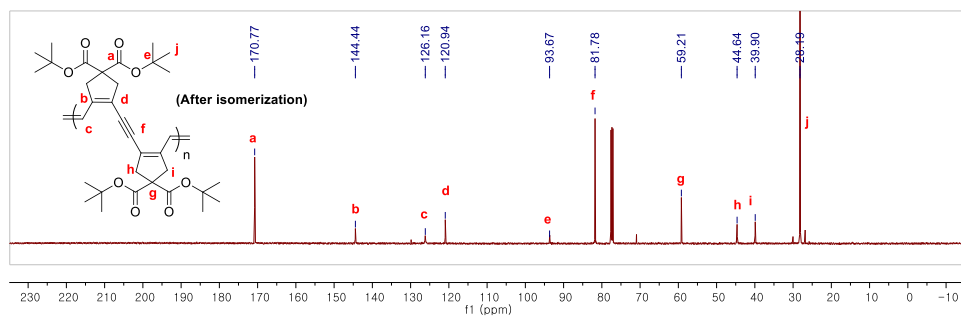
### $^1\text{H}$ NMR of **P3**



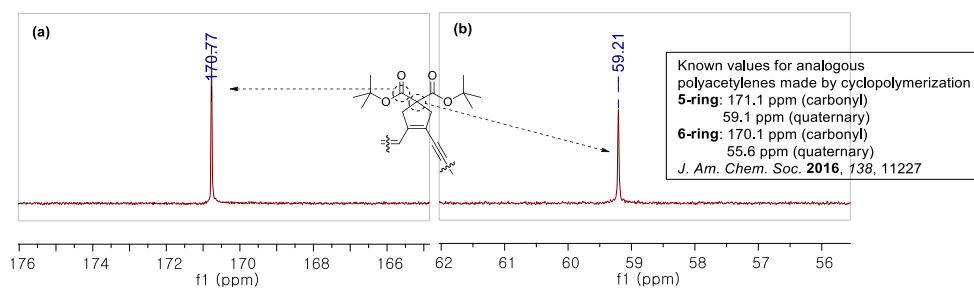
### $^{13}\text{C}$ NMR of **Y**



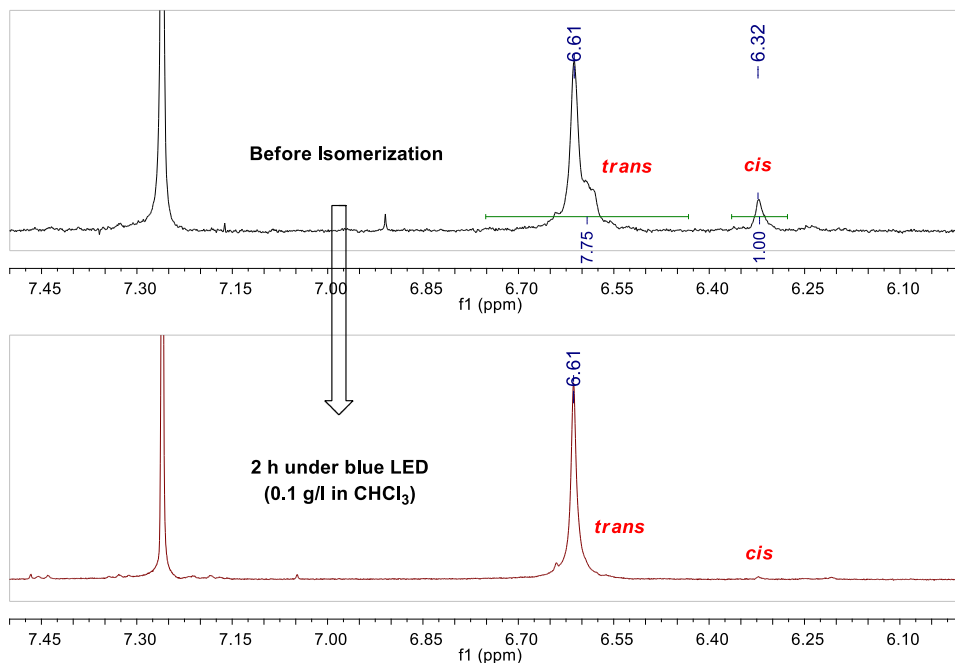
### $^{13}\text{C}$ NMR of **P3**



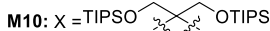
## Ring structure of polymer: $^{13}\text{C}$ NMR spectroscopy



**Figure S4.6.**  $^{13}\text{C}$ -NMR peaks for (a) carbonyl carbon and (b) quaternary carbon of malonate moiety in **P3** (in  $\text{CDCl}_3$ , after *cis*-to-*trans* isomerization by blue LED).<sup>51</sup>



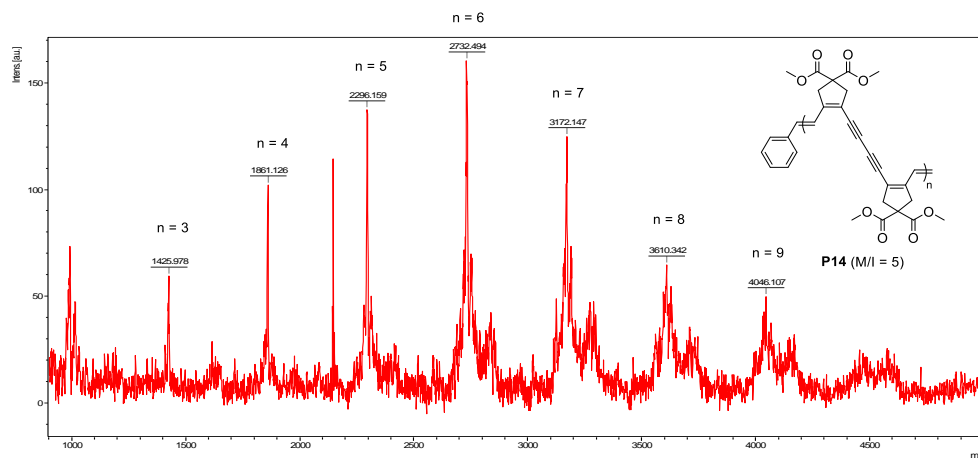
**Figure S4.7.**  $^1\text{H}$  NMR spectra of **P3** before and after isomerization of backbone olefins.<sup>51</sup>



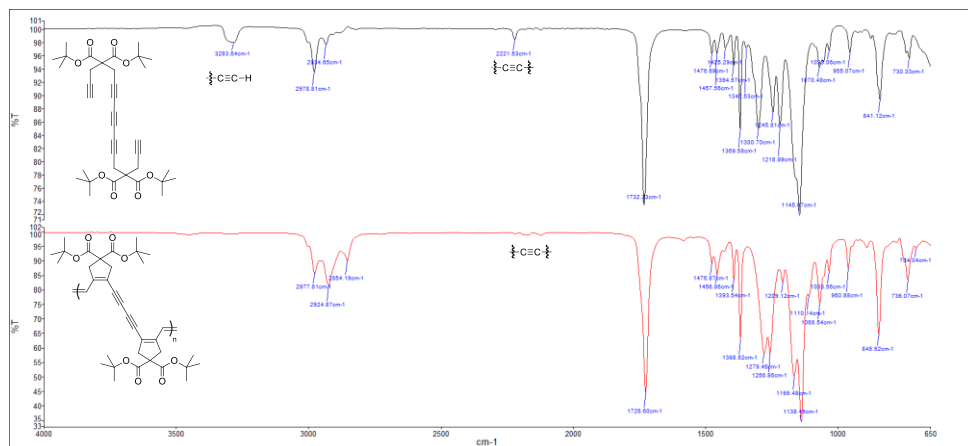
time for the polymerizations of **M10** with M/I/Add = 10/1/2.


$$\mathbf{M/I/Add} = 10/1/5.$$

## Characterization of Polymer Structure



**Figure S4.10.** MALDI spectrum of the oligomers of M14 synthesized by G3 at M/I = 5.



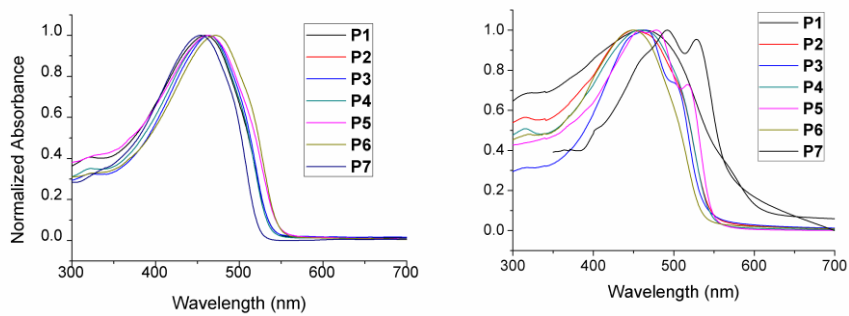
**Figure S4.11.** IR spectra of M15 and P15 indicating the disappearance of terminal alkyne (C-H stretching) and the change of internal alkyne.

## Optical and Physical Properties of Polymers

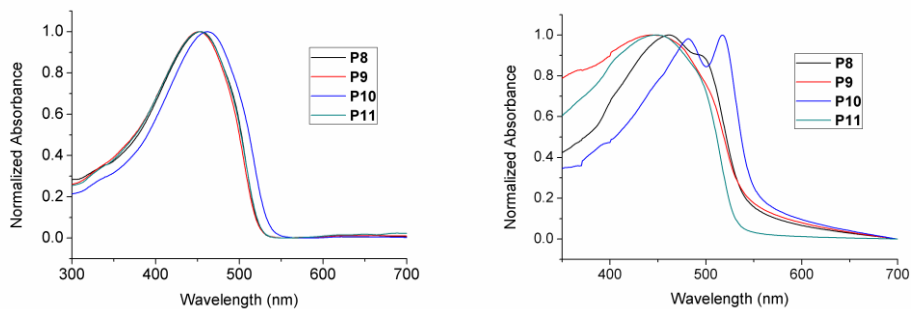
**Table S4.3.** Optical and physical properties of **P1 – P18**

	Solution		Film		$\lambda_{\text{em}}$ (nm)	$\phi_{\text{PL}}$ (%)	$E_{\text{HOMO}}$ (eV)
	$\lambda_{\text{abs}}$ (nm)	$E_{\text{g}}^{\text{opt}}$ (eV)	$\lambda_{\text{abs}}$ (nm)	$E_{\text{g}}^{\text{opt}}$ (eV)			
<b>P1</b>	459	2.30	462	2.04	540	0.1	-5.03
<b>P2</b>	464	2.31	450	2.27	547	0.3	-5.06
<b>P3</b>	464	2.31	465	2.32	550	0.1	-5.07
<b>P4</b>	464	2.32	457	2.28	552	0.2	-5.03
<b>P5</b>	463	2.27	479	2.25	542	0.2	-5.02
<b>P6</b>	472	2.28	450	2.32	553	0.1	-5.03
<b>P7</b>	470	2.22	492, 528	2.19	543	0.16	-5.55
<b>P8</b>	454	2.35	462	2.29	523	0.16	-5.42
<b>P9</b>	452	2.36	443	2.29	522	0.03	-5.50
<b>P10</b>	462	2.30	482, 517	2.25	523	< 0.01	-5.58
<b>P11</b>	453	2.36	448	2.34	523	0.06	-5.49
<b>P14</b>	453	2.34	461	2.13	543	0.05	-5.51
<b>P15</b>	469	2.34	445	2.34	542	< 0.01	-5.52
<b>P16</b>	460	2.34	450	2.28	543	0.05	-5.55
<b>P17</b>	457	2.32	451	2.30	542	0.19	-5.66
<b>P18</b>	453	2.29	456	2.21	546	0.07	-5.44

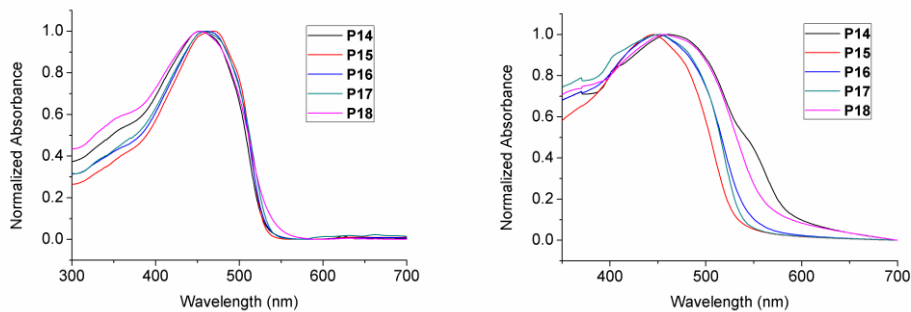




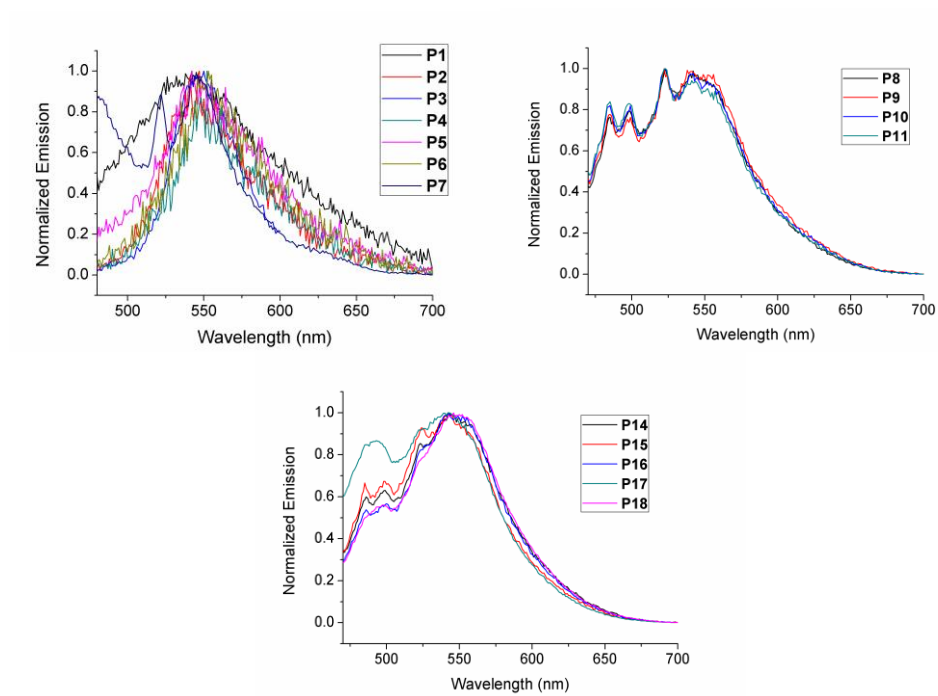
**Figure S4.12.** UV-Vis absorption spectra of **P1-P7** in  $\text{CHCl}_3$  solution (left) and film state (right).



**Figure S4.13.** UV-Vis absorption spectra of **P8-P11** in  $\text{CHCl}_3$  solution (left) and film state (right).



**Figure S4.14.** UV-Vis absorption spectra of **P14-P18** in  $\text{CHCl}_3$  solution (left) and film state (right).



**Figure S4.15.** Emission spectra of **P2-P11** in  $\text{CHCl}_3$  solution.

## 4.6. Experimental Section

### Characterization

$^1\text{H}$  NMR and  $^{13}\text{C}$  NMR were recorded by Varian/Oxford As-500 (500 MHz for  $^1\text{H}$  and 125 MHz for  $^{13}\text{C}$ ) and Bruker DRX-300 (300 MHz for  $^1\text{H}$ , 75 MHz for  $^{13}\text{C}$ ) spectrometers. Size exclusion chromatography (SEC) analyses were carried out with Waters (515 pump) and Wyatt system (Optilab T-rEX Refractive Index Detector) and Shodex GPC LF-804 column eluted with chloroform (HPLC grade, J.T.Baker) and filtered through a 0.2  $\mu\text{m}$  PTFE filter (Whatman®). The flow rate was 1.0 mL/min and temperature of column was maintained at 35 °C. MALDI-TOF analysis was carried out with Bruker Daltonics autoflex II TOF/TOF. IR spectra were measured by Spectrum Two FT-IR Spectrometer (PerkinElmer Inc.). High-resolution mass spectroscopy (HRMS) analyses were performed by ultra high resolution ESI Q-TOF mass spectrometer (Bruker, Germany) in the Sogang Center for Research Facilities. UV/Vis spectra were obtained by Jasco Inc. UV-vis Spectrometer V-650. Emission spectra were obtained by FP-8300 (Jasco Inc.). Absolute quantum yields were measured by QE-2000 (Otsuka Electronics). Cyclic voltammetry (CV) measurements were carried out by CHI 660 Electrochemical Analyzer (CH Instruments, Inc., Texas, USA).

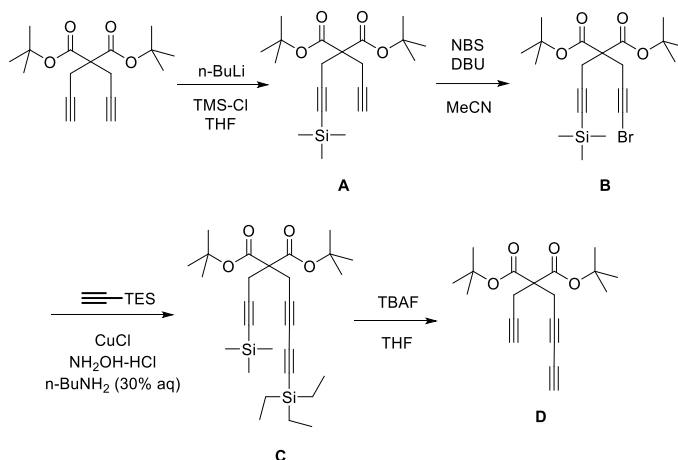
### Materials

All reagents which are commercially available from Sigma-Aldrich®, Tokyo Chemical Industry Co. Ltd., Acros Organics, Alfa Aesar®, without additional notes, were used without further purification. The catalyst **G3** was prepared by a literature method.<sup>57</sup> Dichloromethane (DCM) for the polymerization were purified by Glass Contour Organic Solvent Purification System and degassed further by Ar bubbling for 10 minutes before performing reactions.  $\text{CDCl}_3$  (99.8% D, 0.60 ml in ampoule) and  $\text{DCM-}d_2$  (99.90% D, 0.75mL in ampoule) were purchased from Cambridge Isotope Laboratories, Inc. and Deutero GmbH respectively, and used without further purification.

## Experimental procedures for preparation of monomers

Di-*tert*-butyldipropargyl malonate, 2-(prop-2-yn-1-yl)malonic acid (propargyl malonic acid), and compound **1a**, were prepared by literature methods.

### Synthesis of Compound D (Structure 'b' in Figure 4.2)



To a solution of di-*tert*-butyl dipropargyl malonate (7.31 g, 25 mmol) in THF (125 ml), *n*-butyllithium solution (2.5 M in *n*-hexane, 12 ml, 30 mmol) was added dropwise at  $-78\text{ }^\circ\text{C}$ . After stirring for 1 h, trimethylsilyl chloride (3.81 ml, 30 mmol) was added at  $-78\text{ }^\circ\text{C}$ . The cooling bath was removed after 30 min, and the reaction mixture was stirred for 50 min followed by quenching with saturated  $\text{NH}_4\text{Cl}$  aqueous solution. The organic layer was washed with water and extracted by ethyl acetate, dried with  $\text{MgSO}_4$ , and concentrated. The product was purified by flash column chromatography on silica gel (toluene : hexane = 1 : 2) to afford **A** as colorless liquid (3.65 g, 10.0 mmol, 40%).  $^1\text{H}$  NMR (500 MHz,  $\text{CDCl}_3$ )  $\delta$  2.88 (s, 2H), 2.85 (d,  $J = 2.5\text{ Hz}$ , 2H), 1.99 (t,  $J = 2.0\text{ Hz}$ , 1H), 1.45 (s, 18H), 0.11 (s, 9H).  $^{13}\text{C}$  NMR (125 MHz,  $\text{CDCl}_3$ )  $\delta$  168.09, 101.68, 88.28, 82.33, 79.51, 71.57, 57.57, 28.09, 24.03, 22.64, 0.27. HRMS (ESI):  $m/z$  for  $\text{C}_{20}\text{H}_{32}\text{NaO}_4\text{Si}$   $[\text{M}+\text{Na}]^+$ , calcd. 387.1962, found: 387.1966.

To a solution of **A** (1.59 g, 4.36 mmol) in acetonitrile (9 ml), *N*-bromosuccinimide

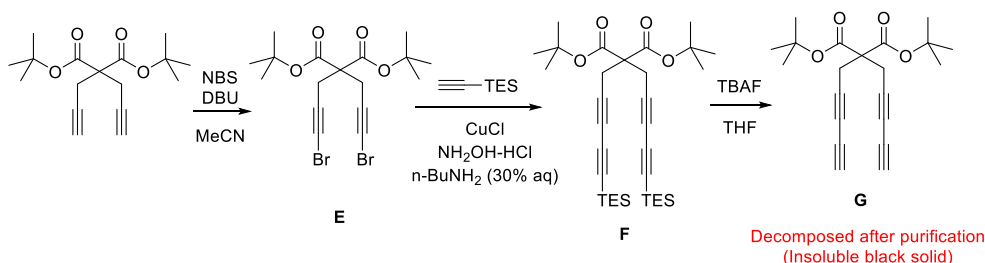
(854 mg, 4.80 mmol) was added. Then, 1,8-diazabicyclo(5.4.0)undec-7-ene (DBU, 0.717 ml, 4.80 mmol) was added and stirred for 30 min. The organic layer was washed with water and extracted by DCM, dried with MgSO<sub>4</sub>, and concentrated. The product was purified by flash column chromatography on silica gel (toluene : hexane = 2 : 1) to afford **B** as white solid (1.16 g, 2.62 mmol, 60%). <sup>1</sup>H NMR (500 MHz, CDCl<sub>3</sub>) δ 2.86 (d, *J* = 6.4 Hz, 4H), 1.45 (s, 18H), 0.12 (s, 9H). <sup>13</sup>C NMR (125 MHz, CDCl<sub>3</sub>) δ 167.97, 101.60, 88.41, 82.40, 75.67, 57.66, 41.35, 28.08, 24.28, 23.92, 0.26. HRMS (ESI): *m/z* for C<sub>20</sub>H<sub>31</sub>BrNaO<sub>4</sub>Si [M+Na]<sup>+</sup>, calcd. 465.1067, found: 465.1068.

To a 30% n-butylamine aqueous solution (10 ml), CuCl (12.7 mg, 0.128 mmol) was added at 0 °C resulting in the formation of a blue solution. A small amount of hydroxylamine hydrochloride was added to make a colorless solution. Then, triethylsilylacetylene (0.16 ml, 0.89 mmol) was added to form a yellow suspension. Compound **B** (262 mg, 0.59 mmol), solvated in 2 ml DCM, was added slowly. After stirring for 15 min at 0 °C, the reaction mixture was further stirred for 10 min at room temperature. Throughout the reaction, more amounts of hydroxylamine hydrochloride were added to prevent the solution from turning blue or green. The reaction was quenched by a saturated NH<sub>4</sub>Cl aqueous solution. The organic layer was washed with water and extracted with DCM, dried with MgSO<sub>4</sub>, and concentrated. The product was purified by flash column chromatography on silica gel (toluene : hexane = 1 : 1) to afford **C** as colorless liquid (239 mg, 0.475 mmol, 81%). <sup>1</sup>H NMR (500 MHz, CDCl<sub>3</sub>) δ 2.93 (s, 2H), 2.85 (s, 2H), 1.44 (s, 18H), 0.96 (t, *J* = 7.8 Hz, 9H), 0.59 (q, *J* = 7.9 Hz, 6H), 0.10 (s, 9H). <sup>13</sup>C NMR (125 MHz, CDCl<sub>3</sub>) δ 167.84, 101.47, 89.39, 88.57, 82.58, 82.33, 74.11, 68.66, 57.77, 28.06, 24.47, 23.63, 7.65, 4.52, 0.25. HRMS (ESI): *m/z* for C<sub>28</sub>H<sub>46</sub>NaO<sub>4</sub>Si<sub>2</sub> [M+Na]<sup>+</sup>, calcd. 525.2827, found: 525.2829.

To a solution of **C** (183 mg, 0.363 mmol) in THF (10 ml), tetra-n-butylammonium

fluoride solution (1M in THF, 0.80 ml, 0.80 mmol) was added at -10 °C. After 20 min, 0 °C water (c.a. 10 ml) was added followed by addition of HCl (6 N, 0.7 ml). The organic layer was washed with water and extracted by ethyl acetate, dried with MgSO<sub>4</sub>, and concentrated. The product was purified by flash column chromatography on silica gel (ethyl acetate : hexane = 1 : 20). The obtained liquid was dried at 0 °C to prevent the compound from turning brown. As a result, compound **D** was obtained as pale yellow solid (102 mg, 0.322 mmol, 89%). <sup>1</sup>H NMR (500 MHz, CDCl<sub>3</sub>) δ 2.97 (s, 2H), 2.86 (d, *J* = 2.5 Hz, 2H), 2.02 (t, *J* = 2.5 Hz, 1H), 1.97 (s, 1H), 1.46 (s, 18H). <sup>13</sup>C NMR (125 MHz, CDCl<sub>3</sub>) δ 167.78, 82.86, 78.99, 73.15, 72.01, 68.34, 67.76, 65.73, 57.44, 28.08, 23.44, 23.07. HRMS (ESI): *m/z* for C<sub>19</sub>H<sub>24</sub>NaO<sub>4</sub> [M+Na]<sup>+</sup>, calcd. 339.1567, found: 339.1567.

#### Synthesis of Compound G (Structure 'c' in Scheme 4.2)



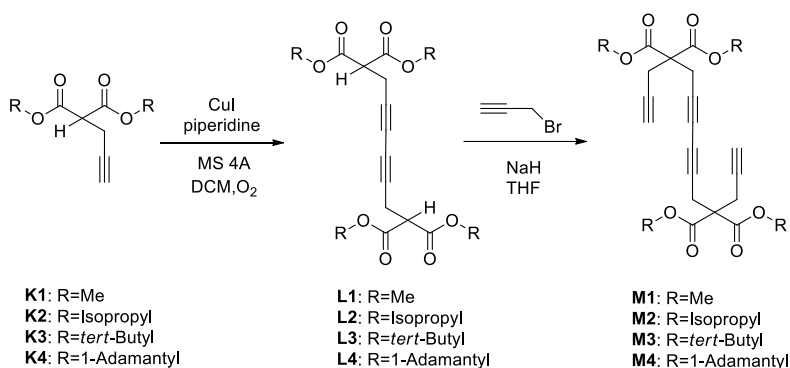
To a solution of di-*tert*-butyldipropargyl malonate (1.75 g, 6.0 mmol) in acetonitrile (12 ml), *N*-bromosuccinimide (1.28 mg, 7.2 mmol) was added. Then, 1,8-diazabicyclo(5.4.0)undec-7-ene (DBU, 4.34 ml, 9 mmol) was added and stirred for 30 min. The organic layer was washed with water and extracted by DCM, dried with MgSO<sub>4</sub>, and concentrated. The product was purified by flash column chromatography on silica gel (toluene : hexane = 2 : 1) to afford **E** as white solid (374 mg, 0.83 mmol) (Originally, we conducted this synthesis for another purpose, and compound **E** was obtained as 14% of byproduct). <sup>1</sup>H NMR (500 MHz, CDCl<sub>3</sub>) δ 2.86 (s, 4H), 1.45 (s, 18H). <sup>13</sup>C NMR (125 MHz, CDCl<sub>3</sub>) δ 167.86, 82.68, 75.35, 57.49, 41.70, 28.05, 24.18. HRMS (ESI): *m/z* for C<sub>17</sub>H<sub>22</sub>Br<sub>2</sub>NaO<sub>4</sub> [M+Na]<sup>+</sup>, calcd. 470.9777, found: 470.9778.

To a 30% n-butylamine aqueous solution (10 ml), CuCl (11.8 mg, 0.119 mmol) was added at 0 °C resulting in the formation of a blue solution. A small amount of hydroxylamine hydrochloride was added to make a colorless solution. Then, triethylsilylacetylene (0.27 ml, 1.49 mmol) was added to form a yellow suspension. Compound **E** (268 mg, 0.59 mmol), solvated in 2 ml DCM, was added slowly. After stirring for 15 min at 0 °C, the reaction mixture was further stirred for 10 min at room temperature. Throughout the reaction, more amounts of hydroxylamine hydrochloride were added to prevent the solution from turning blue or green. The reaction was quenched by a saturated NH<sub>4</sub>Cl aqueous solution. The organic layer was washed with water and extracted with ethyl acetate, dried with MgSO<sub>4</sub>, and concentrated. The product was purified by flash column chromatography on silica gel (ethyl acetate : hexane = 1 : 40) to afford **F** as yellow liquid (258 mg, 0.453 mmol, 76%). <sup>1</sup>H NMR (300 MHz, CDCl<sub>3</sub>) δ 2.96 (s, 4H), 1.46 (s, 18H), 0.98 (t, *J* = 7.8 Hz, 18H), 0.61 (q, *J* = 7.8 Hz, 12H). <sup>13</sup>C NMR (125 MHz, CDCl<sub>3</sub>) δ 167.63, 89.23, 83.05, 82.66, 73.55, 68.99, 57.74, 28.04, 24.07, 7.65, 4.51. HRMS (ESI): *m/z* for C<sub>33</sub>H<sub>52</sub>NaO<sub>4</sub>Si<sub>2</sub> [M+Na]<sup>+</sup>, calcd. 591.3296, found: 591.3299.

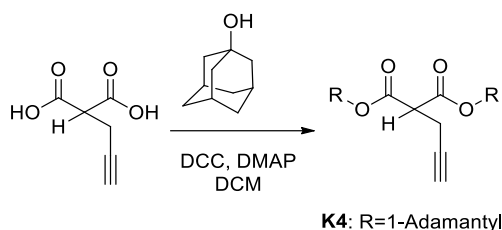
The synthesis of compound **G** was attempted by the same procedure used for the synthesis of compound **D**, using compound **F** as the starting material. It seemed that the deprotection of triethylsilyl group was successful by TLC monitoring. However, after the purification of the reaction mixture and evaporation of the solvent, the compound turned black. The resulting solid was almost insoluble in organic solvents implying the total decomposition of the compound.

### Synthesis of Tetrayne Monomers (M1-M4)

Compounds **K1-K3** were prepared by a literature method and their spectroscopic data were matched with corresponding reported data (**K1**, **K2**, and **K3**).



### Preparation of **K4**



2-(prop-2-yn-1-yl)malonic acid (355 mg, 2.50 mmol) and 1-adamantanol (837 mg, 5.50 mmol) were solvated in THF (20 ml). A mixture of *N,N'*-Dicyclohexylcarbodiimide (1.14 g, 5.50 mmol) and 4-dimethylaminopyridine (30.5 mg, 0.25 mmol) in THF (5ml) was added at 0 °C. The reaction was stirred for 4 h at room temperature, and quenched by acetic acid. After partially removing dicyclohexylurea (generated as a byproduct) by filtering, the organic layer was washed with water and extracted by DCM, dried with MgSO<sub>4</sub>, and concentrated. The product was purified by flash column chromatography on silica gel (ethyl acetate : hexane = 1 : 20) to afford **K4** as white solid (331 mg, 0.806 mmol, 32%).

<sup>1</sup>H NMR (500 MHz, CDCl<sub>3</sub>) δ 3.35 (t, *J* = 7.7 Hz, 2H), 2.66 (dd, *J* = 7.7, 2.4 Hz, 4H), 2.17 (s, 12H), 2.12 (s, 24H), 1.99 (t, *J* = 2.4 Hz, 2H), 1.70 – 1.62 (m, 24H).

<sup>13</sup>C NMR (75 MHz, CDCl<sub>3</sub>) δ 167.35, 82.39, 80.96, 70.31, 53.44, 41.67, 41.48, 36.47, 31.17, 18.73. HRMS (ESI): *m/z* for C<sub>26</sub>H<sub>34</sub>NaO<sub>4</sub> [M+Na]<sup>+</sup>, calcd. 433.2349, found: 433.2350.



### General procedure for Glaser-Hay coupling to afford compound L1-L4

To a dried round-bottom flask containing a stirring bar, CuI (247mg, 1.30 mmol) was added. After adding piperidine (1.54 ml, 15.6 mmol), DCM (130 ml) was added. After all the salts are dissolved (brown colored solution), ca. 5g of 4Å molecular sieve was added. Compound **K1** (2.21 g, 13.0 mmol) in DCM was added, followed by injection of a balloon filled with O<sub>2</sub>. As the reaction proceeded, the reaction mixture turned dark green. Using a large round-bottom flask with vigorous stirring was required to facilitate the O<sub>2</sub> incorporation. The organic layer was washed with water and extracted by DCM, dried with MgSO<sub>4</sub>, and concentrated. The product was purified by flash column chromatography on silica gel (ethyl acetate : hexane = 1 : 2) to afford **L1** as yellow liquid (1.87 g, 5.53 mmol, 85%). <sup>1</sup>H NMR (500 MHz, CDCl<sub>3</sub>) δ 3.77 (s, 12H), 3.59 (t, *J* = 7.5 Hz, 2H), 2.85 (d, *J* = 7.5 Hz, 4H). <sup>13</sup>C NMR (125 MHz, CDCl<sub>3</sub>) δ 168.29, 77.61, 77.36, 77.10, 73.83, 67.16, 53.25, 50.80, 19.56. HRMS (ESI): *m/z* for C<sub>16</sub>H<sub>18</sub>NaO<sub>8</sub> [M+Na]<sup>+</sup>, calcd. 361.0894, found: 361.0891.

**L2** (pale yellow liquid, 75%) <sup>1</sup>H NMR (500 MHz, CDCl<sub>3</sub>) δ 5.06 (hept, *J* = 6.5 Hz, 4H), 3.45 (t, *J* = 7.6 Hz, 2H), 2.81 (d, *J* = 7.6 Hz, 4H), 1.25 (t, *J* = 6.3 Hz, 24H). <sup>13</sup>C NMR (125 MHz, CDCl<sub>3</sub>) δ 167.58, 77.61, 77.36, 77.11, 73.97, 69.82, 67.19, 51.50, 21.99, 21.89, 19.46. HRMS (ESI): *m/z* for C<sub>24</sub>H<sub>34</sub>NaO<sub>8</sub> [M+Na]<sup>+</sup>, calcd. 473.2146, found: 473.2149.

**L3** (colorless liquid, 72%) <sup>1</sup>H NMR (500 MHz, CDCl<sub>3</sub>) δ 3.32 (t, *J* = 7.6 Hz, 2H), 2.72 (d, *J* = 7.7 Hz, 4H), 1.45 (s, 36H). <sup>13</sup>C NMR (125 MHz, CDCl<sub>3</sub>) δ 167.36, 82.44, 74.11, 67.06, 52.95, 28.19, 19.46. HRMS (ESI): *m/z* for C<sub>28</sub>H<sub>42</sub>NaO<sub>8</sub> [M+Na]<sup>+</sup>, calcd. 529.2772, found: 529.2774.

**L4** (white solid, 78%) <sup>1</sup>H NMR (500 MHz, CDCl<sub>3</sub>) δ 3.32 (t, *J* = 7.6 Hz, 2H), 2.72 (d, *J* = 7.6 Hz, 4H), 2.17 (s, 12H), 2.11 (s, 24H), 1.70 – 1.63 (m, 24H). <sup>13</sup>C NMR (100 MHz, CDCl<sub>3</sub>) δ 167.13, 82.49, 74.27, 67.09, 53.16, 41.44, 36.46, 31.18, 19.56. HRMS (ESI): *m/z* for C<sub>52</sub>H<sub>66</sub>NaO<sub>8</sub> [M+Na]<sup>+</sup>, calcd. 841.4650, found: 841.4653.

### General procedure for propargylation to afford compound M1-M4

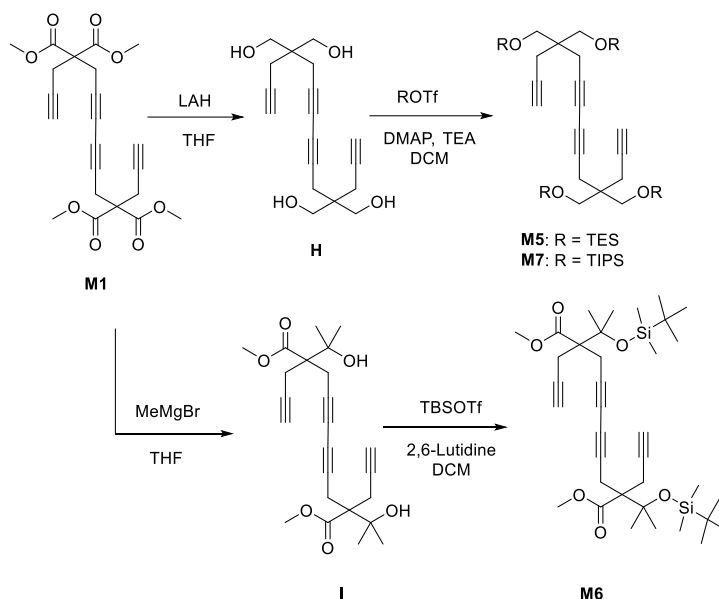
To a solution of compound **L1** (1.87 g, 5.53 mmol) in THF (24 ml), NaH was slowly added at 0 °C. After stirring for 30 min at room temperature, propargyl bromide (80 wt% in toluene) (1.36 ml, 12.2 mmol) was added. The reaction was quenched by saturated NH<sub>4</sub>Cl aqueous solution after 1 h. The organic layer was washed with water and extracted by ethyl acetate, dried with MgSO<sub>4</sub>, and concentrated. The product was purified by flash column chromatography on silica gel (ethyl acetate : hexane = 1 : 3) to afford **M1** as white solid (1.83 g, 4.43 mmol, 80%). <sup>1</sup>H NMR (500 MHz, CDCl<sub>3</sub>) δ 3.78 (s, 12H), 3.08 (s, 4H), 2.98 (d, *J* = 2.5 Hz, 4H), 2.05 (t, *J* = 2.5 Hz, 2H). <sup>13</sup>C NMR (125 MHz, CDCl<sub>3</sub>) δ 169.05, 78.39, 72.42, 72.31, 68.26, 56.73, 53.55, 53.53, 23.77, 23.20. HRMS (ESI): *m/z* for C<sub>22</sub>H<sub>22</sub>NaO<sub>8</sub> [M+Na]<sup>+</sup>, calcd. 437.1207, found: 437.1210.

**M2** (white solid, 80%) <sup>1</sup>H NMR (500 MHz, CDCl<sub>3</sub>) δ 5.06 (hept, *J* = 6.2 Hz, 4H), 3.00 (s, 4H), 2.90 (d, *J* = 2.6 Hz, 4H), 1.99 (t, *J* = 2.6 Hz, 2H), 1.22 (d, *J* = 6.3 Hz, 24H). <sup>13</sup>C NMR (125 MHz, CDCl<sub>3</sub>) δ 168.19, 78.74, 72.58, 72.03, 70.04, 68.19, 56.59, 23.59, 23.00, 21.78. HRMS (ESI): *m/z* for C<sub>30</sub>H<sub>38</sub>NaO<sub>8</sub> [M+Na]<sup>+</sup>, calcd. 549.2459, found: 549.2461.

**M3** (white solid, 86%) <sup>1</sup>H NMR (500 MHz, CDCl<sub>3</sub>) δ 2.93 (s, 4H), 2.82 (d, *J* = 2.6 Hz, 4H), 1.99 (t, *J* = 2.6 Hz, 2H), 1.44 (s, 36H). <sup>13</sup>C NMR (125 MHz, CDCl<sub>3</sub>) δ 167.83, 82.68, 79.12, 72.85, 71.85, 68.10, 57.50, 28.07, 23.56, 22.99. HRMS (ESI): *m/z* for C<sub>34</sub>H<sub>46</sub>NaO<sub>8</sub> [M+Na]<sup>+</sup>, calcd. 605.3085, found: 605.3088.

**M4** (white solid, 67%) <sup>1</sup>H NMR (500 MHz, CDCl<sub>3</sub>) δ 2.92 (s, 4H), 2.82 (d, *J* = 1.8 Hz, 4H), 2.17 (s, 12H), 2.09 (s, 24H), 2.00 (t, *J* = 1.8 Hz, 2H), 1.72 – 1.61 (m, 24H). <sup>13</sup>C NMR (125 MHz, CDCl<sub>3</sub>) δ 167.60, 82.63, 79.29, 72.94, 71.79, 68.16, 57.61, 41.33, 36.45, 31.18, 23.64, 23.05. HRMS (ESI): *m/z* for C<sub>58</sub>H<sub>70</sub>NaO<sub>8</sub> [M+Na]<sup>+</sup>, calcd. 917.4963, found: 916.4967.

## Synthesis of Tetrayne Monomers (M5-M7)



To a solution of **M1** (600 mg, 1.45 mmol) in THF (100 ml), lithium aluminum hydride (434 mg, 11.6 mmol) was added slowly at 0 °C. After 7 h stirring at room temperature, the reaction was quenched by a sequential addition of 0.4 ml H<sub>2</sub>O, 0.8 ml 10% NaOH aqueous solution, and 1.2 ml H<sub>2</sub>O at 0 °C. The insoluble gels were filtered by using Celite 525 powder, and the product was purified by flash column chromatography on silica gel (DCM : MeOH = 10 : 1) to afford **H** as white solid (182 mg, 0.602 mmol, 42%). <sup>1</sup>H NMR (500 MHz, CD<sub>3</sub>OD) δ 3.56 (s, 8H), 2.40 (s, 4H), 2.32 (t, *J* = 2.2 Hz, 2H), 2.29 (d, *J* = 2.3 Hz, 4H). <sup>13</sup>C NMR (500 MHz, CD<sub>3</sub>OD) δ 82.00, 75.55, 72.90, 69.10, 65.06, 45.11, 23.56, 22.94. HRMS (ESI): *m/z* for C<sub>18</sub>H<sub>22</sub>NaO<sub>4</sub> [M+Na]<sup>+</sup>, calcd. 325.1410, found: 325.1412.

To a solution of **H** (86 mg, 0.29 mmol) and 4-dimethylaminopyridine (6.96 mg, 0.057 mmol) in DCM (6 ml), triethylamine (0.32 ml, 2.3 mmol) was added. Triethylsilyl trifluoromethanesulfonate (0.37 ml, 1.7 mmol) was added at 0 °C, and stirred for 5 h at room temperature. After quenching with NaHCO<sub>3</sub> aqueous solution, the organic layer was washed with water and extracted by DCM, dried with MgSO<sub>4</sub>, and concentrated. The product was purified by flash column

chromatography on silica gel (ethyl acetate : hexane = 1 : 200) to afford **M5** as colorless liquid (123 mg, 0.162 mmol, 57%).  $^1\text{H}$  NMR (500 MHz,  $\text{CDCl}_3$ )  $\delta$  3.54 (s, 8H), 2.37 (s, 4H), 2.28 (d,  $J$  = 2.3 Hz, 4H), 1.94 (t,  $J$  = 2.3 Hz, 2H), 0.96 (t,  $J$  = 7.9 Hz, 36H), 0.59 (q,  $J$  = 8.0 Hz, 24H).  $^{13}\text{C}$  NMR (125 MHz,  $\text{CDCl}_3$ )  $\delta$  81.45, 74.34, 70.56, 67.59, 63.40, 44.36, 22.23, 21.43, 7.12, 4.70. HRMS (ESI):  $m/z$  for  $\text{C}_{42}\text{H}_{78}\text{NaO}_4\text{Si}_4$   $[\text{M}+\text{Na}]^+$ , calcd. 781.4869, found: 781.4873.

To a solution of **H** (85 mg, 0.28 mmol) and 4-dimethylaminopyridine (6.84 mg, 0.056 mmol) in DCM (6 ml), triethylamine (0.31 ml, 2.2 mmol) was added. Triisopropylsilyl trifluoromethanesulfonate (0.45 ml, 1.7 mmol) was added at 0 °C, and stirred for 21 h at room temperature. After quenching with  $\text{NaHCO}_3$  aqueous solution, the organic layer was washed with water and extracted by ethyl acetate, dried with  $\text{MgSO}_4$ , and concentrated. The product was purified by flash column chromatography on silica gel (ethyl acetate : hexane = 1 : 200) to afford **M7** as colorless liquid (228 mg, 0.25 mmol, 88%).  $^1\text{H}$  NMR (500 MHz,  $\text{CDCl}_3$ )  $\delta$  3.68 (s, 8H), 2.43 (s, 4H), 2.34 (d,  $J$  = 2.5 Hz, 4H), 1.94 (t,  $J$  = 2.6 Hz, 2H), 1.11 – 1.04 (m, 84H).  $^{13}\text{C}$  NMR (125 MHz,  $\text{CDCl}_3$ )  $\delta$  81.44, 74.26, 70.55, 67.62, 64.09, 44.92, 22.29, 21.47, 18.17, 12.13. HRMS (ESI):  $m/z$  for  $\text{C}_{54}\text{H}_{102}\text{NaO}_4\text{Si}_4$   $[\text{M}+\text{Na}]^+$ , calcd. 949.6747, found: 949.6749.

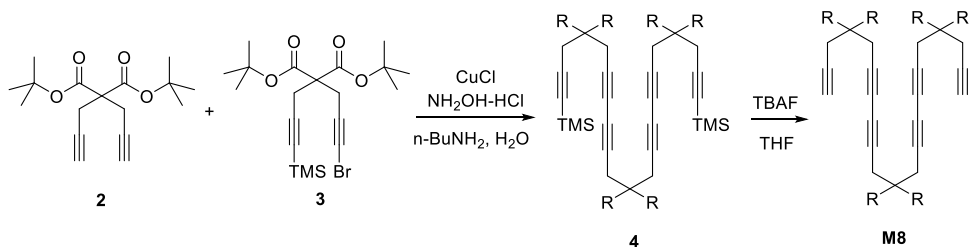
To a solution of **M1** (416 mg, 1.00 mmol) in THF (10 ml), methyl magnesium bromide solution (3 M in ether, 1.34 ml, 4.02 mmol) was added slowly at 0 °C. After stirring for 2 h at room temperature, the reaction was quenched by saturated  $\text{NH}_4\text{Cl}$  aqueous solution. The organic layer was washed with water and extracted by ethyl acetate, dried with  $\text{MgSO}_4$ , and concentrated. The product was purified by flash column chromatography on silica gel (ethyl acetate : hexane = 1 : 2) to afford **I** as white solid (220 mg, 0.53 mmol, 53%).  $^1\text{H}$  NMR (500 MHz,  $\text{CDCl}_3$ )  $\delta$  3.76 (s, 6H), 3.06 – 2.74 (m, 10H), 2.07 (t,  $J$  = 2.5 Hz, 2H), 1.28 (d,  $J$  = 16.0 Hz, 12H).  $^{13}\text{C}$  NMR (125 MHz,  $\text{CDCl}_3$ )  $\delta$  174.10, 81.44, 77.61, 77.36, 77.11, 75.03, 74.20, 72.10,

68.13, 57.08, 52.78, 26.90, 26.71, 22.76, 22.17. HRMS (ESI):  $m/z$  for  $C_{24}H_{30}NaO_6$   $[M+Na]^+$ , calcd. 437.1935, found: 437.1936.

To a solution of **I** (111 mg, 0.268 mmol) in DCM (3 ml), 2,6-lutidine (0.094 ml, 0.80 mmol) was added at 0 °C. *tert*-Butyldimethylsilyl trifluoromethanesulfonate (0.15 ml, 0.67 mmol) was added, and stirred for 7 h at room temperature. After quenching with  $NaHCO_3$  aqueous solution, the organic layer was washed with water and extracted by DCM, dried with  $MgSO_4$ , and concentrated. The product was purified by flash column chromatography on silica gel (ethyl acetate : hexane = 1 : 20) to afford **M6** as white solid (115 mg, 0.179 mmol, 67%).  $^1H$  NMR (500 MHz,  $CDCl_3$ )  $\delta$  3.69 (s, 6H), 3.01 – 2.70 (m, 8H), 1.99 (t,  $J$  = 2.2 Hz, 2H), 1.37 (d,  $J$  = 4.7 Hz, 12H), 0.86 (s, 18H), 0.09 (s, 12H).  $^{13}C$  NMR (125 MHz,  $CDCl_3$ )  $\delta$  173.40, 81.95, 77.16, 75.26, 71.04, 67.88, 58.16, 52.25, 27.58, 27.48, 26.03, 22.76, 22.22, 18.49, -1.83. HRMS (ESI):  $m/z$  for  $C_{36}H_{58}NaO_6Si_2$   $[M+Na]^+$ , calcd. 665.3664, found: 665.3666.

## Synthesis of Hexayne and Pentayne Monomers

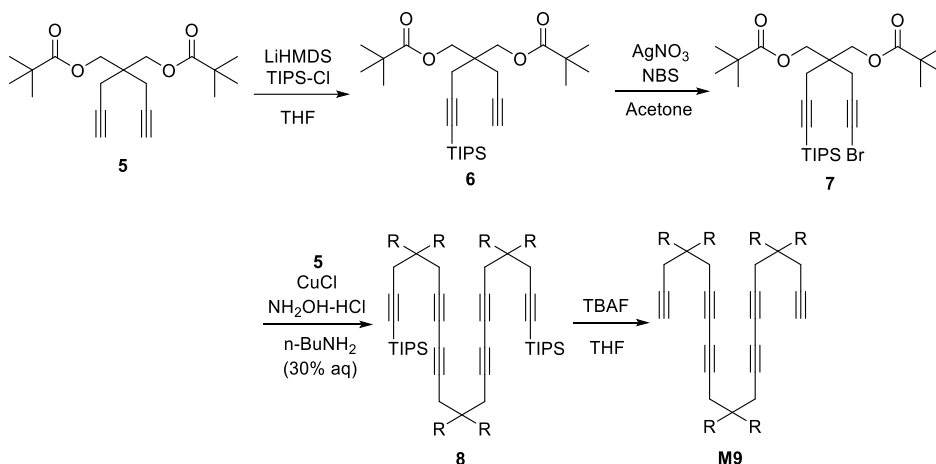
Compounds **2**, **3**, **5**, **9**, **12**, **14**, **17**, and **28**<sup>7</sup> were prepared by literature methods.



To a 30% *n*-butylamine aqueous solution (10 ml),  $CuCl$  (12.7 mg, 0.128 mmol) was added at 0 °C resulting in the formation of a blue solution. A small amount of hydroxylamine hydrochloride was added to make a colorless solution. Then, a solution of compound **2** (187 mg, 0.64 mmol) in DCM (2 ml) was added to form a yellow suspension. Compound **3** (710 mg, 1.6 mmol), solvated in 1.5 ml DCM, was added slowly. After stirring for 15 min at 0 °C, the reaction mixture was

further stirred for 2 h at room temperature. Throughout the reaction, more amounts of hydroxylamine hydrochloride were added to prevent the solution from turning blue or green. The reaction was quenched by a saturated  $\text{NH}_4\text{Cl}$  aqueous solution. The organic layer was washed with water and extracted with DCM, dried with  $\text{MgSO}_4$ , and concentrated. The product was purified by flash column chromatography on silica gel (ethyl acetate : hexane = 1 : 20) to afford **4** as white solid (475 mg, 0.467 mmol, 73%).  $^1\text{H}$  NMR (500 MHz,  $\text{CDCl}_3$ )  $\delta$  2.91 (s, 4H), 2.89 (s, 4H), 2.84 (s, 4H), 1.44 (s, 54H), 0.11 (s, 18H).  $^{13}\text{C}$  NMR (125 MHz,  $\text{CDCl}_3$ )  $\delta$  167.65, 167.46, 101.32, 88.25, 82.63, 82.28, 73.04, 72.37, 68.12, 67.74, 57.54, 27.88, 24.16, 23.67, 23.34, 0.06. HRMS (ESI):  $m/z$  for  $\text{C}_{57}\text{H}_{84}\text{NaO}_{12}\text{Si}_2$   $[\text{M}+\text{Na}]^+$ , calcd. 1039.5394, found: 1039.5389.

To a solution of **4** (455 mg, 0.45 mmol) in THF (5 ml), tetra-*n*-butylammonium fluoride solution (1.0 M in THF, 1.15 ml, 1.15 mmol) was added at  $-10\text{ }^\circ\text{C}$ . After 50 min,  $0\text{ }^\circ\text{C}$  water (c.a. 10 ml) was added, and the organic layer was extracted by ethyl acetate, dried with  $\text{MgSO}_4$ , and concentrated. The product was purified by flash column chromatography on silica gel (ethyl acetate : hexane = 1 : 10). As a result, **M8** was obtained as white solid (266 mg, 0.305 mmol, 68%).  $^1\text{H}$  NMR (500 MHz,  $\text{CDCl}_3$ )  $\delta$  2.94 (s, 4H), 2.89 (s, 4H), 2.83 (d,  $J = 2.1\text{ Hz}$ , 4H), 2.00 (t,  $J = 2.2\text{ Hz}$ , 2H), 1.44 (d,  $J = 4.3\text{ Hz}$ , 54H).  $^{13}\text{C}$  NMR (125 MHz,  $\text{CDCl}_3$ )  $\delta$  167.69, 167.46, 82.66, 82.51, 78.99, 72.82, 72.55, 71.63, 68.08, 67.90, 57.56, 57.37, 27.90, 23.74, 23.43, 22.86. HRMS (ESI):  $m/z$  for  $\text{C}_{51}\text{H}_{68}\text{NaO}_{12}$   $[\text{M}+\text{Na}]^+$ , calcd. 895.4603, found: 895.4605.



To a solution of **5** (5.27 g, 16.4 mmol) in THF (55 ml), Lithium bis(trimethylsilyl)amide solution (1.0 M in THF, 16.4 ml, 16.4 mmol) was added dropwise at -78 °C. After stirring for 1 h, triisopropylsilyl chloride (3.62 ml, 16.4 mmol) was added. The cooling bath was removed and the reaction mixture was stirred for 3 h followed by quenching with saturated NH<sub>4</sub>Cl aqueous solution. The organic layer was washed with water and extracted by ethyl acetate, dried with MgSO<sub>4</sub>, and concentrated. The product was purified by flash column chromatography on silica gel to afford **6** as colorless liquid (4.33 g, 9.02 mmol, 55%). <sup>1</sup>H NMR (500 MHz, CDCl<sub>3</sub>) δ 4.09 (s, 4H), 2.49 (s, 2H), 2.42 (d, *J* = 2.7 Hz, 2H), 2.02 (t, *J* = 2.7 Hz, 1H), 1.20 (s, 18H), 1.05 (s, 21H). <sup>13</sup>C NMR (75 MHz, CDCl<sub>3</sub>) δ 177.91, 102.67, 84.38, 78.96, 71.60, 65.03, 40.79, 39.06, 27.26, 23.73, 22.41, 18.73, 11.32. HRMS (ESI): *m/z* for C<sub>28</sub>H<sub>48</sub>NaO<sub>4</sub>Si [M+Na]<sup>+</sup>, calcd. 499.3214, found: 499.3214.

To a solution of **6** (4.33 g, 9.02 mmol) and *N*-bromosuccinimide (1.28 g, 7.2 mmol) in acetone (45 ml), silver nitrate (154 mg, 0.909 mmol) was added. After stirring for 30 min, the organic layer was washed with water and extracted by ethyl acetate, dried with MgSO<sub>4</sub>, and concentrated. The product was purified by flash column chromatography on silica gel to afford **7** as colorless liquid (4.54 g, 8.17 mmol, 90%). <sup>1</sup>H NMR (300 MHz, CDCl<sub>3</sub>) δ 4.07 (s, 4H), 2.46 (d, *J* = 3.0 Hz, 4H), 1.20 (s,

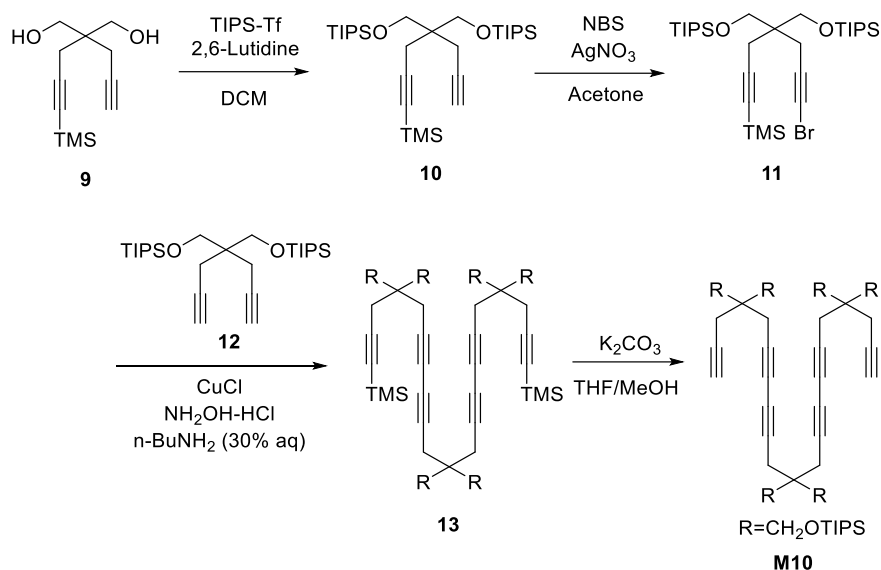
18H), 1.05 (s, 21H).  $^{13}\text{C}$  NMR (75 MHz,  $\text{CDCl}_3$ )  $\delta$  177.90, 102.56, 84.56, 75.14, 65.17, 41.00, 39.07, 27.27, 23.93, 23.82, 18.73, 18.15, 11.32. HRMS (ESI):  $m/z$  for  $\text{C}_{28}\text{H}_{47}\text{BrNaO}_4\text{Si}$   $[\text{M}+\text{Na}]^+$ , calcd. 577.2319, found: 577.2317.

To a 30% n-butylamine aqueous solution (30 ml), CuCl (14 mg, 0.14 mmol) was added at 0 °C resulting in the formation of a blue solution. A small amount of hydroxylamine hydrochloride was added to make a colorless solution. Then, compound **5** (0.23 g, 0.71 mmol) was added to form a yellow suspension. Compound **7** (793 mg, 1.43 mmol), solvated in 2 ml DCM, was added slowly. The reaction mixture was further stirred for 30 min at room temperature. Throughout the reaction, more amounts of hydroxylamine hydrochloride were added to prevent the solution from turning blue or green. The reaction was quenched by a saturated  $\text{NH}_4\text{Cl}$  aqueous solution. The organic layer was washed with water and extracted with ethyl acetate, dried with  $\text{MgSO}_4$ , and concentrated. The product was purified by flash column chromatography on silica gel (ethyl acetate : hexane = 1 : 20) to afford **8** as pale yellow solid (498 mg, 0.392 mmol, 55%).  $^1\text{H}$  NMR (300 MHz,  $\text{CDCl}_3$ )  $\delta$  4.07 (s, 12H), 2.51 (d, 8H), 2.47 (s, 4H), 1.20 (s, 54H), 1.05 (s, 42H).  $^{13}\text{C}$  NMR (75 MHz,  $\text{CDCl}_3$ )  $\delta$  177.86, 102.48, 84.72, 73.01, 72.33, 68.45, 67.96, 65.17, 41.69, 41.35, 39.08, 27.29, 18.76, 11.34. HRMS (ESI):  $m/z$  for  $\text{C}_{75}\text{H}_{120}\text{NaO}_{12}\text{Si}_2$   $[\text{M}+\text{Na}]^+$ , calcd. 1291.8211, found: 1291.8213.

To a solution of **8** (286 mg, 0.23 mmol) in THF (2.3 ml), tetra-n-butylammonium fluoride solution (1.0 M in THF, 0.5 ml, 0.5 mmol) was added at 0 °C. After 40 min, 0 °C water (c.a. 2 ml) and 6 N HCl (0.5 ml) was added, and the organic layer was extracted by dichloromethane, dried with  $\text{MgSO}_4$ , and concentrated. The product was purified by flash column chromatography on silica gel (ether : hexane = 1 : 3). As a result, **M9** was obtained as pale yellow solid (204 mg, 0.213 mmol, 93 %).  $^1\text{H}$  NMR (500 MHz,  $\text{CDCl}_3$ )  $\delta$  4.08 (s, 8H), 4.06 (s, 4H), 2.53 (s, 4H), 2.52 (s, 4H), 2.42 (d,  $J$  = 2.5 Hz, 4H), 2.06 (t,  $J$  = 2.4 Hz, 2H), 1.22 (s, 54H).  $^{13}\text{C}$  NMR (125



MHz, CDCl<sub>3</sub>)  $\delta$  177.89, 177.84, 78.72, 72.88, 72.49, 72.01, 68.40, 68.13, 65.15, 41.70, 41.15, 39.09, 27.28, 23.70, 23.49, 22.73. HRMS (ESI):  $m/z$  for C<sub>57</sub>H<sub>80</sub>NaO<sub>12</sub> [M+Na]<sup>+</sup>, calcd. 979.5542, found: 979.5541.



To a solution of **9** (1.40 g, 6.25 mmol) in DCM (15 ml), 2,6-lutidine (2.18 ml, 18.7 mmol) was added at 0 °C. Triisopropylsilyl trifluoromethanesulfonate (4.21 ml, 15.62 mmol) was added and stirred overnight. After quenching with NaHCO<sub>3</sub> aqueous solution, the organic layer was washed with water and extracted by dichloromethane, dried with MgSO<sub>4</sub>, and concentrated. The product was purified by flash column chromatography on silica gel (hexane elution) to afford **10** as colorless liquid (3.27 g, 6.10 mmol, 98%). <sup>1</sup>H NMR (500 MHz, CDCl<sub>3</sub>)  $\delta$  3.72 (s, 4H), 2.40 (s, 2H), 2.36 (d,  $J$  = 2.6 Hz, 2H), 1.94 (t,  $J$  = 2.5 Hz, 1H), 1.14 – 1.02 (m, 42H), 0.13 (s, 9H). <sup>13</sup>C NMR (125 MHz, CDCl<sub>3</sub>)  $\delta$  104.52, 86.85, 81.79, 70.36, 64.05, 44.43, 22.80, 21.45, 18.19, 12.13, 0.23. HRMS (ESI):  $m/z$  for C<sub>30</sub>H<sub>60</sub>NaO<sub>2</sub>Si<sub>3</sub> [M+Na]<sup>+</sup>, calcd. 559.3793, found: 559.3791.

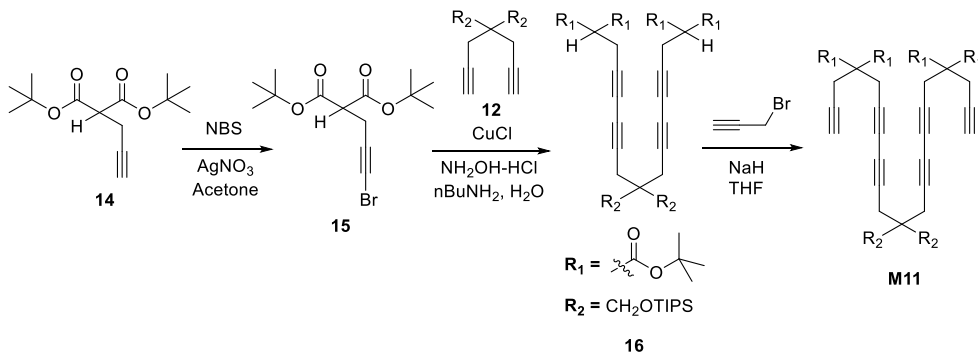
To a solution of **10** (1.55 g, 2.89 mmol) and *N*-bromosuccinimide (618 mg, 3.47 mmol) in acetone (10 ml), silver nitrate (22 mg, 0.14 mmol) was added. After stirring for 1.5 h, *n*-hexane (ca. 10 ml) was poured and precipitated solid was

filtered by celite. Filtrate solution was dried with  $\text{MgSO}_4$ , and concentrated. The product was purified by flash column chromatography (hexane elution) on silica gel to afford **11** as colorless liquid (1.40 g, 2.27 mmol, 79%).  $^1\text{H}$  NMR (300 MHz,  $\text{CDCl}_3$ )  $\delta$  3.69 (d,  $J$  = 1.6 Hz, 4H), 2.37 (d,  $J$  = 1.7 Hz, 4H), 1.20 – 0.99 (m, 42H), 0.12 (s, 9H).  $^{13}\text{C}$  NMR (125 MHz,  $\text{CDCl}_3$ )  $\delta$  104.34, 86.94, 77.88, 64.09, 44.80, 39.36, 22.87, 18.16, 12.11, 0.21. HRMS (ESI):  $m/z$  for  $\text{C}_{30}\text{H}_{59}\text{BrNaO}_2\text{Si}_3$   $[\text{M}+\text{Na}]^+$ , calcd. 637.2898, found: 637.2897.

To a 30% *n*-butylamine aqueous solution (30 ml),  $\text{CuCl}$  (11.6 mg, 0.117 mmol) was added at 0 °C resulting in the formation of a blue solution. A small amount of hydroxylamine hydrochloride was added to make a colorless solution. Then, compound **12** (271 mg, 0.584 mmol) was added to form a yellow suspension. Compound **11** (755 mg, 1.23 mmol), solvated in 2 ml DCM, was added slowly. The reaction mixture was further stirred for 2 h at room temperature. Throughout the reaction, more amounts of hydroxylamine hydrochloride were added to prevent the solution from turning blue or green. The reaction was quenched by a saturated  $\text{NH}_4\text{Cl}$  aqueous solution. The organic layer was washed with water and extracted with dichloromethane, dried with  $\text{MgSO}_4$ , and concentrated. The product was purified by flash column chromatography on silica gel to afford **13** as colorless liquid (339 mg, 0.221 mmol, 38 %).  $^1\text{H}$  NMR (500 MHz,  $\text{CDCl}_3$ )  $\delta$  3.69 (d,  $J$  = 2.2 Hz, 8H), 3.66 (s, 4H), 2.42 (s, 4H), 2.40 (s, 4H), 2.37 (s, 4H), 1.15 – 0.99 (m, 126H), 0.12 (s, 18H).  $^{13}\text{C}$  NMR (125 MHz,  $\text{CDCl}_3$ )  $\delta$  104.37, 86.96, 74.55, 74.06, 67.77, 67.58, 64.17, 45.15, 22.92, 22.40, 18.19, 12.16, 0.23. HRMS (ESI):  $m/z$  for  $\text{C}_{87}\text{H}_{168}\text{NaO}_6\text{Si}_8$   $[\text{M}+\text{Na}]^+$ , calcd. 1556.0887, found: 1556.0917.

To a solution of **13** (299 mg, 0.212 mmol) in MeOH and THF (5 ml + 5 ml), potassium carbonate (304 mg, 2.20 mmol) was added. After stirring for 24 h, followed by celite filtering, the product was purified by flash column chromatography on silica gel to afford **M10** as colorless liquid (152 mg, 0.110

mmol, 52 %).  $^1\text{H}$  NMR (300 MHz,  $\text{CDCl}_3$ )  $\delta$  3.68 (s, 8H), 3.66 (s, 4H), 2.43 (s, 4H), 2.38 (s, 4H), 2.34 (d,  $J = 2.6$  Hz, 4H), 1.94 (t,  $J = 2.6$  Hz, 2H), 1.16 – 1.00 (m, 126H).  $^{13}\text{C}$  NMR (125 MHz,  $\text{CDCl}_3$ )  $\delta$  81.44, 74.31, 74.10, 70.54, 67.70, 67.61, 64.09, 45.66, 44.93, 22.37, 22.30, 21.48, 18.17, 12.13. HRMS (ESI):  $m/z$  for  $\text{C}_{81}\text{H}_{152}\text{NaO}_6\text{Si}_6$   $[\text{M}+\text{Na}]^+$ , calcd. 1412.0097, found: 1412.0099.

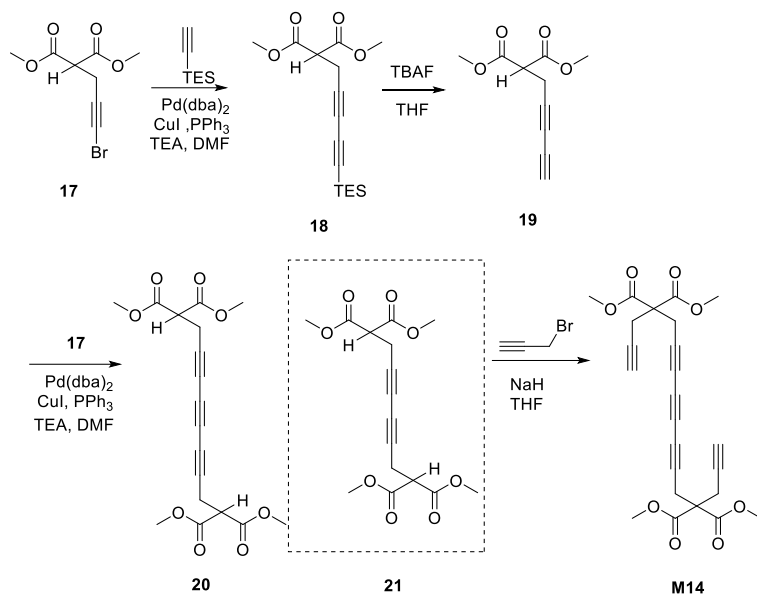


To a solution of **14** (139 mg, 0.547 mmol) and *N*-bromosuccinimide (195 mg, 1.09 mmol) in acetone (5 ml), silver nitrate (8.4 mg, 0.055 mmol) was added. After stirring for 1.5 h, the organic layer was washed with water and extracted with dichloromethane, dried with  $\text{MgSO}_4$ , and concentrated. The product was purified by flash column chromatography (ethyl acetate : hexane = 1 : 20) on silica gel to afford **15** as colorless liquid (165 mg, 0.494 mmol, 90%).  $^1\text{H}$  NMR (500 MHz,  $\text{CDCl}_3$ )  $\delta$  3.35 (t,  $J = 7.7$  Hz, 1H), 2.69 (d,  $J = 7.8$  Hz, 2H), 1.47 (s, 18H).  $^{13}\text{C}$  NMR (125 MHz,  $\text{CDCl}_3$ )  $\delta$  167.31, 82.19, 76.54, 52.78, 40.37, 28.00, 19.67. HRMS (ESI):  $m/z$  for  $\text{C}_{14}\text{H}_{21}\text{BrNaO}_4$   $[\text{M}+\text{Na}]^+$ , calcd. 355.0515, found: 355.0514.

To a 30% *n*-butylamine aqueous solution (10 ml),  $\text{CuCl}$  (8.6 mg, 0.087 mmol) was added at 0 °C resulting in the formation of a blue solution. A small amount of hydroxylamine hydrochloride was added to make a colorless solution. Then, compound **12** (202 mg, 0.434 mmol) was added to form a yellow suspension. Compound **15** (304 mg, 0.912 mmol), solvated in 3 ml DCM, was added slowly. The reaction mixture was further stirred for 30 min at room temperature.

Throughout the reaction, more amounts of hydroxylamine hydrochloride were added to prevent the solution from turning blue or green. The reaction was quenched by a saturated  $\text{NH}_4\text{Cl}$  aqueous solution. The organic layer was washed with water and extracted with dichloromethane, dried with  $\text{MgSO}_4$ , and concentrated. The product was purified by flash column chromatography on silica gel to afford **16** as colorless liquid (205 mg, 0.212 mmol, 49%).  $^1\text{H}$  NMR (500 MHz,  $\text{CDCl}_3$ )  $\delta$  3.63 (s, 4H), 3.34 (t,  $J = 7.7$  Hz, 2H), 2.74 (d,  $J = 7.7$  Hz, 4H), 2.39 (s, 4H), 1.47 (s, 36H), 1.13 – 0.98 (m, 42H).  $^{13}\text{C}$  NMR (125 MHz,  $\text{CDCl}_3$ )  $\delta$  167.26, 82.22, 75.16, 72.96, 67.42, 67.20, 64.25, 52.90, 45.58, 28.04, 22.39, 19.36, 18.14, 12.12. HRMS (ESI):  $m/z$  for  $\text{C}_{55}\text{H}_{92}\text{NaO}_{10}\text{Si}_2$   $[\text{M}+\text{Na}]^+$ , calcd. 991.6121, found: 991.6127.

To a solution of compound **16** (187 mg, 0.193 mmol) in THF (2 ml), NaH (17 mg, 0.42 mmol) was slowly added at 0 °C. After stirring for 30 min at room temperature, propargyl bromide (80 wt% in toluene, 47  $\mu\text{l}$ , 0.42 mmol) was added. The reaction was quenched by saturated  $\text{NH}_4\text{Cl}$  aqueous solution after 3 h. The organic layer was washed with water and extracted by ethyl acetate, dried with  $\text{MgSO}_4$ , and concentrated. The product was purified by flash column chromatography on silica gel to afford **M11** as colorless liquid (170 mg, 0.163 mmol, 84%).  $^1\text{H}$  NMR (500 MHz,  $\text{CDCl}_3$ )  $\delta$  3.63 (s, 4H), 2.95 (s, 4H), 2.85 (d,  $J = 2.5$  Hz, 4H), 2.38 (s, 4H), 2.00 (t,  $J = 2.6$  Hz, 2H), 1.45 (s, 36H), 1.06 (s, 42H).  $^{13}\text{C}$  NMR (125 MHz,  $\text{CDCl}_3$ )  $\delta$  167.74, 82.42, 79.09, 75.25, 71.55, 68.30, 67.37, 64.24, 57.42, 45.60, 27.91, 23.45, 22.81, 22.44, 18.14, 12.14. HRMS (ESI):  $m/z$  for  $\text{C}_{61}\text{H}_{96}\text{NaO}_{10}\text{Si}_2$   $[\text{M}+\text{Na}]^+$ , calcd. 1067.6434, found: 1067.6432.



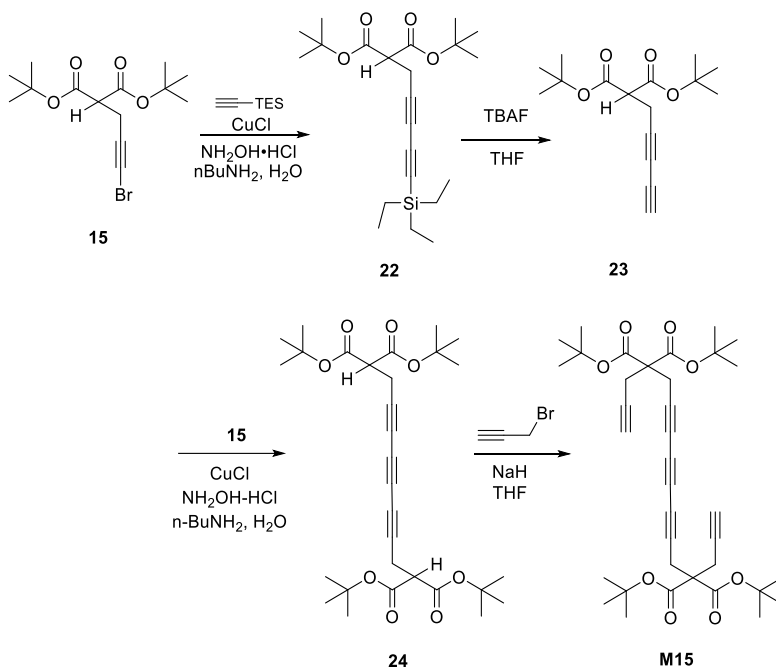
To a solution of  $\text{Pd}(\text{dba})_2$  (139 mg, 0.243 mmol),  $\text{CuI}$  (23 mg, 0.12 mmol),  $\text{PPh}_3$  (64 mg, 0.24 mmol), triethylamine (1.69 ml, 12.1 mmol) in DMF (12 ml), triethylacetylene (1.23 ml, 6.67 mmol) was added. Then, compound **17** (1.51 g, 6.06 mmol, solvated in 2 ml DCM) was added slowly. After stirring overnight, the organic layer was washed with water and extracted by ethyl acetate, dried with  $\text{MgSO}_4$ , and concentrated. The product was purified by flash column chromatography on silica gel to afford **18** as pale yellow liquid (1.08 g, 3.50 mmol, 58%).  $^1\text{H}$  NMR (500 MHz,  $\text{CDCl}_3$ )  $\delta$  3.77 (s, 1H), 3.60 (t,  $J = 7.6$  Hz, 1H), 2.88 (d,  $J = 7.6$  Hz, 1H), 0.98 (t,  $J = 7.9$  Hz, 1H), 0.60 (q,  $J = 7.9$  Hz, 1H).  $^{13}\text{C}$  NMR (75 MHz,  $\text{CDCl}_3$ )  $\delta$  168.12, 88.86, 82.87, 74.03, 67.69, 53.12, 50.57, 19.45, 7.46, 4.27. HRMS (ESI):  $m/z$  for  $\text{C}_{16}\text{H}_{24}\text{NaO}_4\text{Si}$   $[\text{M}+\text{Na}]^+$ , calcd. 331.1336, found: 331.1339.

To a solution of **18** (2.20 g, 7.14 mmol) in THF (35 ml), tetra-*n*-butylammonium fluoride solution (1.0 M in THF, 7.86 ml, 7.86 mmol) was added at 0 °C. After 10 min, 0 °C water (c.a. 10 ml) and 6 N HCl (5 ml) was added, and the organic layer was extracted by ethyl acetate, dried with  $\text{MgSO}_4$ , and concentrated. The product was purified by flash column chromatography on silica gel (ether : hexane = 1 : 10). As a result, **19** was obtained as pale yellow liquid (1.22 g, 6.28 mmol, 88 %).  $^1\text{H}$

NMR (500 MHz, CDCl<sub>3</sub>)  $\delta$  3.78 (s, 6H), 3.62 (t,  $J$  = 7.6 Hz, 1H), 2.88 (dd,  $J$  = 7.6, 1.1 Hz, 2H), 2.00 (t,  $J$  = 1.1 Hz, 1H). <sup>13</sup>C NMR (125 MHz, CDCl<sub>3</sub>)  $\delta$  168.02, 73.37, 68.01, 66.78, 65.95, 53.10, 50.48, 19.25. HRMS (ESI):  $m/z$  for C<sub>10</sub>H<sub>10</sub>NaO<sub>4</sub> [M+Na]<sup>+</sup>, calcd. 217.0471, found: 217.0469.

To a solution of Pd(dba)<sub>2</sub> (130 mg, 0.226 mmol), CuI (21.5 mg, 0.113 mmol), PPh<sub>3</sub> (59.3 mg, 0.226 mmol), triethylamine (1.60 ml, 11.3 mmol) in DMF (11 ml), compound **19** (1.21 g, 6.23 mmol) was added. Then, compound **17** (1.41 g, 5.65 mmol, solvated in 2 ml DCM) was added slowly. After stirring overnight, the organic layer was washed with water and extracted by ether, dried with MgSO<sub>4</sub>, and concentrated. The product was purified by flash column chromatography on silica gel to afford a mixture of **20** and **21**, and the next step was conducted without further purification.

To a solution of compound mixture of **20** and **21** (505 mg) in THF (5 ml), NaH (123 mg, 3.07 mmol) was slowly added at 0 °C. After stirring for 30 min at room temperature, propargyl bromide (80 wt% in toluene, 0.34 ml, 3.07 mmol) was added. The reaction was quenched by saturated NH<sub>4</sub>Cl aqueous solution after 2 h. The organic layer was washed with water and extracted by ethyl acetate, dried with MgSO<sub>4</sub>, and concentrated. The product was purified by flash column chromatography on silica gel and further recrystallization afforded **M14** as white solid (403 mg, 0.919 mmol, 24 % yield for two steps). <sup>1</sup>H NMR (500 MHz, CDCl<sub>3</sub>)  $\delta$  3.77 (s, 12H), 3.11 (s, 4H), 2.97 (d,  $J$  = 2.6 Hz, 4H), 2.04 (t,  $J$  = 2.6 Hz, 2H). <sup>13</sup>C NMR (125 MHz, CDCl<sub>3</sub>)  $\delta$  168.77, 78.12, 73.61, 72.25, 68.63, 61.09, 56.66, 53.45, 23.91, 23.17. HRMS (ESI):  $m/z$  for C<sub>24</sub>H<sub>22</sub>NaO<sub>8</sub> [M+Na]<sup>+</sup>, calcd. 461.1207, found: 461.1208.



To a 30% n-butylamine aqueous solution (150 ml), CuCl (149 mg, 1.508 mmol) was added at 0 °C resulting in the formation of a blue solution. A small amount of hydroxylamine hydrochloride was added to make a colorless solution. Then, triethylsilylacetylene (2.70 ml, 15.1 mmol) was added to form a yellow suspension. Compound **15** (2.51 g, 7.54 mmol), solvated in 10 ml DCM, was added slowly. The reaction mixture was further stirred for 30 min at room temperature. Throughout the reaction, more amounts of hydroxylamine hydrochloride were added to prevent the solution from turning blue or green. The reaction was quenched by a saturated  $\text{NH}_4\text{Cl}$  aqueous solution. The organic layer was washed with water and extracted with dichloromethane, dried with  $\text{MgSO}_4$ , and concentrated. The product was purified by flash column chromatography on silica gel to afford **22** as colorless liquid (2.55 g, 6.51 mmol, 86 %).  $^1\text{H}$  NMR (500 MHz,  $\text{CDCl}_3$ )  $\delta$  3.36 (t,  $J$  = 7.7 Hz, 1H), 2.76 (d,  $J$  = 7.7 Hz, 2H), 1.47 (s, 18H), 0.98 (t,  $J$  = 7.9 Hz, 9H), 0.60 (q,  $J$  = 7.9 Hz, 6H).  $^{13}\text{C}$  NMR (75 MHz,  $\text{CDCl}_3$ )  $\delta$  167.21, 89.19, 82.41, 74.98, 67.56, 52.60, 28.00, 19.33, 7.47, 4.32. HRMS (ESI):  $m/z$  for  $\text{C}_{22}\text{H}_{36}\text{NaO}_4\text{Si}$   $[\text{M}+\text{Na}]^+$ , calcd. 415.2275, found: 415.2277.

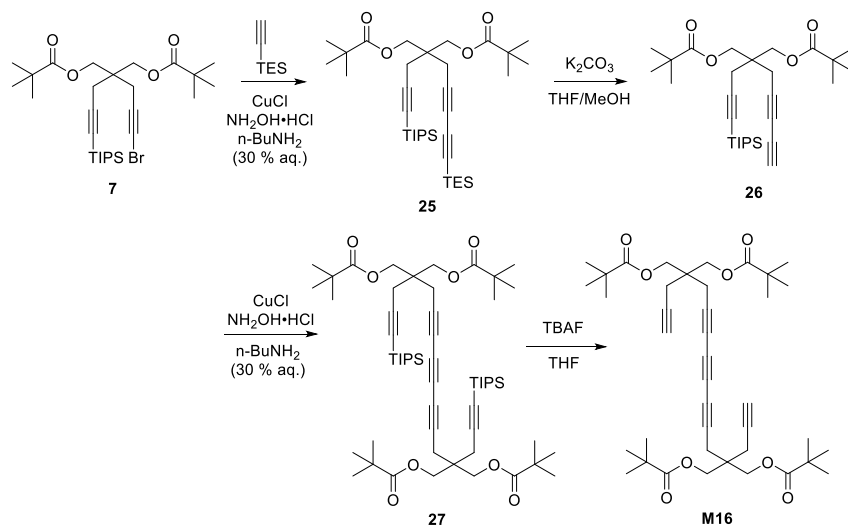
To a solution of **22** (2.55 g, 6.51 mmol) in THF (30 ml), tetra-*n*-butylammonium fluoride solution (1.0 M in THF, 7.16 ml, 7.16 mmol) was added at 0 °C. After 40 min, 0 °C water (c.a. 10 ml) and 6 N HCl (5 ml) was added, and the organic layer was extracted by ethyl acetate, dried with MgSO<sub>4</sub>, and concentrated. The product was purified by flash column chromatography on silica gel. As a result, **23** was obtained as dark brown liquid (1.80 g, 6.48 mmol, 99 %). <sup>1</sup>H NMR (500 MHz, CDCl<sub>3</sub>) δ 3.37 (t, *J* = 7.7 Hz, 1H), 2.75 (d, *J* = 7.7 Hz, 2H), 1.97 (s, 1H), 1.47 (s, 18H). <sup>13</sup>C NMR (125 MHz, CDCl<sub>3</sub>) δ 167.05, 82.43, 74.23, 68.25, 66.54, 65.47, 52.54, 28.01, 19.14. HRMS (ESI): *m/z* for C<sub>16</sub>H<sub>22</sub>NaO<sub>4</sub> [M+Na]<sup>+</sup>, calcd. 301.1410, found: 301.1412.

To a 30% *n*-butylamine aqueous solution (63 ml), CuCl (62 mg, 0.63 mmol) was added at 0 °C resulting in the formation of a blue solution. A small amount of hydroxylamine hydrochloride was added to make a colorless solution. Then, compound **23** (873 mg, 3.14 mmol) was added to form a yellow suspension. Compound **15** (1.05 g, 3.14 mmol), solvated in 5 ml DCM, was added slowly. The reaction mixture was further stirred for 30 min at room temperature. Throughout the reaction, more amounts of hydroxylamine hydrochloride were added to prevent the solution from turning blue or green. The reaction was quenched by a saturated NH<sub>4</sub>Cl aqueous solution. The organic layer was washed with water and extracted with dichloromethane, dried with MgSO<sub>4</sub>, and concentrated. The product was purified by flash column chromatography on silica gel, and further recrystallization afforded **24** as white solid (238 mg, 0.449 mmol, 14 % was obtained as the pure product). <sup>1</sup>H NMR (500 MHz, CDCl<sub>3</sub>) δ 3.35 (t, *J* = 7.6 Hz, 2H), 2.77 (d, *J* = 7.6 Hz, 4H), 1.46 (s, 36H). <sup>13</sup>C NMR (125 MHz, CDCl<sub>3</sub>) δ 167.02, 82.50, 75.38, 67.40, 60.90, 52.52, 28.02, 19.49. HRMS (ESI): *m/z* for C<sub>30</sub>H<sub>42</sub>NaO<sub>8</sub> [M+Na]<sup>+</sup>, calcd. 553.2772, found: 553.2774.

To a solution of compound **24** (122 mg, 0.230 mmol) in THF (2.5 ml), NaH (19 mg,



0.48 mmol) was slowly added at 0 °C. After stirring for 30 min at room temperature, propargyl bromide (80 wt% in toluene, 56  $\mu$ l, 0.51 mmol) was added. The reaction was quenched by saturated  $\text{NH}_4\text{Cl}$  aqueous solution after 1.5 h. The organic layer was washed with water and extracted by ethyl acetate, dried with  $\text{MgSO}_4$ , and concentrated. The product was purified by flash column chromatography on silica gel to afford **M15** as colorless liquid (125 mg, 0.206 mmol, 89%).  $^1\text{H}$  NMR (300 MHz,  $\text{CDCl}_3$ )  $\delta$  3.01 (s, 4H), 2.87 (d,  $J$  = 2.6 Hz, 4H), 2.03 (t,  $J$  = 2.6 Hz, 2H), 1.48 (s, 36H).  $^{13}\text{C}$  NMR (125 MHz,  $\text{CDCl}_3$ )  $\delta$  167.53, 82.71, 78.79, 74.23, 71.82, 68.38, 60.85, 57.33, 27.90, 23.64, 22.96. HRMS (ESI):  $m/z$  for  $\text{C}_{36}\text{H}_{46}\text{NaO}_8$   $[\text{M}+\text{Na}]^+$ , calcd. 629.3085, found: 629.3088.



To a 30%  $n$ -butylamine aqueous solution (50 ml),  $\text{CuCl}$  (109 mg, 1.10 mmol) was added at 0 °C resulting in the formation of a blue solution. A small amount of hydroxylamine hydrochloride was added to make a colorless solution. Then, triethylsilylacetylene (1.09 ml, 6.06 mmol) was added to form a yellow suspension. Compound **7** (3.06 g, 5.51 mmol), solvated in 10 ml DCM, was added slowly. The reaction mixture was further stirred for 40 min at room temperature. Throughout the reaction, more amounts of hydroxylamine hydrochloride were added to prevent the solution from turning blue or green. The reaction was

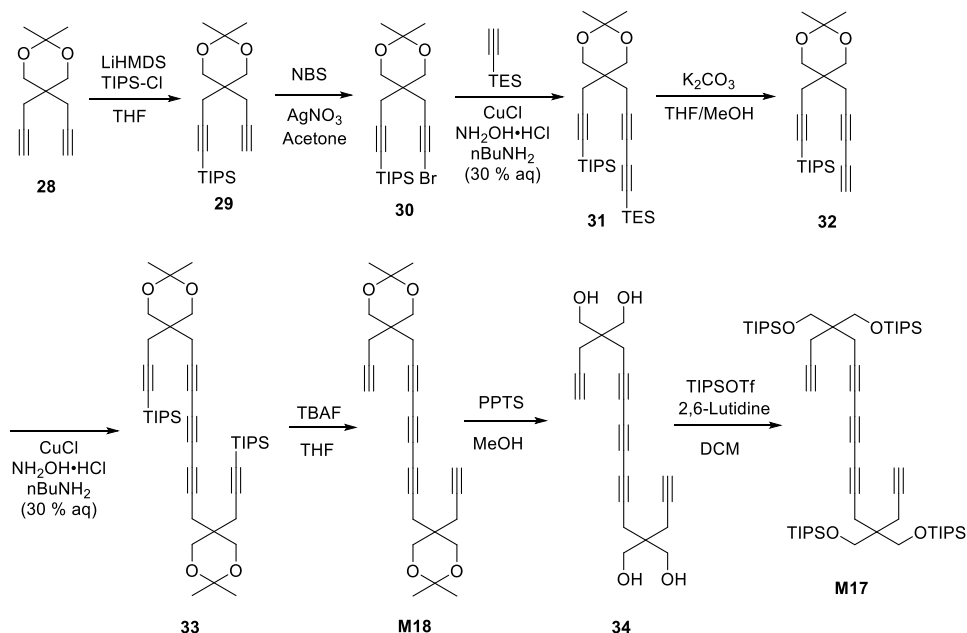
quenched by a saturated  $\text{NH}_4\text{Cl}$  aqueous solution. The organic layer was washed with water and extracted with dichloromethane, dried with  $\text{MgSO}_4$ , and concentrated. The product was purified by flash column chromatography on silica gel to afford **25** as colorless liquid (2.78 g, 4.52 mmol, 82 %).  $^1\text{H}$  NMR (500 MHz,  $\text{CDCl}_3$ )  $\delta$  4.08 (s, 4H), 2.54 (s, 2H), 2.48 (s, 2H), 1.20 (s, 18H), 1.04 (s, 21H), 0.99 (t,  $J = 7.9$  Hz, 9H), 0.62 (q,  $J = 7.9$  Hz, 6H).  $^{13}\text{C}$  NMR (75 MHz,  $\text{CDCl}_3$ )  $\delta$  177.87, 102.45, 89.06, 84.76, 82.34, 73.60, 68.63, 65.25, 41.37, 39.07, 27.27, 24.09, 23.62, 18.73, 11.32, 7.47, 4.29. HRMS (ESI):  $m/z$  for  $\text{C}_{36}\text{H}_{62}\text{NaO}_4\text{Si}_2$   $[\text{M}+\text{Na}]^+$ , calcd. 637.4079, found: 637.4080.

To a solution of **25** (431 mg, 0.701 mmol) in MeOH and THF (1.8 ml + 3.6 ml), potassium carbonate (407 mg, 2.95 mmol) was added. After stirring for 4 h, followed by celite filtering, the product was purified by flash column chromatography on silica gel to afford **26** as pale yellow liquid (297 mg, 0.593 mmol, 84 %).  $^1\text{H}$  NMR (500 MHz,  $\text{CDCl}_3$ )  $\delta$  4.08 (s, 4H), 2.52 (s, 2H), 2.47 (s, 2H), 2.01 (s, 1H), 1.20 (s, 18H), 1.09 – 0.95 (m, 21H).  $^{13}\text{C}$  NMR (125 MHz,  $\text{CDCl}_3$ )  $\delta$  177.88, 102.30, 84.87, 72.95, 68.16, 67.69, 65.59, 65.14, 41.36, 39.10, 27.28, 24.04, 23.35, 18.75, 11.34. HRMS (ESI):  $m/z$  for  $\text{C}_{30}\text{H}_{48}\text{NaO}_4\text{Si}$   $[\text{M}+\text{Na}]^+$ , calcd. 523.3214, found: 523.3216.

To a 30% n-butylamine aqueous solution (6 ml),  $\text{CuCl}$  (6.3 mg, 0.063 mmol) was added at 0 °C resulting in the formation of a blue solution. A small amount of hydroxylamine hydrochloride was added to make a colorless solution. Then, **26** (206 mg, 0.412 mmol) was added to form a yellow suspension. Compound **7** (176 mg, 0.317 mmol), solvated in 2 ml DCM, was added slowly at 50 °C. The reaction mixture was further stirred for 1 h. Throughout the reaction, more amounts of hydroxylamine hydrochloride were added to prevent the solution from turning blue or green. The reaction was quenched by a saturated  $\text{NH}_4\text{Cl}$  aqueous solution. The organic layer was washed with water and extracted with ether, dried with  $\text{MgSO}_4$ ,

and concentrated. The product was purified by flash column chromatography on silica gel to afford a product mixture containing **27**, and the next step was conducted without further purification.

To a solution mixture of **27** in THF (3 ml), tetra-*n*-butylammonium fluoride solution (1.0 M in THF, 0.71 ml, 0.71 mmol) was added at 0 °C. After 15 min, 0 °C water (c.a. 1 ml) and 6 N HCl (ca. 0.5 ml) was added, and the organic layer was extracted by ethyl acetate, dried with MgSO<sub>4</sub>, and concentrated. The product was purified by flash column chromatography on silica gel. Further recrystallization afforded **M16** as pale yellow solid (175 mg, 0.264 mmol, 55 % yield for two steps). <sup>1</sup>H NMR (500 MHz, CDCl<sub>3</sub>) δ 4.07 (s, 8H), 2.52 (s, 4H), 2.41 (d, *J* = 2.5 Hz, 4H), 2.05 (t, *J* = 2.5 Hz, 2H), 1.21 (s, 36H). <sup>13</sup>C NMR (125 MHz, CDCl<sub>3</sub>) δ 177.82, 78.52, 74.27, 72.13, 68.57, 65.08, 60.94, 41.30, 39.07, 27.25, 23.71, 22.78. HRMS (ESI): *m/z* for C<sub>40</sub>H<sub>54</sub>NaO<sub>8</sub> [M+Na]<sup>+</sup>, calcd. 685.3711, found: 685.3713.



To a solution of **28** (3.98 g, 20.7 mmol) in THF (69 ml), Lithium bis(trimethylsilyl)amide solution (1.0 M in THF, 20.7 ml, 20.7 mmol) was added

dropwise at -78 °C. After stirring for 1 h, triisopropylsilyl chloride (4.56 ml, 20.7 mmol) was added. The cooling bath was removed and the reaction mixture was stirred for 3 h followed by quenching with saturated NH<sub>4</sub>Cl aqueous solution. The organic layer was washed with water and extracted by ethyl acetate, dried with MgSO<sub>4</sub>, and concentrated. The product was purified by flash column chromatography on silica gel to afford **29** as colorless liquid (5.33 g, 15.3 mmol, 74%). <sup>1</sup>H NMR (500 MHz, CDCl<sub>3</sub>) δ 3.84 (d, *J* = 11.8 Hz, 2H), 3.76 (d, *J* = 11.8 Hz, 2H), 2.50 (d, *J* = 2.5 Hz, 2H), 2.44 (s, 2H), 2.03 (t, *J* = 2.5 Hz, 1H), 1.42 (d, *J* = 5.2 Hz, 6H), 1.10 – 1.00 (m, 21H). <sup>13</sup>C NMR (125 MHz, CDCl<sub>3</sub>) δ 98.35, 84.00, 80.26, 71.34, 66.18, 35.49, 25.22, 24.42, 23.02, 22.65, 18.80, 11.46. HRMS (ESI): *m/z* for C<sub>21</sub>H<sub>36</sub>NaO<sub>2</sub>Si [M+Na]<sup>+</sup>, calcd. 371.2377, found: 371.2376.

To a solution of **29** (5.33 g, 15.3 mmol) and *N*-bromosuccinimide (2.72 g, 15.3 mmol) in acetone (51 ml), silver nitrate (260 mg, 1.53 mmol) was added. After stirring for 2 h, the organic layer was washed with water and extracted with dichloromethane, dried with MgSO<sub>4</sub>, and concentrated. The product was purified by flash column chromatography on silica gel to afford **30** as colorless liquid (5.74 g, 13.4 mmol, 88 %). <sup>1</sup>H NMR (300 MHz, CDCl<sub>3</sub>) δ 3.87 (d, *J* = 12.0 Hz, 2H), 3.74 (d, *J* = 12.0 Hz, 2H), 2.56 (s, 2H), 2.41 (s, 2H), 1.44 (d, *J* = 4.5 Hz, 6H), 1.15 – 1.05 (m, 21H). <sup>13</sup>C NMR (75 MHz, CDCl<sub>3</sub>) δ 103.46, 98.36, 84.19, 77.36, 76.40, 66.16, 40.77, 35.78, 31.74, 25.73, 24.50, 24.29, 22.03, 18.79, 11.40. HRMS (ESI): *m/z* for C<sub>21</sub>H<sub>35</sub>BrNaO<sub>2</sub>Si [M+Na]<sup>+</sup>, calcd. 449.1482, found: 449.1481.

To a 30% *n*-butylamine aqueous solution (70 ml), CuCl (128 mg, 1.29 mmol) was added at 0 °C resulting in the formation of a blue solution. A small amount of hydroxylamine hydrochloride was added to make a colorless solution. Then, triethylsilylacetylene (1.43 ml, 7.74 mmol) was added to form a yellow suspension. Compound **30** (2.76 g, 6.45 mmol), solvated in 10 ml DCM, was added slowly at 50 °C. The reaction mixture was further stirred for 1 h. Throughout the

reaction, more amounts of hydroxylamine hydrochloride were added to prevent the solution from turning blue or green. The reaction was quenched by a saturated  $\text{NH}_4\text{Cl}$  aqueous solution. The organic layer was washed with water and extracted with dichloromethane, dried with  $\text{MgSO}_4$ , and concentrated. The product was purified by flash column chromatography on silica gel to afford **31** as colorless liquid (1.95 g, 4.00 mmol, 62 %).  $^1\text{H}$  NMR (500 MHz,  $\text{CDCl}_3$ )  $\delta$  3.85 (d,  $J$  = 12.0 Hz, 2H), 3.72 (d,  $J$  = 12.0 Hz, 2H), 2.62 (s, 2H), 2.39 (s, 2H), 1.41 (d,  $J$  = 8.2 Hz, 6H), 1.15 – 1.01 (m, 21H), 0.99 (t,  $J$  = 7.9 Hz, 9H), 0.61 (q,  $J$  = 7.9 Hz, 6H).  $^{13}\text{C}$  NMR (125 MHz,  $\text{CDCl}_3$ )  $\delta$  103.35, 98.39, 89.33, 84.37, 81.86, 75.18, 68.64, 66.21, 36.22, 25.85, 24.64, 23.96, 18.79, 11.44, 7.48, 4.39. HRMS (ESI):  $m/z$  for  $\text{C}_{29}\text{H}_{50}\text{NaO}_2\text{Si}_2$   $[\text{M}+\text{Na}]^+$ , calcd. 509.3242, found: 509.3245.

To a solution of **31** (475 mg, 0.975 mmol) in MeOH and THF (2.5 ml + 5 ml), potassium carbonate (566 mg, 4.09 mmol) was added. After stirring for 4 h, followed by celite filtering, the product was purified by flash column chromatography on silica gel to afford **32** as pale yellow liquid (322 mg, 0.864 mmol, 89 %).  $^1\text{H}$  NMR (500 MHz,  $\text{CDCl}_3$ )  $\delta$  3.84 (d,  $J$  = 12.1 Hz, 2H), 3.71 (d,  $J$  = 12.1 Hz, 2H), 2.61 (s, 2H), 2.39 (s, 2H), 1.99 (s, 1H), 1.41 (d,  $J$  = 7.1 Hz, 6H), 1.11 – 0.95 (m, 21H).  $^{13}\text{C}$  NMR (125 MHz,  $\text{CDCl}_3$ )  $\delta$  103.17, 98.42, 84.44, 74.43, 68.37, 67.60, 66.18, 65.17, 36.17, 25.84, 24.56, 23.68, 21.90, 18.78, 11.41. HRMS (ESI):  $m/z$  for  $\text{C}_{23}\text{H}_{36}\text{NaO}_2\text{Si}$   $[\text{M}+\text{Na}]^+$ , calcd. 395.2377, found: 395.2379.

To a 30% n-butylamine aqueous solution (20 ml),  $\text{CuCl}$  (73 mg, 0.73 mmol) was added at 0 °C resulting in the formation of a blue solution. A small amount of hydroxylamine hydrochloride was added to make a colorless solution. Then, **32** (1.64 g, 4.39 mmol) was added to form a yellow suspension. Compound **30** (1.56 g, 3.66 mmol), solvated in 10 ml DCM, was added slowly at 50 °C. The reaction mixture was further stirred for 1 h. Throughout the reaction, more amounts of hydroxylamine hydrochloride were added to prevent the solution from turning blue

or green. The reaction was quenched by a saturated  $\text{NH}_4\text{Cl}$  aqueous solution. The organic layer was washed with water and extracted with ether, dried with  $\text{MgSO}_4$ , and concentrated. The product was purified by flash column chromatography on silica gel to afford **33** (2.26 g, 3.14 mmol, 86 %).  $^1\text{H}$  NMR (500 MHz,  $\text{CDCl}_3$ )  $\delta$  3.83 (d,  $J$  = 11.9 Hz, 4H), 3.71 (d,  $J$  = 11.9 Hz, 4H), 2.62 (s, 4H), 2.39 (s, 4H), 1.42 (d,  $J$  = 6.9 Hz, 12H), 1.12 – 0.97 (m, 42H).  $^{13}\text{C}$  NMR (75 MHz,  $\text{CDCl}_3$ )  $\delta$  103.07, 98.45, 84.50, 77.36, 68.45, 66.19, 60.72, 36.35, 31.09, 25.86, 24.57, 24.03, 21.87, 18.79, 11.38. HRMS (ESI):  $m/z$  for  $\text{C}_{44}\text{H}_{70}\text{NaO}_4\text{Si}_2$   $[\text{M}+\text{Na}]^+$ , calcd. 741.4705, found: 741.4708.

To a solution of **33** (2.26 g, 3.14 mmol) in THF (15 ml), tetra-*n*-butylammonium fluoride solution (1.0 M in THF, 6.9 ml, 6.9 mmol) was added at 0 °C. After 30 min, 0 °C water (c.a. 5 ml) and 6 N HCl (ca. 3 ml) was added, and the organic layer was extracted by ethyl acetate, dried with  $\text{MgSO}_4$ , and concentrated. The product was purified by flash column chromatography on silica gel. Further recrystallization afforded **M18** as pale yellow solid (323 mg, 0.795 mmol, 25 %).  $^1\text{H}$  NMR (500 MHz,  $\text{CDCl}_3$ )  $\delta$  3.75 (dd,  $J$  = 28.0, 11.9 Hz, 8H), 2.59 (s, 4H), 2.38 (d,  $J$  = 2.7 Hz, 4H), 2.06 (t,  $J$  = 2.7 Hz, 2H), 1.42 (s, 12H).  $^{13}\text{C}$  NMR (125 MHz,  $\text{CDCl}_3$ )  $\delta$  98.48, 79.37, 75.38, 71.87, 68.53, 66.03, 60.78, 36.07, 24.56, 23.86, 23.11, 23.05. HRMS (ESI):  $m/z$  for  $\text{C}_{26}\text{H}_{30}\text{NaO}_4$   $[\text{M}+\text{Na}]^+$ , calcd. 429.2036, found: 429.2038.

To a solution of **M18** (105 mg, 0.259 mmol) in MeOH (2.6 ml), pyridinium *p*-toluenesulfonate (65 mg, 0.26 mmol) was added. After stirring overnight, the solution was concentrated and the product was purified by flash column chromatography on silica gel (MeOH : DCM = 1 : 10) to afford **34** as white solid (79 mg, 0.24 mmol, 93 %).  $^1\text{H}$  NMR (500 MHz,  $\text{CD}_3\text{OD}$ )  $\delta$  3.54 (s, 8H), 2.45 (s, 4H), 2.31 (t,  $J$  = 2.4 Hz, 2H), 2.28 (d,  $J$  = 2.6 Hz, 4H).  $^{13}\text{C}$  NMR (125 MHz,  $\text{CD}_3\text{OD}$ )  $\delta$  81.01, 77.24, 72.12, 68.17, 64.31, 61.01, 44.44, 22.98, 22.20. HRMS (ESI):  $m/z$  for  $\text{C}_{20}\text{H}_{22}\text{NaO}_4$   $[\text{M}+\text{Na}]^+$ , calcd. 349.1410, found: 349.1411.

To a solution of **34** (79 mg, 0.24 mmol) in DCM (3 ml), 2,6-lutidine (0.17 ml, 1.45 mmol) was added at 0 °C. Triisopropylsilyl trifluoromethanesulfonate (0.34 ml, 1.21 mmol) was added and stirred overnight. After quenching with NaHCO<sub>3</sub> aqueous solution, the organic layer was washed with water and extracted by dichloromethane, dried with MgSO<sub>4</sub>, and concentrated. The product was purified by flash column chromatography on silica gel (hexane elution) to afford **M17** as colorless liquid (187 mg, 0.196 mmol, 82 %). <sup>1</sup>H NMR (500 MHz, CD<sub>2</sub>Cl<sub>2</sub>) δ 3.68 (d, *J* = 9.7 Hz, 8H), 2.47 (s, 4H), 2.34 (d, *J* = 2.6 Hz, 4H), 1.99 (t, *J* = 2.6 Hz, 2H), 1.15 – 0.96 (m, 84H). <sup>13</sup>C NMR (125 MHz, CDCl<sub>3</sub>) δ 81.22, 76.65, 70.75, 67.93, 64.20, 60.37, 45.17, 22.64, 21.63, 18.16, 12.15. HRMS (ESI): *m/z* for C<sub>56</sub>H<sub>102</sub>NaO<sub>4</sub>Si<sub>4</sub> [M+Na]<sup>+</sup>, calcd. 973.6747, found: 973.6744.

## General procedure for polymerization

A 4-mL sized screw-cap vial with septum was flame dried and charged with monomer and a magnetic bar. The vial was purged with argon three times, and degassed anhydrous DCM was added. After the Ar-purged mixture of initiator (and additive) in another 4-mL vial was dissolved in DCM, the solution was rapidly injected to the monomer solution at experimental temperature under vigorous stirring. Low reaction temperature (0 °C) was regulated by fuzzy control system with refrigerated bath circulators (Wisecircu®). The reaction was quenched by excess ethyl vinyl ether after desired reaction time, and partially precipitated in methanol, remaining small amount of crude mixture (c.a. 10%). Obtained solid was filtered and dried *in vacuo*. Monomer conversion was calculated from the <sup>1</sup>H NMR spectrum of the remained crude mixture.

## <sup>1</sup>H and <sup>13</sup>C NMR characterization of polymers

**P1:** <sup>1</sup>H NMR (500 MHz, CDCl<sub>3</sub>) δ 6.79 – 6.04 (m, 2H), 3.93 – 3.54 (m, 12H), 3.54 – 2.98 (m, 8H). <sup>13</sup>C NMR (125 MHz, CDCl<sub>3</sub>) δ 171.98, 144.32, 126.18, 120.85, 93.69, 58.07, 53.35, 44.73, 40.17.

**P2:** <sup>1</sup>H NMR (300 MHz, CDCl<sub>3</sub>) δ 6.82 – 6.08 (m, 2H), 5.28 – 4.89 (m, 4H), 3.28 (br, 8H), 1.24 (br, 24H). <sup>13</sup>C NMR (100 MHz, CDCl<sub>3</sub>) δ 171.06, 144.42, 126.21, 120.91, 93.63, 69.55, 58.08, 44.69, 40.06, 21.86.

**P3:** <sup>1</sup>H NMR (300 MHz, CDCl<sub>3</sub>) δ 6.78 – 6.17 (m, 2H), 3.65 – 2.80 (m, 8H), 1.46 (br, 36H). <sup>13</sup>C NMR (75 MHz, CDCl<sub>3</sub>) δ 170.78, 144.38, 126.19, 120.93, 93.62, 81.77, 59.19, 44.63, 39.89, 28.18.

**P4** <sup>1</sup>H NMR (500 MHz, CDCl<sub>3</sub>) δ 6.61 (br, 2H), 3.21 (br, 8H), 2.12 (br, 36H), 1.66 (br, 24H). <sup>13</sup>C NMR (75 MHz, CDCl<sub>3</sub>) δ 170.58, 144.52, 126.13, 121.04, 93.71, 81.68, 59.43, 44.75, 41.35, 39.97, 36.52, 31.18.

**P5:** <sup>1</sup>H NMR (500 MHz, CDCl<sub>3</sub>) δ 6.81 – 6.12 (m, 2H), 3.52 (br, 8H), 2.44 (br, 8H), 0.95 (t, *J* = 7.5 Hz, 36H), 0.58 (d, *J* = 7.7 Hz, 24H). <sup>13</sup>C NMR (75 MHz, CDCl<sub>3</sub>) δ 146.18, 126.42, 122.17, 94.30, 65.55, 48.43, 43.02, 37.55, 7.19, 4.77.



**P6:**  $^1\text{H}$  NMR (500 MHz,  $\text{CDCl}_3$ )  $\delta$  6.89 – 6.03 (m, 2H), 3.66 (br, 6H), 3.40 – 2.57 (m, 8H), 1.28 (br, 12H), 0.84 (br, 18H), 0.20 – 0.02 (m, 12H).  $^{13}\text{C}$  NMR (125 MHz,  $\text{CDCl}_3$ )  $\delta$  176.31, 145.68, 126.08, 121.99, 94.24, 76.29, 63.14, 52.40, 42.95, 37.85, 27.42, 26.11, 18.56, -1.73.

**P7:**  $^1\text{H}$  NMR (500 MHz,  $\text{CDCl}_3$ )  $\delta$  6.76 – 6.18 (m, 2H), 3.63 (s, 8H), 2.84 – 2.03 (m, 8H), 1.20 – 0.88 (m, 84H).  $^{13}\text{C}$  NMR (125 MHz,  $\text{CDCl}_3$ )  $\delta$  145.90, 126.16, 122.10, 94.08, 66.38, 49.03, 42.94, 37.30, 18.30, 12.26.

**P8:**  $^1\text{H}$  NMR (500 MHz,  $\text{CDCl}_3$ )  $\delta$  6.73 – 6.18 (m, 2H), 3.36 – 2.96 (m, 12H), 1.52 – 1.39 (m, 54H).  $^{13}\text{C}$  NMR (125 MHz,  $\text{CDCl}_3$ )  $\delta$  170.50, 170.11, 144.82, 126.58, 126.10, 120.79, 93.44, 92.90, 81.54, 59.42, 59.06, 44.32, 44.02, 39.74, 29.82, 28.00.

**P9:**  $^1\text{H}$  NMR (500 MHz,  $\text{CDCl}_3$ )  $\delta$  6.59 – 6.19 (m, 2H), 4.12 – 3.90 (m, 12H), 2.69 – 2.42 (m, 12H), 1.23 – 1.15 (m, 54H).  $^{13}\text{C}$  NMR (75 MHz,  $\text{CDCl}_3$ )  $\delta$  178.02, 145.51, 127.32, 126.25, 121.58, 93.80, 93.23, 66.86, 66.65, 45.09, 44.59, 43.50, 43.28, 39.02, 27.30.

**P10:**  $^1\text{H}$  NMR (500 MHz,  $\text{CDCl}_3$ )  $\delta$  6.66 – 6.22 (m, 2H), 3.74 – 3.45 (m, 12H), 2.66 – 2.18 (m, 12H), 1.08 – 1.00 (m, 126H).  $^{13}\text{C}$  NMR (125 MHz,  $\text{CDCl}_3$ )  $\delta$  146.56, 127.72, 126.32, 122.16, 93.91, 93.53, 66.30, 49.52, 49.08, 42.88, 37.18, 29.86, 18.30, 12.24.

**P11:**  $^1\text{H}$  NMR (500 MHz,  $\text{CDCl}_3$ )  $\delta$  6.74 – 6.16 (m, 2H), 3.86 – 3.43 (m, 4H), 3.33 – 2.91 (m, 8H), 2.62 – 2.34 (m, 4H), 1.50 – 1.33 (m, 36H), 1.18 – 0.97 (m, 42H).  $^{13}\text{C}$  NMR (75 MHz,  $\text{CDCl}_3$ )  $\delta$  170.55, 144.12, 128.61, 125.95, 120.88, 94.63, 92.24, 81.41, 66.08, 58.94, 49.71, 44.50, 42.32, 39.68, 27.97, 18.25, 12.13.

**P14:**  $^1\text{H}$  NMR (500 MHz,  $\text{CDCl}_3$ )  $\delta$  6.49 (br, 2H), 3.73 (br, 12H), 3.26 (br, 8H).  $^{13}\text{C}$  NMR (125 MHz,  $\text{CDCl}_3$ )  $\delta$  171.55, 147.91, 126.68, 120.18, 82.64, 80.14, 57.94, 53.25, 44.07, 40.16.

**P15:**  $^1\text{H}$  NMR (500 MHz,  $\text{CDCl}_3$ )  $\delta$  6.54 (br, 2H), 3.11 (br, 8H), 1.45 (br, 36H).  $^{13}\text{C}$  NMR (125 MHz,  $\text{CDCl}_3$ )  $\delta$  170.46, 148.11, 126.72, 120.18, 81.94, 59.18, 44.13, 39.85, 37.26, 29.85, 28.02, 19.89.

**P16:**  $^1\text{H}$  NMR (300 MHz,  $\text{CDCl}_3$ )  $\delta$  7.00 – 6.18 (m, 2H), 3.94 (br, 8H), 2.72 (br,

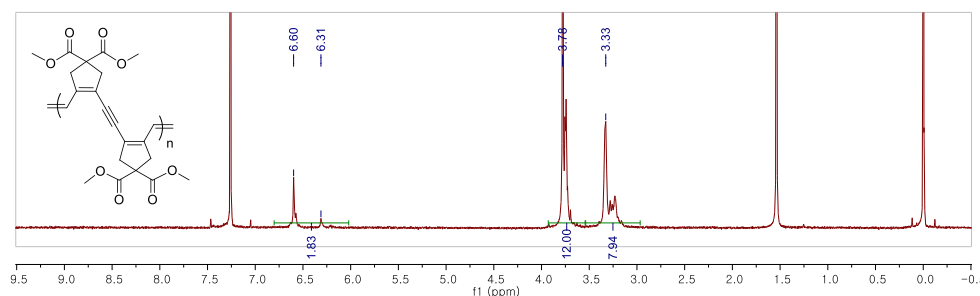
8H), 1.16 (br, 36H).  $^{13}\text{C}$  NMR (75 MHz,  $\text{CDCl}_3$ )  $\delta$  178.27, 149.08, 149.03, 128.90, 127.10, 120.95, 82.21, 80.64, 66.96, 44.76, 43.15, 39.09, 29.82, 27.32.

**P17:**  $^1\text{H}$  NMR (300 MHz,  $\text{CDCl}_3$ )  $\delta$  6.53 (br, 2H), 3.60 (br, 8H), 2.46 (br, 8H), 1.02 (br,  $J = 17.9$  Hz, 84H).  $^{13}\text{C}$  NMR (75 MHz,  $\text{CDCl}_3$ )  $\delta$  150.51, 127.03, 121.30, 81.57, 66.17, 53.56, 49.34, 42.34, 37.25, 29.85, 18.24, 12.20.

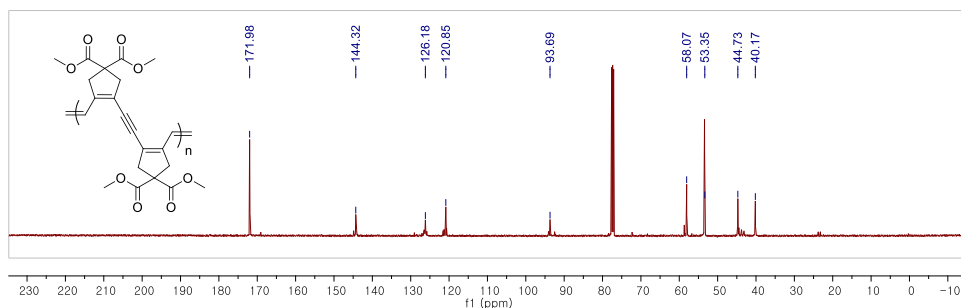
**P18:**  $^1\text{H}$  NMR (300 MHz,  $\text{CD}_2\text{Cl}_2$ )  $\delta$  6.78 (br, 2H), 3.68 (br, 8H), 2.79 (br, 8H), 1.41 (br, 12H).  $^{13}\text{C}$  NMR (75 MHz,  $\text{CD}_2\text{Cl}_2$ )  $\delta$  149.94, 127.29, 121.30, 98.22, 82.17, 81.35, 77.96, 68.99, 44.49, 40.36, 30.08, 24.26, 23.77.

## $^1\text{H}$ and $^{13}\text{C}$ NMR spectra of polymers

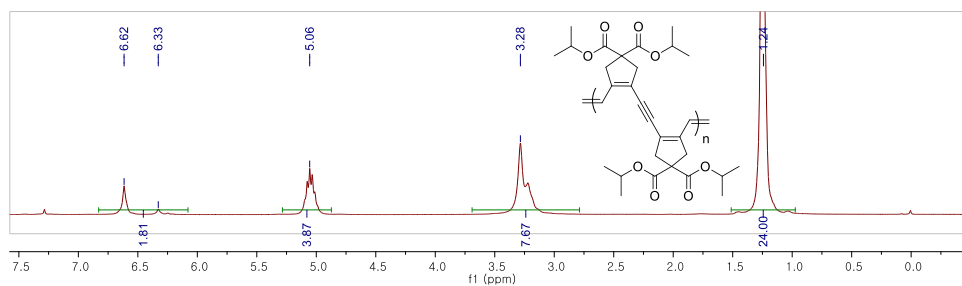
**P1** ( $^1\text{H}$  NMR,  $\text{CDCl}_3$ )



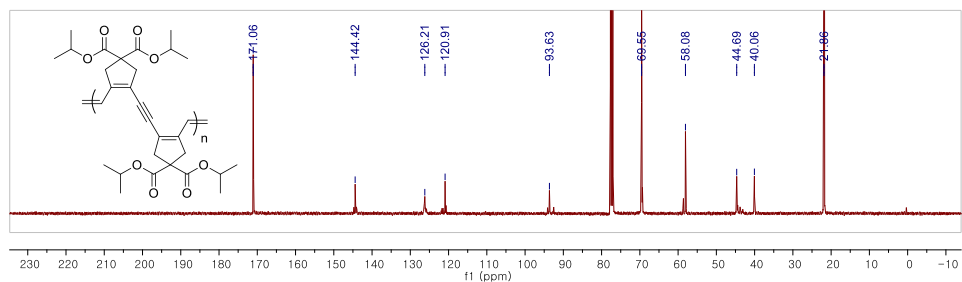
**P1** ( $^{13}\text{C}$  NMR,  $\text{CDCl}_3$ )



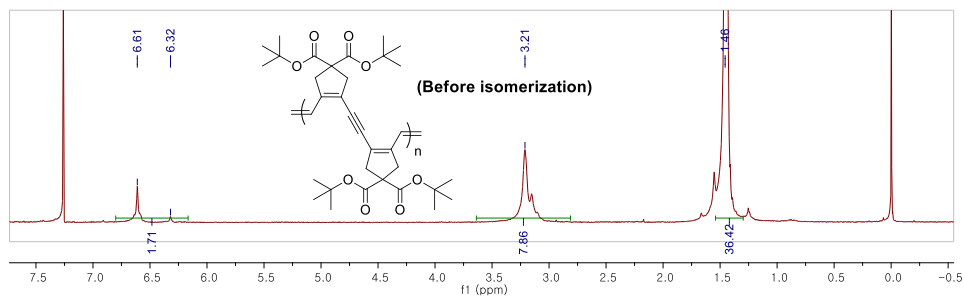
**P2** ( $^1\text{H}$  NMR,  $\text{CDCl}_3$ )



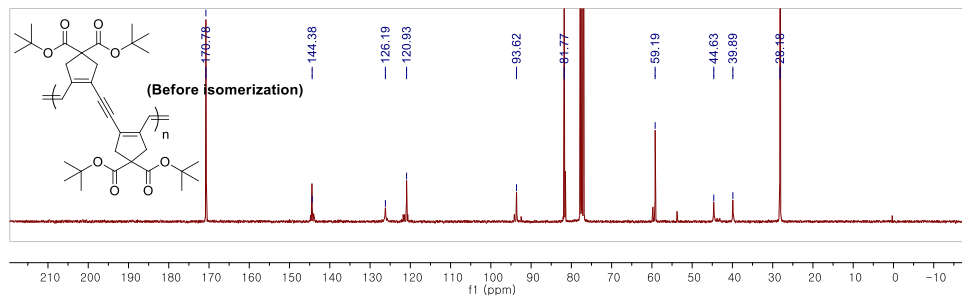
**P2** ( $^{13}\text{C}$  NMR,  $\text{CDCl}_3$ )



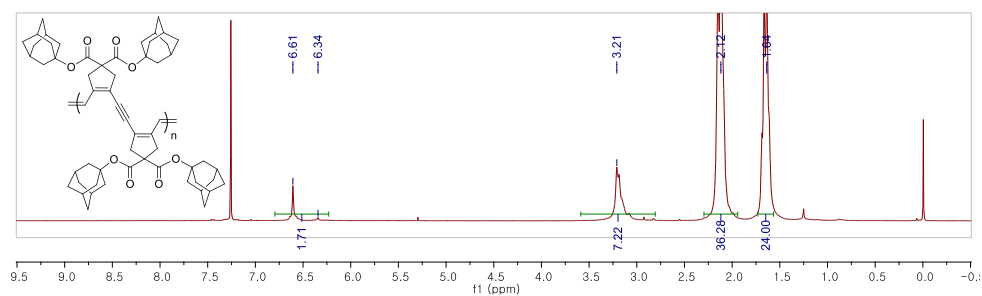
**P3** ( $^1\text{H}$  NMR,  $\text{CDCl}_3$ )



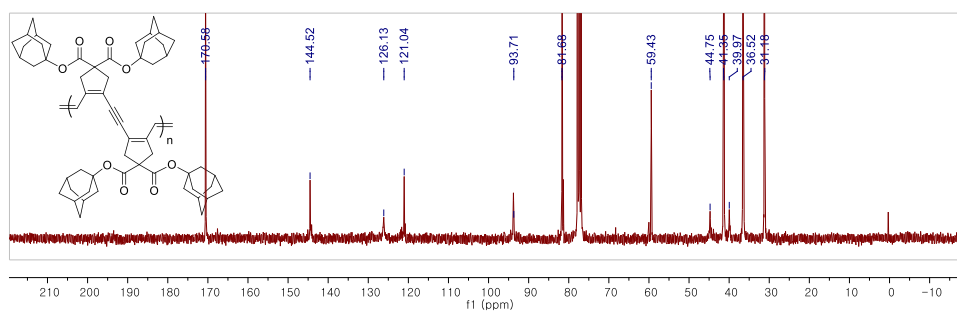
**P3** ( $^{13}\text{C}$  NMR,  $\text{CDCl}_3$ )



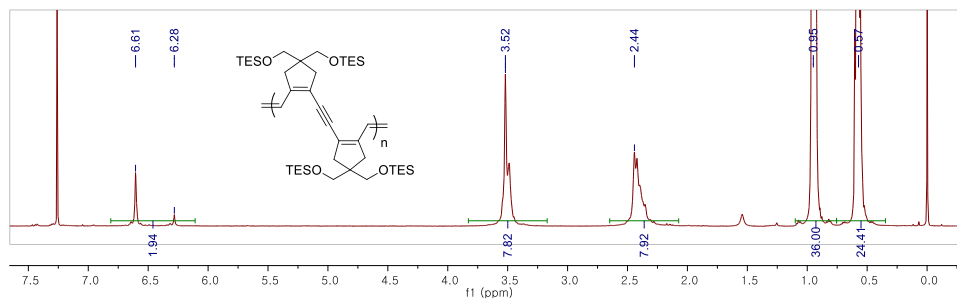
**P4** ( $^1\text{H}$  NMR,  $\text{CDCl}_3$ )



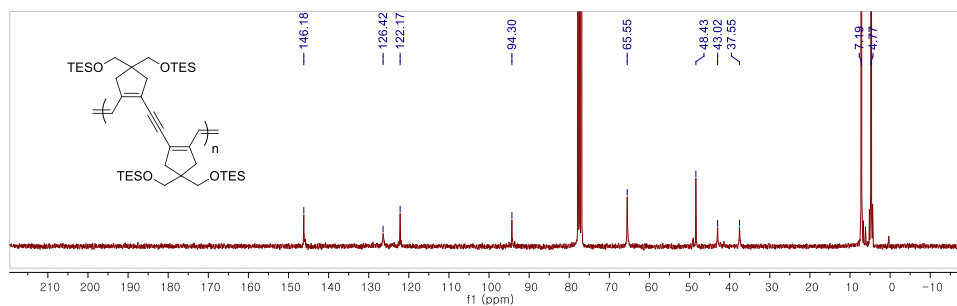
**P4** ( $^{13}\text{C}$  NMR,  $\text{CDCl}_3$ )



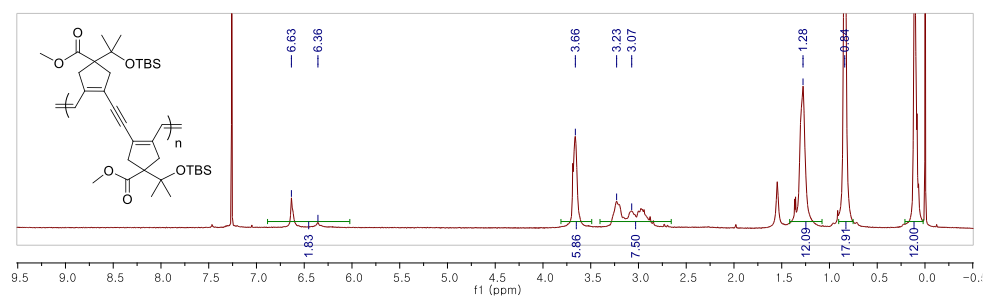
**P5** ( $^1\text{H}$  NMR,  $\text{CDCl}_3$ )



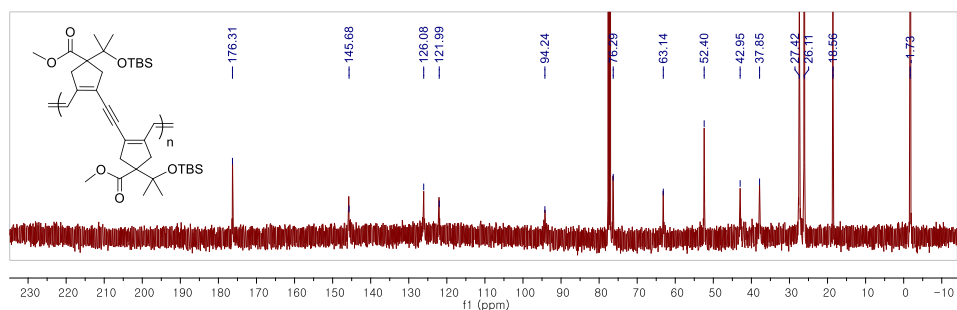
**P5** ( $^{13}\text{C}$  NMR,  $\text{CDCl}_3$ )



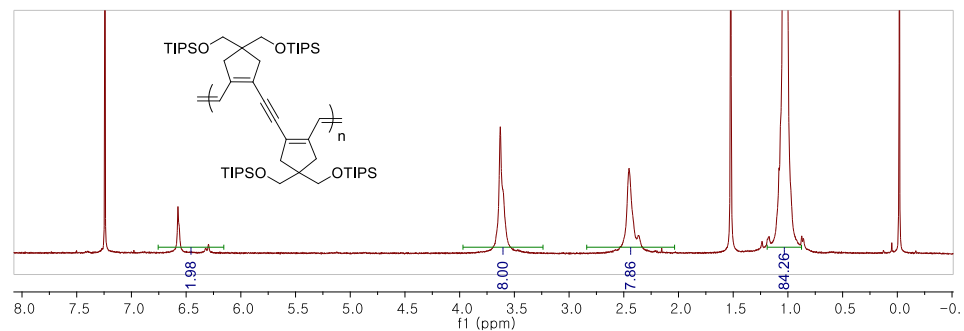
**P6** ( $^1\text{H}$  NMR,  $\text{CDCl}_3$ )



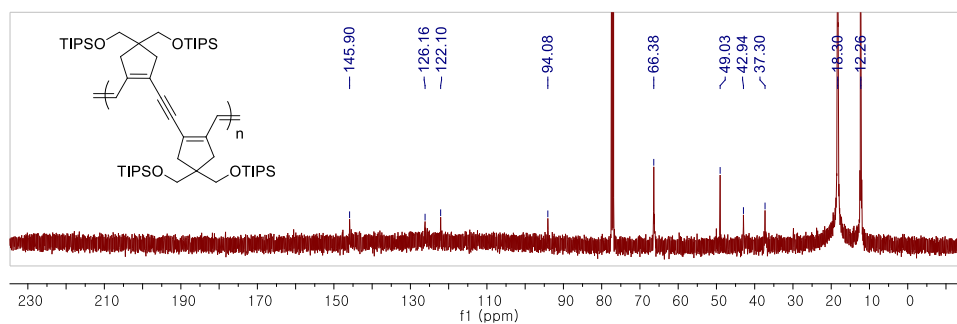
**P6** ( $^{13}\text{C}$  NMR,  $\text{CDCl}_3$ )



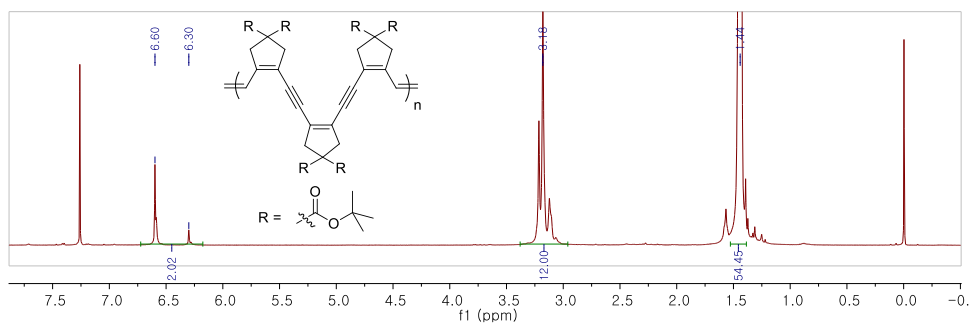
**P7**  $^1\text{H}$  NMR (500 MHz,  $\text{CDCl}_3$ )



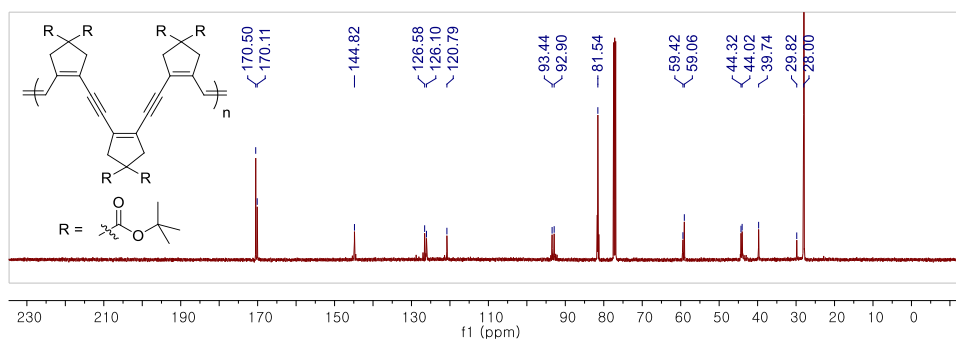
**P7**  $^{13}\text{C}$  NMR (125 MHz,  $\text{CDCl}_3$ )



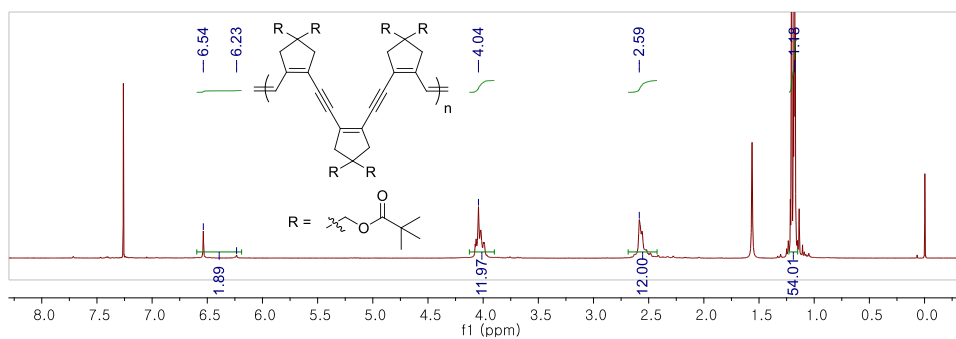
**P8**  $^1\text{H}$  NMR (500 MHz,  $\text{CDCl}_3$ )



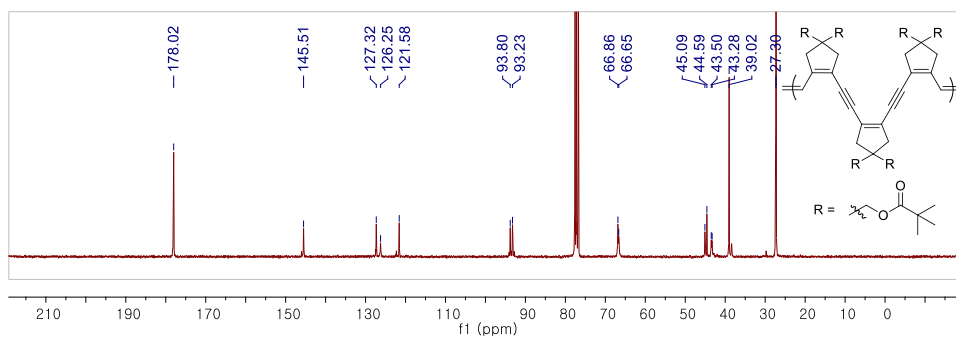
**P8**  $^{13}\text{C}$  NMR (125 MHz,  $\text{CDCl}_3$ )



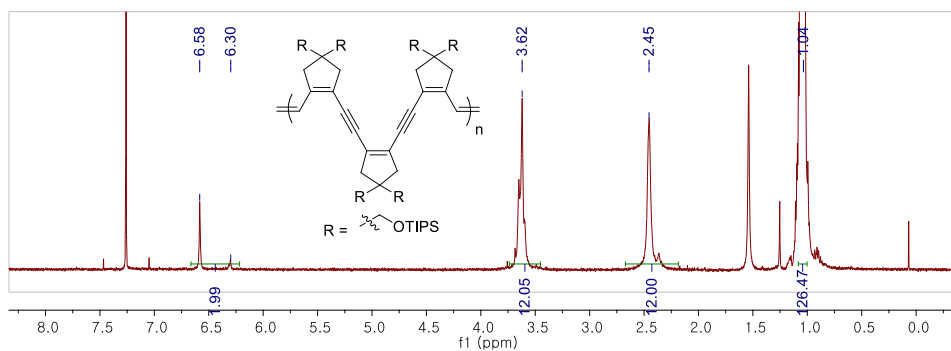
**P9**  $^1\text{H}$  NMR (500 MHz,  $\text{CDCl}_3$ )



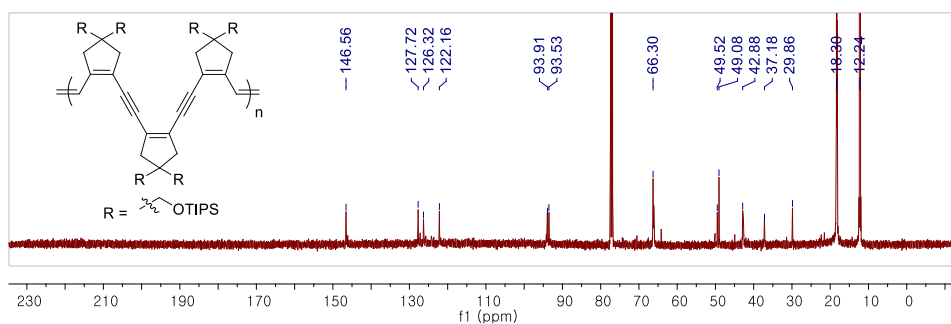
**P9**  $^{13}\text{C}$  NMR (75 MHz,  $\text{CDCl}_3$ )



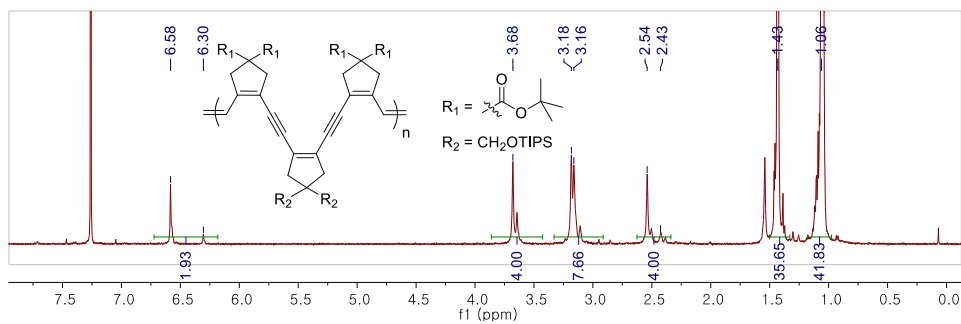
**P10**  $^1\text{H}$  NMR (500 MHz,  $\text{CDCl}_3$ )



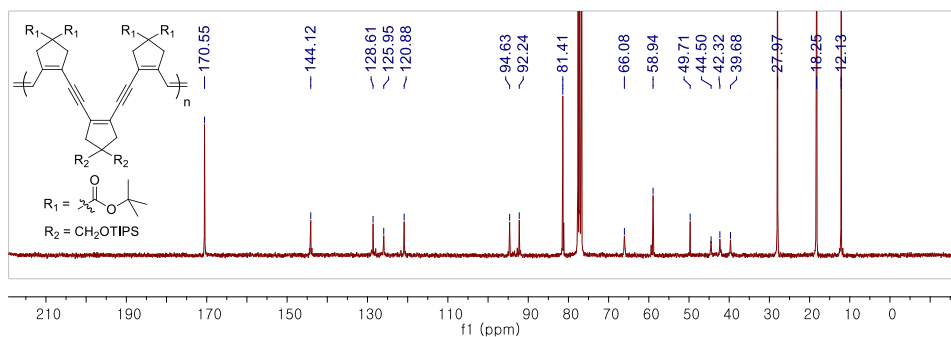
**P10**  $^{13}\text{C}$  NMR (125 MHz,  $\text{CDCl}_3$ )



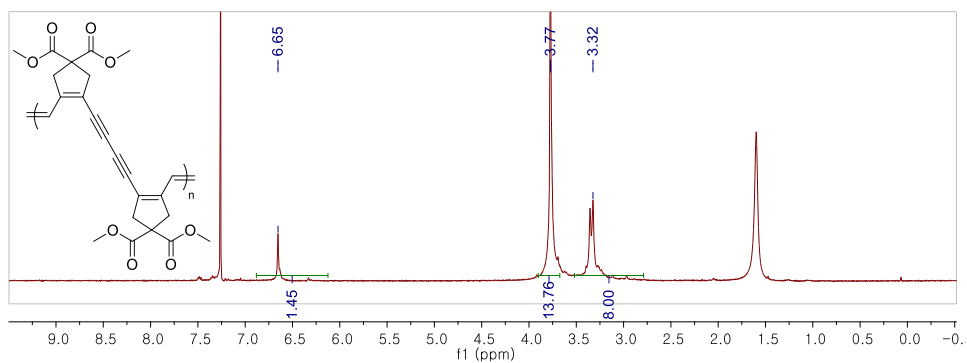
**P11**  $^1\text{H}$  NMR (500 MHz,  $\text{CDCl}_3$ )



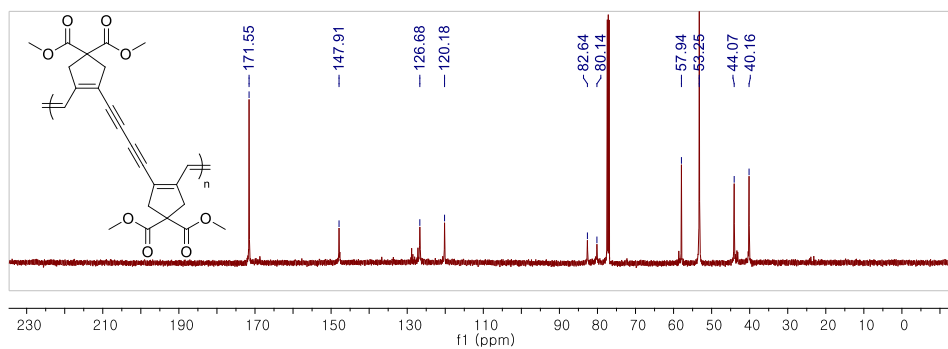
**P11**  $^{13}\text{C}$  NMR (75 MHz,  $\text{CDCl}_3$ )



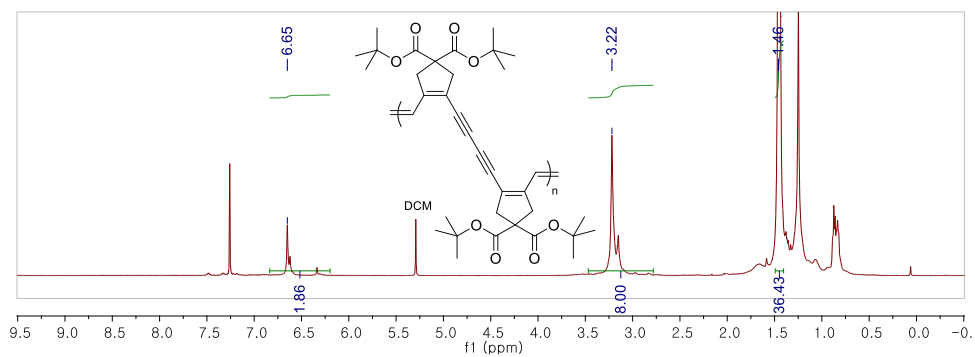
**P14**  $^1\text{H}$  NMR (500 MHz,  $\text{CDCl}_3$ )



**P14**  $^{13}\text{C}$  NMR (125 MHz,  $\text{CDCl}_3$ )

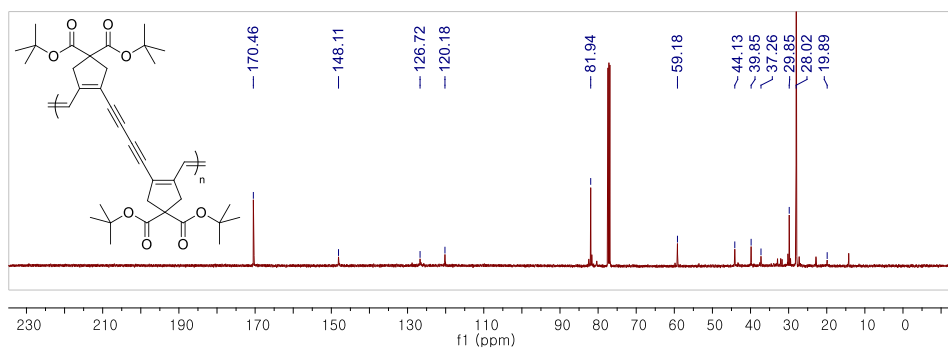


**P15**  $^1\text{H}$  NMR (500 MHz,  $\text{CDCl}_3$ )

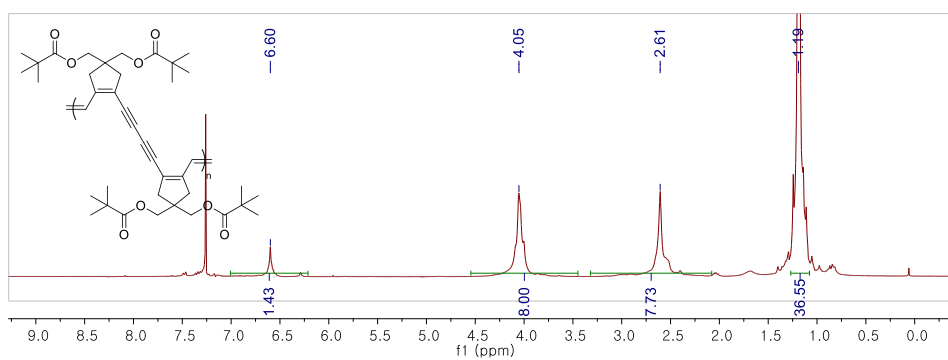




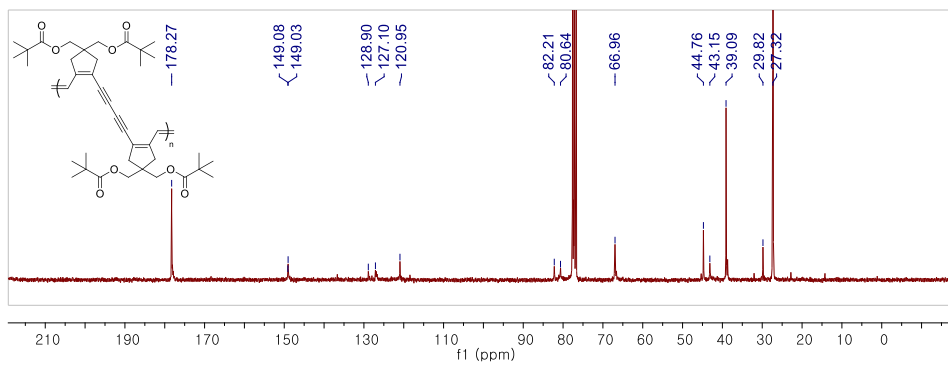
**P15**  $^{13}\text{C}$  NMR (125 MHz,  $\text{CDCl}_3$ )



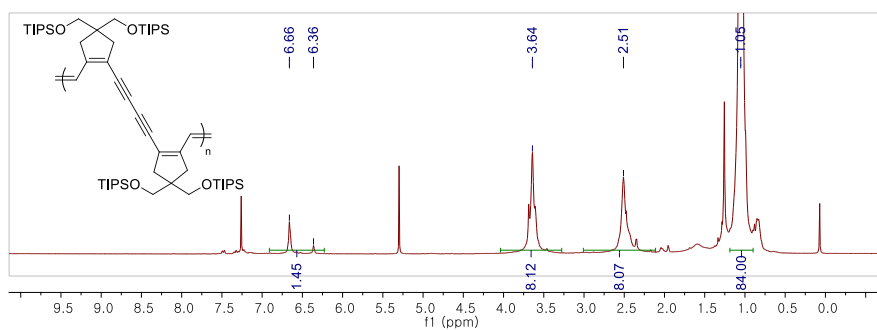
**P16**  $^1\text{H}$  NMR (300 MHz,  $\text{CDCl}_3$ )



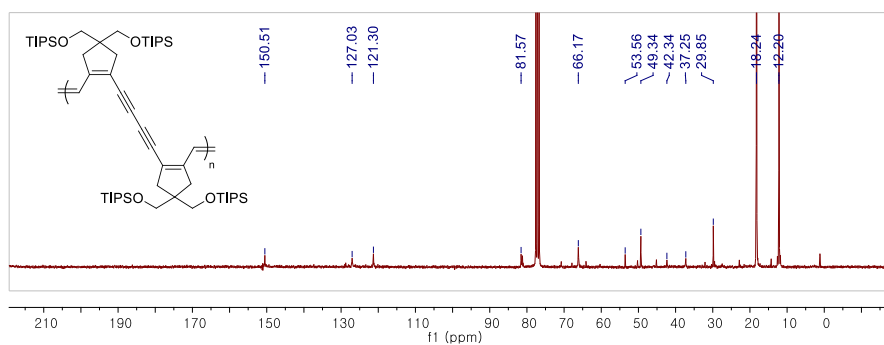
**P16**  $^{13}\text{C}$  NMR (75 MHz,  $\text{CDCl}_3$ )



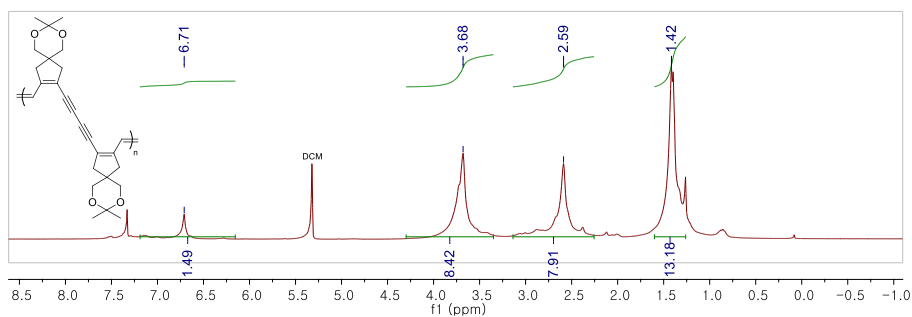
**P17**  $^1\text{H}$  NMR (300 MHz,  $\text{CDCl}_3$ )



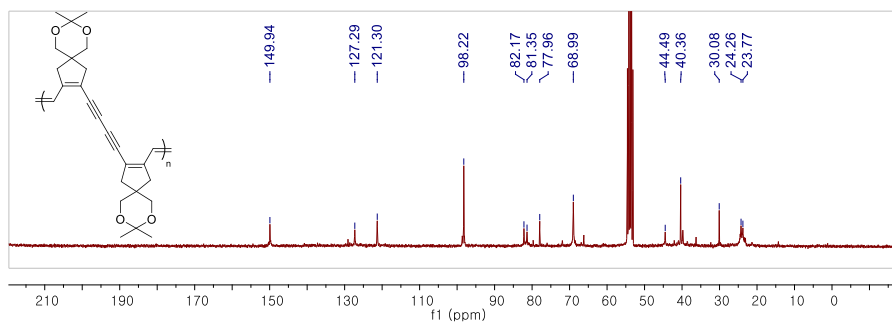
**P17**  $^{13}\text{C}$  NMR (75 MHz,  $\text{CDCl}_3$ )



**P18**  $^1\text{H}$  NMR (300 MHz,  $\text{CD}_2\text{Cl}_2$ )



**P18**  $^{13}\text{C}$  NMR (75 MHz,  $\text{CD}_2\text{Cl}_2$ )



## 4.7. References

† Portions of this chapter has been reported:

Kang, C.; Park, H.; Lee, J. K.; Choi, T.-L. *J. Am. Chem. Soc.* **2017**, *139*, 11309-11312.

Kang, C.; Kwon, S.; Sung, J. C.; Kim, J.; Baik, M. H.; Choi, T. L. *J. Am. Chem. Soc.* **2018**, *140*, 16320-16329.

- (1) Yoon, B.; Lee, S.; Kim, J. M. *Chem. Soc. Rev.* **2009**, *38*, 1958.
- (2) Sun, X.; Chen, T.; Huang, S.; Li, L.; Peng, H. *Chem. Soc. Rev.* **2010**, *39*, 4244.
- (3) Lee, S.; Kim, J. Y.; Chen, X.; Yoon, J. *Chem. Commun.* **2016**, *52*, 9178.
- (4) Eichele, H.; Schwoerer, M.; Huber, R.; Bloor, D. *Chem. Phys. Lett.* **1976**, *42*, 342–346
- (5) Stevens, G. C.; Bloor, D. *Chem. Phys. Lett.* **1976**, *40*, 37–40.
- (6) Lee, D.; Kim, M. *Org. Biomol. Chem.* **2007**, *5*, 3418-3427.
- (7) Padwa, A.; Austin, D. J.; Gareau, Y.; Kassir, J. M.; Xu, S. L. *J. Am. Chem. Soc.* **1993**, *115*, 2637-2647.
- (8) Barluenga, H.; de la Rúa, R. B.; de Súa, D.; Ballesteros, A.; Tomás, M. *Angew. Chem. Int. Ed.* **2005**, *44*, 4981-4983.
- (9) Barluenga, J.; García-García, P.; de Súa, D.; Fernández-Rodríguez, M. A.; Bernardo de la Rúa, R.; Ballesteros, A.; Aguilar, E.; Tomás, M. *Angew. Chem. Int. Ed.* **2007**, *46*, 2610–2612.
- (10) Ohe, K.; Fujita, M.; Matsumoto, H.; Tai, Y.; Miki, K. *J. Am. Chem. Soc.* **2006**, *128*, 9270–9271.
- (11) Kim, M.; Miller, R. L.; Lee, D. *J. Am. Chem. Soc.* **2005**, *127*, 12818–12819.
- (12) Kim, M.; Lee, D. *J. Am. Chem. Soc.* **2005**, *127*, 18024–18025.
- (13) Yun, S. Y.; Kim, M.; Lee, D.; Wink, D. J. *J. Am. Chem. Soc.* **2009**, *131*, 24-25
- (14) Wang, K.-P.; Yun, S. Y.; Lee, D.; Wink, D. L. *J. Am. Chem. Soc.* **2009**, *131*, 15114-15115.
- (15) Yun, S. Y.; Wang, K. P.; Kim, M.; Lee, D. *J. Am. Chem. Soc.* **2010**, *132*, 8840-8841.

- (16) Wang, K. P.; Cho, E. J.; Yun, S. Y.; Rhee, J. Y.; Lee, D. *Tetrahedron*, **2013**, *69*, 9105-9110.
- (17) Cho, E. J.; Lee, D. *Org. Lett.* **2008**, *10*, 257-259.
- (18) Li, J.; Miller, R. L.; Lee, D. *Org. Lett.* **2009**, *11*, 571-574.
- (19) Grubbs, R. H. *Handbook of Metathesis*, 2nd ed., Vols. 2, 3; Wiley-VCH: Weinheim, 2015.
- (20) Grela, K. *Olefin Metathesis: Theory and Practice*. Wiley-VCH: Weinheim, 2014.
- (21) Peterson, G. I.; Yang, S.; Choi, T. L. *Acc. Chem. Res.* **2019**, *52*, 994–1005.
- (22) Buchmeiser, M. R. *Polym. Rev.* **2017**, *57*, 15-30.
- (23) Park, H.; Choi, T.-L. *J. Am. Chem. Soc.* **2012**, *134*, 7270– 7273.
- (24) Park, H.; Lee, H.-K.; Choi, T.-L. *J. Am. Chem. Soc.* **2013**, *135*, 10769-10775.
- (25) Park, H.; Kang, E. H.; Müller, L.; Choi, T. L. *J. Am. Chem. Soc.* **2016**, *138*, 2244-2251.
- (26) Lee, H. K.; Bang, K. T.; Hess, A.; Grubbs, R. H.; Choi, T. L. *J. Am. Chem. Soc.* **2015**, *137*, 9262-9265.
- (27) Carnes, M.; Buccella, D.; Siegrist, T.; Steigerwald, M. L.; Nuckolls, C. *J. Am. Chem. Soc.* **2008**, *130*, 14078-14079.
- (28) von Kugelgen, S.; Bellone, D. E.; Cloke, R. R.; Perkins, W. S.; Fischer, F. R. *J. Am. Chem. Soc.* **2016**, *138*, 6234-6239.
- (29) Katsumata, T.; Shiotsuki, M.; Masuda, T.; *Macromol. Chem. Phys.* **2006**, *207*, 1244-1252.
- (30) Katsumata, T.; Shiotsuki, M.; Sanda, F.; Sauvage, X.; Delaude, L.; Masuda, T. *Macromol. Chem. Phys.* **2009**, *210*, 1891–1902.
- (31) Kang, E.-H.; Yu, S. Y.; Lee, I. S.; Park, S. E.; Choi, T.-L. *J. Am. Chem. Soc.* **2014**, *136*, 10508-10514.
- (32) Kang, E. H.; Kang, C.; Yang, S.; Oks, E.; Choi, T. L. *Macromolecules* **2016**, *49*, 6240–6250
- (33) Park, H.; Lee, H. K.; Choi, T. L. *Polym. Chem.* **2013**, *4*, 4676-4681.

- (34) Kang, E.-H.; Choi, T.-L. *ACS Macro Lett.* **2013**, *2*, 780–784.
- (35) Wenz, G.; Mueller, M. A.; Schmidt, M.; Wegner, G. *Macromolecules* **1984**, *17*, 837.
- (36) Bredas, J. L.; Heeger, A. J. *Macromolecules* **1990**, *23*, 1150.
- (37) Magyar, R. J.; Tretiak, S.; Gao, Y.; Wang, H. L.; Shreve, A. P. *Chem. Phys. Lett.* **2005**, *401*, 149.
- (38) Jung, K.; Kim, K.; Sung, J. C.; Ahmed, T. S.; Hong, S. H.; Grubbs, R. H.; Choi, T.-L. *Macromolecules* **2018**, *51*, 4564.
- (39) Rughooputh, S. D. D. V.; Phillips, D.; Bloor, D.; Ando, D. *J. Chem. Phys. Lett.* **1984**, *106*, 247.

## Chapter 5. $\beta$ -Selective Cascade Metathesis and Metallotropy Polymerization

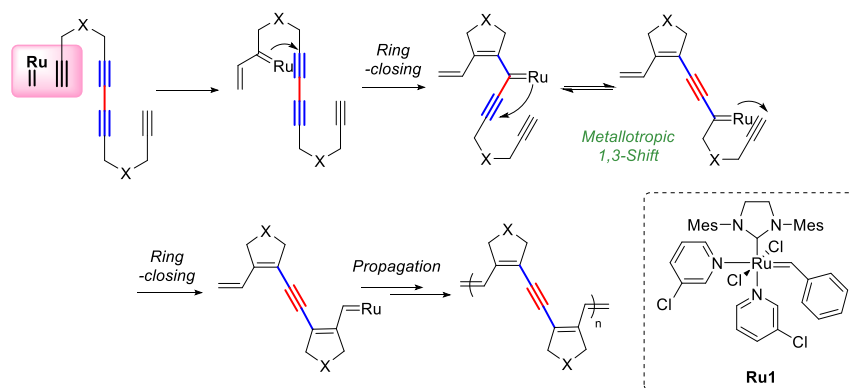
### 5.1. Abstract

Previously, we synthesized various conjugated polyenynes containing cyclopentene units in the backbone via exclusive  $\alpha$ -addition by using the third-generation Grubbs catalyst. In this chapter, we demonstrate the complete switch of regioselectivity toward  $\beta$ -addition using a Ru carbene containing a dithiolate ligand, and thus, synthesized new unique conjugated polyenynes having alternating cyclohexene and cyclopentene units in the backbone. Furthermore, detailed *in situ* NMR studies revealed that the adjacent triple bond strongly chelates to the propagating Ru carbene during the polymerization.

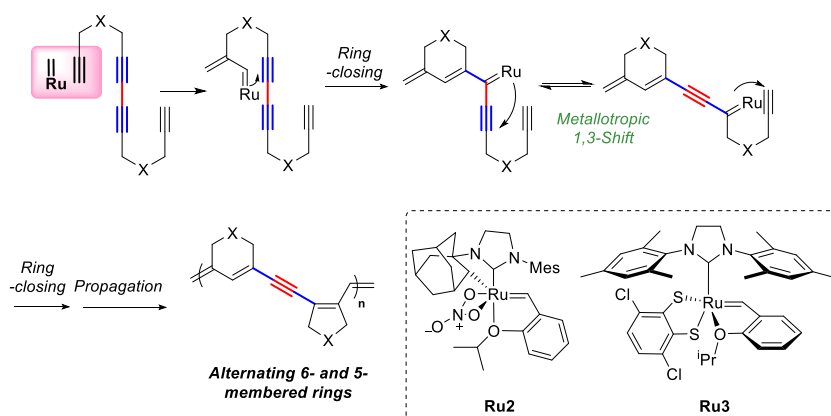
## 5.2. Introduction

In Chapter 4, we demonstrated the chain-growth synthesis of conjugated polyenynes by designing tetrayne monomers, where cascade olefin metathesis and metallotropic 1,3-shift reactions occurred in the presence of the 3<sup>rd</sup> generation Grubbs catalyst, **Ru1** (Scheme 5.1.a).<sup>1</sup> Furthermore, the design of pentayne and hexayne monomers enabled the incorporation of various sequences of conjugated double and triple bonds in the backbone, and even living polymerization was possible, thus allowing control of the molecular weights with narrow dispersities and the synthesis of conjugated block copolyenynes.<sup>2</sup>

(a)  $\alpha$ -addition (Previous work)



(b)  $\beta$ -addition (This work)



**Scheme 5.1.** Mechanism of Cascade Metathesis and Metallotropy (M&M) Polymerization via (a)  $\alpha$ - or (b)  $\beta$ -Addition

Meanwhile, one of the most important issues related to the cyclopolymerization of 1,6-heptadiynes,<sup>3</sup> is controlling the regioselectivity of the catalyst insertion, i.e.,  $\alpha$ - or  $\beta$ -addition to produce polyacetylenes containing five- or six-membered ring, respectively.<sup>4,5</sup> Historically, this selectivity issue was addressed by modifying the ligands of Schrock-type Mo catalysts.<sup>6-8</sup> However, only Ru-based catalysts were known to promote the M&M reaction, and for more than two decades, all the conventional Grubbs-type Ru catalysts produced only  $\alpha$ -addition products, thereby limiting the scope of M&M polymerization. Fortunately, recent advances in catalyst design have led to the discovery of the so-called Grubbs *Z*-selective catalyst (**Ru2**)<sup>9</sup> and stereo-retentive Hoveyda catalyst (**Ru3**),<sup>10</sup> which contain a chelating *N*-heterocyclic ligand and a dithiolate ligand, respectively. Using these new Ru catalysts, cyclopolymerization via  $\beta$ -addition in a highly selective manner became possible.<sup>11-14</sup> Accordingly, we envisioned that selective  $\beta$ -addition using **Ru2** or **Ru3** would afford a new type of conjugated polyenynes containing alternating six- and five-membered rings in the backbone via sequential ring-closing (to form a six-membered ring)/metallotropic 1,3-shift/ring-closing (to form a five-membered ring) reactions (Scheme 5.1.b). In this chapter, we demonstrate the  $\beta$ -selective M&M polymerization from various tetrayne monomers and provide deeper insights into the polymerization mechanism by in-depth NMR studies.

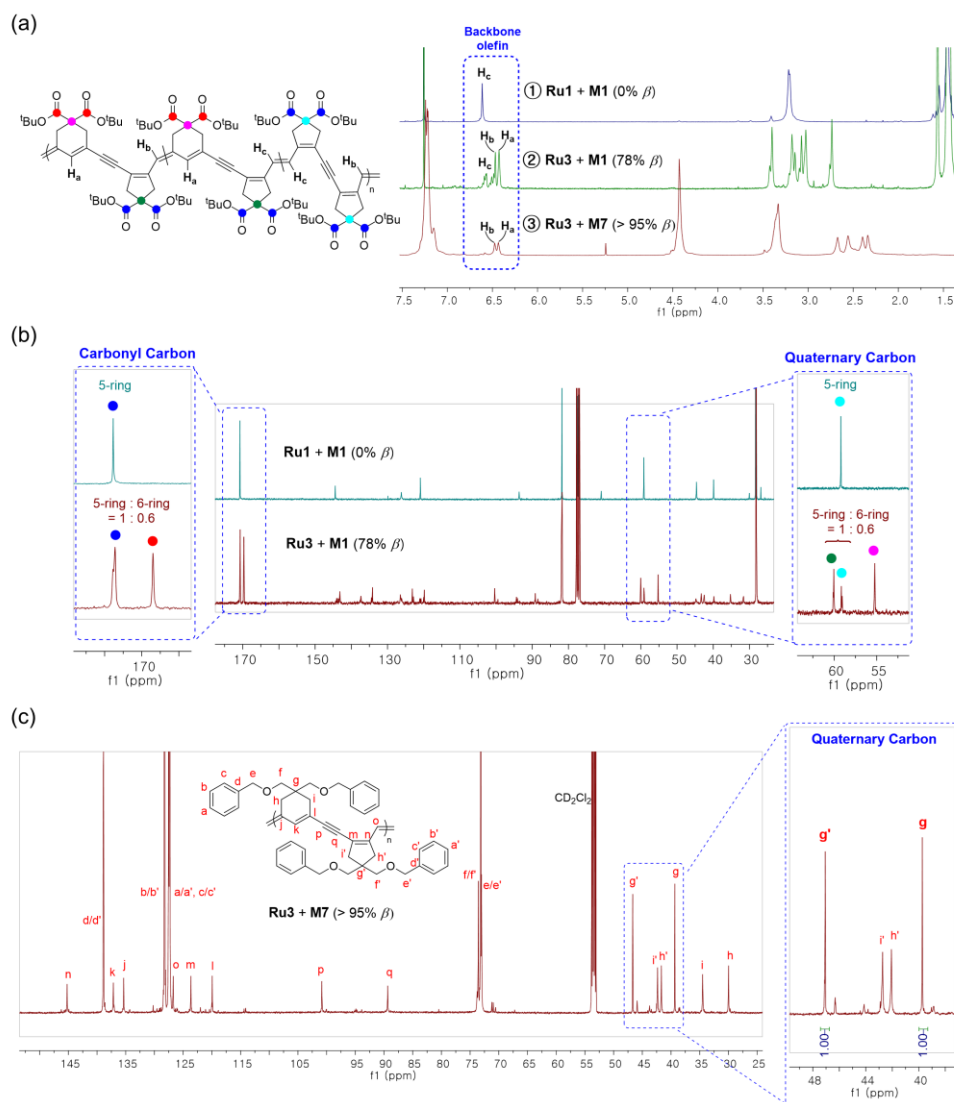


## 5.3. Results and Discussion

### 5.3.1. Polymerization and characterization

First, we optimized the polymerization conditions by using **M1**, which was one of the most efficient tetrayne monomers for the previous  $\alpha$ -selective M&M polymerization using **Ru1**.<sup>1</sup> After screening, we observed that **Ru3** was much more active than **Ru2** at 40 °C in DCM with 3,5-dichloropyridine additive (Table S5.1), affording polyenyne **P1** with a high conversion of 91% (M/I/Add = 25/1/5) and  $M_n$  = 20 kDa (Table 5.1, entry 1). Disappointingly, **P1** showed only moderate  $\beta$ -selectivity of 75%, which was much lower than that observed with the previous cyclopolymerizations.<sup>12-14</sup> However, when the side chains were altered from *tert*-butyl (**M1**) to the smaller isopropyl (**M2**) and methyl (**M3**) malonate moieties, the  $\beta$ -selectivities increased from 75% to 85 and 88%, respectively (entries 2 and 3, Figure S5.1) while maintaining comparable conversions (89% and 82%, respectively). Similarly, the smaller acetyl-containing **M4** showed higher  $\beta$ -selectivity (89%) than that of the bulkier pivaloyl-containing **M5** (78%), while yielding high conversions at M/I = 15 (90% and 83%, respectively) to give  $M_n$ s of 10.8 kDa and 14.6 kDa (entries 4 and 5). While triethylsilyl (**M6**)- and benzyl ether (**M7**)-containing monomers showed high conversions of 83% and 96%, respectively, to afford polymers with molecular weights of 9–11 kDa (entries 6 and 7), both **P6** and **P7** interestingly showed very high regioselectivity toward  $\beta$ -addition (92%–93%) to form a well-defined polymer structure containing almost perfectly alternating six- and five-membered rings. Furthermore, monomers **M8**–**M10** having one ester group and silyl ether groups with a *gem*-dimethyl group showed even higher  $\beta$ -selectivities (93%–97%) with moderate to good polymerization efficiency (68%–94%), affording 10–14 kDa polymers (entries 8–10).





**Figure 5.1.** (a) Comparison of  $^1\text{H}$  NMR spectra of polymers having different  $\alpha/\beta$  selectivity for **P1** and **P7**. (b)  $^{13}\text{C}$  NMR spectra of polymers having different  $\alpha/\beta$  selectivity from **M1**. (c) Full characterization of **P7** by  $^{13}\text{C}$  NMR.

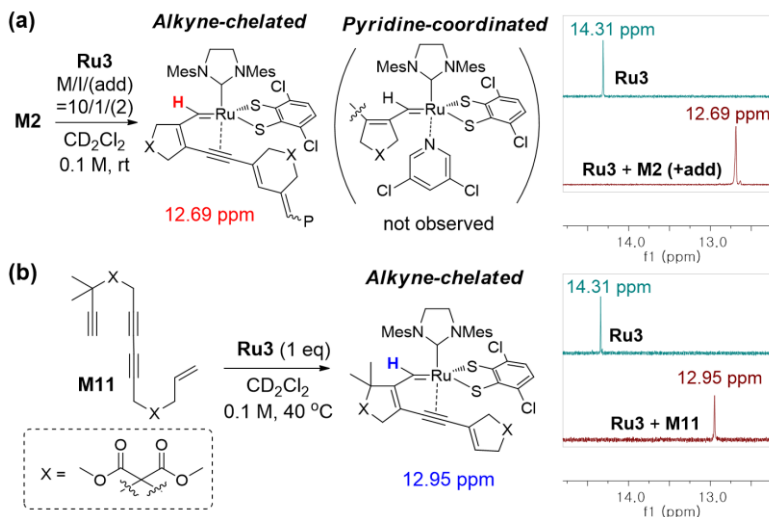
All the new polymer structures, including the  $\beta$ -selectivities, were readily determined by  $^1\text{H}$  and  $^{13}\text{C}$  NMR analyses. When **M1** was polymerized via  $\alpha$ -selective M&M polymerization using **Ru1**,<sup>1</sup> the olefinic proton in the backbone containing only five-membered rings showed a single peak at 6.61 ppm ( $\text{H}_c$ ) in the  $^1\text{H}$  NMR spectrum (Figure 5.1.a-①). In contrast, the  $^1\text{H}$  NMR spectrum of **P1** prepared from **Ru3** showed multiple peaks at 6.47–6.61 ppm ( $\text{H}_b$  and  $\text{H}_c$ ) and a

sharp peak at 6.43 ppm ( $H_a$ ), with a ratio of approximately 1:0.6, which corresponded to the olefins adjacent to the five- and six-membered rings, respectively (Figure 5.1.a-②, Figure S5.2). This observation was consistent with the  $^{13}\text{C}$  NMR spectrum, which also confirmed the approximate ratio of 1:0.6 for the five- and six-membered rings from the carbonyl carbon and the quaternary carbon region (Figure 5.1.b, Figure S5.3). In the  $^1\text{H}$  NMR spectrum of **P7**, two clear peaks were observed at 6.53 ( $H_b$ ) ppm and 6.49 ppm ( $H_a$ ) in an 1:1 ratio, showing only a small amount of  $H_c$  (6.64 ppm, 7%) corresponding to the five-membered ring in a consecutive manner (Figure 5.1.a-③). This result was further supported by the  $^{13}\text{C}$  NMR spectrum, which showed a 1:1:0.16 ratio of the quaternary carbon peaks from  $\beta$ -addition ( $g$  and  $g'$ ) and  $\alpha$ -addition ( $g'-\alpha$ ), respectively (Figure 5.1.c, Figure S5.4). All other peaks could be assigned explicitly to the expected polymer structure having alternating six- and five-membered rings, which gave six different olefin peaks (j-o) (Figures S5.5–S5.8).

### 5.3.2. *In situ* NMR and UV-Vis measurements

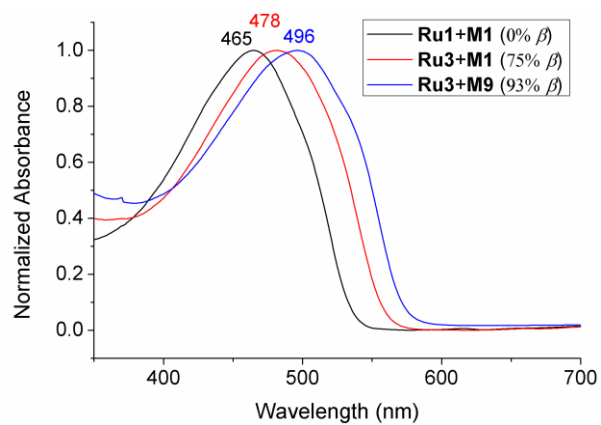
In order to obtain detailed mechanistic insights, we monitored the polymerization kinetics of **M2** ( $M/I = 10$ ) by *in situ*  $^1\text{H}$  NMR analysis. Initially, the benzyldiene carbene proton of **Ru3** was observed at 14.31 ppm, and the new peak at 12.69 ppm grew after the addition of the monomer (Figure 5.2.a). Interestingly, the same propagating carbene peak was observed even with the addition of 3,5-dichloropyridine (2 equiv with respect to **Ru3**). A new peak, which could be putatively assigned to the pyridine-bound Ru complex, appeared at 15.48 ppm (~58%) only after the addition of an excess amount (30 equiv) of the stronger 3-chloropyridine ligand (Figure S5.9). This implied that the adjacent triple bond is strongly chelated to the propagating Ru carbene, similar to the structure reported by the Lee group (alkyne chelation).<sup>15</sup> Analogous to their strategy, the reaction of **Ru3** with **M11**, consisting of a tetradeca-1-en-6,8,13-triyne moiety, produced an alkyne-chelated Ru complex, which showed a single carbene peak at 12.95 ppm (Figure 5.2.b). This further supported that the propagating carbene from **M2** (12.69 ppm, Figure 5.2.a) corresponded to a similar alkyne-chelated species, the peak for which was more upfield-shifted than that of the pyridine-bound Ru carbene (15.48 ppm, Figure S5.9). This strong chelation could explain the highly retarded propagation with **Ru3** (Figure S5.10, 3 h to reach a degree of polymerization (DP) of 8 at room temperature) as compared to the reaction using **Ru1**, which showed no alkyne chelation (only 10 min to reach a DP of 20).<sup>1</sup> The addition of pyridine to **Ru3** did not significantly retard the propagation or improve the stability of the propagating carbene (Figure S5.10); however, we added pyridine because the results were slightly better than those without the pyridine (Table S5.1). This is contrast to the case of using **Ru1**, where the pyridine additives played a crucial role in stabilizing the propagating carbene.<sup>1</sup> Furthermore, the electronic nature of various pyridine additives did not affect the regioselectivity of the M&M polymerization when using **Ru3** (75–79% with **M1**, Table S5.2), unlike the cyclopolymerization of 1,6-heptadiynes using **Ru3**, where the regioselectivity

drastically changed with the type of pyridine additive.<sup>13,14</sup> All these observations indicated that the strong intramolecular alkyne chelation impeded any other intermolecular reactions/interactions such as propagation or pyridine coordination.



**Figure 5.2.** (a) <sup>1</sup>H NMR spectra of initial **Ru3** and the propagating carbene with and without additive. (b) Formation of alkyne-chelated Ru complex from the reaction of **M11** and **Ru3**.

Having synthesized these new conjugated polyenyynes by  $\beta$ -selective M&M polymerization, we next investigated their optoelectronic and physical properties (Table S5.3). The UV-Vis absorption spectra of the polymers were more red-shifted as the  $\beta$ -addition% increased from 0% ( $\lambda_{\text{max}} = 465$  nm) to 93% (496 nm) (Figure 5.3, Figure S5.11), and accordingly, the optical band-gaps ( $E_g$ ) became narrower (2.31 and 2.16 eV, respectively). It seems that the higher amount of the 6-membered ring resulted in a longer effective conjugation length due to its more planar conformation. Analogous to the polymers obtained by  $\alpha$ -selective M&M polymerization,<sup>1,2</sup> all the new polymers showed very weak emissions at 536–552 nm (Figure S5.13). Finally, the thermal decomposition temperatures of the polymers ranged from 200 to 342 °C, as measured by thermogravimetric analysis.



**Figure 5.3.** UV-Vis spectra of polymers having different  $\alpha/\beta$  selectivities.

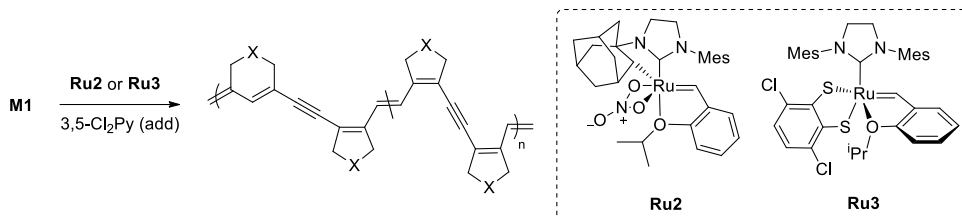
## 5.4. Conclusion

In conclusion, we demonstrated cascade metathesis and metallotropy (M&M) polymerization by completely switching the regioselectivity from  $\alpha$ -addition to  $\beta$ -addition, thereby producing conjugated polyenynes having alternating six- and five-membered rings in the backbone. Detailed *in situ* NMR studies revealed that a stable alkyne-chelated Ru complex was formed during polymerization, thus explaining the slow propagation and insignificant role of the pyridine additive in the kinetics and regioselectivity of the polymerization. The findings of this study will broaden the utility of cascade M&M polymerization due to precise control of the regioselectivity.



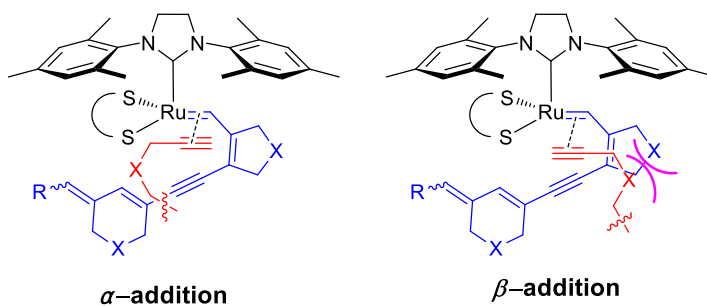
## 5.5. Supporting Figures

**Table S5.1.** Optimization of Polymerization of **M1** Using **Ru2** and **Ru3**

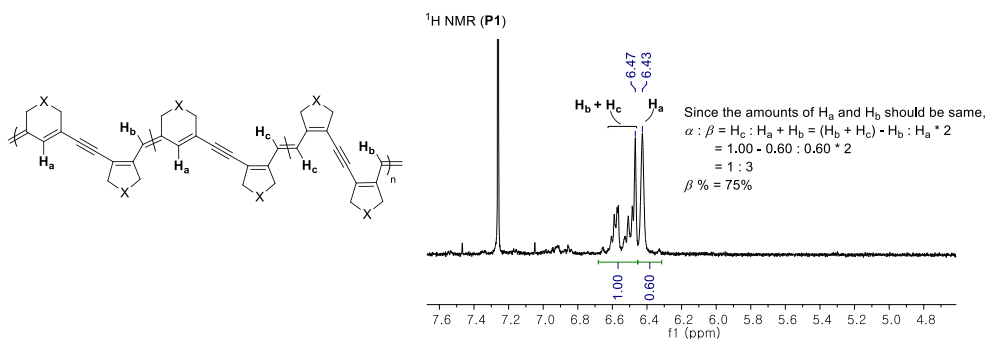


entry	cat	M/I/add	solvent	temp (°C)	time (h)	conv (%) <sup>a</sup>	yield (%) <sup>b</sup>	<i>M<sub>n</sub></i> <sup>c</sup> (kDa)	<i>D<sub>w</sub></i> <sup>c</sup>	<i>β</i> (%) <sup>a</sup>
1	<b>Ru2</b>	25/1/0	THF	rt	26	< 5	-	-	-	-
2	<b>Ru2</b>	25/1/0	DCE	70	13	25	-	-	-	-
3	<b>Ru3</b>	25/1/0	DCE	70	4	99	65	21.3	1.47	72%
4	<b>Ru3</b>	25/1/0	DCM	40	6	93	78	14.8	1.58	74%
5	<b>Ru3</b>	25/1/0	DCM	rt	22	48	44	10.6	1.36	73%
6	<b>Ru3</b>	25/1/5	DCM	40	6	91	84	20.0	1.36	75%

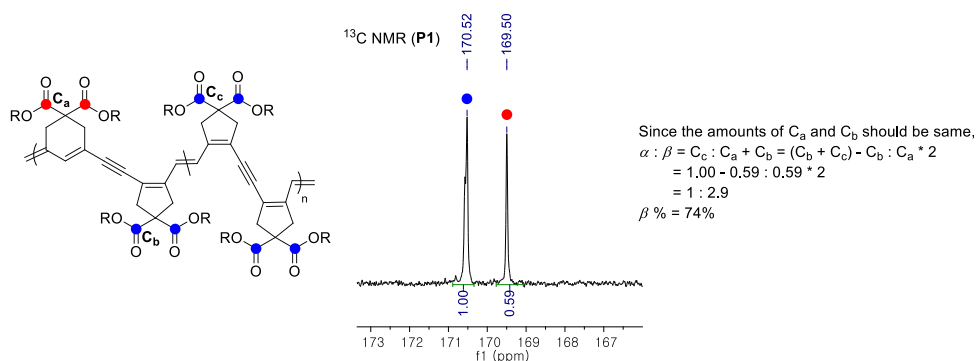
<sup>a</sup>Calculated from crude <sup>1</sup>H NMR. <sup>b</sup>Isolated yield. <sup>c</sup>Determined by tetrahydrofuran (THF) size-exclusion chromatography (SEC) calibrated using polystyrene standards.



**Figure S5.1.** Larger side chain (X) tends to give higher steric repulsion between the propagating species and monomer impeding the  $\beta$ -addition pathway.

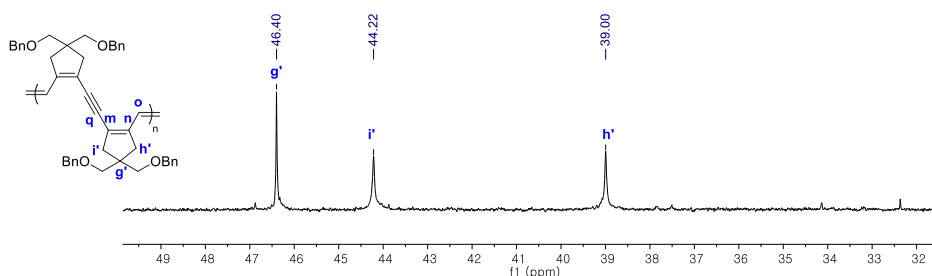


**Figure S5.2.** Calculation of  $\beta$  % by using olefin peaks in the backbone from  $^1\text{H}$  NMR spectrum (P1).  $\beta$  % values of other polymers (P2 – P10) were calculated by the same method.

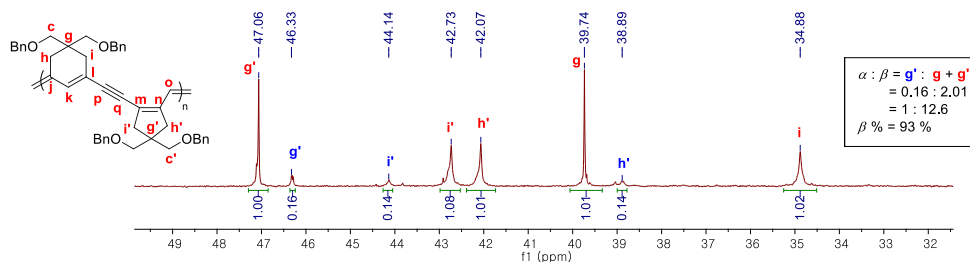


**Figure S5.3.** Calculation of  $\beta$  % by using carbonyl carbon peaks from  $^{13}\text{C}$  NMR spectrum.  $\beta$  % values of other polymers containing carbonyl groups (**P2**, **P3**, **P4**, **P5**, **P8**, **P9**, and **P10**) were calculated by the same method.

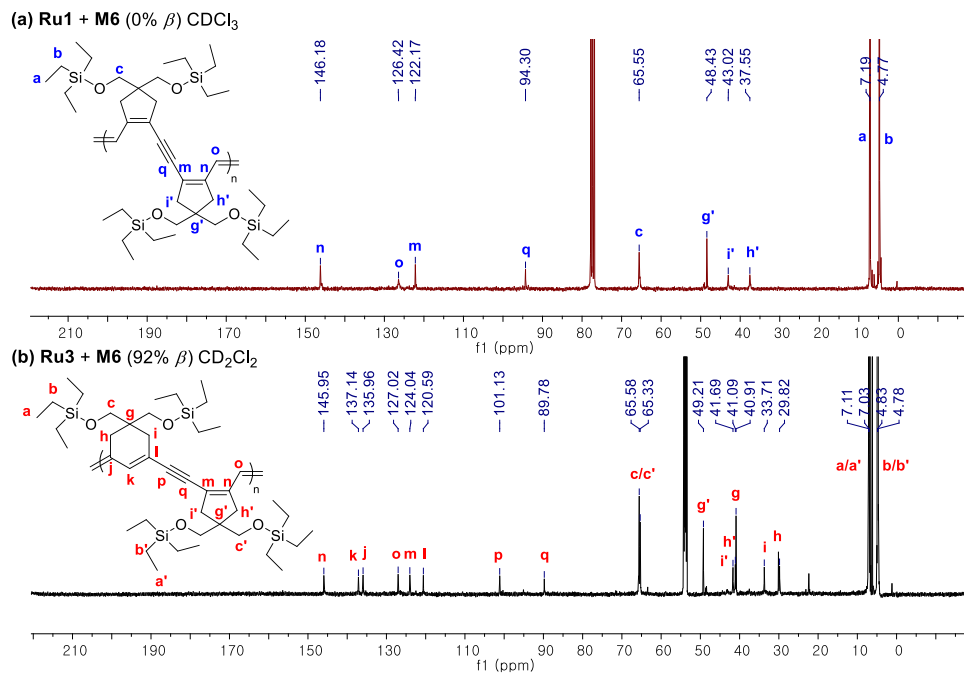
**(a) Ru1 + M7**  $^{13}\text{C}$  NMR ( $\text{CD}_2\text{Cl}_2$ )



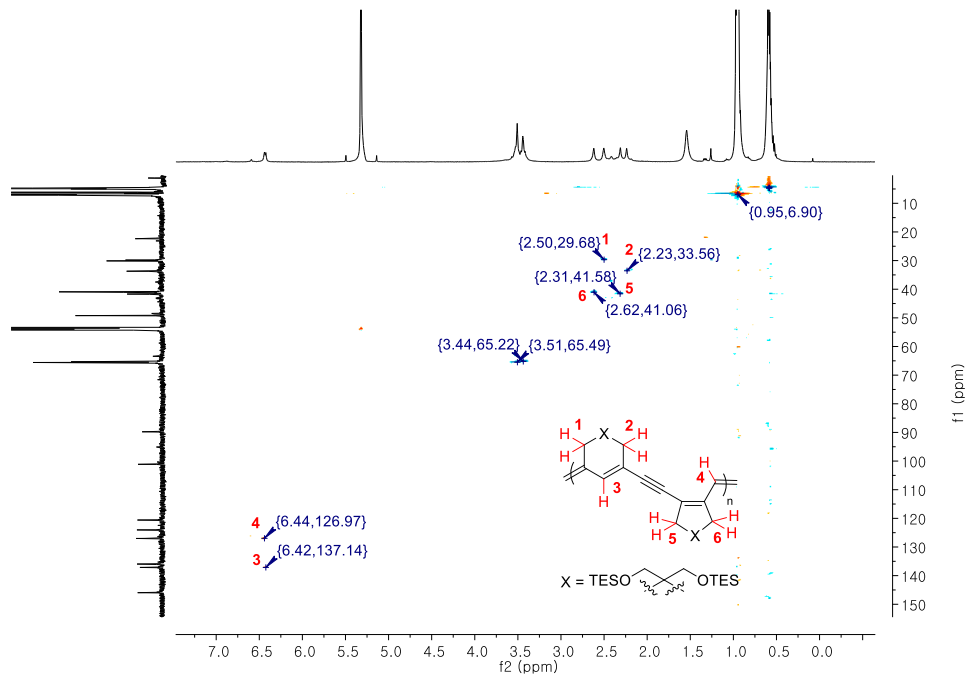
**(b) Ru3 + M7**  $^{13}\text{C}$  NMR ( $\text{CD}_2\text{Cl}_2$ )



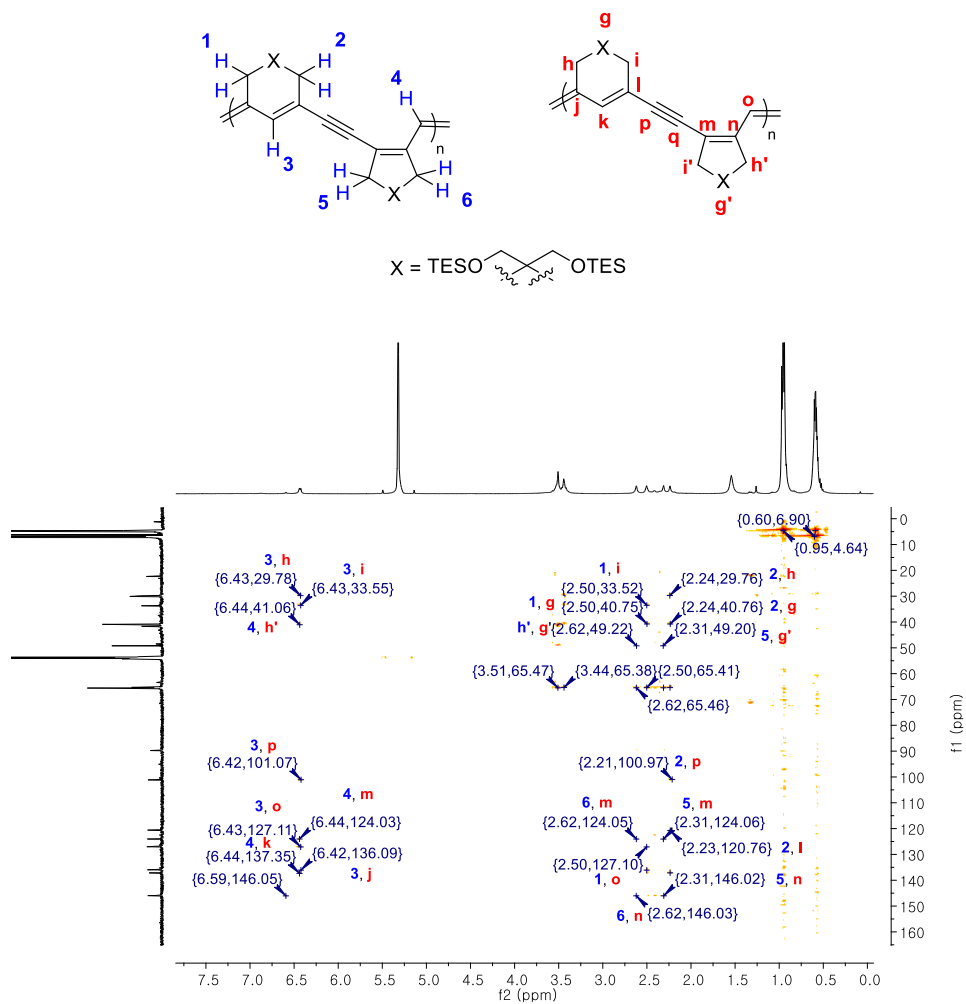
**Figure S5.4.** Quaternary carbon region of  $^{13}\text{C}$  NMR spectra of **P7** synthesized by (a) **Ru1** and (b) **Ru3**, respectively.  $\beta$  % values of **P6** and **P7** were calculated by using quaternary carbon peaks.



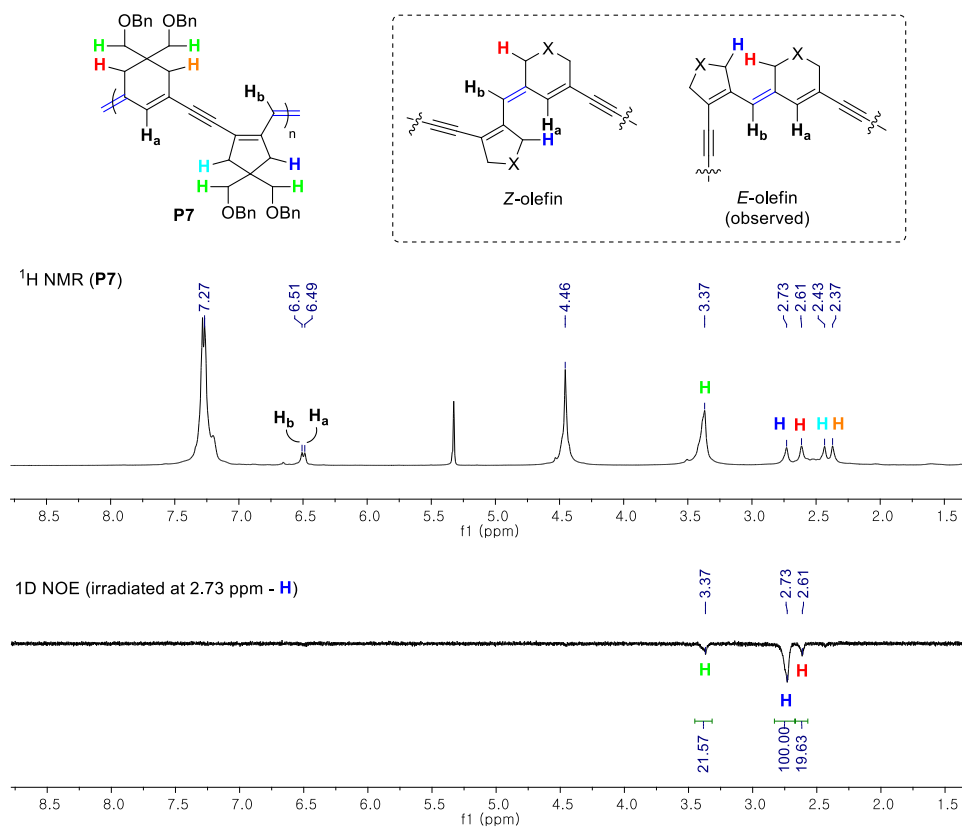
**Figure S5.5.** Comparison of  $^{13}\text{C}$  NMR spectra of **P6** synthesized by (a) **Ru1** and (b) **Ru3**, respectively.



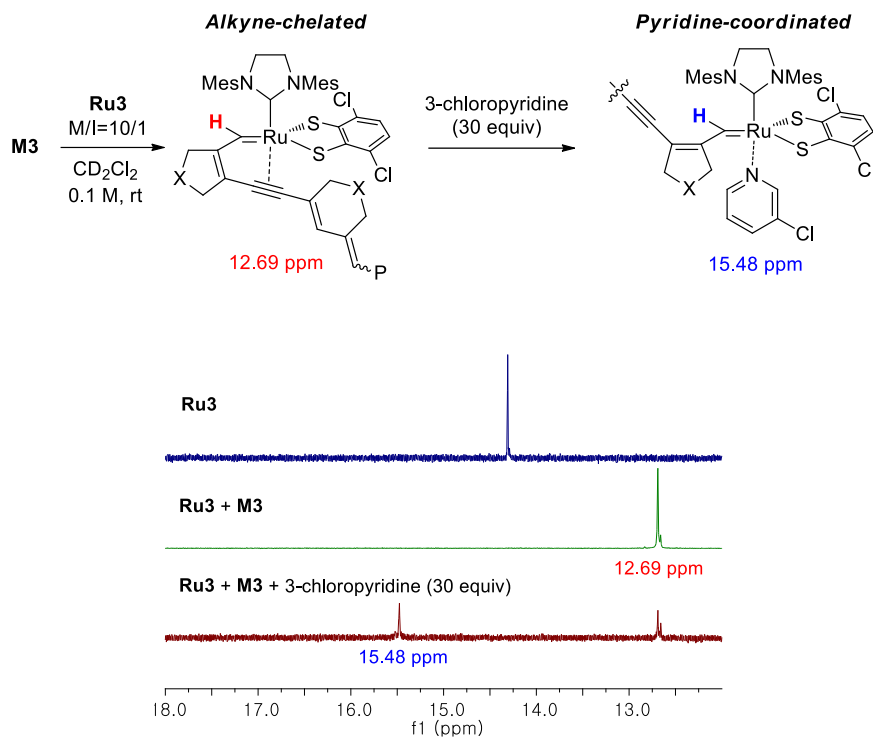
**Figure S5.6.**  $^1\text{H}$  –  $^{13}\text{C}$  HSQC (Heteronuclear Single Quantum Coherence) NMR spectrum of **P6** in CD<sub>2</sub>Cl<sub>2</sub>.



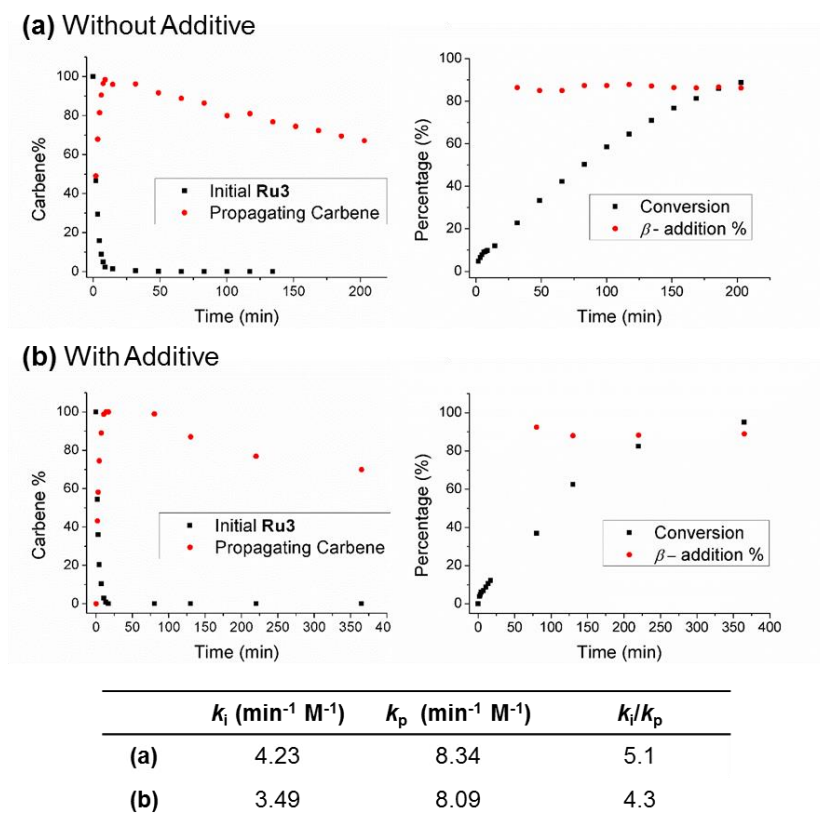
**Figure S5.7.**  $^1\text{H} - ^{13}\text{C}$  HMBC (Heteronuclear Multiple Bond Correlation) NMR spectrum of **P6** in  $\text{CD}_2\text{Cl}_2$ .



**Figure S5.8.** 1D  $^1\text{H}$  NOE difference spectrum of **P6** (irradiated at 2.73 ppm). Strong NOE between 2.73 ppm (**H**) and 2.61 ppm (**H**) indicates exclusive  $E$ -configuration of the backbone olefin.

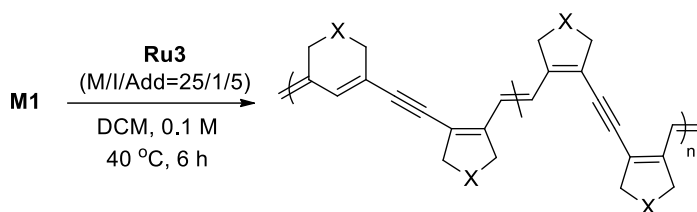


**Figure S5.9.**  $^1\text{H}$  NMR spectra (carbene region) of initial **Ru3**, the propagating carbene, and the pyridine-coordinated Ru complex



**Figure S5.10.** Carbene, conversion, and  $\beta$ -addition % changes for the polymerization of **M2** ( $M/I = 10/1$ ) (a) without and (b) with 3,5-dichloropyridine additive (20 mol%). The reaction was conducted in  $\text{CD}_2\text{Cl}_2$  (0.1 M for monomer) at room temperature and monitored by in-situ  $^1\text{H}$  NMR analysis.



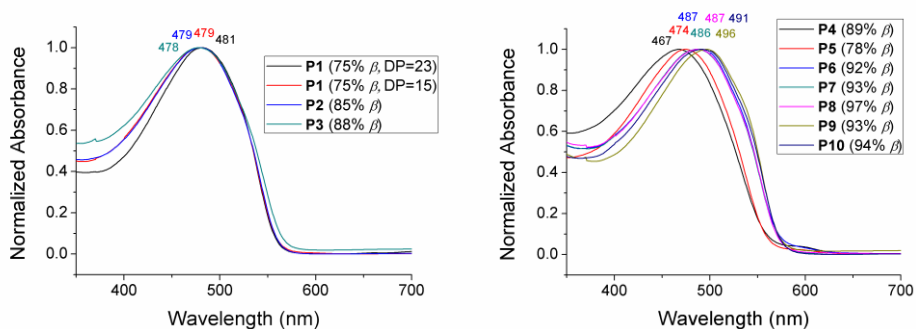
**Table S5.2.** Polymerization of **M1** Using Various Pyridine Additives

entry	additive	conv <sup>a</sup>	yield <sup>b</sup>	$M_n$ <sup>c</sup>	$\bar{D}$ <sup>c</sup>	$\beta$ (%) <sup>a</sup>
1	3,5-dichloropyridine	91%	84%	20.0 k	1.36	75%
2	3-chloropyridine	74%	59%	18.8 k	1.37	77%
3	pyridine	76%	72%	18.9 k	1.35	77%
4	4-methylpyridine	47%	42%	-	-	79%
5	4-methoxypyridine	69%	67%	-	-	79%

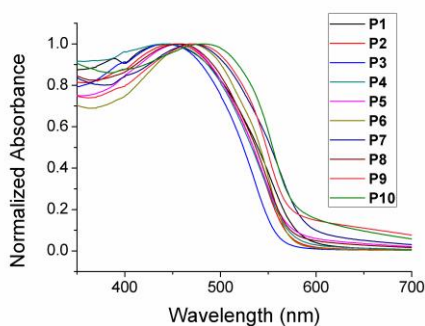
<sup>a</sup>Calculated from crude <sup>1</sup>H NMR. <sup>b</sup>Isolated yield. <sup>c</sup>Determined by tetrahydrofuran (THF) size-exclusion chromatography (SEC) calibrated using polystyrene standards.

**Table S5.3.** Optical and Physical Properties of **P1** – **P10**

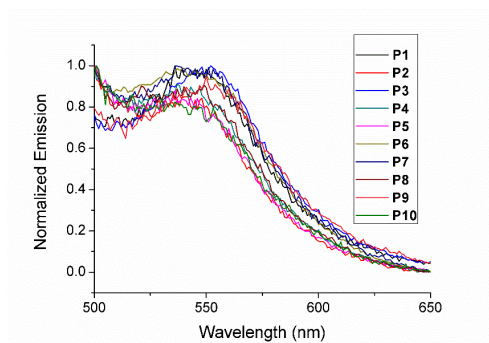
	Expt. DP	Solution		Film		$\lambda_{em}$ (nm)	$\phi_{PL}$ (%)	$E_{HOMO}$ (eV)	$T_d$ (°C)
		$\lambda_{abs}$ (nm)	$E_g^{opt}$ (eV)	$\lambda_{abs}$ (nm)	$E_g^{opt}$ (eV)				
<b>P1</b>	23	481	2.22	446	2.13	536	< 0.01	-5.36	196
<b>P2</b>	22	479	2.20	453	2.17	541	-	-5.22	282
<b>P3</b>	21	478	2.19	442	2.21	552	0.07	-5.22	301
<b>P4</b>	14	467	2.21	442	2.16	537	< 0.01	-5.23	311
<b>P5</b>	12	474	2.22	459	2.17	536	-	-5.28	332
<b>P6</b>	12	487	2.16	469	2.17	540	< 0.01	-5.30	359
<b>P7</b>	14	486	2.16	470	2.11	536	-	-5.13	316
<b>P8</b>	13	487	2.17	458	2.17	549	-	-5.06	242
<b>P9</b>	14	496	2.16	473	2.18	550	< 0.01	-5.23	244
<b>P10</b>	10	491	2.16	481	2.15	536	-	-5.19	228



**Figure S5.11.** UV-Vis spectra of **P1 – P10** in  $\text{CHCl}_3$  solution (ca. 0.01 g/L).



**Figure S5.12.** UV-Vis spectra of **P1 – P10** in film state.



**Figure S5.13.** Emission spectra of **P1 – P10** in  $\text{CHCl}_3$  solution ( $\lambda_{\text{ex}} = 400$  nm, ca. 0.01 g/L).

## 5.6. Experimental Section

### Characterization

$^1\text{H}$  NMR and  $^{13}\text{C}$  NMR were recorded by Varian/Oxford As-500 (500 MHz for  $^1\text{H}$ , 125 MHz for  $^{13}\text{C}$ ) and Bruker DRX-300 (300 MHz for  $^1\text{H}$ , 75 MHz for  $^{13}\text{C}$ ) spectrometers. 2D NMR ( $^1\text{H} - ^{13}\text{C}$  HSQC,  $^1\text{H} - ^{13}\text{C}$  HMBC) were recorded by Bruker AVANCE 600 (600 MHz for  $^1\text{H}$  and 150 MHz for  $^{13}\text{C}$ ) in the Seoul National University National Instrumentation Center for Environmental Management. Size exclusion chromatography (SEC) analyses were carried out with Waters system (1515 pump and 2707 autosampler) and Shodex GPC LF-804 column eluted with THF (GPC grade, Honeywell Burdick & Jackson<sup>®</sup>) and filtered through a 0.2  $\mu\text{m}$  PTFE filter (Whatman<sup>®</sup>). The flow rate was 1.0 mL/min and temperature of the column was maintained at 35  $^{\circ}\text{C}$ . Wyatt OptiLab T-rEx refractive index detector was used for molecular weight measurement. High-resolution mass spectroscopy (HRMS) analyses were performed by ultra high resolution ESI Q-TOF mass spectrometer (Bruker, Germany) in the Sogang Organic Chemistry Research Center. UV/Vis spectra were obtained by UV-vis Spectrometer V-650 (Jasco Inc.). Emission spectra were obtained by FP-8300 (Jasco Inc.). Cyclic voltammetry (CV) measurements were carried out by CHI 660 Electrochemical Analyzer (CH Instruments, Inc., Texas, USA). Thermogravimetric analysis (TGA) was carried out under  $\text{N}_2$  gas at a scan rate of 10  $^{\circ}\text{C}/\text{min}$  with Q50 model device (TA Instruments).

### Materials

All reagents which are commercially available from Sigma-Aldrich<sup>®</sup>, Tokyo Chemical Industry Co. Ltd., Acros Organics, Alfa Aesar<sup>®</sup>, without additional notes, were used without further purification. The catalyst **Ru3** was prepared by a literature method.<sup>10</sup> Dichloromethane (DCM), 1,2-dichloroethane (DCE), and tetrahydrofuran (THF) for the polymerization were purified by Glass Contour



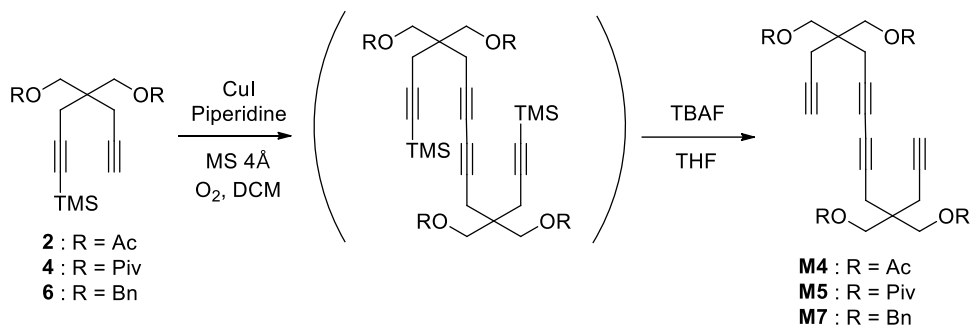


$[M+Na]^+$ , calcd: 415.2275, found: 415.2277.



gel to afford **6** as colorless liquid (23 mg, 0.056 mmol, 30%). <sup>1</sup>H NMR (500 MHz,

CDCl<sub>3</sub>)  $\delta$  7.48 – 7.26 (m, 10H), 4.52 (s, 4H), 3.54 – 3.46 (m, 4H), 2.49 – 2.38 (m, 4H), 1.95 (s, 1H), 0.12 (s, 9H). <sup>13</sup>C NMR (125 MHz, CD<sub>2</sub>Cl<sub>2</sub>)  $\delta$  128.65, 127.88, 127.83, 81.05, 73.84, 71.75, 71.62, 70.78, 70.70, 42.32, 23.86, 23.79, 22.35, 0.24. HRMS (ESI): m/z for C<sub>26</sub>H<sub>32</sub>NaO<sub>2</sub>Si [M+Na]<sup>+</sup>, calcd: 427.2064, found: 427.2065.



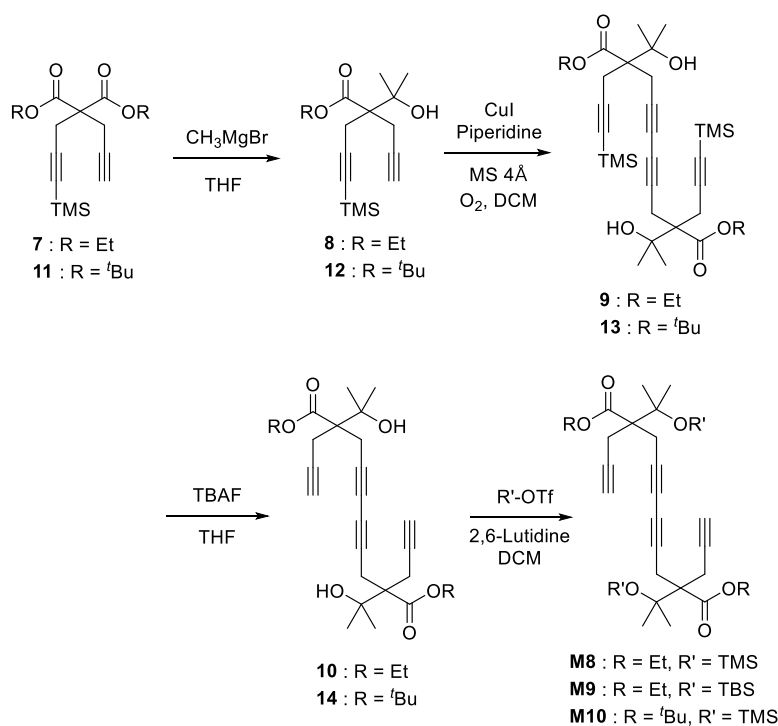
### General procedure for Glaser-Hay coupling and TMS deprotection to afford **M4**, **M5**, and **M7**

To a dried round-bottom flask containing a stirring bar, CuI (49.1 mg, 0.258 mmol) was added. After adding piperidine (0.31 ml, 3.1 mmol), DCM (23 ml) was added. After all the salts dissolved (brown solution), ca. 1 g of 4Å molecular sieve was added. Then, compound **2** (795 mg, 2.58 mmol) in DCM (3 ml) was added, followed by injection of a balloon filled with O<sub>2</sub>. As the reaction proceeded, the reaction mixture turned dark green. Using a large round-bottom flask with vigorous stirring was required to facilitate the O<sub>2</sub> incorporation. After quenching with a saturated NH<sub>4</sub>Cl aqueous solution, the organic layer was washed with water and extracted by DCM, dried with MgSO<sub>4</sub>, and concentrated. This crude product was dissolved in THF (10 ml), then tetrabutylammonium fluoride solution (1.0 M in THF, 2.26 ml, 2.26 mmol) was added at -10 °C. After stirring for 15 min, the reaction mixture was quenched with cold water and 6 N HCl. The organic layer was washed with water and extracted by ethyl acetate, dried with MgSO<sub>4</sub>, and concentrated. The product was purified by flash column chromatography on silica gel to afford **M4** as white powder (364 mg, 0.775 mmol, 61%). <sup>1</sup>H NMR (500 MHz, CDCl<sub>3</sub>)  $\delta$  4.09 (s, 8H), 2.50 (s, 4H), 2.40 (d, *J* = 2.6 Hz, 4H), 2.07 (s, 12H), 2.05 (t,

$J = 2.6$  Hz, 2H).  $^{13}\text{C}$  NMR (125 MHz,  $\text{CDCl}_3$ )  $\delta$  170.63, 78.75, 72.76, 72.07, 68.17, 65.17, 40.63, 23.26, 22.54, 20.89. HRMS (ESI):  $m/z$  for  $\text{C}_{26}\text{H}_{30}\text{NaO}_8$   $[\text{M}+\text{Na}]^+$ , calcd: 493.1833, found: 493.1832.

**M5** : white powder (205 mg, 0.310 mmol, 56%).  $^1\text{H}$  NMR (500 MHz,  $\text{CDCl}_3$ )  $\delta$  4.07 (s, 8H), 2.52 (s, 4H), 2.41 (d,  $J = 2.5$  Hz, 4H), 2.05 (t,  $J = 2.5$  Hz, 2H), 1.21 (s, 36H).  $^{13}\text{C}$  NMR (125 MHz,  $\text{CDCl}_3$ )  $\delta$  177.85, 78.70, 72.71, 71.99, 68.15, 65.13, 41.12, 39.06, 27.25, 23.47, 22.71. HRMS (ESI):  $m/z$  for  $\text{C}_{38}\text{H}_{54}\text{NaO}_8$   $[\text{M}+\text{Na}]^+$ , calcd: 661.3711, found: 661.3713.

**M7** : colorless liquid (160 mg, 0.233 mmol, 40%).  $^1\text{H}$  NMR (500 MHz,  $\text{CDCl}_3$ )  $\delta$  7.48 – 7.15 (m, 20H), 4.53 (s, 8H), 3.51 (s, 8H), 2.53 (s, 4H), 2.44 (d,  $J = 2.5$  Hz, 4H), 1.97 (t,  $J = 2.6$  Hz, 2H).  $^{13}\text{C}$  NMR (125 MHz,  $\text{CDCl}_3$ )  $\delta$  138.66, 128.42, 127.58, 127.54, 80.80, 74.01, 73.54, 71.39, 70.80, 67.64, 42.76, 23.12, 22.40. HRMS (ESI):  $m/z$  for  $\text{C}_{46}\text{H}_{46}\text{NaO}_4$   $[\text{M}+\text{Na}]^+$ , calcd: 685.3288, found: 685.3286.



### General procedure for the synthesis of compounds **8** and **12**

To a solution of **7** (6.55 g, 21.3 mmol) in THF (70 ml), methyl magnesium bromide

solution (3 M in ether, 24.8 ml, 8.27 mmol) was added slowly at 0 °C. After stirring for 2 h at room temperature, the reaction was quenched by a saturated NH<sub>4</sub>Cl aqueous solution. The organic layer was washed with water and extracted by ethyl acetate, dried with MgSO<sub>4</sub>, and concentrated. The product was purified by flash column chromatography on silica gel to afford **8** as colorless liquid (3.80 g, 12.0 mmol, 56 %). <sup>1</sup>H NMR (500 MHz, CDCl<sub>3</sub>) δ 4.21 (q, *J* = 7.1 Hz, 2H), 3.25 (br, 1H), 2.93 – 2.78 (m, 4H), 2.03 (t, *J* = 2.7 Hz, 1H), 1.32 (s, 3H), 1.29 (t, *J* = 7.2 Hz, 3H), 1.27 (s, 3H), 0.13 (s, 9H). <sup>13</sup>C NMR (125 MHz, CDCl<sub>3</sub>) δ 173.46, 104.33, 88.58, 81.71, 74.20, 71.26, 61.51, 56.50, 26.72, 26.54, 23.11, 21.76, 14.23, 0.02. HRMS (ESI): *m/z* for C<sub>16</sub>H<sub>26</sub>NaO<sub>3</sub>Si [M+Na]<sup>+</sup>, calcd: 317.1543, found: 317.1542.

**12** : colorless liquid (2.84 g, 8.83 mmol, 88 %) <sup>1</sup>H NMR (500 MHz, CDCl<sub>3</sub>) δ 3.41 (br, 1H), 2.90 – 2.73 (m, 4H), 2.03 (t, *J* = 2.7 Hz, 1H), 1.49 (s, 9H), 1.31 (d, *J* = 13.7 Hz, 6H), 0.14 (s, 9H). <sup>13</sup>C NMR (125 MHz, CDCl<sub>3</sub>) δ 172.65, 104.58, 88.20, 82.67, 82.00, 74.19, 71.11, 56.43, 28.05, 26.66, 26.57, 23.27, 21.93, 0.07. HRMS (ESI): *m/z* for C<sub>18</sub>H<sub>30</sub>NaO<sub>3</sub>Si [M+Na]<sup>+</sup>, calcd: 345.1856, found: 345.1857.

### General procedure for the synthesis of compounds **9** and **13**

To a dried round-bottom flask containing a stirring bar, CuI (50 mg, 0.26 mmol) was added. After adding piperidine (0.31 ml, 3.1 mmol), DCM (26 ml) was added. After all the salts dissolved (brown solution), ca. 1 g of 4Å molecular sieve was added. Compound **12** (841 mg, 2.61 mmol) in DCM was added, followed by injection of a balloon filled with O<sub>2</sub>. As the reaction proceeded, the reaction mixture turned dark green. Using a large round-bottom flask with vigorous stirring was required to facilitate the O<sub>2</sub> incorporation. The organic layer was washed with water and extracted by DCM, dried with MgSO<sub>4</sub>, and concentrated. The product was purified by flash column chromatography on silica gel to afford **13** as yellow liquid (495 mg, 0.770 mmol, 59%).

**9** : <sup>1</sup>H NMR (500 MHz, CDCl<sub>3</sub>) δ 4.27 – 4.15 (m, 4H), 3.21 (br, 2H), 2.98 – 2.79 (m, 8H), 1.32 (s, 6H), 1.29 (t, *J* = 7.1 Hz, 6H), 1.24 (s, 6H), 0.13 (s, 18H). <sup>13</sup>C



NMR (125 MHz, CDCl<sub>3</sub>)  $\delta$  173.39, 104.06, 88.92, 74.93, 74.10, 67.80, 61.61, 56.78, 26.72, 26.38, 23.40, 22.63, 14.24, -0.00. HRMS (ESI):  $m/z$  for C<sub>32</sub>H<sub>50</sub>NaO<sub>6</sub>Si<sub>2</sub> [M+Na]<sup>+</sup>, calcd: 609.3038, found: 609.3040.

**13** : <sup>1</sup>H NMR (500 MHz, CDCl<sub>3</sub>)  $\delta$  3.43 (s, 2H), 2.93 – 2.70 (m, 8H), 1.49 (s, 18H), 1.29 (d,  $J$  = 27.1 Hz, 12H), 0.13 (s, 18H). <sup>13</sup>C NMR (125 MHz, CDCl<sub>3</sub>)  $\delta$  172.70, 104.30, 88.53, 82.89, 75.15, 74.09, 67.74, 56.77, 28.05, 26.67, 26.42, 23.55, 22.84, 0.06. HRMS (ESI):  $m/z$  for C<sub>36</sub>H<sub>58</sub>NaO<sub>6</sub>Si<sub>2</sub> [M+Na]<sup>+</sup>, calcd: 665.3664, found: 665.3665.

### General procedure for the synthesis of compounds **10** and **14**

Compound **13** (495 mg, 0.770 mmol) was dissolved in THF (10 ml), then tetrabutylammonium fluoride solution (1.0 M in THF, 1.69 ml, 1.69 mmol) was added at -10 °C. After stirring for 15 min, the reaction mixture was quenched with cold water and 6 N HCl. The organic layer was washed with water and extracted by ethyl acetate, dried with MgSO<sub>4</sub>, and concentrated. The product was purified by flash column chromatography on silica gel to afford **14** as colorless liquid (243 mg, 0.488 mmol, 63%).

**10** : <sup>1</sup>H NMR (500 MHz, CDCl<sub>3</sub>)  $\delta$  4.23 (q,  $J$  = 7.1 Hz, 4H), 3.07 – 2.66 (m, 9H), 2.06 (t,  $J$  = 2.6 Hz, 2H), 1.33 – 1.26 (m, 18H). <sup>13</sup>C NMR (125 MHz, CDCl<sub>3</sub>)  $\delta$  173.43, 81.33, 74.89, 74.00, 71.83, 67.94, 61.75, 56.59, 26.68, 26.49, 22.60, 22.00, 14.25. HRMS (ESI):  $m/z$  for C<sub>26</sub>H<sub>34</sub>NaO<sub>6</sub> [M+Na]<sup>+</sup>, calcd: 465.2248, found: 465.2249.

**14** : <sup>1</sup>H NMR (500 MHz, CDCl<sub>3</sub>)  $\delta$  3.22 (br, 2H), 2.99 – 2.66 (m, 8H), 2.05 (t,  $J$  = 2.6 Hz, 2H), 1.49 (s, 18H), 1.29 (d,  $J$  = 14.5 Hz, 12H). <sup>13</sup>C NMR (125 MHz, CDCl<sub>3</sub>)  $\delta$  172.72, 83.13, 81.57, 75.07, 73.96, 71.63, 67.84, 56.58, 28.05, 26.62, 26.45, 22.76, 22.13. HRMS (ESI):  $m/z$  for C<sub>30</sub>H<sub>42</sub>NaO<sub>6</sub> [M+Na]<sup>+</sup>, calcd: 521.2874, found: 521.2875.

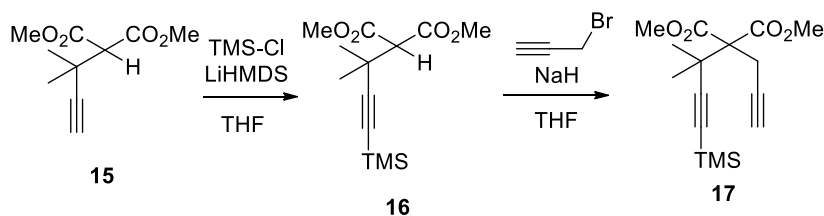
### General procedure for the synthesis of **M8** – **M10**

To a solution of **10** (219 mg, 0.495 mmol) and 2,6-lutidine (0.17 ml, 1.4 mmol) in DCM (5 ml), Trimethylsilyl trifluoromethanesulfonate (0.26 ml, 1.4 mmol) was added at 0 °C and stirred overnight at room temperature. The reaction mixture was concentrated and the product was purified by flash column chromatography on silica gel to afford **M8** as colorless liquid (171 mg, 0.292 mmol, 59%). <sup>1</sup>H NMR (500 MHz, CDCl<sub>3</sub>) δ 4.17 – 4.10 (m, 4H), 2.88 (dd, *J* = 31.8, 16.9 Hz, 4H), 2.77 (ddd, *J* = 47.5, 16.7, 2.4 Hz, 4H), 1.94 (t, *J* = 2.6 Hz, 2H), 1.33 (d, *J* = 5.4 Hz, 12H), 1.26 (t, *J* = 7.1 Hz, 6H), 0.09 (s, 18H). <sup>13</sup>C NMR (125 MHz, CDCl<sub>3</sub>) δ 172.78, 81.96, 76.85, 75.06, 70.52, 67.49, 61.03, 57.58, 27.40, 22.39, 21.79, 14.20, 2.45. HRMS (ESI): *m/z* for C<sub>32</sub>H<sub>50</sub>NaO<sub>6</sub>Si<sub>2</sub> [M+Na]<sup>+</sup>, calcd: 609.3038, found: 609.3040.

Following the same procedure, compound **10** was reacted with *tert*-butyldimethylsilyl trifluoromethanesulfonate to afford **M9**: <sup>1</sup>H NMR (500 MHz, CDCl<sub>3</sub>) δ 4.22 – 4.07 (m, 4H), 3.01 – 2.64 (m, 8H), 1.96 (t, *J* = 2.6 Hz, 2H), 1.36 (d, *J* = 4.4 Hz, 12H), 1.27 (t, *J* = 7.1 Hz, 6H), 0.86 (s, 18H), 0.08 (s, 12H). <sup>13</sup>C NMR (125 MHz, CDCl<sub>3</sub>) δ 172.63, 81.89, 76.99, 75.19, 70.78, 67.69, 61.12, 57.75, 27.45, 27.37, 25.91, 22.65, 22.14, 18.34, 14.17, -1.99. HRMS (ESI): *m/z* for C<sub>38</sub>H<sub>62</sub>NaO<sub>6</sub>Si<sub>2</sub> [M+Na]<sup>+</sup>, calcd: 693.3975, found: 693.3977.

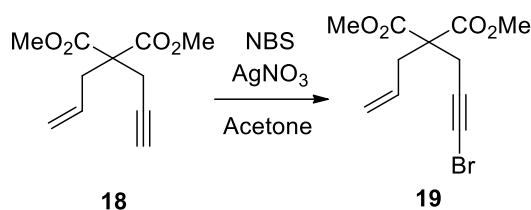
Following the same procedure, compound **14** was reacted with trimethylsilyl trifluoromethanesulfonate to afford **M10**: <sup>1</sup>H NMR (500 MHz, CDCl<sub>3</sub>) δ 2.91 – 2.62 (m, 8H), 1.93 (t, *J* = 2.5 Hz, 2H), 1.44 (s, 18H), 1.33 (d, *J* = 2.5 Hz, 12H), 0.11 (s, 18H). <sup>13</sup>C NMR (125 MHz, CDCl<sub>3</sub>) δ 171.74, 82.35, 81.42, 76.86, 75.38, 70.27, 67.38, 57.68, 28.03, 27.50, 22.60, 22.02, 2.57. HRMS (ESI): *m/z* for C<sub>36</sub>H<sub>58</sub>NaO<sub>6</sub>Si<sub>2</sub> [M+Na]<sup>+</sup>, calcd: 665.3664, found: 665.3668.

## Synthesis of M11

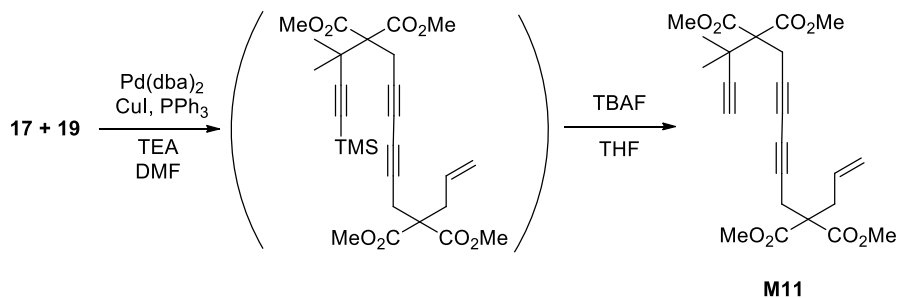


To a solution of **15** (1.11 g, 5.59 mmol) in THF (19 ml), lithium bis(trimethylsilyl)amide solution (1.0 M in THF, 14.0 ml, 14.0 mmol) was added dropwise at  $-78\text{ }^{\circ}\text{C}$ . After stirring for 1.5 h, trimethylsilyl chloride (0.85 ml, 6.7 mmol) was added. The cooling bath was removed and the reaction mixture was stirred for 1.5 h followed by quenching with a saturated  $\text{NH}_4\text{Cl}$  aqueous solution. The organic layer was washed with water and extracted by ethyl acetate, dried with  $\text{MgSO}_4$ , and concentrated. The product was purified by flash column chromatography on silica gel to afford **16** as colorless liquid (1.38 g, 5.11 mmol, 91%).  $^1\text{H}$  NMR (500 MHz,  $\text{CDCl}_3$ )  $\delta$  3.72 (s, 6H), 3.52 (s, 1H), 1.43 (s, 6H), 0.11 (s, 9H).  $^{13}\text{C}$  NMR (125 MHz,  $\text{CDCl}_3$ )  $\delta$  167.81, 111.11, 85.41, 60.37, 52.28, 33.75, 27.20, 0.19. HRMS (ESI):  $m/z$  for  $\text{C}_{13}\text{H}_{22}\text{NaO}_4\text{Si}$   $[\text{M}+\text{Na}]^+$ , calcd: 293.1180, found: 293.1180.

$\text{NaH}$  (60% dispersion in mineral oil, 241 mg, 6.02 mmol) was slowly added to a solution of compound **16** (1.36 g, 5.02 mmol) in THF (20 ml) at  $0\text{ }^{\circ}\text{C}$ . After stirring for 30 min at room temperature, propargyl bromide (80 wt% in toluene, 0.67 ml, 6.02 mmol) was added. The reaction was quenched by saturated  $\text{NH}_4\text{Cl}$  aqueous solution after 4 h. The organic layer was washed with water and extracted by ethyl acetate, dried with  $\text{MgSO}_4$ , and concentrated. The product was purified by flash column chromatography on silica gel to afford **17** as colorless liquid (1.13 g, 3.68 mmol, 73%).  $^1\text{H}$  NMR (500 MHz,  $\text{CDCl}_3$ )  $\delta$  3.76 (s, 6H), 3.03 (d,  $J = 2.6\text{ Hz}$ , 2H), 2.00 (t,  $J = 2.6\text{ Hz}$ , 1H), 1.47 (s, 6H), 0.13 (s, 9H).  $^{13}\text{C}$  NMR (125 MHz,  $\text{CDCl}_3$ )  $\delta$  169.23, 110.49, 86.60, 80.93, 70.69, 63.78, 52.29, 38.03, 26.82, 23.68, 0.11. HRMS (ESI):  $m/z$  for  $\text{C}_{16}\text{H}_{24}\text{NaO}_4\text{Si}$   $[\text{M}+\text{Na}]^+$ , calcd: 331.1336, found: 331.1337.



To a solution of **18** (621 mg, 2.96 mmol) and *N*-bromosuccinimide (789 mg, 4.43 mmol) in acetone (10 ml), silver nitrate (46 mg, 0.30 mmol) was added. After stirring for 3 h, *n*-hexane (ca. 10 ml) was poured and the precipitated solid was filtered out by celite. The filtrate was concentrated and the product was purified by flash column chromatography on silica gel to afford **19** as colorless liquid (474 mg, 1.64 mmol, 55%).  $^1\text{H}$  NMR (500 MHz,  $\text{CDCl}_3$ )  $\delta$  5.61 (ddt,  $J = 17.5, 10.1, 7.5$  Hz, 1H), 5.17 (d,  $J = 17.0$  Hz, 1H), 5.15 – 5.11 (m, 1H), 3.74 (s, 6H), 2.82 (s, 2H), 2.78 (d,  $J = 7.5$  Hz, 2H).  $^{13}\text{C}$  NMR (125 MHz,  $\text{CDCl}_3$ )  $\delta$  170.18, 131.72, 120.12, 74.97, 57.02, 52.96, 41.61, 36.89, 24.12. HRMS (ESI):  $m/z$  for  $\text{C}_{11}\text{H}_{13}\text{BrNaO}_4$   $[\text{M}+\text{Na}]^+$ , calcd: 310.9889, found: 310.9891.



To a solution of  $\text{Pd(dba)}_2$  (46 mg, 0.080 mmol),  $\text{CuI}$  (7.6 mg, 0.040 mmol),  $\text{PPh}_3$  (21 mg, 0.080 mmol), and triethylamine (0.44 ml, 3.2 mmol) in DMF (5 ml), compound **17** (639 mg, 2.07 mmol) and **19** (461 mg, 1.59 mmol) in DCM (ca. 3 ml) were added at 0 °C. After stirring 6 h at 50 °C, the organic layer was washed with water and extracted by DCM, dried with  $\text{MgSO}_4$ , and concentrated. This crude product was dissolved in THF (8 ml), then tetrabutylammonium fluoride solution (1.0 M in THF, 0.90 ml, 0.90 mmol) was added at -10 °C. After stirring for 15 min,

the reaction mixture was quenched with cold water and 6 N HCl. The organic layer was washed with water and extracted by ethyl acetate, dried with MgSO<sub>4</sub>, and concentrated. The product was purified by flash column chromatography on silica gel to afford **M11** as colorless liquid (327 mg, 0.736 mmol, 50%). <sup>1</sup>H NMR (500 MHz, CD<sub>2</sub>Cl<sub>2</sub>) δ 5.61 (ddt, *J* = 17.4, 10.0, 7.5 Hz, 1H), 5.17 (d, *J* = 17.0 Hz, 1H), 5.13 (d, *J* = 10.2 Hz, 1H), 3.75 (s, 6H), 3.71 (s, 6H), 3.09 (s, 2H), 2.84 (s, 2H), 2.74 (d, *J* = 7.5 Hz, 2H), 2.29 (s, 1H). <sup>13</sup>C NMR (75 MHz, CDCl<sub>3</sub>) δ 170.20, 169.30, 131.01, 120.11, 88.54, 74.69, 73.00, 72.68, 69.38, 68.08, 67.40, 63.65, 57.25, 37.28, 27.79, 26.11, 24.67. HRMS (ESI): *m/z* for C<sub>24</sub>H<sub>28</sub>NaO<sub>8</sub> [M+Na]<sup>+</sup>, calcd: 467.1676, found: 467.1672.

### General Procedure for Polymerization

A 4-mL sized screw-cap vial with septum was flame dried and charged with monomer (ca. 20 ~ 30 mg). The vial was purged with Ar three times, and degassed anhydrous solvent was added. A mixture of initiator and additive in another 4-mL vial was dissolved in solvent under Ar atmosphere. The initiator solution was rapidly injected to the monomer solution at experimental temperature under vigorous stirring. The reaction was quenched by excess ethyl vinyl ether after desired reaction time, and resulting polymer was partially precipitated in methanol, remaining small amount of crude mixture (c.a. 2 mg). Obtained solid was filtered and dried *in vacuo*. Monomer conversion was calculated from the <sup>1</sup>H NMR spectrum of the remained crude mixture.

### <sup>1</sup>H and <sup>13</sup>C NMR characterization of polymers

**P1**: <sup>1</sup>H NMR (500 MHz, CDCl<sub>3</sub>) δ 6.68 – 6.45 (m, 1H), 6.43 (s, 1H), 3.52 – 2.61 (m, 7H), 1.50 – 1.37 (m, 30H).

<sup>13</sup>C NMR (75 MHz, CDCl<sub>3</sub>) δ 170.52, 169.50, 142.99, 137.15, 133.95, 126.24, 122.94, 119.62, 100.17, 94.17, 88.98, 81.75, 81.53, 59.83, 58.95, 55.03, 44.60, 43.12, 42.27, 39.62, 35.06, 31.42, 27.93.

**P2:**  $^1\text{H}$  NMR (500 MHz,  $\text{CDCl}_3$ )  $\delta$  6.66 – 6.45 (m, 1H), 6.45 – 6.30 (m, 1H), 5.04 (td,  $J$  = 12.0, 6.1 Hz, 4H), 3.57 – 2.72 (m, 8H), 1.28 – 1.16 (m, 24H).

$^{13}\text{C}$  NMR (75 MHz,  $\text{CDCl}_3$ )  $\delta$  171.04, 169.90, 151.77, 143.49, 134.52, 127.25, 125.35, 123.26, 120.05, 100.48, 89.11, 70.74, 68.66, 58.83, 24.06, 22.47, 20.85, 19.28.

**P3:**  $^1\text{H}$  NMR (300 MHz,  $\text{CDCl}_3$ )  $\delta$  6.64 – 6.47 (m, 1H), 6.47 – 6.26 (m, 1H), 3.76 (s, 12H), 3.58 – 2.76 (m, 8H).

$^{13}\text{C}$  NMR (125 MHz,  $\text{CDCl}_3$ )  $\delta$  171.77, 170.79, 142.87, 137.47, 133.60, 126.36, 123.11, 119.31, 100.44, 89.12, 58.78, 57.91, 54.12, 53.20, 44.59, 43.20, 42.51, 39.97, 34.95, 31.49.

**P4:**  $^1\text{H}$  NMR (500 MHz,  $\text{CDCl}_3$ )  $\delta$  6.54 (s, 1H), 6.45 (s, 1H), 4.46 – 3.55 (m, 8H), 2.90 – 2.23 (m, 8H), 2.08 (s, 12H).

$^{13}\text{C}$  NMR (125 MHz,  $\text{CDCl}_3$ )  $\delta$  170.90, 170.71, 143.73, 137.44, 133.61, 127.29, 123.80, 118.83, 100.67, 88.98, 66.70, 66.31, 44.90, 44.12, 43.27, 41.80, 41.51, 38.23, 37.40, 34.16, 29.97, 29.75, 20.91.

**P5:**  $^1\text{H}$  NMR (500 MHz,  $\text{CDCl}_3$ )  $\delta$  6.67 – 6.47 (m, 1H), 6.47 – 6.24 (m, 1H), 4.33 – 3.80 (m, 8H), 2.94 – 2.20 (m, 8H), 1.19 (d,  $J$  = 5.0 Hz, 36H).

$^{13}\text{C}$  NMR (125 MHz,  $\text{CDCl}_3$ )  $\delta$  178.18, 177.89, 143.80, 137.27, 133.71, 127.32, 124.02, 118.86, 100.77, 89.13, 66.86, 66.08, 45.33, 42.47, 42.07, 39.09, 37.93, 34.31, 30.54, 29.82, 27.33, 22.36.

**P6:**  $^1\text{H}$  NMR (500 MHz,  $\text{CD}_2\text{Cl}_2$ )  $\delta$  6.43 (d,  $J$  = 7.7 Hz, 2H), 4.08 – 3.05 (m, 8H), 2.86 – 1.96 (m, 8H), 1.06 – 0.77 (m, 36H), 0.70 – 0.52 (m, 24H).

$^{13}\text{C}$  NMR (150 MHz,  $\text{CD}_2\text{Cl}_2$ )  $\delta$  145.95, 137.14, 135.96, 127.02, 124.04, 120.59, 101.13, 89.78, 65.58, 65.33, 49.21, 41.69, 41.09, 40.91, 33.71, 29.82, 7.11, 7.03, 4.83, 4.78.

**P7:**  $^1\text{H}$  NMR (500 MHz,  $\text{CDCl}_3$ )  $\delta$  7.53 – 7.03 (m, 20H), 6.53 (s, 1H), 6.49 (s, 1H), 4.48 (s, 8H), 3.38 (s, 8H), 2.92 – 2.23 (m, 8H).

$^{13}\text{C}$  NMR (125 MHz,  $\text{CDCl}_3$ )  $\delta$  145.18, 138.89, 137.45, 135.29, 128.39, 127.54, 127.42, 123.70, 119.87, 100.97, 89.51, 73.61, 73.30, 46.85, 42.62, 41.77, 39.56,

34.75, 30.10, 22.37.

**P8:**  $^1\text{H}$  NMR (500 MHz,  $\text{CD}_2\text{Cl}_2$ )  $\delta$  6.46 (s, 1H), 6.42 (s, 1H), 4.21 – 3.93 (m, 4H), 3.74 – 2.27 (m, 8H), 1.49 – 1.22 (m, 15H), 1.17 (s, 3H), 0.28 – 0.11 (m, 18H).

$^{13}\text{C}$  NMR (125 MHz,  $\text{CD}_2\text{Cl}_2$ )  $\delta$  175.64, 173.87, 145.92, 137.24, 125.70, 123.56, 122.17, 100.85, 89.96, 76.63, 76.03, 64.96, 63.80, 61.26, 60.92, 56.58, 56.38, 41.23, 40.79, 34.04, 29.97, 29.59, 27.60, 27.39, 26.96, 26.80, 14.39, 2.67, 2.59.

**P9:**  $^1\text{H}$  NMR (500 MHz,  $\text{CDCl}_3$ )  $\delta$  6.40 (br, 2H), 4.11 (s, 4H), 3.76 – 2.04 (m, 8H), 1.54 – 1.02 (m, 18H), 1.01 – 0.61 (m, 18H), 0.22 – 0.01 (m, 12H).

$^{13}\text{C}$  NMR (125 MHz,  $\text{CDCl}_3$ )  $\delta$  175.50, 173.52, 145.09, 136.45, 125.69, 123.53, 121.63, 100.58, 89.68, 76.17, 63.18, 60.91, 56.33, 40.62, 33.54, 29.41, 27.16, 26.78, 26.11, 18.35, 14.21, -1.97.

**P10:**  $^1\text{H}$  NMR (500 MHz,  $\text{CD}_2\text{Cl}_2$ )  $\delta$  6.42 (s, 1H), 6.40 (s, 1H), 3.75 – 2.07 (m, 8H), 1.51 – 1.17 (m, 30H), 0.33 – -0.04 (m, 18H).

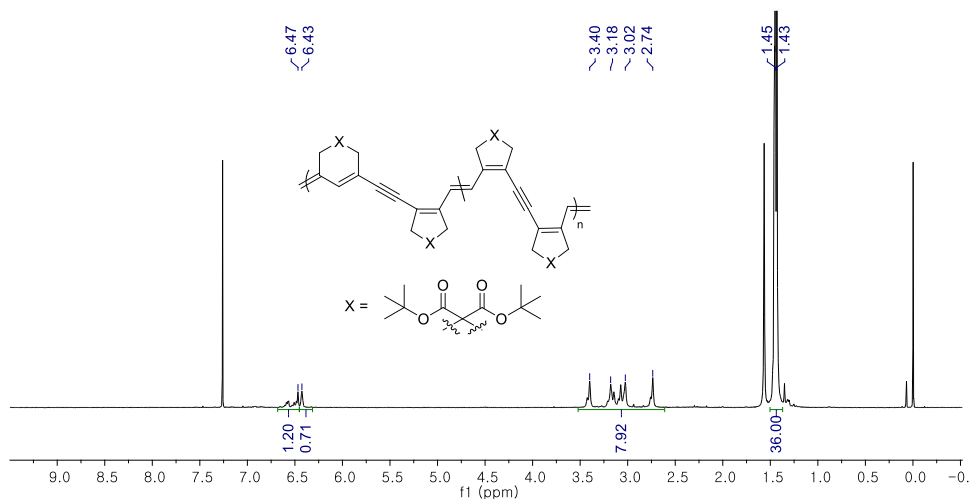
$^{13}\text{C}$  NMR (125 MHz,  $\text{CD}_2\text{Cl}_2$ )  $\delta$  174.28, 172.33, 145.51, 137.20, 136.56, 125.07, 123.18, 122.13, 100.43, 89.47, 80.40, 76.13, 63.38, 56.31, 40.85, 33.74, 29.70, 27.72, 27.63, 26.64, 2.25.

### Procedure for *In situ* NMR Experiment

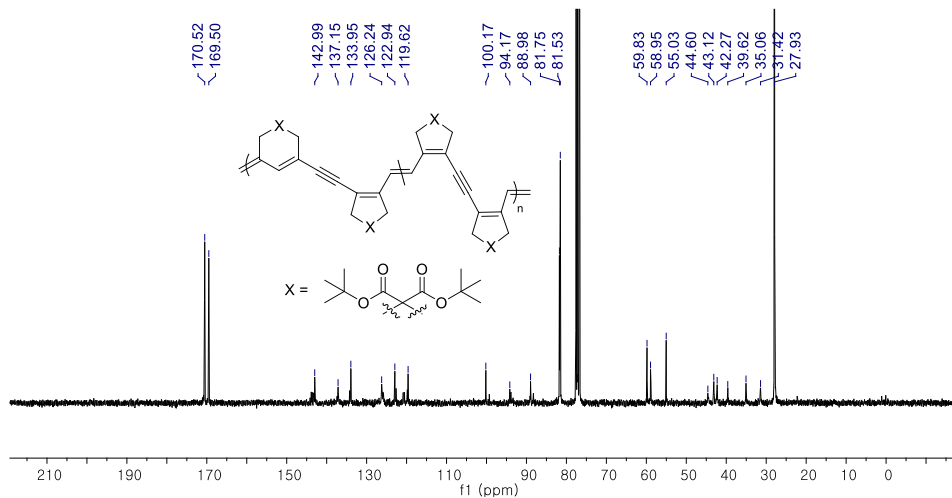
An NMR tube was filled with monomer (0.05 mmol, 20 eq), purged with argon, and  $\text{DCM-}d_2$  (300  $\mu\text{L}$ ) was added. A 5-mL vial containing initiator (0.0025 mmol, 1 eq) (and 2 eq of additive) was argon-purged, and hexamethyldisilane was added as an internal standard. The total amount of initiator and additive was 5/4 of the amount used for the reaction; after dissolving those using  $\text{DCM-}d_2$  (250  $\mu\text{L}$ ), 1/5 (50  $\mu\text{L}$ ) of it was diluted in another NMR tube and used for checking the ratio between initial carbene and the internal standard. Then, the remaining 200  $\mu\text{L}$  of initiator solution was added to monomer solution and  $^1\text{H}$  NMR measurement was recorded over time.

# $^1\text{H}$ and $^{13}\text{C}$ NMR Spectra of Polymers

## P1 $^1\text{H}$ NMR (500 MHz, $\text{CDCl}_3$ )

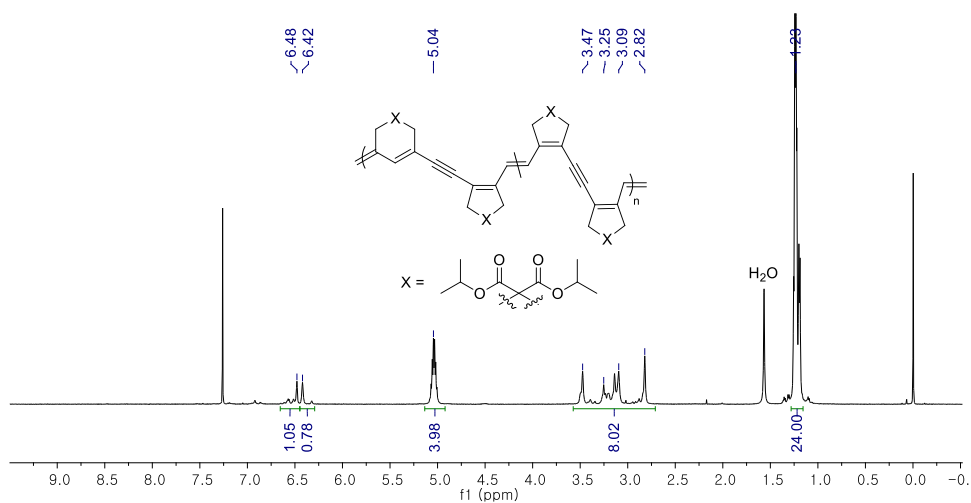


## P1 $^{13}\text{C}$ NMR (75 MHz, $\text{CDCl}_3$ )

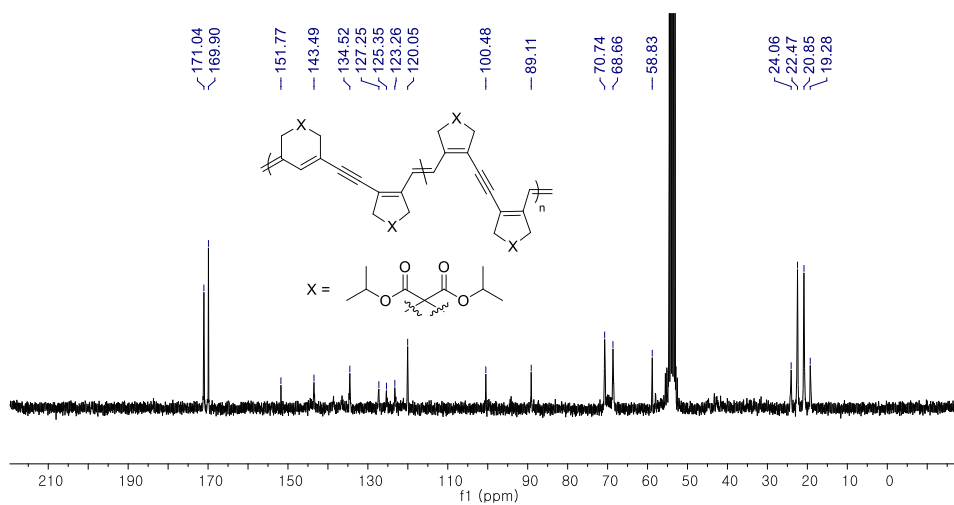




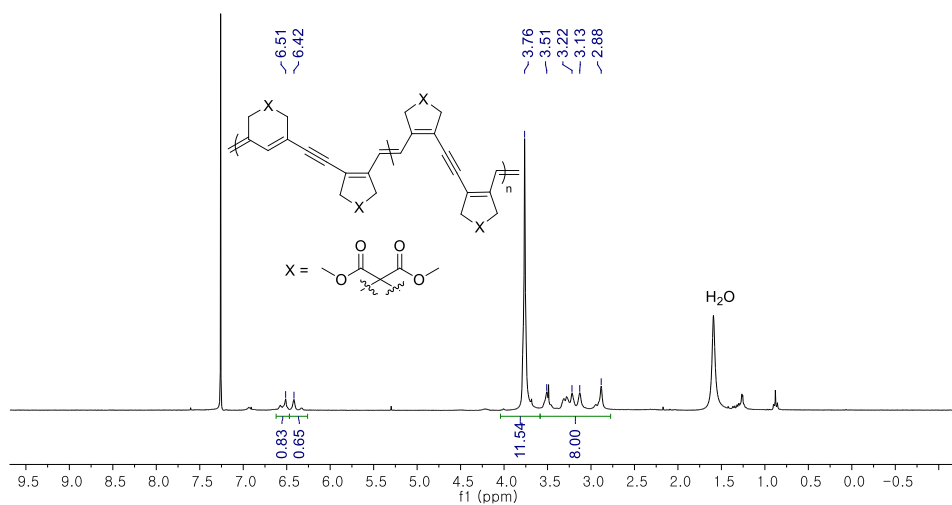
**P2**  $^1\text{H}$  NMR (500 MHz,  $\text{CDCl}_3$ )



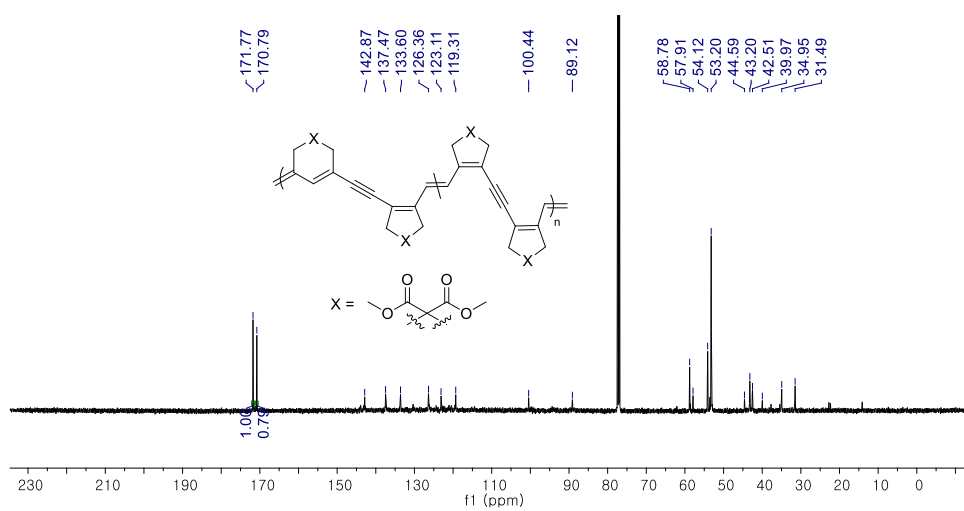
**P2**  $^{13}\text{C}$  NMR (75 MHz,  $\text{CDCl}_3$ )



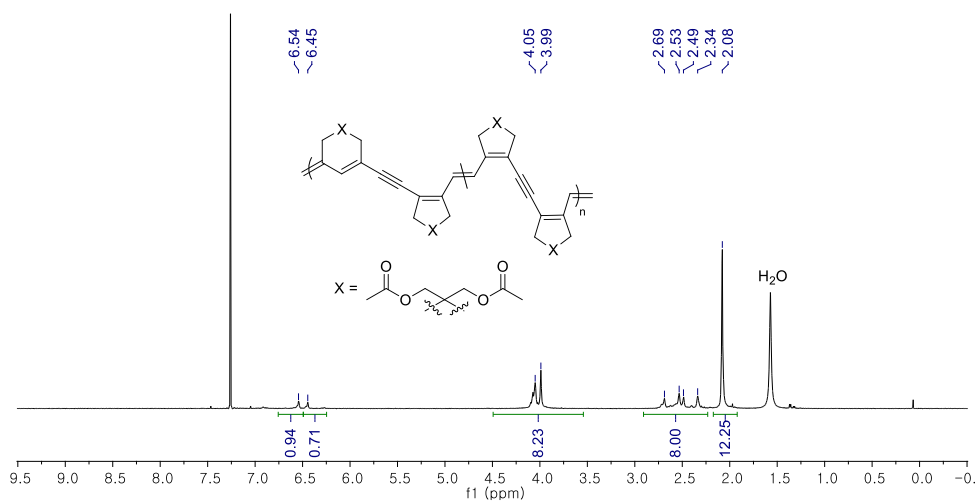
**P3**  $^1\text{H}$  NMR (300 MHz,  $\text{CDCl}_3$ )



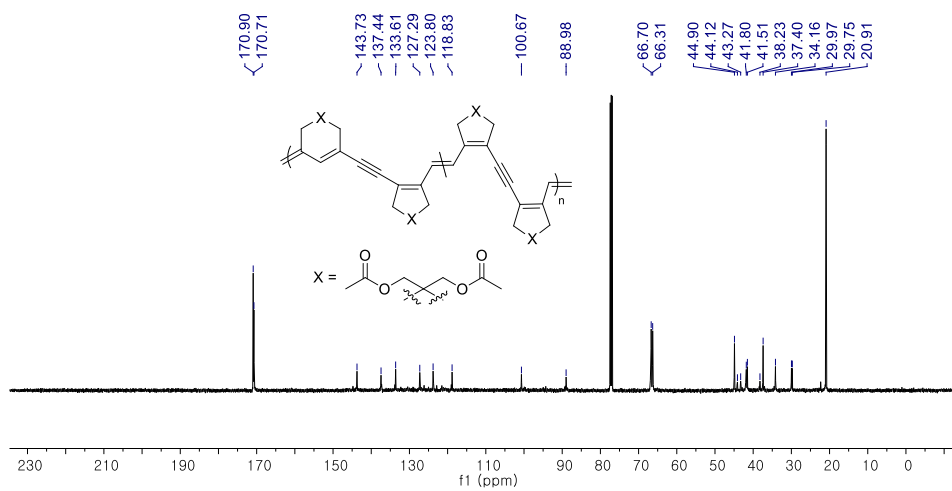
**P3**  $^{13}\text{C}$  NMR (125 MHz,  $\text{CDCl}_3$ )



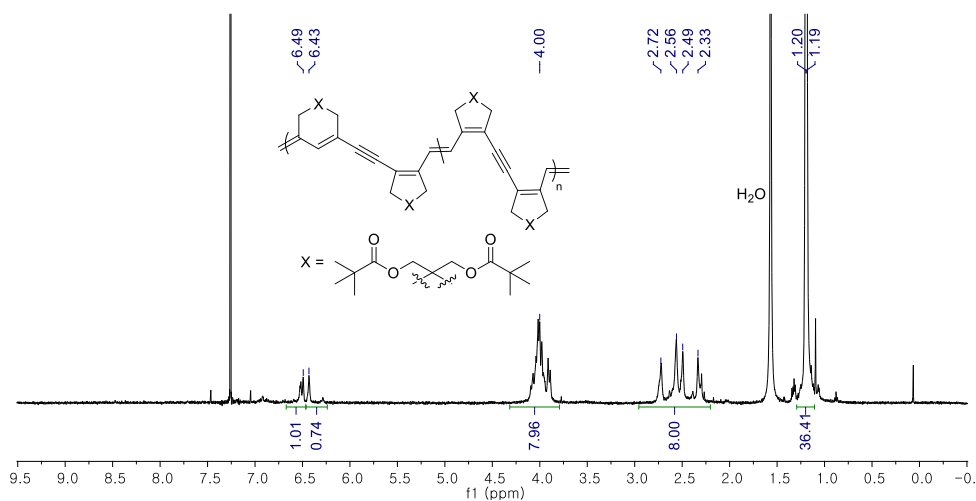
**P4**  $^1\text{H}$  NMR (500 MHz,  $\text{CDCl}_3$ )



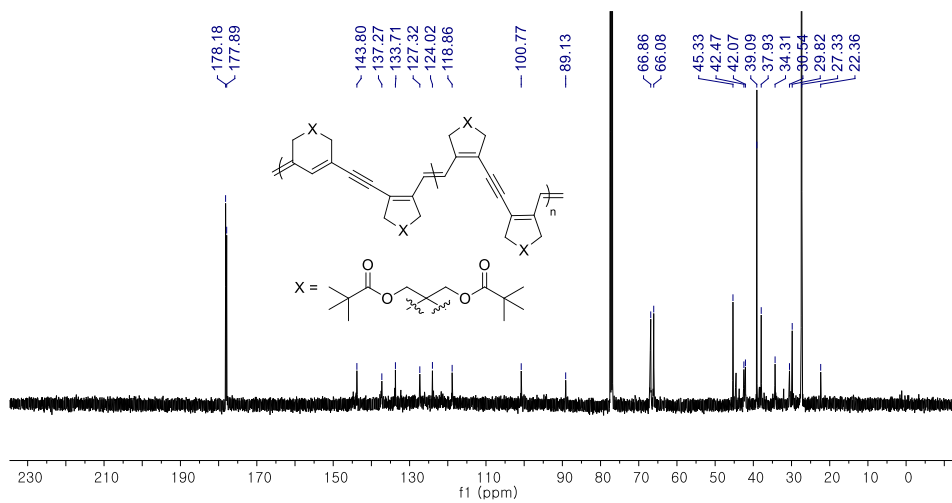
**P4**  $^{13}\text{C}$  NMR (125 MHz,  $\text{CDCl}_3$ )



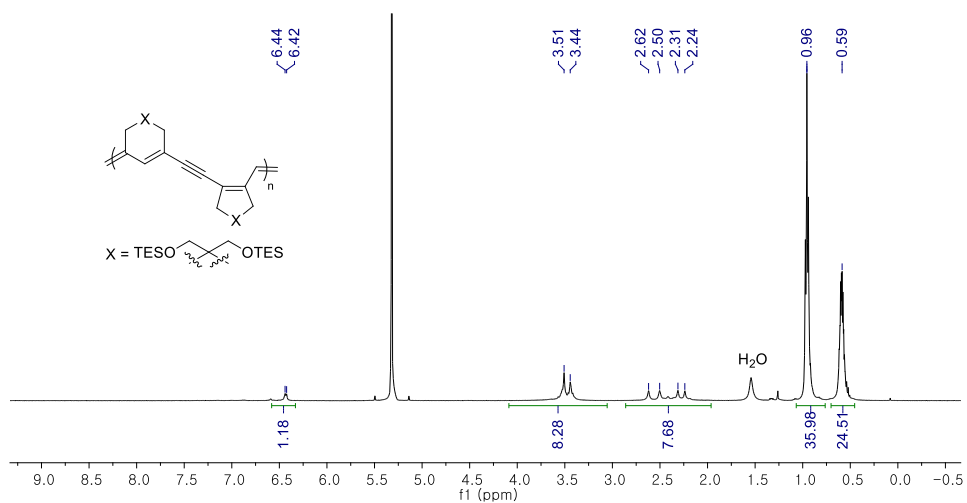
**P5**  $^1\text{H}$  NMR (500 MHz,  $\text{CDCl}_3$ )



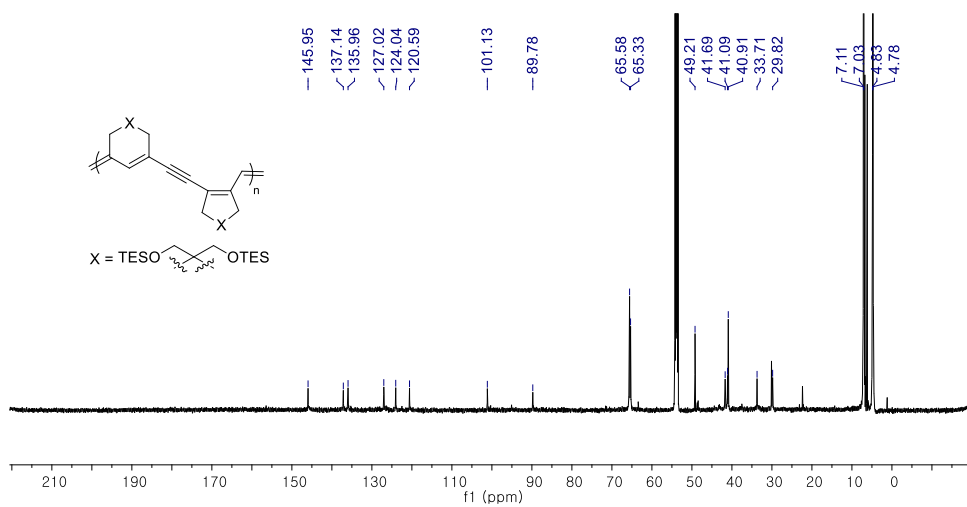
**P5**  $^{13}\text{C}$  NMR (125 MHz,  $\text{CDCl}_3$ )



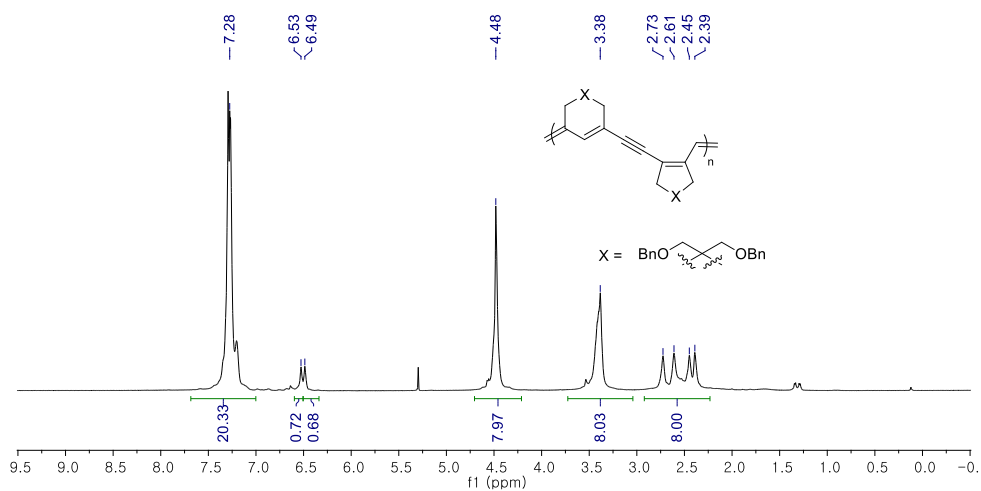
**P6**  $^1\text{H}$  NMR (500 MHz,  $\text{CD}_2\text{Cl}_2$ )



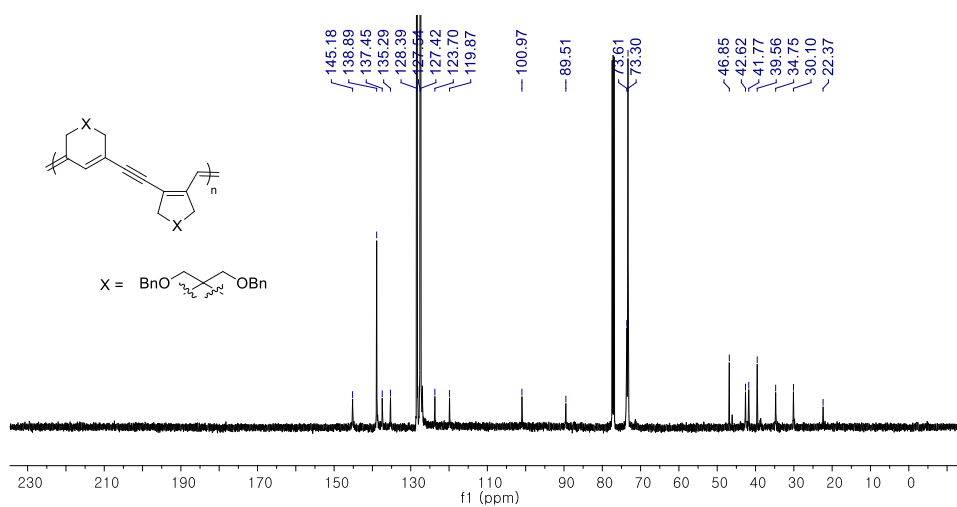
**P6**  $^{13}\text{C}$  NMR (150 MHz,  $\text{CD}_2\text{Cl}_2$ )



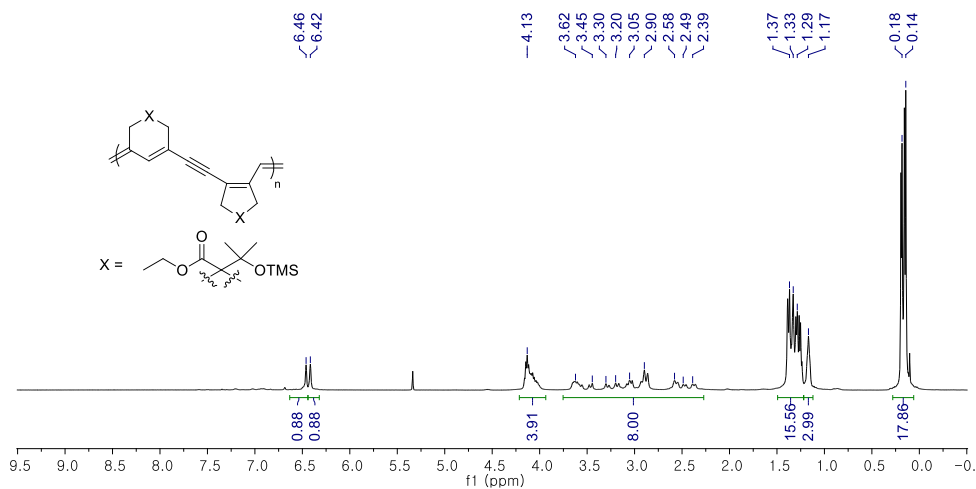
**P7**  $^1\text{H}$  NMR (500 MHz,  $\text{CDCl}_3$ )



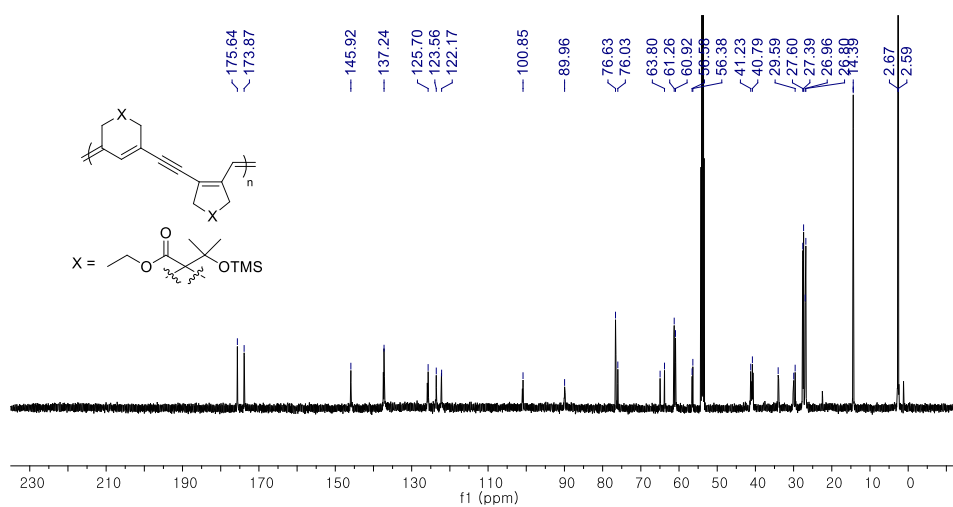
**P7**  $^{13}\text{C}$  NMR (125 MHz,  $\text{CDCl}_3$ )



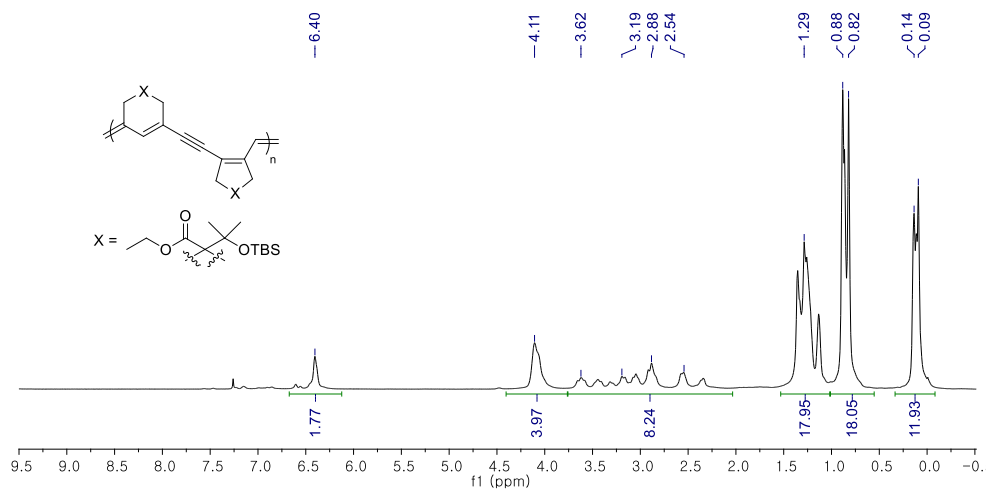
**P8**  $^1\text{H}$  NMR (500 MHz,  $\text{CD}_2\text{Cl}_2$ )



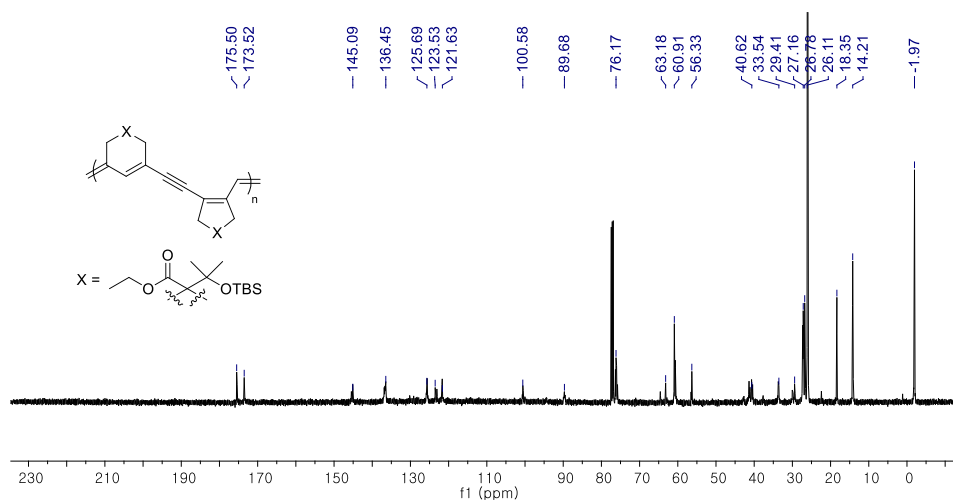
**P8**  $^{13}\text{C}$  NMR (125 MHz,  $\text{CD}_2\text{Cl}_2$ )



**P9**  $^1\text{H}$  NMR (500 MHz,  $\text{CDCl}_3$ )

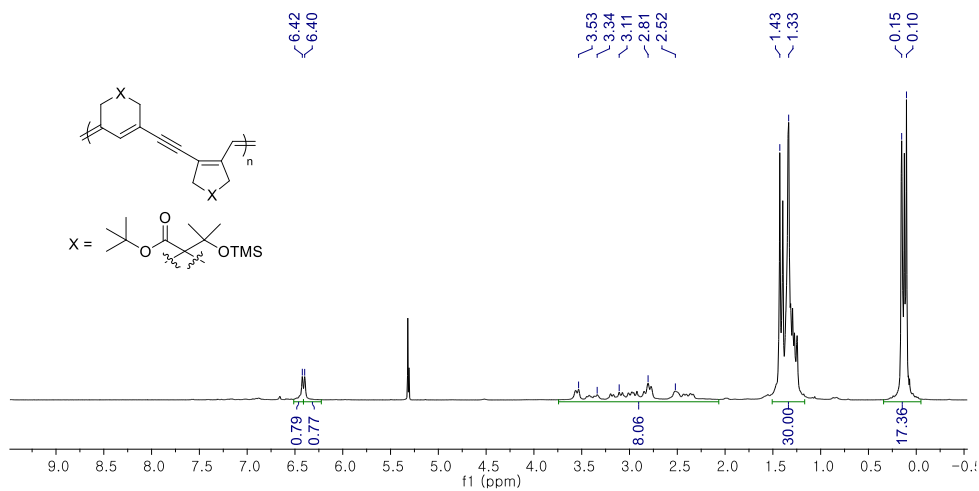


**P9**  $^{13}\text{C}$  NMR (125 MHz,  $\text{CDCl}_3$ )

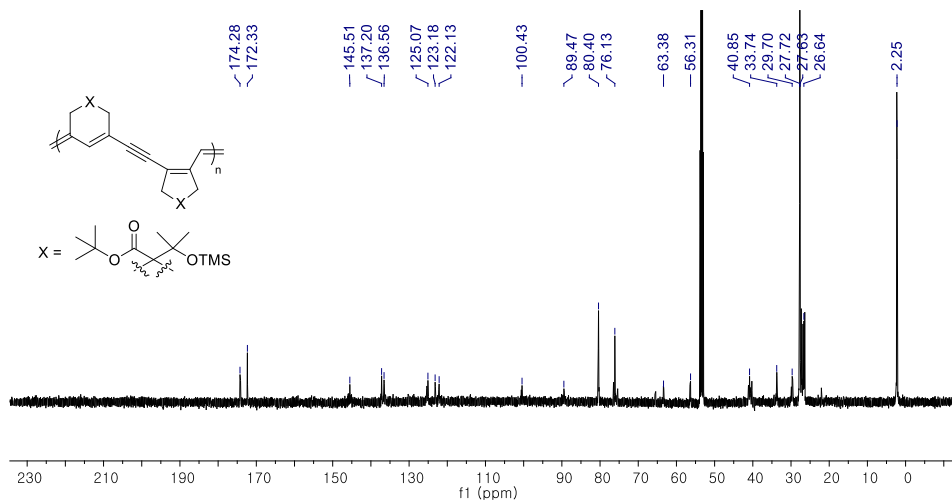




**P10** <sup>1</sup>H NMR (500 MHz, CD<sub>2</sub>Cl<sub>2</sub>)



**P10**  $^{13}\text{C}$  NMR (125 MHz,  $\text{CD}_2\text{Cl}_2$ )



## 5.7. References

† This chapter has been previously reported: Kang, C.; Sung, J.-C.; Kim, K.; Hong, S. H.; Choi T.-L. *ACS Macro Lett.*, **2020**, *9*, 339 —343

- (1) Kang, C.; Park, H.; Lee, J. K.; Choi, T.-L. *J. Am. Chem. Soc.* **2017**, *139*, 11309-11312.
- (2) Kang, C.; Kwon, S.; Sung, J. C.; Kim, J.; Baik, M. H.; Choi, T. L. *J. Am. Chem. Soc.* **2018**, *140*, 16320-16329.
- (3) Peterson, G. I.; Yang, S.; Choi, T. L. *Acc. Chem. Res.* **2019**, *52*, 4994-1005.
- (4) Fox, H. H.; Schrock, R. R. *Organometallics* **1992**, *11*, 2763–2765.
- (5) Fox, H. H.; Wolf, M. O.; O'Dell, R.; Lin, B. L.; Schrock, R. R.; Wrighton, M. S. *J. Am. Chem. Soc.* **1994**, *116*, 2827–2843.
- (6) Anders, U.; Nuyken, O.; Buchmeiser, M. R.; Wurst, K. *Macromolecules* **2002**, *35*, 9029–9038.
- (7) Schattenmann, F. J.; Schrock, R. R.; Davis, W. M. *J. Am. Chem. Soc.* **1996**, *118*, 3295–3296.
- (8) Schattenmann, F. J.; Schrock, R. R. *Macromolecules* **1996**, *29*, 8990–8991.
- (9) Keitz, B. K.; Endo, K.; Patel, P. R.; Herbert, M. B.; Grubbs, R. H. *J. Am. Chem. Soc.* **2012**, *134*, 693-699.
- (10) Koh, M. J.; Khan, R. K. M.; Torker, S.; Yu, M.; Mikus, M. S.; Hoveyda, A. H. *Nature*, **2015**, *517*, 181-186.
- (11) Jung, K.; Kang, E. H.; Sohn, J. H.; Choi, T. L. *J. Am. Chem. Soc.* **2016**, *138*, 11227-11233.
- (12) Jung, K. Jung, M. Hong, S. Kwon, K. Kim, S. H. Hong, T.-L. Choi and M. H. Baik, *J. Am. Chem. Soc.* **2018**, *140*, 834-841.
- (13) Jung, K.; Kim, K.; Sung, J. C.; Ahmed, T. S.; Hong, S. H.; Grubbs, R. H.; Choi, T. L. *Macromolecules* **2018**, *51*, 4564-4571.
- (14) Jung, K.; Ahmed, T. S.; Lee, J., Sung, J. C.; Keum, H.; Grubbs, R. H.; Choi, T. L. *Chem. Sci.* **2019**, *10*, 8955-8963.

- (15) Wang, K. P.; Yun, S. Y.; Lee, D.; Wink, D. J. Structure and Reactivity of Alkyne-Chelated Ruthenium Alkylidene Complexes. *J. Am. Chem. Soc.* **2009**, *131*, 15114-15115.
- (16) Koh, M. J.; Khan, R. K.; Torker, S.; Yu, M.; Mikus, M. S.; Hoveyda, A. H., *Nature* **2015**, *517*, 181.
- (17) Seo, S.; Marks, T. J. *Chem.–A Eur. J.* **2010**, *16*, 5148.
- (18) Madine, J. W.; Wang, X.; Widenhoefer, R. A. *Org. Lett.* **2001**, *3*, 385.
- (19) Murai, M.; Uemura, E.; Hori, S.; Takai, K. *Angew. Chem.* **2017**, *129*, 5956.
- (20) Stulgies, B.; Prinz, P.; Magull, J.; Rauch, K.; Meindl, K.; Ruhl, S.; Meijere, A. *Chem. Eur. J.* **2005**, *11*, 308.
- (21) Zhu, S.; Liang, R.; Jiang, H.; Wu, W. *Angew. Chem. Int. Ed.* **2012**, *51*, 10861.

## Abstract (Korean)

폴리엔 (폴리아세틸렌) 구조를 가지는 반도체성 고분자의 발견 이후, 다양한 공액 고분자는 여러 전기·광학적 재료에 사용되어 왔다. 특히, 양 끝에 삼중 결합을 갖는 다이아인 단량체는 고리화중합을 거쳐 사이클로알켄 구조를 포함하는 폴리아세틸렌을 형성할 수 있다. 지난 수십년 간의 연구를 통해 몰리브데넘과 루테튬 기반의 촉매를 사용하는 고리화중합 방법이 개발되어 왔지만, 여전히 몇몇 종류의 촉매나 단량체를 사용할 수 없다는 한계가 있다.

폴리엔뿐만 아니라 폴리에나인 구조를 갖는 공액 고분자 또한 흥미로운 광학적 성질로 인해 많은 관심을 받아 왔다. 그러나 이러한 고분자를 합성하는 방법은 토포케미컬 중합이나 단계 중합 반응에 의존해 왔기 때문에 정교한 분자량 조절을 할 수 없었다.

본 연구에서는 루테튬 촉매를 사용한 고리화 중합 반응 연구를 확장하여 기존에 사용할 수 없었던 촉매와 단량체를 효율적으로 활용하는 방안을 제시하고자 한다. 또한, 루테튬 촉매로부터 올레핀 복분해와 금속 이동 반응이 일어나는 연쇄 중합 방법을 개발함으로써 처음으로 사슬 중합 메커니즘을 통해 폴리에나인을 합성하는 사례를 보고한다.

2 장에서는 기존에 고리화 중합 반응에 사용되지 못했던 1 세대 그럽스 촉매 (G1)를 사용하여 성공적으로 폴리엔을 합성하는 것을 보고한다. 여러 종류의 첨가제를 시도했을 때, 벤조산과 벤조산 나트륨이 G1 의 반응성을 증가시키는 것을 발견하였고, 이를 통해 효율적으로 1,6-헵타다이아인의 고리화 반응 중합을 진행시킬 수 있었다. NMR 분석을 이용한 대조 실험들을 통해 이 두 종류의 첨가제가 어떤 역할을 하는지 고찰하였다.

1,6-헵타다이아인을 단량체로 사용하는 고리화중합 연구가 많이 진행된 것과는 달리, 1,5-헥사다이아인의 경우에는 고리화 반응 이후에 생성되는 사이클로뷰텐의 불안정성 때문에 단량체로 사용하기 어려웠다. 3 장에서는 1,5-헥사다이아인을 사용하여 4 각 고리를 형성하는 중합 과정을 통해 새로운 종류의 폴리엔을 합성한 연구에 대해 소개하고자 한다. 커다란 입체 구조의 작용기를 가진 촉매와 단량체를 사용했을 때 고리화중합이 효율적으로 진행되어 고분자의 분자량을 조절할 수 있을 뿐 아니라 블록공중합체의 합성도 가능하였다. 또, 4 각 고리를 가지는 새로운 폴리엔이 기존의 경우보다 특히 비편재화된  $\pi$ -시스템을 가지는 것을 실험적·계산적 방법을 통해 밝혀내었다.

더 나아가, 루테튬 촉매를 이용한 고분자 합성 확장의 일환으로 폴리에나인 공액 고분자를 합성하고자 하였다. 4 장에서는 여러 종류의 멀티아인 단량체 디자인을 통해, 올레핀 복분해와 금속 이동 반응이 연속적이고 선택적으로 일어나는 중합 방법 개발에 대해 서술한다. 새로운 M&M 중합을 통해 이중 결합과 삼중 결합의 다양한 조합으로 뼈대가 구성되는 특이한 폴리에나인을 합성할 수 있었다. 또, 리빙 중합을 통해 고분자의 분자량 조절과 블록공중합체의 합성도 가능하였다.

마지막으로, 5 장에서는 기존의 M&M 중합의 위치 선택성을 전환함으로써 본 연구를 보다 확장하는 것에 대해 기술하였다. 이전의 M&M 중합은  $\alpha$  (알파) 배향을 통해 5 각 고리를 선택적으로 생성하였는데, 루테튬 다이싸이올레이트 촉매를 사용한 경우  $\beta$  (베타) 방향으로 선택성이 전환되어 결과적으로 6 각 고리와 5 각 고리가 번갈아 나타나는 새로운 폴리에나인을 형성할 수 있었다. 추가적인 NMR 분석을 통해 중합 과정에서 인접한 알카인이 킬레이트를 형성하여 중합 특성에 큰 영향을 미치는 것을 확인하였다.

**주요어:** 고리화 중합, M&M 중합, 공액 폴리엔, 공액 폴리에나인, 루테늄 촉매, 그럽스 촉매, 리빙 중합

**학번:** 2014-22387